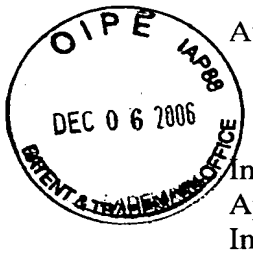

Attorney Docket No. 9013-67

PATENT

IN THE UNITED STATES PATENT AND TRADEMARK OFFICE

In re: Foster et al.
Application No.: 10/518,471
Int'l Filing Date: December 17, 2004
For: ***REMOVAL OF PRION INFECTIVITY***

Confirmation No.: 7924
Group Art Unit: 1746
Examiner: Bibi S. Carrillo

Date: December 8, 2006

Mail Stop RCE
Commissioner for Patents
P.O. Box 1450
Alexandria, VA 22313-1450

Appendix A

Attorney Docket No. 9013-67 PATENT

IN THE UNITED STATES PATENT AND TRADEMARK OFFICE

In re: Foster et al.
Application No.: 10/518,471
Int'l Filing Date: December 17, 2004
For: *REMOVAL OF PRION INFECTIVITY*

Confirmation No.: 7924
Group Art Unit: 1746
Examiner: Bibi S. Carrillo

Declaration of Ian MacGregor, Ph.D. Pursuant to 37 C.F.R. § 1.132

I, Ian R. Mac Gregor, do hereby declare and say as follows:

1. I have a Ph.D. in Biochemistry, from University of London (King's College Medical School). I am Lead Scientist (Consultant Level Research Scientist), in the Products & Components Research Group for the Scottish National Blood Transfusion Service, Edinburgh. I am involved in prion research and have authored or co-authored more than 16 publications related to this area. A *curriculum vitae* is attached herewith at Appendix B.

2. I have read and am familiar with the contents of the James et al. publication (U.S. Application Serial No. 2003/0162225) cited by the Examiner in connection with the '471 application.

3. James et al. discusses treatment of recombinant prion proteins and not abnormal, infectious proteins, which are the subject of the present invention. It is well known that there are significant structural differences between normal and abnormal prions. In fact, it is these structural differences, which give rise to the abnormal infectious behaviour of infectious prion proteins. Thus, behaviour which could be ascribed to normal prion proteins could not be regarded as a good basis for treatment of abnormal prion proteins. These differences are discussed below in greater detail.

4. Differences in properties are attributed to differences in conformation since sequences and secondary structures are the same.

It is generally accepted that the primary and secondary structures of normal and infectious prion proteins are the same. However their physico-chemical properties are quite different and this is attributed to their differing tertiary structures. While both forms have a

disordered N terminus, the globular C domain of an infectious prion protein has much more β-pleated sheet structure than that of a normal prion. Conversely, normal prion protein has much more α-helix (Turk *et al.*, 1889; James *et al.*, 1997). These differences are reflected in different exposure of hydrophobic regions of the molecule and in turn in different physico-chemical properties. In addition, normal prion protein is soluble in non-ionic detergent while, in contrast, infectious prion protein is insoluble. Normal prion protein is readily digested by the broad specificity proteinase K while only the N-terminus of infectious prion protein is degraded with the major part of the molecule remaining intact. Further evidence for differences in conformation is given by the inability of a monoclonal antibody, 3F4, directed to an epitope expressed in normal prion protein, to bind to infectious prion protein. However, upon denaturation of the latter, binding to 3F4 is obtained (Safar *et al.*, 1998).

Furthermore, sodium phosphotungstic acid has been used to selectively precipitate infectious prion protein in the presence of normal prion protein. A 10% NaCl solution also will allow enrichment of infectious prion protein from brain homogenate (Polymenidou *et al.*, 2002).

5. A 'most infectious particle' has been characterized and its properties can be distinguished from normal prion protein in several ways.

Infectious prion protein is often found in fibrils. However, recently it has been shown that the most infectious prion protein particles are not fibrillar but are of 17-27 nm (300-600 kDa) while prion infectivity and prion converting activity was virtually absent in oligomers of ≤ 5 prion molecules (Silveira *et al.*, 2005). In contrast, normal prion protein exists in nature mainly as a monomer although some dimeric forms have also been reported (Meyer *et al.*, 2000).

6. Procedures have been developed by which the normal prion protein can be converted to forms similar to infectious forms, underlining the differences.

Protein misfolding cyclic amplifications has been used to convert substrate normal hamster prion protein into infectious prion protein. The substrate prion was not infectious but the generated prion protein, which shared the properties of infectious protein regarding proteinase K resistance, was infectious when injected into hamsters. (Castilla *et al.*, 2005).

7. A number of ways of discriminating normal from infectious prion have been devised. These illustrate the differences in the properties of the two forms.

Antibodies which have specificity for infectious prion protein over normal prion protein have been described. These utilize differences in the conformation of the two forms or the fact that the former is multimeric. Peptoids and chemical ligands have been used in a similar way, using conditions that allow binding of infectious but not normal prion protein.

8. Reference List

All references listed are attached at Appendix C.

Castilla, J., Saa, Ph., Hetz, C., & Soto, C. (2005) In vitro generation of infectious scrapie prions. *Cell*, **121**, 195-206.

James, T.L., Liu, H., Ulyanov, N.B., FarrJones, S., Zhang, H., Donne, D.G., Kaneko, K., Groth, D., Mehlhorn, I., Prusiner, S.B., and Cohen, F.E., Solution structure of a 142-residue recombinant prion protein corresponding to the infectious fragment of the scrapie isoform. *Proceedings of the National Academy of Sciences of the United States of America*, 94(19), 10086-10091, 1997.

Meyer, R.K., Lustig, A., Oesch, B., Fatzer, R., Zurbriggen, A., and Vandevelde, M. A monomer-dimer equilibrium of a cellular prion protein (PrPC) not observed with recombinant PrP. *J. Biol. Chem.*, 275(48), 38081-38087, 2000.

Polymenidou, M., Verghse-Nikolai, S., Groshup, M., Chaplin, M.J., Stack, M.G., Plaitakis, A. & Sklaviadis, T. (2002) A short purification process for quantitative isolation of PrP^{SC} from naturally occurring and experimental transmissible spongiform encephalopathies. *BMC.Infect.Dis.*, 2, 1-8.

Safar, J., Wille, H., Itri, V., Groth, D., Serban, H., Torchia, M., Cohen, F.E. & Prusiner, S.B. (1998) Eight prion strains have PrPSc molecules with different conformations. *Nature Medicine*, 4, 1157-1165.

Silveira, J.R., Raymond, G.J., Hughson, A.G., Race, R.E., Sim, V.L., Hayes, S.F., & Caughey. B. (2005) The most infectious prion protein particles. *Nature*, 437, 257-261.

Turk, E., Teplow, D.B., Hood, L.E., & Prusiner, S.B. (1988) Purification properties of the cellular and scrapie hamster prion proteins. *European Journal of Biochemistry*, 176, 21-30.

9. I hereby declare that all statements made herein of my own knowledge are true and that all statements made on information and belief are believed to be true; and further that these statements were made with the knowledge that willful false statements and the like so made are punishable by fine or imprisonment, or both, under Section 1001 of Title 18 of the United States Code and that such willful false statements may jeopardize the validity of the application or any patent issued thereon.

Ian MacGregor

Ian R. MacGregor, Ph.D.

5th December 2006

Date

Attorney Docket No. 9013-67 PATENT

IN THE UNITED STATES PATENT AND TRADEMARK OFFICE

In re: Foster et al.
Application No.: 10/518,471
Int'l Filing Date: December 17, 2004
For: ***REMOVAL OF PRION INFECTIVITY***

Confirmation No.: 7924
Group Art Unit: 1746
Examiner: Bibi S. Carrillo

Date: December 8, 2006

Mail Stop RCE
Commissioner for Patents
P.O. Box 1450
Alexandria, VA 22313-1450

Appendix B

Brief CV: Ian Randle MacGregor

Degrees and qualifications

- BSc. Hons Pharmacology, University of Edinburgh 1974
- PhD Biochemistry, University of London (King's College Medical School) 1980
- Clinical Scientist, Health Professions Council.
- Certificate in Continuing Professional Development (RCPath UK).

Job History

1999- Present: Lead Scientist (Consultant Level Research Scientist) , Products & Components Research Group, Scottish National Blood Transfusion Service, Edinburgh. Tenured post on SNBTS permanent staff establishment.

1980- 1999: Basic Grade Scientist promoted to Senior Scientist then to Principal Scientist in R&D Departments of SNBTS.

1976-1980: MRC Research Assistant at Thrombosis Research Unit, King's College Hospital Medical School, London.

1974-1976: Research Pharmacologist at Weddell Pharmaceuticals, St Albans.

Principal Elements of Present Post

Line and Financial Manager for a department of 7 tenured Scientists, Technicians and Support Staff as well as grant-funded staff and visiting scientists. Main current R&D responsibilities are:

- Lead SNBTS vCJD R&D Group
- Develop methods to detect the agent of variant Creutzfeldt-Jakob disease in blood.
- Improve storage and safety of clinical blood components.

Principal Scientific Contributions.

- SNBTS Principal Investigator on two current grant-funded vCJD projects and co-applicant on others. Previous grants funded by MRC, BHF, DH, EU etc.
- Development and application of prion assays to blood.
- Member of UK & Ireland Blood Services Prion Assay Working Group.
- On Management Committee of Scottish Transmissible Spongiform Encephalopathies Network.
- Establishment of pre-clinical safety evaluation methods for immunogenicity and thrombogenicity of new blood products.
- Active member of British Blood Transfusion Society, American Association of Blood Banks, British Society for Haemostasis and Thrombosis, International Society on Thrombosis and Haemostasis, Scottish TSE Network.
- Author of over 70 peer-reviewed full publications in the field of blood products and prion diseases, granted patents, and invited presentations at meetings e.g. of International Blood Transfusion Societies and Medicines Evaluation Agencies.
- Examiner of PhDs and Master's Degrees; Supervisor for Post-graduate Degrees; regular referee for journals and grant applications.

Grants awarded on prion topics

"Development of a conformation dependent immunoassay for the detection of abnormal prion protein in blood". To Drs M. Head, I. MacGregor, A. Williamson, G. Moroncini, M. Turner and J Ironside. 2006 – 2008 from Chief Scientist Office (Scotland) Value £188,172.

"The effect of leucodepletion on transmission of BSE by transfusion of sheep blood components". To Drs F. Houston, C. Prowse, I. MacGregor, V. Hornsey, J. Foster, N. Hunter, M. Turner and M. Groschup. 2005 – 2011 from UK Department of Health, Value £3,319,707.

"Screening Blood for High Risk Donations". To Drs M. Clinton, D. Anstee and I. MacGregor. Funded by UK Department of Health 3 years from April 2002 Value £472,723

"Novel Application-Specific Monoclonal Antibodies to PrP". To: Drs M. Head, I. MacGregor, C. Farquhar and J. Connolly. Funded by UK Department of Health 3 years from April 2002 Value £445,540

"A study of normal and abnormal isoforms of prion protein in the peripheral blood and tissues of patients with variant Creutzfeldt Jakob disease". To Drs M Turner, I MacGrergor, R Barclay, M Head and J Ironside. From Chief Scientist Office (Scotland). June 2001 – May 2003. Value £145,600.

"Assessment and improvement of selected technologies to remove or inactivate TSE-causing agents (prions)". I MacGregor for SNBTS and with Dutch BTS, Finnish Red Cross and commercial collaborators. From EU CRAFT, January 1999 – December 2001. Value 500,000 Euro.

"The effect of leucocyte depletion on the generation and removal of microvesicles and prion protein in blood components" M Turner, I MacGregor, C Prowse, L Williamson, P Krailadsiri, J Seghatchian, D Anstee, T Barrowcliffe. From Department of Health, Jan 1999 – July 2001. Value £240,000.

Publications on prion topics: 2000 to date.

Starke R., Mackie I., Drummond O., MacGregor I., Harrison P., Machin, S. Prion protein (PrPc) in patients with renal failure. *Transf. Med.* 2006: 16: 165-168

Krailadsiri P., Seghatchian J., MacGregor I., Drummond O., Perrin R., Spring F., Prescott R., Williamson L., Prowse C., Anstee D. and Turner M. The effects of leucodepletion on the generation and removal of microvesicles and prion protein in blood components. *Transfusion* 2006: 46: 407-417

Fagge T., Barclay GR., MacGregor IR., Head M., Ironside J. and Turner M. Variation in concentration of prion protein in the peripheral blood of patients with variant and sporadic Creutzfeldt-Jakob disease detected by dissociation enhanced lanthanide fluoroimmunoassay and flow cytometry. Transfusion 2005;45: 504-513.

Jones M., Head MW.; Connolly JG., Farquhar CF.; Hornsey VS., Pepper DS., and MacGregor IR. Purification of normal cellular prion protein from human platelets and the formation of a high molecular weight prion protein complex following platelet activation. Biochem. Biophys. Res. Comm. 2005; 335: 48-56.

MacGregor IR. Screening assays for Transmissible Spongiform Encephalopathies (TSEs). Vox Sang. 2004: 87: Suppl. 2: 3-6

MacGregor IR. and Prowse CV. Impacts and concerns for vCJD in blood transfusion: Current Status. Current Molecular Medicine 2004: 4: 361-373

Foster PR., Griffin BD., Bienek C., McIntosh RV., MacGregor IR., Somerville RA., Steele PJ. and Reichl H.E. Distribution of a bovine spongiform encephalopathy-derived agent over ion-exchange chromatography used in the preparation of concentrates of fibrinogen and factor VIII. *Vox Sang.* 2004: 86: 92-99.

Prowse CV. and MacGregor IR. Assays for detection of Creutzfeldt-Jakob disease in donors: Progress to date. In Emerging Technologies in Transfusion Medicine. eds: Christopher Stowell and Walter Dzik AABB Press. Chapter 1; 2003 p. 1-22

Starke R., Harrison P., Gale R., Mackie I., Drummond O., MacGregor IR. and Machin S. Endothelial cells express normal cellular prion protein. Br. J. Haematol. 123; 372-373.

Starke R., Drummond O, MacGregor IR, Biggerstaff J., Camilleri R., Gale R., Lee CA., Nitu-Whalley, IC, Machin, S and Harrison, P. The expression of prion protein by endothelial cells. Br J Haematol. 2002; 119: 863-873

Prowse CV. and MacGregor IR. Mad Cows and Englishmen: An update on blood and vCJD. Vox Sang. 2002, 83: Suppl. 1, 341-349

Reichl H., Foster PR., Welch AG., Li Q., MacGregor IR., Somerville RA., Fernie K., Steele PJ. and Taylor DM. Studies on the removal of a BSE-derived agent by processes used in the manufacture of human immunoglobulin. Vox Sang. 2002, 83:137-145.

Bessos H., Prowse C., Turner M. and MacGregor IR. The release of prion protein from platelets during storage of apheresis platelet concentrates. Transfusion 2001;41:61-66.

MacGregor IR. Prion protein and developments in its detection. Transfusion Medicine. 2001;11:3-14.

MacGregor IR. and Drummond O. Species differences in the blood content of the normal cellular isoform of prion protein, PrPc, measured by time-resolved fluoroimmunoassay. Vox Sang 2001;81:236-240.

Hornsey V., MacGregor IR., Bethel H., Krailadsiri P., Smith K., Seghatchian J. and Prowse CV. Leucofiltration, retention/generation of soluble prion and annexin V and storage of blood components. Transfusion Science, 2000;22:75-76

Attorney Docket No. 9013-67 PATENT

IN THE UNITED STATES PATENT AND TRADEMARK OFFICE

In re: Foster et al.
Application No.: 10/518,471
Int'l Filing Date: December 17, 2004
For: ***REMOVAL OF PRION INFECTIVITY***

Confirmation No.: 7924
Group Art Unit: 1746
Examiner: Bibi S. Carrillo

Date: December 8, 2006

Mail Stop RCE
Commissioner for Patents
P.O. Box 1450
Alexandria, VA 22313-1450

Appendix C

CASTILLA, J.

Cell, Vol. 121, 195–206, April 22, 2005, Copyright ©2005 by Elsevier Inc. DOI 10.1016/j.cell.2005.02.011

TSE

In Vitro Generation of Infectious Scrapie Prions

Joaquín Castilla,[1] Paula Saá,[1,2] Claudio Hetz,[1,3] and Claudio Soto[1,*]
[1]Department of Neurology
University of Texas Medical Branch
Galveston, Texas 77555
[2]Centro de Biología Molecular
Universidad Autónoma de Madrid
28049 Madrid
Spain
[3]University of Chile, Instituto de Ciencias Biomédicas
P.O. Box 625
Santiago
Chile

Summary

Prions are unconventional infectious agents responsible for transmissible spongiform encephalopathy (TSE) diseases. They are thought to be composed exclusively of the protease-resistant prion protein (PrP^{res}) that replicates in the body by inducing the misfolding of the cellular prion protein (PrP^{C}). Although compelling evidence supports this hypothesis, generation of infectious prion particles in vitro has not been convincingly demonstrated. Here we show that $PrP^{C} \rightarrow PrP^{res}$ conversion can be mimicked in vitro by cyclic amplification of protein misfolding, resulting in indefinite amplification of PrP^{res}. The in vitro-generated forms of PrP^{res} share similar biochemical and structural properties with PrP^{res} derived from sick brains. Inoculation of wild-type hamsters with in vitro-produced PrP^{res} led to a scrapie disease identical to the illness produced by brain infectious material. These findings demonstrate that prions can be generated in vitro and provide strong evidence in support of the protein-only hypothesis of prion transmission.

Introduction

Prion diseases, also called transmissible spongiform encephalopathies (TSEs), are some of the most intriguing infectious disorders affecting the brains of humans and animals. The group is comprised of Creutzfeldt-Jakob disease (CJD), kuru, Gerstmann-Sträussler Sheinker syndrome (GSS), and fatal familial insomnia (FFI) in humans and scrapie, bovine spongiform encephalopathy (BSE), and chronic wasting disease (CWD) in animals (Collinge, 2001). TSEs can have sporadic, inherited, and infectious origins. The nature of the transmissible agent has been the subject of intense debate (Prusiner, 1998; Mestel, 1996; Chesebro, 1998; Soto and Castilla, 2004). Initially the agent was thought to be a slow virus (Sigurdsson, 1954), but further research has indicated that the infectious particle is significantly different from viruses and other conventional agents (Prusiner, 1998). Accordingly, a new hypothesis regarding the nature of the transmissible agent has emerged and recently gained widespread acceptance. This hypothesis proposes that the material responsible for the disease transmission is uniquely composed of a protein that has the surprising ability to replicate itself within the body (Prusiner, 1982; Prusiner, 1998). This newly discovered pathogen is called a proteinaceous infectious particle, or prion (Prusiner, 1982).

An important step in understanding the nature of this novel infectious agent was the isolation of the protease-resistant prion protein (PrP^{res}) from the infectious material (Bolton et al., 1982). Using biochemical and immunological methods, it was shown that PrP^{Sc} and infectivity copurified and that the concentration of the protein was proportional to the infectivity titer (Gabizon et al., 1988). Infectivity was retained in highly purified preparations of PrP^{res}, in which no other component is detectable. In addition, infectivity was convincingly reduced by agents that destroy protein structure and by anti-PrP antibodies (Gabizon et al., 1988). Purification of PrP led to the identification of the gene containing the sequence that encodes PrP (Basler et al., 1986). PrP mRNA is the product of a single gene that is synthesized in the brains of healthy animals and is also constitutively expressed in many cell types (Basler et al., 1986). Thus, PrP has two alternate forms: the normal cellular protein (PrP^{C}) and the pathological isoform (PrP^{res}). Chemical differences between the PrP^{C} and PrP^{res} isoforms have not been detected (Stahl et al., 1993), and the conversion seems to involve a conformational change in which the α-helical content of the normal protein is reduced while the β sheet content is increased (Pan et al., 1993). Structural changes are accompanied by alterations in the biochemical properties (Prusiner, 1998; Cohen and Prusiner, 1998). As such, PrP^{C} is soluble in nondenaturing detergents while PrP^{res} is insoluble, and PrP^{C} is readily digested by proteases while PrP^{res} is mostly resistant, resulting in the formation of an N-terminally truncated fragment known as PrP27–30.

The structural conversion of PrP^{C} into PrP^{res} catalyzed by PrP^{res} has been done in vitro. The cell-free conversion system developed by Caughey and coworkers (Kocisko et al., 1994) using purified PrP^{C} mixed with stoichiometric amounts of purified PrP^{res} produced a low yield of PrP^{res} formation under nonphysiological conditions, making it difficult to evaluate the infectious properties of in vitro-produced misfolded protein. However, the fact that PrP^{res} was able to induce the transformation of the normal protein into more of itself represented important evidence in favor of the prion hypothesis. More recently, we developed a new in vitro conversion system to convert large quantities of PrP^{C} into PrP^{res} using minute amounts of PrP^{res} (Saborio et al., 2001). This system, called PMCA (protein misfolding cyclic amplification), confirms a central facet of the prion hypothesis, which is that prion replication is a cyclical process and that newly produced PrP^{res} can further propagate the protein misfolding (Soto et al., 2002).

*Correspondence: clsoto@utmb.edu

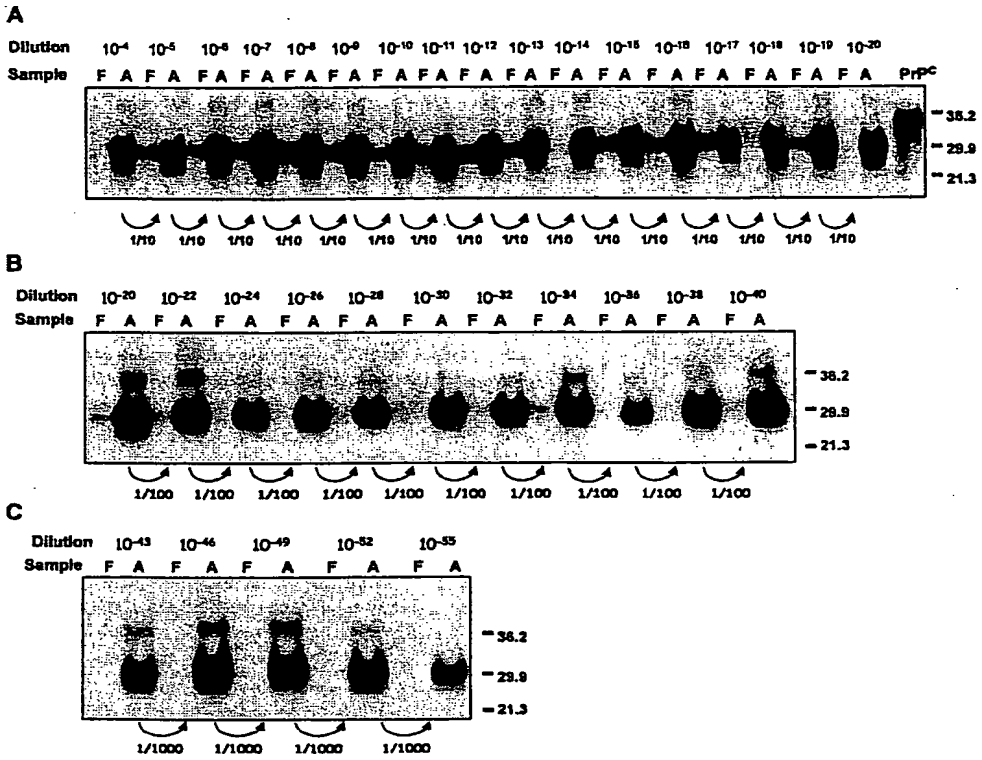

Figure 1. Infinite PrP^{res} Replication In Vitro by Serial PMCA

(A) Hamster scrapie brain homogenate was diluted 10^4-fold into normal brain homogenate and subjected to 20 cycles of PMCA as described in Experimental Procedures. The amplified material was diluted 10-fold into normal brain homogenate and amplified again. This procedure was repeated several times to reach a 10^{-20} dilution of scrapie brain homogenate. Mathematical estimations indicate that the last molecule of PrP^{res} from the inoculum was lost at the 10^{-14} dilution.

(B) PrP^{res} samples from the 10^{-20} dilution were further replicated up to 10^{-40} by serial PMCA after 100-fold dilutions followed by 48 PMCA cycles.

(C) PrP^{res} samples from the 10^{-40} dilution were further replicated to reach a 10^{-55} dilution by performing 48 PMCA cycles and 1000-fold dilutions of the samples. F, frozen samples; A, amplified samples.

The PMCA technology was experimentally designed to mimic some of the fundamental steps involved in PrP^{res} replication in vivo at an accelerated rate (Soto et al., 2002). In a cyclic manner conceptually analogous to PCR cycling, a minute quantity of PrP^{res} is incubated with excess PrP^{C} to enlarge the PrP^{res} aggregates that are then sonicated to generate multiple smaller units for the continued formation of new PrP^{res} (Saborio et al., 2001). A modest level of amplification has also been observed without sonication (Saborio et al., 2001; Lucassen et al., 2003; Deleault et al., 2003), and the extent of conversion depends upon the number of PMCA cycles (Saborio et al., 2001; Bieschke et al., 2004; Piening et al., 2005).

In spite of the compelling evidence supporting the prion hypothesis, there is still considerable skepticism among scientists (Chesebro, 1998; Mestel, 1996; Soto and Castilla, 2004). It is widely accepted that the prion hypothesis can ultimately only be proven once infectivity can be generated in a test tube. If the infectious agent is misfolded PrP^{res} and its replication is promoted by interaction with PrP^{C}, then it should be possible to reproduce the whole process entirely in vitro. Several strategies have been employed to achieve this aim, but all have failed or have produced infectivity after a very long time of incubation and only in transgenic animals highly overexpressing mutated or truncated versions of PrP (May et al., 2004; Soto and Castilla, 2004; Legname et al., 2004).

The aim of this study was to evaluate the biochemical, structural, and infectious properties of in vitro-generated PrP^{res}. For this purpose we have optimized the PMCA procedure to produce high levels of PrP^{res} formation in vitro and developed the conditions to maintain PrP^{res} indefinitely propagating in vitro at the expense of PrP^{C} with the goal of producing misfolded protein free from brain PrP^{res} inoculum. Our results indicate that PrP^{res} generated in vitro under conditions in which no brain-derived PrP^{res} is present in the sample has the same structural and biochemical properties as the disease-associated protein. More importantly, we have shown that the PMCA-generated protein is infectious to wild-type animals, leading to a disease that has clinical, histological, and biochemical properties that

are identical to the illness produced by the prion infectious agent. These findings represent the first time that wild-type animals have been infected with PrP^{res} generated in vitro and thus constitute some of the strongest evidence yet available supporting the prion hypothesis.

Results

Infinite Replication of PrP^{res} In Vitro

Hamster brains infected with 263K scrapie were homogenized and diluted 10^4-fold into a 10% normal hamster brain homogenate. Samples were either immediately frozen or subjected to 20 PMCA cycles. After this first round of PMCA, a small aliquot of the amplified samples was taken and diluted 10-fold into more normal brain homogenate. These samples were again immediately frozen or amplified by 20 PMCA cycles. This procedure was repeated several times, and PrP^{res} generation was determined by Western blot after proteinase K (PK) digestion to remove the remaining PrP^{C}. Figure 1A shows the results of an experiment in which 17 rounds of PMCA were performed. In the final series of PMCA, the amount of scrapie brain homogenate is equivalent to a 10^{20}-fold dilution. Estimation of the amount of PrP^{res} inoculum present indicates that after this dilution no molecules of brain-derived protein were present, whereas the amount of newly generated PrP^{res} corresponds to approximately 1×10^{11} molecules. The amplified samples for the 10^{-20} dilution were further diluted and subjected to several rounds of PMCA separated by 100-fold dilutions to reach a final dilution of scrapie brain homogenate equivalent to 10^{-40} (Figure 1B). The serial replication of PrP^{res} was additionally continued up to a 10^{-55} dilution by performing a series of 1000-fold dilutions followed by 48 cycles of PMCA (Figure 1C). We conclude from these results that PMCA enables an infinite replication of PrP^{res} in vitro. Interestingly, the signal can be fully recovered even after 1000-fold dilution of the sample, suggesting that the amplification rate is at least 1000. Moreover, the rate of PrP replication was not altered upon dilution, which suggests that newly converted protein is capable of inducing PrP^{res} formation with an efficiency similar to that of brain-derived PrP^{res}. A control experiment in which the healthy brain homogenate was serially diluted into itself and subjected to the same number of PMCA cycles as described above but in the absence of PrP^{res} inoculum did not show any protease-resistant PrP under any conditions (data not shown).

Biochemical and Structural Properties of In Vitro-Generated PrP^{res}

An in vitro-generated PrP^{res} sample that does not contain any brain-derived PrP^{res} provides an ideal material for analyzing the biochemical and structural properties of the in vitro-produced protein and comparing them with the properties of in vivo-generated PrP^{res}. A first comparison using Western blot profiles indicates that in vitro replication leads to a protein with identical electrophoretic mobility and glycosylation pattern to the disease-associated misfolded protein (Figure 2A). Indeed, experiments using PrP^{res} inoculum from different species/strains with distinct Western blot profiles showed that newly generated PrP^{res} always follows the pattern of the misfolded protein used as template (Soto et al., 2005). Furthermore, amino acid composition analysis of highly purified PrP^{res} produced in vitro shows very similar results to those found using brain-derived PrP^{res} (data not shown), indicating that the cleavage site after PK digestion is the same in both proteins. This is important because PrP^{res} from different strains has been shown to have a distinct PK cleavage site due to the different folding or aggregation of the protein (Chen et al., 2000; Collinge et al., 1996). The similar glycosylation pattern of newly generated and brain-derived PrP^{res} was further confirmed in experiments in which the proteins were treated with endoglycosidase (Figure 2A). The results demonstrate that the enzymatic removal of glycosylated chains occurs with similar efficiency in both proteins and that the unglycosylated bands have the same molecular weight.

A typical feature of misfolded PrP that has been extensively used to distinguish it from the normal protein isoform is the high resistance of the pathological protein to protease degradation. To compare the protease-resistance profile, similar quantities of PMCA-generated PrP^{res} (produced after a 10^{-20} dilution of scrapie brain homogenate) and brain-derived PrP^{res} were treated for 60 min with 50, 100, 150, 200, 250, 1,000, 2,500, 5,000 and 10,000 μg/ml of PK (Figure 2B). Both proteins were highly resistant to these large PK concentrations, and, strikingly, the pattern of resistance was virtually identical. This result is very significant because protease resistance is one of the hallmark properties of disease-associated PrP, and its quantity correlates tightly with infectivity (McKinley et al., 1983). Several procedures have been reported to produce protease-resistant forms of PrP, but in most of these cases the protease resistance was only detected at low concentrations of the enzyme and was thus not comparable to the extent of protease resistance seen in bona fide PrP^{res} (Jackson et al., 1999; Lehmann and Harris, 1996; Lee and Eisenberg, 2003).

Another typical property of misfolded PrP is its high insolubility in nonionic detergents. More than 95% of PrP^{res} derived both from brain and from PMCA was detected in the pellet after incubation and centrifugation in the presence of 10% sarkosyl, indicating that the two proteins are highly and similarly insoluble (Figure 3A). Insolubility of PrP^{res} was lost when the proteins were treated with >2 M guanidine hydrochloride, indicating that PrP^{res} from both origins was equally sensitive to denaturation by a chaotropic agent (Figure 3B).

The main difference between PrP^{C} and PrP^{res}, which is responsible for the other biochemical distinctions, is the secondary structure of the two proteins: whereas PrP^{C} is mainly α-helical, PrP^{res} is rich in β sheet conformation (Pan et al., 1993; Cohen and Prusiner, 1998). To study the secondary structure, PrP^{res} was highly purified from the brain of scrapie-sick hamsters or from samples amplified after a 10^{-20} dilution, as described in Figure 1. The standard purification procedure based on differential precipitation in detergents and protease degradation was used, and purity was estimated to be

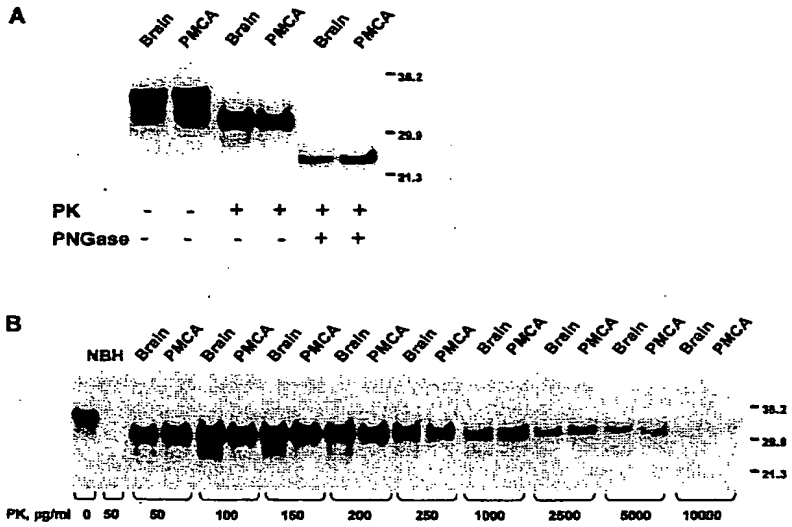

Figure 2. Electrophoretic Pattern, Deglycosylation, and Protease-Resistance Properties of In Vitro-Generated PrP^{res}

(A) Aliquots containing similar quantities of brain-derived PrP^{res} and the misfolded protein obtained by PMCA after a 10^{-20} dilution of scrapie brain homogenate (as shown in Figure 1A) were subjected to proteinase K (PK) digestion (50 μg/ml for 60 min) and loaded onto SDS-PAGE. Immunoreactive bands were observed using Western blot and a 3F4 monoclonal antibody. Similar aliquots of both proteins were subjected to deglycosylation by treatment with peptide N-glycosidase F for 2 hr at 37°C. Western blot analyses of different dilutions before and after deglycosylation were performed.

(B) Aliquots of PrP^{res} generated in vitro after a 10^{-20} dilution of brain PrP^{res} or misfolded protein obtained from scrapie brain homogenate were incubated for 60 min at 45°C, with the indicated concentrations of PK and PrP^{res} signal being detected by Western blot analysis as described in Experimental Procedures.

>90% by silver staining after electrophoresis and by amino acid composition analysis. Structural studies conducted using Fourier transform infrared (FTIR) spectroscopy of in vitro-generated PrP^{res} showed a spectrum consisting of high levels of β sheet content that was very similar to the spectrum obtained for purified brain-derived PrP^{res} (Figure 4). Deconvolution and fitting analysis of the spectra showed a virtually identical profile of secondary structures for both proteins (Figure 4), which are consistent with those previously reported for hamster PrP^{res} (Caughey et al., 1998; Pan et al., 1993). Importantly, the spectra show a still relatively high content of α-helical structure, as expected for disease-associated misfolded prion protein (May et al., 2004). The lack of α-helical structure is considered a drawback for most of the in vitro PrP refolding assays in which the PrP^{res}-like form is almost entirely organized in an aggregated β sheet structure (May et al., 2004). The high levels of β sheet structure, as well as the presence of random coil and α helix for PMCA-generated PrP^{res}, were also confirmed by circular dichroism studies. FTIR spectra of recombinant full-length hamster PrP^{C} produced in bacteria showed the expected high proportion of α helix and random coil and <10% of β sheet structure (data not shown).

The high content of β sheet structure of PrP^{res} results in a high tendency to form larger-order aggregates in vitro and in vivo (Prusiner et al., 1983; Ghetti et al., 1996). To study the ultrastructural characteristics of the aggregates, samples from highly purified brain-derived and PMCA-generated PrP^{res} were analyzed by electron microscopy after negative staining. Both proteins make

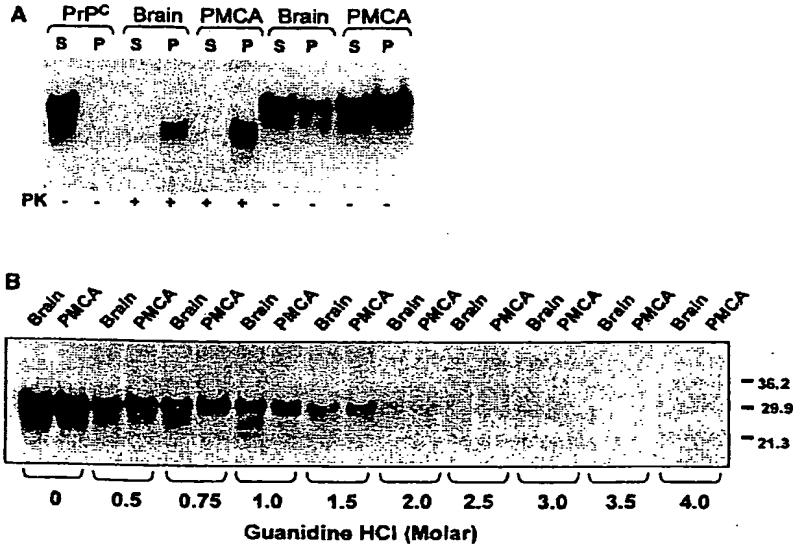

Figure 3. Detergent Solubility Studies

(A) Samples containing PMCA-generated or brain-derived PrP^{res} in 10% sarkosyl (final concentration) were centrifuged at 100,000 × g for 1 hr at 4°C, and the pellet (P) and supernatant (S) were treated with PK. PrP signal was detected using Western blotting. The distribution of PrP^{C} not treated with PK is shown as a control.

(B) Samples of PrP^{res} produced in vitro and in vivo were treated with the indicated concentrations of guanidine hydrochloride for 2 hr and thereafter centrifuged as described earlier. PrP^{res} in the pellet was detected by Western blot after PK digestion.

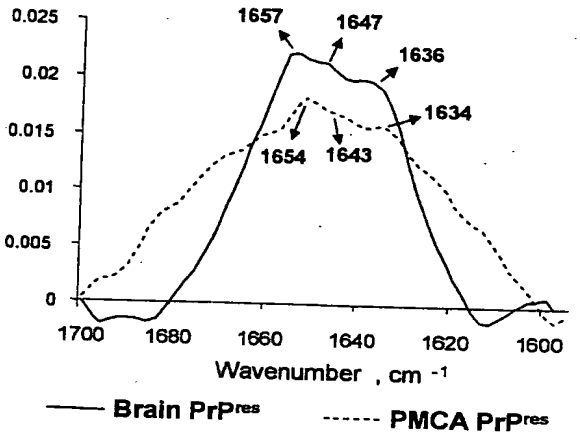

Secondary structure	Brain PrP^{res}	PMCA PrP^{res}
α-helix (1652-1657 cm^{-1})	36	36
β-sheet (1632-1636 cm^{-1})	31	32
Unordered (1642-1648 cm^{-1})	33	32

Figure 4. Secondary Structure of PMCA-Generated and Brain-Derived PrP^{res}

Samples of highly purified PrP27–30 (5 mg/ml in phosphate-buffered saline) obtained from PrP^{res} generated in vitro after a 10^{-20} dilution of brain PrP^{res} or from 263K scrapie hamster brain were loaded into Fourier transform infrared spectroscopy cuvettes and dried by passing a flow of nitrogen. Fourier self-deconvolution and curve fitting of the amide I region of the spectra was done using the Grams software. The table shows the estimation of the percentage of different secondary-structure motifs.

typical prion rod-like structures that are 10 to 20 nm in diameter and 50 to 100 nm in length (Figure S1), as previously described (Prusiner et al., 1983; Wille et al., 2000).

A hallmark property of prions is their capability to sustain autocatalytic replication in vivo (Prusiner, 1998). Injection of brain extracts containing PrP^{res} into an animal can further direct the conversion of normal PrP^{C}, and the misfolded protein can in this way keep replicating across animals and generations (Prusiner, 1998). The results shown in Figure 1 suggest that newly formed PrP^{res} is able to maintain replication in vitro even in the absence of brain-derived PrP^{res}. However, in order to analyze whether the efficiency of conversion is the same, we compared the rate of PrP^{C} conversion induced by brain-derived and PMCA-produced PrP^{res}. For these experiments, aliquots of both samples containing a similar amount of PrP^{res} equivalent to a 100-fold dilution of scrapie brain homogenate were further diluted into normal brain homogenate and subjected to 20 amplification cycles. As shown in Figure 5A, both samples were able to convert high levels of PrP^{C} to produce a similar amount of PrP^{res}. The efficient conversion was lost under these conditions when the samples were diluted more than 160-fold (16,000-fold in total). This result indicates that an approximately 300-fold amplification rate was obtained for both brain and PMCA PrP^{res} using 20 amplification cycles (Figure 5A). As described before, the rate of amplification depends upon the number of cycles performed (for example, a >6500-fold amplification was obtained when samples were subjected to 140 cycles), but, again, this rate was similar regardless of whether PrP^{res} came from in vivo brain samples or from in vitro-produced protein (data not shown).

Finally, we studied whether the converting activity of in vitro-generated PrP^{res} is as resistant to denaturation as has been reported for brain PrP^{res}. Samples of brain-derived and in vitro-generated PrP^{res} were subjected to thermal denaturation by incubation at 100°C, 110°C, 120°C, and 140°C for 1 hr. Thereafter, these samples were used to trigger PrP^{res} formation by diluting them into normal brain homogenate and performing 20 PMCA cycles. Generation of new PrP^{res} was not altered by previously heating the samples at 100°C or 110°C, but this activity was dramatically reduced by incubating PrP^{res} at 120°C and completely abolished after heating at 140°C (Figure 5B). Interestingly, the heat-resistance profile of both brain-derived and PMCA-produced PrP^{res} was very similar, further supporting the hypothesis that the two forms resemble each other.

PrP^{res} Generated In Vitro Is Infectious

One objective that has long been pursued is the in vitro production of prion infectious material by inducing the misfolding of PrP. Successful completion of this experiment is widely regarded as the final proof for the controversial protein-only hypothesis of prion propagation (Soto and Castilla, 2004). The serial replication of PrP^{res} in vitro by PMCA provides a perfect system to achieve this aim because, after many rounds of amplification following serial dilution of PrP^{res} inoculum, we were able to produce a preparation of misfolded protein that was biochemically and structurally identical to brain-derived PrP^{res} but lacked any molecules of the initial scrapie-infected inoculum. To determine the infectious capability of in vitro-generated PrP^{res}, groups of wild-type Syrian hamsters were inoculated intracerebrally (i.c.) with samples generated by 6 or 16 rounds of serial PMCA separated by 10-fold dilutions as described in Figure 1 (see Figure S2 for a schematic description of the groups used in this study). Since at the first PMCA the dilution of scrapie brain homogenate was 10^{-4}, the final dilution of scrapie material in these groups corresponds to 10^{-9} and 10^{-19}, respectively. An additional 10-fold dilution in phosphate-buffered saline was performed in all samples before inoculation. As shown in Figure 1, despite the large dilution, the quantity of PrP^{res} remained constant after amplification. Detailed estimation by quantitative Western blot analysis indicated that the amount of PrP^{res} in these samples was similar to the quantity of PK-resistant protein present in a 10^{-4} dilution of 263K hamster brain, which contains approximately 10^{10} molecules of the misfolded protein.

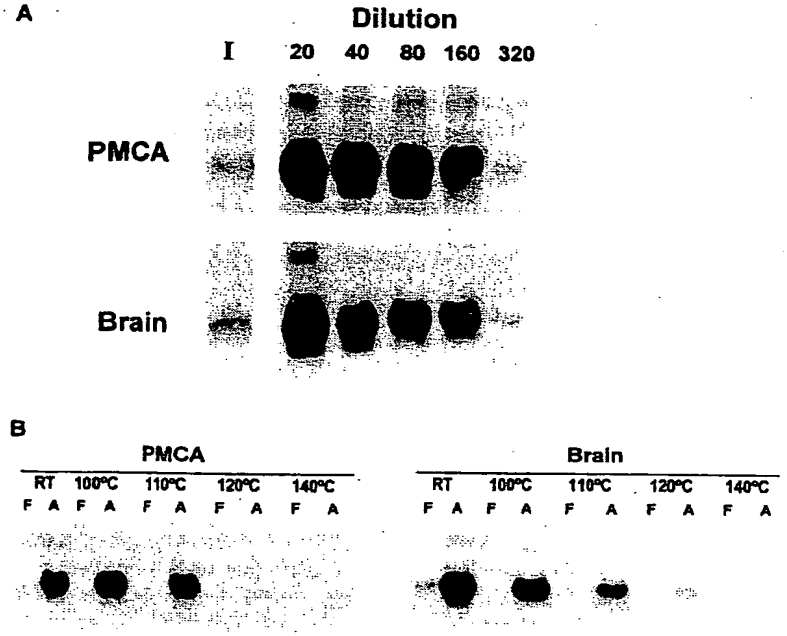

Figure 5. Self-Propagation and Heat Inactivation of PrP^{res}

(A) The efficiency with which PMCA-generated PrP^{res} induced the conversion of PrP^{C} in vitro was compared to the rate of conversion induced by brain-derived PrP^{res}. For this purpose, small and equivalent aliquots of both proteins (lane 1, I) were diluted 20-, 40-, 80-, 160-, and 320-fold into normal brain homogenate and subjected to 20 cycles of PMCA. The formation of newly generated PrP^{res} was determined using Western blot analysis.

(B) The resistance of PrP^{res} from both origins to heat inactivation was determined by incubating equivalent aliquots of the proteins at the indicated temperatures for 20 min. Thereafter, the samples were diluted 100-fold into normal brain homogenate and tested for their ability to induce the conversion of normal PrP^{C} into the protease-resistant isoform using 20 cycles of PMCA. F: frozen samples; A: amplified samples.

In the animals infected with the 10^{-10} dilution (group 6 in Table 1), 99.99999% of this material corresponded to newly generated PrP^{res} (0.99999×10^{10} molecules) and only 0.000001% to brain-derived PrP^{res} (1×10^{4} molecules). In the 10^{-20} dilution (group 7), 100% of PrP^{res} was newly generated protein (1×10^{10} molecules). Strikingly, all of the animals in these two sets (groups 6 and 7) showed typical signs of scrapie and died of the disease at around 170 days after inoculation (Table 1).

Based on our experience with the 263K experimental model and the literature reports, the 10^{-8} dilution of scrapie brain homogenate is the last dilution in which infectivity is observed (and only in some animals). Therefore, we hypothesized that dilutions equivalent to 10^{-10} and 10^{-20} would not produce any detectable disease (Table 1). This estimation was confirmed by the results obtained in our control groups (Table 1; groups 1, 2, 3, and 4). Two different negative control groups

Table 1. Infectivity Associated with In Vitro-Generated PrP^{res}

Group	Experimental Condition	Scrapie Brain Dilution	Molecules of PrP^{res} (Brain/PMCA)	Predicted Survival Time (% Sick Animals)	Observed Survival Time (Number of Sick/Total Animals)
1	Negative control: SBH diluted in NBH nonamplified	10^{-10}	$\sim 10^{4}$ (10^{4}/0)	>600 days (0%)	>400 days (0/6)
2	Negative control: SBH diluted in NBH nonamplified	10^{-20}	0 (0/0)	>600 days (0%)	>400 days (0/6)
3	Negative control: SBH diluted in null BH amplified	10^{-10}	$\sim 10^{4}$ (10^{4}/0)	>600 days (0%)	>400 days (0/6)
4	Negative control: SBH diluted in null BH amplified	10^{-20}	0 (0/0)	>600 days (0%)	>400 days (0/6)
5	Positive control: SBH diluted in NBH nonamplified	10^{-4}	$\sim 10^{10}$ (10^{10}/0)	94 ± 2.7 days (100%)	106 ± 2.9 days (6/6)
6	Experiment: SBH diluted in NBH amplified	10^{-10}	$\sim 10^{10}$ (10^{4}/0.99 × 10^{10})	?	177 ± 7.3 days (6/6)
7	Experiment: SBH diluted in NBH amplified	10^{-20}	$\sim 10^{10}$ (0/10^{10})	?	162 ± 3.5 days (6/6)

The number of molecules of PrP^{res} were estimated based on quantitative Western blot, using known concentrations of recombinant hamster PrP as standard. The predicted survival times are based on our previous data as well as published observations. Observed survival time is expressed as average ± standard error.

were used: the first one contained 10^{-10} and 10^{-20} dilutions of the scrapie brain homogenate into normal hamster brain homogenate done in serial 10-fold dilutions in parallel to the samples for PMCA but kept frozen without amplification (groups 1 and 2). The second control consisted of the scrapie brain homogenate diluted serially into PrP-knockout mouse brain homogenate up to 10^{10}- and 10^{20}-fold dilutions and subjected to the PMCA cycling (groups 3 and 4) in the same way as the study samples. None of the animals in these four groups of negative control samples had shown any signs of disease up to 400 days after infection (Table 1). This result clearly indicates that infectivity seen in the PMCA-amplified samples is associated with newly in vitro-generated PrP^{res}.

To compare the infectious capacity of PMCA-produced PrP^{res} with brain-derived infectivity, a group of animals were inoculated with a sample containing a similar amount of PrP^{res} as the ones produced after 6 and 16 serial PMCA rounds. As mentioned above, careful estimation using Western blot analysis showed that the quantity of PrP^{res} after the serial PMCA assays was equivalent to a 10^{-3} dilution of scrapie brain homogenate (10^{-4} considering the further 10-fold dilution prior to inoculation). A positive control group of animals (group 5) injected with this dilution of scrapie brain developed the disease with a mean survival time of 106 days (Table 1). The material for this experiment and the dilution used correspond exactly to the sample utilized to begin PMCA amplification, so it serves as the double control of the infectivity present in the sample prior to any dilution and amplification as well as the infectivity associated with this amount of PrP^{res}. The survival time was shorter than the one obtained with the equivalent quantity of PMCA-generated PrP^{res}, indicating that the in vitro-generated misfolded protein was significantly less infectious. We are currently doing infectivity titration studies to find out exactly how much lower the infectivity in the samples is, but based on the survival time, in vitro-generated PrP^{res} seems to be between 10 and 100 times less infectious than the same quantity of brain-derived PrP^{res}.

The clinical signs observed in the disease produced by the amplified samples were identical to those of the animals inoculated with infectious brain material and included hyperactivity, motor impairment, head wobbling, muscle weakness, and weight loss. In order to evaluate whether the biochemical and neuropathological characteristics of the disease were also the same, we performed a detailed comparative study of the brains of animals affected by the disease induced by brain-derived PrP^{res} (group 5) and PMCA-generated PrP^{res} (groups 6 and 7). Brain samples from all the animals in these three groups contained a large and similar quantity of PrP^{res}, which has an identical glycosylation profile (Figure 6A). Conversely, no protease-resistant protein was detected in the brains of negative control animals. To further evaluate whether or not PMCA-generated infectivity represents a new strain, we compared the electrophoretic mobility after PK treatment and the glycoform pattern of PrP^{res} with those of two other standard scrapie strains in hamsters, namely, 263K and drowsy. As shown in Figure 6B, whereas the Western blot pattern of the PMCA-generated PrP^{res} is identical to that of 263K (the strain used to produce new PrP^{res} by PMCA), it is substantially different from that of drowsy, a strain known to differ biochemically from 263K.

Histological analysis showed typical spongiform degeneration of the brain (Figure 6C), and samples from animals infected with in vitro-produced PrP^{res} showed a pattern and extent of vacuolation that was indistinguishable from those coming from the brains of hamsters inoculated with infectious brain material (Figure S3). The same similarities were also seen when tissue samples were stained for PrP accumulation (Figure 6D) and astrogliosis (Figure 6E). Thus, based on all of the biochemical, histological, and clinical analyses of the animals, we concluded that in vitro-generated PrP^{res} triggers a similar neurological disorder as brain-derived PrP^{res}.

To evaluate whether infectious properties of in vitro-generated PrP^{res} were stable over time, serial transmission experiments were done. Brain from one of the animals inoculated with 10^{-20} dilution of scrapie brain homogenate subjected to 16 rounds of PMCA (group 7 in Table 1) was homogenized and injected intraperitoneally (i.p.) into a group of six wild-type hamsters. All animals inoculated with this material exhibited typical signs of the disease with a mean survival time of 136.5 days (Table 2). Hamsters inoculated i.p. with the same dilution of brain homogenate from an animal originally infected with brain-derived PrP^{res} (group 5 in Table 1) developed the disease at 100.2 days postinoculation (Table 2). No clinical signs were observed in negative control animals inoculated with normal brain homogenate. All animals in groups 2 and 3 of the experiment in Table 2 showed protease-resistant PrP in the brain after postmortem analysis (data not shown). These results indicate that the infectious agent generated in vitro is stable over time.

Discussion

Compelling evidence has accumulated over the last several years in support of the protein-only hypothesis of prion propagation (Soto and Castilla, 2004; Prusiner, 1998). However, the prion concept is still highly controversial, and it is widely accepted that the final proof for this hypothesis consists of the generation of infectious material in vitro by inducing the misfolding of the prion protein (Soto and Castilla, 2004). Although extensively attempted, the generation of infectious mammalian prions in vitro has been elusive. Paradoxically, de novo generation of infectious proteins has been successfully done in a simpler system in yeast. A yeast prion has been defined as an infectious protein that behaves as a non-Mendelian genetic element, which transmits biological information in the absence of nucleic acid. Diverse genetic, biochemical, and structural evidence has been provided in support of the prion nature of the yeast determinants Sup35p and Ure2p (for references, see Uptain and Lindquist, 2002). Recent studies showed that bacterially produced N-terminal fragments of Sup35p, when transformed into amyloid fibrils, were able to propagate the prion phenotype to yeast cells (King and Diaz-Avalos, 2004; Tanaka et al., 2004). Infec-

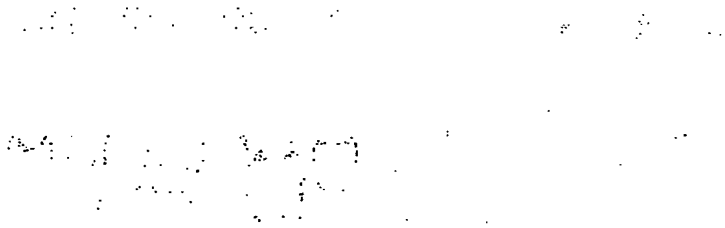

Figure 6. Biochemical and Histopathological Features of the Disease Induced by Inoculation with PMCA-Generated PrP^{res}

(A) The presence and quantity of PrP^{res} in the brains of animals in the terminal stage of the disease produced by inoculation with brain infectious material (group 5) or with the 10^{10}- and 10^{20}-fold diluted and amplified material (groups 6 and 7, respectively) were analyzed using Western blotting.

(B) The electrophoretic mobility and glycoform pattern of PrP^{res} obtained in the animals inoculated with PMCA-generated PrP^{res} were compared with the profile of 263K and drowsy (DY) strains of prions.

(C) Spongiform degeneration was evaluated after hematoxylin and eosin staining of medulla sections from symptomatic animals inoculated with either brain-derived or in vitro-produced PrP^{res}.

(D) PrP accumulation in these animals was evaluated by staining the tissue with the 3F4 anti-PrP monoclonal antibody as described in Experimental Procedures.

(E) Reactive astrogliosis in animals from both groups was evaluated by histological staining with glial fibrillary acidic protein antibodies.

For the results shown in this figure, all animals in groups 5–7 (Table 1) were analyzed, and the figure corresponds to a representative picture of these animals. As a control, brain samples from one animal in group 1 sacrificed without signs of the disease at 280 days after inoculation were used.

tion of yeast with different conformers led to generation of distinct [PSI+] strains in vivo, indicating that differences in the conformation of the infectious protein determine prion strain variation.

Different strategies have been used to attempt the in vitro generation of mammalian prion infectious material (Soto and Castilla, 2004; May et al., 2004). An approach that has been explored for the purpose of generating de novo infectivity involved the production of PrP containing mutations associated with inherited TSEs. Several mutant PrP^{res}-like molecules have been generated, some of which have been shown to acquire various biochemical properties of PrP^{res}, but so far, none of them have been shown to be infectious (Lehmann and Harris, 1996; Chiesa et al., 1998). Another strategy consisted of inducing the misfolding of recombinant protein or short PrP synthetic peptides into β sheet-rich structures exhibiting some of the biochemical and biological properties of PrP^{res} (Jackson et al., 1999; Baskakov et al., 2000; Zhang et al., 1995; Lee and Eisenberg, 2003). The hope in these experiments was that infectivity might be generated even if a very small percentage of the protein altered in vitro adopted the "infectious folding." Unfortunately, these experiments have largely failed. Very recently, however, a recombinant mouse PrP fragment (residues 89–230) assembled into amyloid fibrils was found to induce a TSE-like disease with PrP^{res} formation when injected in transgenic mice overexpressing the same PrP sequence (Legname et al., 2004). The disease was later transmitted to wild-type animals in a second passage. These findings have come close to being the long-awaited definitive proof

Table 2. Secondary Transmission of In Vitro-Generated PrP^{res}

Group	Experimental Condition	Scrapie Brain Dilution	Survival Time (Number of Sick/Total Animals)
1	Negative control NBH	2×10^{-2}	>200 days (0/6)
2	Positive control[a]: animals infected with brain PrP^{res}	2×10^{-2}	100.2 ± 7.7 days (6/6)
3	Experiment[b]: animals infected with PMCA PrP^{res}	2×10^{-2}	136.5 ± 12.9 days (6/6)

The quantity of PrP^{res} inoculated in animals in groups 2 and 3 was similar as evaluated by Western blot. Survival time is expressed as average ± standard error.

[a] Animals were inoculated i.p. with 200 μl of a 1:50 dilution of brain homogenate from one animal in group 5 in Table 1.

[b] Animals were inoculated i.p. with 200 μl of a 1:50 dilution of brain homogenate from one animal in group 7 in Table 1.

of the prion hypothesis, but some experimental caveats remain to be addressed. The fact that the disease was originally transmitted to transgenic animals largely overexpressing the PrP gene and not to wild-type animals is a matter of concern because it is well known that this type of animals develops a prion-like disease spontaneously (Westaway et al., 1994; Castilla et al., 2004a; Chiesa et al., 1998). In other words, the effect seen might just be an acceleration of the disease process that was set to occur spontaneously at a later time. In this sense, an important missing control was the inoculation of animals in a second passage with brain homogenate of transgenic mice not injected with synthetic prions. Finally, the clinical and histopathological presentation of the disease was different from the usual disease in mice. The authors argued that this result may be due to the creation of a new strain of prions.

A strategy that is regarded as more promising is the generation of infectivity by in vitro conversion of PrP^{C} because in these experiments the transformation process is triggered, catalyzed, and templated by brain-derived PrP^{res}. The cell-free conversion system developed by Caughey and coworkers (Kocisko et al., 1994) uses purified PrP^{C} mixed with stoichiometric amounts of purified PrP^{res}. The low yield of PrP^{res} formation resulting from this system and the nonphysiological conditions used had made it difficult to evaluate the biological and structural properties of the newly converted protein. However, Collinge and coworkers took advantage of the species-barrier phenomenon to test infectivity of newly generated PrP^{res} under conditions in which the PrP^{res} from the inoculum would not be infectious (Hill et al., 1999). The results of these experiments argued that cell-free-generated PrP^{res} was not infectious. A recent study attempting to analyze infectivity of PMCA-generated PrP^{res} produced inconclusive results (Bieschke et al., 2004). The most likely reason for this was that the level of PrP^{res} produced in vitro was still not high enough to have a clear separation from the infectivity of the material used to generate the misfolded protein. In addition, an important control experiment analyzing the parallel effect of the sonication procedure on brain-derived infectivity was missing. We have obtained similar results in other infectivity studies in which animals inoculated with PrP^{res} obtained after a low level (10- to 50-fold) of amplification led to inconclusive results regarding the infectivity of newly generated protein (data not shown). However, in experiments in which a higher level of amplification (>200-fold) was obtained in a single round of PMCA, a significant increase in infectivity was observed (data not shown).

In this study we have further optimized the PMCA procedure to reach very high levels of PrP^{res} conversion. Furthermore, we have been able to serially amplify PrP^{res} in vitro indefinitely. As a result of many rounds of PMCA following serial dilution of brain infectious material, we have been able to generate large quantities of newly synthesized PrP^{res} in the absence of any molecules of the brain-derived misfolded protein. This in vitro-generated PrP^{res} isoform has identical biochemical and structural properties to the protein used to begin the conversion, and, more importantly, the in vitro-generated PrP^{res} is clearly associated with infectivity. Our results represent the first time in which prion infectious material has been generated in vitro to produce an in vivo disease in wild-type animals with characteristics identical to the disease produced by brain-isolated prions. These results provide some of the strongest evidence in support of the prion hypothesis. The fact that a given quantity of in vitro-generated PrP^{res} is associated with a lower degree of infectivity as compared with brain-derived infectious material may explain the inconclusive results from Bieschke and coworkers (Bieschke et al., 2004) and our own previous data using a low level of amplified material for inoculation. The reason for the lower level of infectivity in PMCA-produced PrP^{res} is unknown and currently under investigation, but we can envision at least three possibilities. First, although the samples contained the same amount of PrP^{res} as analyzed by Western blot after SDS-PAGE, the protein molecules might have been organized into a different number of infectious units. For example, a large production of PrP^{res} in vitro may have led to the formation of big aggregates that might be less efficient for propagating infectivity in vivo, or sonication may have produced too small aggregates that were not very efficient in maintaining infectivity. Second, it is possible that in vitro-generated and in vivo-derived infectious agents may contain different proportions of resistant and sensitive forms of PrP. In our biochemical quantitation we only take PrP^{res} into account. Third, we may have generated a different prion strain after repeated in vitro amplification reactions. Although the biochemical, histological, and clinical characteristics of the disease produced by in vitro-generated PrP^{res} were identical to the disease originating from brain-derived infectious material, the extended incubation periods, both in the first and second passages, support a possible new strain. Additional experiments of serial transmission and titration are needed to reach definitive conclusions.

A central facet of the prion hypothesis is that prion replication is a cyclical process and that newly produced PrP^{res} can further propagate protein misfolding; in this way, prions can continue replicating across animals and generations. Our results show that this process of autocatalytic generation of PrP^{res} can be mimicked in vitro by PMCA, indicating that prions can be "cultured" in vitro indefinitely, thus enabling the detailed study of their properties. In vitro-produced PrP^{res} exhibited properties strikingly similar to those of the protein isolated from scrapie-affected animals, including secondary structure, Western blot profile, protease resistance, detergent insolubility, resistance to denaturation by heat and chaotropic agents, aggregation into rod-like structures, efficiency in inducing the misfolding of the normal PrP^{C}, and in vivo infectivity. These findings indicate that PMCA is a valuable tool for studying the molecular basis of prion conversion and the factors involved in this process as well as for identifying novel compounds that inhibit this pathological event. PMCA might also be useful for studying the mechanism of the species barrier and assessing whether the nature of the prion strains is indeed encoded on the structure of the misfolded protein. Finally, the high levels of amplification resulting from our improved and automated PMCA procedure may have important applications for TSE di-

agnosis by allowing the highly sensitive detection of PrP^{res}.

Experimental Procedures

Preparation of Tissue Homogenates

Healthy and sick animals were perfused with phosphate-buffered saline (PBS) plus 5 mM EDTA previous to harvesting the tissue. Ten percent brain homogenates (w/v) were prepared in conversion buffer (PBS containing 150 mM NaCl, 1.0% Triton X-100, 4 mM EDTA, and the complete™ cocktail of protease inhibitors [Boehringer Mannheim, Mannheim, Germany]). The samples were clarified by a brief low-speed centrifugation (1500 rpm for 30 s) using an Eppendorf (Hamburg, Germany) centrifuge, model 5414.

PrP^{res} Purification

One gram of brain tissue was homogenized in 5 ml of cold PBS containing protease inhibitors. For PMCA-generated PrP^{res}, the total sample was processed after the last amplification in the same way as brain homogenate. The samples were mixed with 1 volume of 20% sarkosyl, and the mixture was homogenized and sonicated until a clear preparation was obtained. Samples were centrifuged at 5000 rpm for 15 min at 4°C. The pellet was discarded, the supernatant was mixed with 1/3 volume of PBS containing 0.1% SB-314, and samples were centrifuged in a Biosafe Optima MAX ultracentrifuge (Beckman Coulter, Fullerton, California) at 100,000 × g for 3 hr at 4°C. The supernatant was discarded and the pellet was resuspended in 600 μl of PBS containing 0.1% SB-314 and 10% NaCl and sonicated. The resuspended pellet was layered over 600 μl of PBS containing 20% saccharose, 10% NaCl, and 0.1% SB-314 and centrifuged for 3 hr at 4°C. The supernatant was discarded and the pellet was resuspended in 300 μl of PBS containing 0.1% SB-314 and sonicated again. After sonication the samples were incubated with PK (100 μg/ml) for 2 hr at 37°C and shaken. The digested sample was layered over 100 μl of PBS containing 20% sarkosyl, 0.1% SB-314, and 10% NaCl and centrifuged for 1 hr 30 min at 100,000 × g. The final pellet was resuspended in 100 μl of PBS and sonicated. The sample was stored at −80°C. Purity was analyzed by silver staining and amino acid composition analysis.

PMCA Procedure

Although the principle of PMCA remains the same as in our original publication (Saborio et al., 2001), the system has been optimized and automated, thus enabling the routine processing of many more samples at the same time and reaching a higher conversion efficiency. The detailed protocol, including troubleshooting, has been recently published elsewhere (Castilla et al., 2004b; Saá et al., 2004). Aliquots of normal and scrapie brain homogenate prepared in conversion buffer were mixed and loaded onto 0.2 ml PCR tubes. Tubes were positioned on an adaptor placed on the plate holder of a microsonicator (Misonix Model 3000, Farmingdale, New York) and programmed to perform cycles of 30 min incubation at 37°C followed by a 40 s pulse of sonication set at 60% potency. Samples were incubated, without shaking, immersed in the water of the sonicator bath.

Protease-Resistance Assay

The profile of PK sensitivity for in vitro- and in vivo-generated PrP^{res} was studied by subjecting samples to incubation for 60 min at 45°C with different concentrations of PK ranging from 0 to 10,000 μg/ml. The digestion was stopped by adding electrophoresis sample buffer. For all other experiments involving PK digestion, the standard conditions used consisted of incubating the samples with 50 μg/ml of the enzyme for 60 min at 45°C.

PrP^{res} Quantification

PrP^{res} concentration was estimated by Western blotting followed by densitometric analysis, using known concentrations of hamster recombinant PrP^{C} (Prionics Inc, Zurich, Switzerland). To obtain a reliable and robust quantification, we ran several different dilutions of the sample in the same gel as the standard, thus avoiding artifacts due to saturation of the signal or to too weak a signal. In some selected samples, quantification was confirmed by single ELISA technique after PK digestion, using plates coated with 3F4 antibody.

Detergent Solubility Assay

Samples containing brain homogenate and in vitro- or in vivo-generated PrP^{res} were incubated in the presence of 10% sarkosyl for 30 min at 4°C. Thereafter, samples were centrifuged at 100,000 × g for 1 hr in a Biosafe Optima MAX ultracentrifuge (Beckman Coulter), and the pellet of the centrifugation was then resuspended in conversion buffer plus electrophoresis sample buffer. Equivalent aliquots of supernatant and pellet were analyzed using immunoblotting. In some experiments, prior to the addition of sarkosyl, samples were incubated with different concentrations of guanidine hydrochloride for 2 hr at room temperature and shaken. Thereafter, sarkosyl was added and the soluble and insoluble proteins were separated using centrifugation.

PrP^{res} Detection

Proteins were fractionated by sodium dodecyl sulfate-polyacrylamide gel electrophoresis (SDS-PAGE) under reducing conditions, electroblotted into nitrocellulose membrane, and probed with 3F4 antibody (Kascsak et al., 1987) (dilution 1:5000). The immunoreactive bands were visualized by enhanced chemiluminescence assay (Amersham, Piscataway, New Jersey).

Protein Deglycosylation Assay

PrP^{res} samples were first digested with PK as described above. After addition of 10% sarkosyl (final concentration), samples were centrifuged at 100,000 × g for 1 hr at 4°C, the supernatant was discarded, and the pellet was resuspended in 100 μl of glycoprotein denaturing buffer (New England Biolabs, Beverly, Massachusetts) and incubated for 10 min at 100°C. Thereafter, 26 μl of 50 mM sodium phosphate (pH 7.5) containing 1% nonidet P-40 and 3 μl of peptide N-glycosidase F (New England Biolabs) was added. Samples were incubated for 2 hr at 37°C, the reaction was stopped by adding electrophoresis buffer, and samples were analyzed by Western blot.

Fourier Transform Infrared Spectroscopy

Solutions or suspensions containing highly purified PrP^{res} (5 mg/ml) were prepared in PBS. Two hundred microliters was loaded into an infrared cell, and samples were dried for 30 min under a nitrogen flow. Spectra were recorded with a Bruker (Billerica, Massachusetts) model 66v/S FTIR spectrophotometer at 25°C. For each spectrum, 512 scans were collected with a 2 cm^{-1} resolution and a 1 cm^{-1} interval from 4000–700 cm^{-1}. Smoothing and Fourier self-deconvolution were applied to increase the spectral resolution in the amide I region (1700–1600 cm^{-1}), and iterative fitting to lorentzian line shapes was carried out using the Grams software from Thermo Corporation (San Jose, California) to estimate the proportion of each secondary-structure element.

Electron Microscope

Samples of PrP^{res} either highly purified from the brain or generated by PMCA amplification were resuspended in PBS, placed onto carbon formvar-coated 300-mesh nickel grids, and stained for 60 s with 2% uranyl acetate. Grids were analyzed using a Philips EM 410 (FEI Company, Hillsboro, Oregon) electron microscope at 60 kV.

PrP^{res} Thermal Inactivation

Equivalent samples of brain homogenates containing in vivo-derived and PMCA-generated PrP^{res} were incubated for 20 min at different temperatures (room temperature, 100°C, 110°C, 120°C, and 140°C). Thereafter, aliquots were taken, diluted into normal brain homogenate, and subjected to PMCA amplification. Formation of new PrP^{res} was monitored using Western blot after PK digestion.

In Vivo Infectivity Studies

Syrian golden hamsters were used. Animals were 4 to 6 weeks old at the time of inoculation. Anesthesized animals were injected stereotaxically in the right hippocampus with 1 μl of the sample using a computerized perfusion machine that delivered the sample into

the brain at a rate of 0.1 μl/min. For the second-passage experiments, animals were inoculated i.p. with 100 μl of the material. The onset of clinical disease was measured by scoring the animals twice per week using the following scale: 1, normal animal; 2, mild behavioral abnormalities, including hyperactivity and hypersensitivity to noise; 3, moderate behavioral problems, including tremor of the head, ataxia, wobbling gait, head bobbing, irritability, and aggressiveness; 4, severe behavioral abnormalities, including all of the above plus jerks of the head and body and spontaneous backrolls; 5, terminal stage of the disease, in which the animal lies in the cage and is no longer able to stand up. Animals scoring level 4 for two consecutive weeks were considered sick and were sacrificed to avoid excessive pain using exposure to carbonic dioxide. Brains and other tissues were extracted and analyzed histologically. The right cerebral hemisphere was frozen and stored at −70°C for biochemical examination of PrP^{res} using Western blot analysis; the left hemisphere was fixed in 10% formaldehyde solution, cut into sections, and embedded in paraffin. Serial sections (6 μm thick) from each block were stained with hematoxylin and eosin, using standard protocols or incubated with monoclonal antibodies recognizing PrP or the glial fibrillary acidic protein. Immunoreactions were developed using the peroxidase-antiperoxidase method, following manufacturer specifications. Antibody specificity was verified by absorption.

Supplemental Data

Supplemental Data include three figures and one reference and are available with this article online at http://www.cell.com/cgi/content/full/121/2/195/DC1/.

Acknowledgments

We thank Drs. Javier Navarro and Stan Watowich (University of Texas Medical Branch) for kindly letting us use their Fourier transform infrared spectrometer and circular dichroism, respectively. We are also grateful to Dr. Jesus Requena (University of Santiago de Compostela, Spain) for helpful discussions. C.S. is part of the European Community project TSELAB. This research was supported in part by NIH grants R03 AG0224642 and R01 N549173. Claudio Hetz is a postdoctoral fellow from the Damon Runyon Cancer Research Foundation.

Received: October 12, 2004
Revised: December 20, 2004
Accepted: February 11, 2005
Published: April 21, 2005

References

Baskakov, I.V., Aagaard, C., Mehlhorn, I., Wille, H., Groth, D., Baldwin, M.A., Prusiner, S.B., and Cohen, F.E. (2000). Self-assembly of recombinant prion protein of 106 residues. Biochemistry *39*, 2792–2804.

Basler, K., Oesch, B., Scott, M., Westaway, D., Walchli, M., Groth, D.F., McKinley, M.P., Prusiner, S.B., and Weissmann, C. (1986). Scrapie and cellular PrP isoforms are encoded by the same chromosomal gene. Cell *46*, 417–428.

Bieschke, J., Weber, P., Sarafoff, N., Beekes, M., Giese, A., and Kretzschmar, H. (2004). Autocatalytic self-propagation of misfolded prion protein. Proc. Natl. Acad. Sci. USA *101*, 12207–12211.

Bolton, D.C., McKinley, M.P., and Prusiner, S.B. (1982). Identification of a protein that purifies with the scrapie prion. Science *218*, 1309–1311.

Castilla, J., Gutierrez-Adan, A., Brun, A., Doyle, D., Pintado, B., Ramirez, M.A., Salguero, F.J., Parra, B., Diaz, S.S., Sanchez-Vizcaino, J.M., et al. (2004a). Subclinical bovine spongiform encephalopathy infection in transgenic mice expressing porcine prion protein. J. Neurosci. *24*, 5063–5069.

Castilla, J., Saá, P., and Soto, C. (2004b). Cyclic Amplification of Prion Protein Misfolding. In Techniques in Prion Research, S. Lehmann and J. Grassi, eds. (Basel, Switzerland: Birkhauser Verlag), pp. 198–213.

Caughey, B., Raymond, G.J., and Bessen, R.A. (1998). Strain-dependent differences in beta-sheet conformations of abnormal prion protein. J. Biol. Chem. *273*, 32230–32235.

Chen, S.G., Zou, W., Parchi, P., and Gambetti, P. (2000). PrP(Sc) typing by N-terminal sequencing and mass spectrometry. Arch. Virol. *16* (Suppl.), 209–216.

Chesebro, B. (1998). BSE and prions: uncertainties about the agent. Science *279*, 42–43.

Chiesa, R., Piccardo, P., Ghetti, B., and Harris, D.A. (1998). Neurological illness in transgenic mice expressing a prion protein with an insertional mutation. Neuron *21*, 1339–1351.

Cohen, F.E., and Prusiner, S.B. (1998). Pathologic conformations of prion proteins. Annu. Rev. Biochem. *67*, 793–819.

Collinge, J. (2001). Prion diseases of humans and animals: their causes and molecular basis. Annu. Rev. Neurosci. *24*, 519–550.

Collinge, J., Sidle, K.C., Meads, J., Ironside, J., and Hill, A.F. (1996). Molecular analysis of prion strain variation and the aetiology of 'new variant' CJD. Nature *383*, 685–690.

Deleault, N.R., Lucassen, R.W., and Supattapone, S. (2003). RNA molecules stimulate prion protein conversion. Nature *425*, 717–720.

Gabizon, R., McKinley, M.P., Groth, D., and Prusiner, S.B. (1988). Immunoaffinity purification and neutralization of scrapie prion infectivity. Proc. Natl. Acad. Sci. USA *85*, 6617–6621.

Ghetti, B., Piccardo, P., Frangione, B., Bugiani, O., Giaccone, G., Young, K., Prelli, F., Farlow, M.R., Dlouhy, S.R., and Tagliavini, F. (1996). Prion protein amyloidosis. Brain Pathol. *6*, 127–145.

Hill, A.F., Antoniou, M., and Collinge, J. (1999). Protease-resistant prion protein produced in vitro lacks detectable infectivity. J. Gen. Virol. *80*, 11–14.

Jackson, G.S., Hosszu, L.L., Power, A., Hill, A.F., Kenney, J., Saibil, H., Craven, C.J., Waltho, J.P., Clarke, A.R., and Collinge, J. (1999). Reversible conversion of monomeric human prion protein between native and fibrilogenic conformations. Science *283*, 1935–1937.

Kascsak, R.J., Rubenstein, R., Merz, P.A., Tonna-DeMasi, M., Fersko, R., Carp, R.I., Wisniewski, H.M., and Diringer, H. (1987). Mouse polyclonal and monoclonal antibody to scrapie-associated fibril proteins. J. Virol. *61*, 3688–3693.

King, C.Y., and Diaz-Avalos, R. (2004). Protein-only transmission of three yeast prion strains. Nature *428*, 319–323.

Kocisko, D.A., Come, J.H., Priola, S.A., Chesebro, B., Raymond, G.J., Lansbury, P.T., and Caughey, B. (1994). Cell-free formation of protease-resistant prion protein. Nature *370*, 471–474.

Lee, S., and Eisenberg, D. (2003). Seeded conversion of recombinant prion protein to a disulfide-bonded oligomer by a reduction-oxidation process. Nat. Struct. Biol. *10*, 725–730.

Legname, G., Baskakov, I.V., Nguyen, H.O., Riesner, D., Cohen, F.E., DeArmond, S.J., and Prusiner, S.B. (2004). Synthetic mammalian prions. Science *305*, 673–676.

Lehmann, S., and Harris, D.A. (1996). Two mutant prion proteins expressed in cultured cells acquire biochemical properties reminiscent of the scrapie isoform. Proc. Natl. Acad. Sci. USA *93*, 5610–5614.

Lucassen, R., Nishina, K., and Supattapone, S. (2003). In vitro amplification of protease-resistant prion protein requires free sulfhydryl groups. Biochemistry *42*, 4127–4135.

May, B.C., Govaerts, C., Prusiner, S.B., and Cohen, F.E. (2004). Prions: so many fibers, so little infectivity. Trends Biochem. Sci. *29*, 162–165.

McKinley, M.P., Bolton, D.C., and Prusiner, S.B. (1983). A protease-resistant protein is a structural component of the scrapie prion. Cell *35*, 57–62.

Mestel, R. (1996). Putting prions to the test. Science *273*, 184–189.

Pan, K.M., Baldwin, M., Njuyen, J., Gassett, M., Serban, A., Groth, D., Mehlhorn, I., and Prusiner, S.B. (1993). Conversion of alpha-helices into beta-sheets features in the formation of scrapie prion poteins. Proc. Natl. Acad. Sci. USA *90*, 10962–10966.

Piening, N., Weber, P., Giese, A., and Kretzschmar, H. (2005). Breakage of PrP aggregates is essential for efficient autocatalytic propagation of misfolded prion protein. Biochem. Biophys. Res. Commun. *326*, 339–343.

Prusiner, S.B. (1982). Novel proteinaceous infectious particles cause scrapie. Science *216*, 136–144.

Prusiner, S.B. (1998). Prions. Proc. Natl. Acad. Sci. USA *95*, 13363–13383.

Prusiner, S.B., McKinley, M.P., Bowman, K.A., Bolton, D.C., Bendheim, P.E., Groth, D.F., and Glenner, G.G. (1983). Scrapie prions aggregate to form amyloid-like birefringent rods. Cell *35*, 349–358.

Saá, P., Castilla, J., and Soto, C. (2004). Cyclic amplification of protein misfolding and aggregation. In Amyloid Proteins: Methods and Protocols, E.M. Sigurdsson, ed. (Totowa, NJ: Humana Press), pp. 53–65.

Saborio, G.P., Permanne, B., and Soto, C. (2001). Sensitive detection of pathological prion protein by cyclic amplification of protein misfolding. Nature *411*, 810–813.

Sigurdsson, B. (1954). Maedi, a slow progressing pemumonia of sheep: an epizoological and pathological study. Br. Vet. J. *110*, 255–258.

Soto, C., and Castilla, J. (2004). The controversial protein-only hypothesis of prion propagation. Nat. Med. *10*, S63–S67.

Soto, C., Saborio, G.P., and Anderes, L. (2002). Cyclic amplification of protein misfolding: application to prion-related disorders and beyond. Trends Neurosci. *25*, 390–394.

Soto, C., Anderes, L., Suardi, S., Cardone, F., Castilla, J., Frossard, M.J., Peano, S., Saá, P., Limido, L., Carbonatto, M., et al. (2005). Pre-symptomatic detection of prions by cyclic amplification of protein misfolding. FEBS Lett. *579*, 638–642.

Stahl, N., Baldwin, M.A., Teplow, D.B., Hood, L., Gibson, B.W., Burlingame, A.L., and Prusiner, S.B. (1993). Structural studies of the scrapie prion protein using mass spectrometry and amino acid sequencing. Biochemistry *32*, 1991–2002.

Tanaka, M., Chien, P., Naber, N., Cooke, R., and Weissman, J.S. (2004). Conformational variations in an infectious protein determine prion strain differences. Nature *428*, 323–328.

Uptain, S.M., and Lindquist, S. (2002). Prions as protein-based genetic elements. Annu. Rev. Microbiol. *56*, 703–741.

Westaway, D., DeArmond, S.J., Cayetano-Canlas, J., Groth, D., Foster, D., Yang, S.L., Torchia, M., Carlson, G.A., and Prusiner, S.B. (1994). Degeneration of skeletal muscle, peripheral nerves, and the central nervous system in transgenic mice overexpressing wild-type prion proteins. Cell *76*, 117–129.

Wille, H., Prusiner, S.B., and Cohen, F.E. (2000). Scrapie infectivity is independent of amyloid staining properties of the N-terminally truncated prion protein. J. Struct. Biol. *130*, 323–338.

Zhang, H., Kaneko, K., Nguyen, J.T., Livshits, T.L., Baldwin, M.A., Cohen, F.E., James, T.L., and Prusiner, S.B. (1995). Conformational transitions in peptides containing two putative alpha-helices of the prion protein. J. Mol. Biol. *250*, 514–526.

JAMES 2

TSE

Proc. Natl. Acad. Sci. USA
Vol. 94, pp. 10086–10091, September 1997
Biochemistry

Solution structure of a 142-residue recombinant prion protein corresponding to the infectious fragment of the scrapie isoform

(NMR structure/conformational change)

THOMAS L. JAMES*†‡, HE LIU*, NIKOLAI B. ULYANOV*, SHAUNA FARR-JONES*, HONG ZHANG*, DAVID G. DONNE§, KIYOTOSHI KANEKO¶, DARLENE GROTH¶, INGRID MEHLHORN¶, STANLEY B. PRUSINER¶‖, AND FRED E. COHEN*‖**††

Departments of *Pharmaceutical Chemistry, †Radiology, ¶Neurology, **Cellular and Molecular Pharmacology, ††Medicine, and ‖Biochemistry and Biophysics, University of California, San Francisco, CA 94143; and §Department of Molecular Biology, The Scripps Research Institute, La Jolla, CA 92037

Contributed by Stanley B. Prusiner, July 16, 1997

ABSTRACT **The scrapie prion protein (PrP^{Sc}) is the major, and possibly the only, component of the infectious prion; it is generated from the cellular isoform (PrP^{C}) by a conformational change. N-terminal truncation of PrP^{Sc} by limited proteolysis produces a protein of ≈142 residues designated PrP 27–30, which retains infectivity. A recombinant protein (rPrP) corresponding to Syrian hamster PrP 27–30 was expressed in *Escherichia coli* and purified. After refolding rPrP into an α-helical form resembling PrP^{C}, the structure was solved by multidimensional heteronuclear NMR, revealing many structural features of rPrP that were not found in two shorter PrP fragments studied previously. Extensive side-chain interactions for residues 113–125 characterize a hydrophobic cluster, which packs against an irregular β-sheet, whereas residues 90–112 exhibit little defined structure. Although identifiable secondary structure is largely lacking in the N terminus of rPrP, paradoxically this N terminus increases the amount of secondary structure in the remainder of rPrP. The surface of a long helix (residues 200–227) and a structured loop (residues 165–171) form a discontinuous epitope for binding of a protein that facilitates PrP^{Sc} formation. Polymorphic residues within this epitope seem to modulate susceptibility of sheep and humans to prion disease. Conformational heterogeneity of rPrP at the N terminus may be key to the transformation of PrP^{C} into PrP^{Sc}, whereas the discontinuous epitope near the C terminus controls this transition.**

Prions cause neurodegenerative illnesses in humans and animals (1). Those illnesses in humans include kuru, Creutzfeldt–Jakob disease (CJD), Gerstmann–Sträussler–Scheinker disease (GSS), and fatal familial insomnia (FFI) (2–4). Familial CJD, GSS, and FFI are autosomal dominant diseases caused by mutations in the PrP gene and are transmissible to experimental animals. In animals, bovine spongiform encephalopathy, or "mad cow" disease, has caused more than 160,000 cattle deaths in Great Britain. It is thought to be caused by a meat and bone meal dietary supplement containing prion-contaminated offal from sheep and cattle (5). Recent reports suggest that bovine prions may have been transmitted to humans (6, 7).

In contrast to viruses and viroids, prions do not contain a nucleic acid genome encoding their progeny. Rather, prions are composed largely, if not entirely, of a modified host-encoded glycoprotein denoted PrP^{Sc}. Through a posttranslational process, PrP^{Sc} is formed from the normal, cellular prion protein (PrP) isoform designated PrP^{C}. No posttranslational chemical modification responsible for conversion of PrP^{C} into PrP^{Sc} has been identified. Both PrP^{C} and PrP^{Sc} possess a glycosylphosphatidyl inositol (GPI) anchor at the C terminus and are glycosylated at Asp^{181} and Asp^{197}, but no covalent chemical differences between the two isoforms have been found (8). The GPI anchor of PrP^{C} apparently targets it to caveolar-like structures within or adjacent to the plasma membrane where PrP^{C} is either degraded or converted into PrP^{Sc} (9). Differences between PrP^{Sc} and PrP^{C} lie in their properties: PrP^{C} is soluble in nondenaturing detergents, and PrP^{Sc} is not, and whereas PrP^{C} is largely α-helical and readily degraded by proteases, PrP^{Sc} has substantial β-sheet structure and a proteolytically stable core, termed PrP 27–30. Prediction efforts suggested that PrP^{C} could form a four-helix bundle (H1-H4), whereas PrP^{Sc} would lose two of the four helices in favor of a substantial β-sheet (10, 11). Preparations containing this truncated PrP retain scrapie infectivity (12), and similarly truncated recombinant PrP (rPrP) promotes formation of PrP^{Sc} in cultured cells and in transgenic mice (13, 14). Recombinant antibody fragments (rFabs) that bind the N terminus (residues 90–112) of PrP 27–30 recognize native PrP^{C} but not PrP^{Sc}, whereas other rFabs to epitopes in the C-terminal region bind to both native PrP^{C} and PrP^{Sc} (15, 16). Because both N- and C-terminal rFabs bind to denatured PrP^{Sc}, we conclude that as PrP^{Sc} is formed, epitopes exposed in PrP^{C} become buried (17).

Production of rPrP in large quantities for structural studies recently has been successful with expression in *Escherichia coli* of a 142-residue polypeptide corresponding to the Syrian hamster (SHa) sequence of PrP 27–30 (18). While this protein was being investigated, smaller segments of PrP were studied extensively by NMR spectroscopy. A 56-residue peptide consisting of PrP residues 90–145 was found to exist as an α-helical structure or one with intermolecular β-sheets depending on the microenvironment (19). In a hydrophobic environment, chemical shift and nuclear Overhauser effect (NOE) connectivities confirmed the existence of helices in the predicted H1 region and, more weakly, in the H2 region. A 111-residue polypeptide spanning mouse (Mo) PrP residues 121–231 [Mo-PrP(121–231)] was expressed in *E. coli* and found to contain H3 and H4 as predicted, with these helices stabilized by a disulfide bond joining the two Cys residues in PrP (20). An additional α-helix and two antiparallel four-residue β-strands were observed (20). One β-strand corresponds to a portion of H2 that was predicted to participate in a β-sheet of PrP^{Sc} (10).

The publication costs of this article were defrayed in part by page charge payment. This article must therefore be hereby marked "*advertisement*" in accordance with 18 U.S.C. §1734 solely to indicate this fact.

Abbreviations: PrP, prion protein; PrP^{Sc}, scrapie isoform of PrP; PrP^{C}, cellular isoform of PrP; PrP 27–30, N-terminally truncated fragment of PrP^{Sc}; rPrP, recombinant PrP consisting of residues 90–231; SHa, Syrian hamster; Mo, mouse; rFabs, recombinant antibody fragments; NOE(SY), nuclear Overhauser effect (spectroscopy); HSQC, heteronuclear single quantum coherence.

Data deposition: The coordinates from the NMR studies have been deposited in the Protein Data Bank, Brookhaven National Laboratory, Upton, NY 11973.

‡To whom reprint requests should be addressed.

Both PrP^C and PrP^{Sc} possess a disulfide bond (21). We report here on the NMR structure of rPrP(90–231) corresponding to the sequence of PrP 27–30 in an α-helical form that appears to resemble PrP^C (18, 22).

MATERIALS AND METHODS

Isotopic Labeling of rPrP. Uniform isotopic labeling of the protein was done by minimal modifications of the protocol (described by ref. 18). The bacteria were grown overnight in a shaker flask containing 100 ml of Celtone microbial growth media either ^{15}N- or $^{15}N/^{13}C$-labeled. The culture then was used for inoculation of a 1-liter fermentation where the following components were substituted for the isotopically labeled ones: isoleucine, ammonium sulfate, ammonium hydroxide, glucose, and 10% reconstituted Celtone powdered media for the 20% yeast extract and NZ amines. The fermentation was allowed to proceed for either 24 hr (^{15}N) or 12–14 hr ($^{15}N/^{13}C$) depending on the reagents that were limiting. Wet cell paste yield was between 40 and 50 g, ultimately obtaining a minimum of 100 mg of purified protein.

Expression and Purification of rPrP. SHa rPrP was expressed using an alkaline phosphatase promoter in a protease-deficient strain of *E. coli* (27C7), as described (18). Insoluble particles containing rPrP were extruded by a microfluidizer and pelleted by centrifugation. The extruded material was solubilized in 8 M guanidinium hydrochloride (GdnHCl)/100 mM DTT, pH 8.0 and subjected to purification by two sequential chromatographic procedures: size-exclusion chromatography (Pharmacia Superdex 200) eluted by 6 M GdnHCl/50 mM Tris·acetate, pH 8.0/1 mM EDTA, followed by reversed-phase chromatography using a C-4 column (Vydac) eluted by a gradient of acetonitrile/trifluoroacetic acid/water. Purified rPrP subsequently was lyophilized before refolding. Lyophilized rPrP was solubilized at 1 mg/ml in 8 M GdnHCl and rapidly diluted into 20 mM Tris·acetate, pH 8.0/5 mM EDTA to a final concentration of 0.1 mg/ml. The refolded protein was dialyzed against 20 mM sodium acetate, pH 5.0/0.005% sodium azide. Insoluble material was removed by filtration through a 0.2-μm filter. Solutions were concentrated by Centriplus 10 (Amicon) to a final protein concentration of 0.7–1.3 mM for NMR studies. Deuterated buffer exchange was done simultaneously with the final concentration step. Samples were analyzed by mass spectroscopy, Fourier transform infrared spectroscopy, and circular dichroism spectroscopy.

NMR Spectral Acquisition and Analysis. NMR spectra for resonance assignments were acquired at 30°C, with 1 mM uniformly ^{15}N-labeled and $^{15}N/^{13}C$-labeled rPrP at pH 5.2, in 10% ^2H_2O on the following spectrometers: a Bruker DMX750, a Bruker AMX500, or a Varian UnityPlus600, each equipped with a 5-mm $^{13}C/^{15}N/^1H$ triple resonance probe. Backbone and C_β assignments were made using CBCA(CO)NH, HNCACB, and HNCA experiments (23). Side-chain ^{13}C and ^1H assignments were obtained using (H)C(CO)NH-total correlated spectroscopy (24) and HCCH-total correlated spectroscopy (25) spectra. NOE spectroscopy (NOESY) experiments were run at 750 MHz on a Bruker DMX750 spectrometer. Distance restraints were obtained from the NOESY data, using a ^{15}N-labeled sample, from a three-dimensional ^{15}N-resolved NOESY with a 100-ms mixing time (modified from ref. 26) and, using a $^{13}C/^{15}N$-labeled sample, from a three-dimensional ^{13}C-resolved NOESY with a 100-ms mixing time (27).

Structure Determination. Spectra were processed using the program NMRPIPE (28). Spectra were analyzed, and assignments managed using the locally written program SPARKY (29). All spectra were referenced relative to 3-(trimethylsilyl)-tetradeutero-sodium propionate. The backbone ^1H, ^{15}N, and $^{13}C_\alpha$ resonance assignments of rPrP(90–231) are complete. Ninety-two percent of the side-chain resonances are assigned,

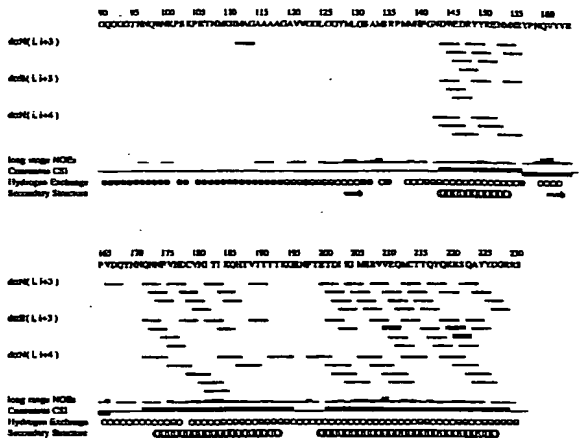

FIG. 1. Secondary structure diagram for rPrP. NOE connectivities are denoted by lines, where the thickness qualitatively represents the relative intensity (weak, medium, or strong) of the NOE crosspeaks, and i designates the residue number for rPrP. $d_{\alpha N}(i, i+3)$ denotes an NOE between the α-proton of residue i and the amide proton of residue $i+3$. The long-range NOE line indicates by height the relative number of NOE crosspeaks between residues $i \rightarrow i + \geq 4$. In the consensus chemical shift index (59), contiguous up bars designate α-helix and down bars designate β-strand. Regions of secondary structure are depicted by helices for α-helices and broad arrows for β-strands. Hydrogen exchange was calculated from the intensity of proton NOE crosspeak between the amide and water: open circles for slow, filled for fast, and half-filled circles for medium exchange rate. No circle indicates spectral overlap or proline. The secondary structure diagram was created using the program VINCE (60).

with the unassigned resonances mainly concerning residues with aromatic rings. From the NOE crosspeaks, 2,401 experimental distance restraints were used to generate low-resolution structures via the program DIANA (30), followed by minimization with AMBER 4.1 (31).

RESULTS

To investigate the basis of the PrP structural transitions, we prepared rPrP with the SHaPrP sequence corresponding to residues 90–231 of PrP 27–30 (18, 22). The rPrP was uniformly labeled with ^{15}N or with both ^{15}N and ^{13}C; it was refolded into a conformer that resembles PrP^C based on optical spectroscopic and immunochemical measurements (15, 32). The pH of the rPrP solution was found to be critical: N-terminal epitopes (residues 90–112) in rPrP that were observed to be partially buried at pH 5.2–8.0 by ELISA using N-terminal rFabs (17) (Y. Matsunaga and S.B.P., unpublished work) became completely exposed at pH 4.8 or lower. Whether the pH-dependent conformational transition detected by rFabs extends to other parts of the protein remains to be established, but it may be pertinent to structural differences between rPrP and MoPrP(121–231), because the latter structure was determined at pH 4.5 (20) (*vide infra*). When rPrP (0.9 mM) was poised in the middle of this structural transition at pH 5.0 in 20 mM Na acetate and 0.005% Na azide, its α-helical state was stable for at least 15 days at temperatures from 4°C to 30°C as judged by circular dichroism. In contrast, 1 day at 35°C led to a substantial loss of α-helix and a concomitant acquisition of β-sheet that was concentration-dependent (data not shown). At 35°C, incremental increases in the concentration of rPrP from 0.03 mM to 0.75 mM steadily increased the rate of α-helix to β-sheet conversion.

Multidimensional heteronuclear NMR studies were performed with rPrP. Signal linewidths and spectral dispersion indicated that most of the protein is well structured at the concentration (ca. 1 mM) and solution conditions used: 20 mM

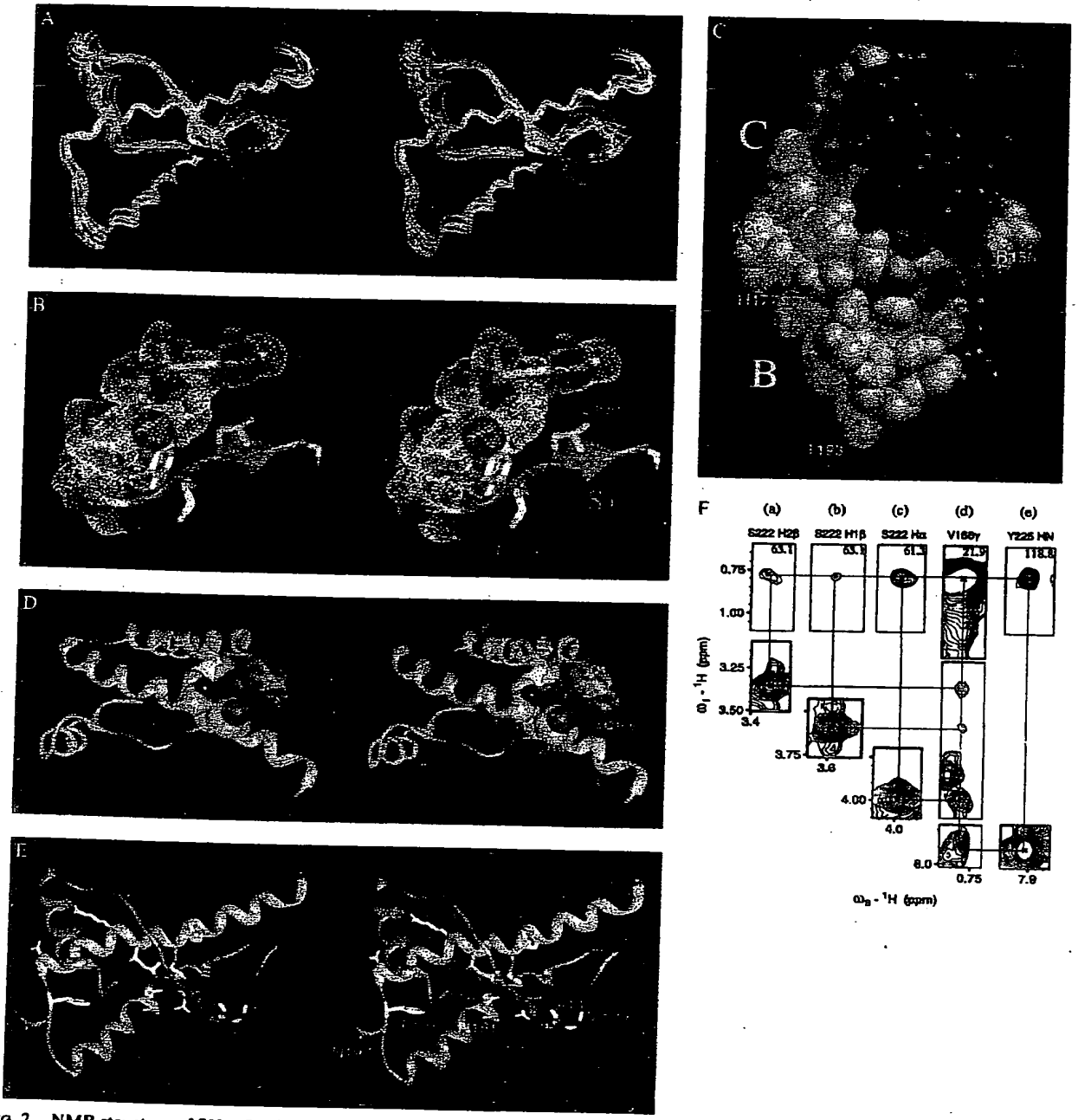

FIG. 2. NMR structure of SHa rPrP(90–231). (*A*) Comparison of the 15 best-scoring structures of rPrP shown with a best-fit superposition of backbone atoms for residues 113–227 (stereoview). In all figures except *C*, the color scheme is: disulfide between Cys^{179} and Cys^{214}, yellow; sites of glycosidation in PrP^C, i.e., Asn^{181} and Asn^{197}, gold; hydrophobic cluster composed of residues 113–126, red; helices, pink; loops, gray; residues 129–134, green, encompassing strand S1 and residues 159–165, blue, encompassing strand S2; the arrows span residues 129–131 and 161–163, as these show a closer resemblance to β-sheet. The structures were generated with the program DIANA (30), followed by energy minimization with AMBER 4.1 (31). Structure generation parameters are as follows: 2,401 distance restraints (intraresidue, 858; sequential ($i \rightarrow i+1$), 753; ($i \rightarrow i+2$), 195; ($i \rightarrow i+3$), 233; ($i \rightarrow i+4$), 109; and ($i \rightarrow i+\geq 5$), 253 for amino acid i); hydrogen bond restraints, 44; distance restraint violations >0.5 Å per structure, 30; AMBER energy, −1,443 ± 111 kcal/mol. Precision of structures: atomic rms deviation for all backbone heavy atoms of residues 128–227, <1.9 Å. The distance restraint violations and precision in some molecular moities reflect the conformational heterogeneity of rPrP. (*B*) Residues 113–132 illustrating (stereoview) in one representative structure the interaction of the hydrophobic cluster, with van der Waals rendering of atoms in residues 113–127, with the first β-strand. (*C*) Van der Waals surface of rPrP turned approximately 180° from *A*, illustrating the interaction of helix A with helix C. Helices A, B, and C are colored magenta, cyan, and gold, respectively. (*D*) Stereoview, using RIBBONJR, illustrating the proximity of helix C to the 165–171 loop and the end of helix B, where residues Gln^{168} and Gln^{172} are depicted with a low-density van der Waals rendering and helix C residues Thr^{215} and Gln^{219} are depicted with a high-density van der Waals rendering. (*E*) Stereoview, highlighting in white the residues corresponding to point mutations that lead to human prion diseases. Illustrations were generated with MIDASPLUS. (*F*) Portion of the three-dimensional ^{13}C-NOESY spectrum corresponding to ^{13}C

sodium acetate, pH 5.2, 30°C. Analytical sedimentation indicated that the protein was essentially monomeric at 25° (22). However, ^{15}N spin-lattice and spin-spin relaxation time measurements indicate that the protein is undergoing rapid interconversion between a weak dimer and monomer. No specific intermolecular interactions have been identified to date.

Essentially three parts to the protein are readily reflected in simple NMR spectral features: residues 90–112 are characterized by narrow (18 Hz) ^{15}N heteronuclear single quantum coherence (HSQC) spectral signals and few long-range NOE crosspeaks; residues 113–126 have relatively narrow (ca. 18 Hz) ^{15}N HSQC spectral (ca. 18Hz) signals and many NOE crosspeaks; and most of the remaining residues exhibit ca. 6 Hz broader HSQC signals and numerous NOE crosspeaks. The consensus chemical shift indices (33), as well as the proton NOE connectivities evident in NOESY spectra, consistently indicate that rPrP contains three α-helical regions (Fig. 1). The locations of these correspond largely, but not entirely, to those found for MoPrP(121–231) under similar solution conditions (0.8 mM protein, pH 4.5, no buffer, 20°C) (20) and to two of the four helices predicted for the entire sequence (10).

A best-fit superposition of backbone atoms for residues 113–228 of rPrP is shown in Fig. 2*A*. To distinguish the α-helices found in rPrP by NMR from those predicted by molecular modeling, we provisionally designate these helices A, B, and C. Helix A spans residues 144–156 with the last turn distorted, corresponding to helix 144–154 found for MoPrP(121–231). Helix B spans residues 172–193, with the first turn irregular at the present stage of structure refinement. This helix is about two turns longer than the 179–193 helix found for MoPrP(121–231), which agrees well with predicted helix H3 (179–191). Helix C extends from residues 200 to 227 with the 225–227 turn irregular. This helix is about three turns longer than the helix corresponding to residues 200–217 in MoPrP(121–231). It is notable that predicted helix H4 (residues 202–218) corresponds well with that found in MoPrP(121–231). Two four-residue β-strands (128–131 and 161–164) were identified in the MoPrP(121–231) structure. We found a similar antiparallel β-sheet, with S2 spanning residues 161–163 and S1 spanning 129–131 possessing β-sheet characteristics, but the two strands do not manifest standard β-sheet geometry. In fact, a β-bridge occurs only between Leu^{130} and Tyr^{162}, although extensive cross-strand connectivities of residues are in segment 129–134 with proximate residues on the antiparallel segment 159–165.

The loop between S2 and helix B (i.e., residues 165–171) yields resonances clearly exhibiting long-range as well as medium-range restraints, which were not seen for the backbone atoms of residues 167–176 in the shorter MoPrP(121–231). Our results indicate that the loop is reasonably ordered, whereas this region is disordered in MoPrP(121–231) (20). Fig. 2*F* shows only one example: ^1H-^1H crosspeaks between the unresolved methyl protons of Val^{166} with Ser^{222} and Tyr^{225}. The methyl protons of Val^{166} also exhibit 15 long-range crosspeaks with protons in the same loop, e.g., Tyr^{169}, and in the extension of helix C, e.g., Tyr^{218} and Tyr^{225}. Connectivities of Val^{166} to residues two turns apart on helix C suggest that the loop may exist in at least two conformations. Apparently, the interaction of the 165–171 loop with the helix C extension is important in stabilizing the structure (see Fig. 2*A*).

The mature human, Mo, and SHa prions manifest >90% sequence homology (34). Nevertheless, we must consider whether variations in sequence might cause the differences in structures observed for MoPrP(121–231) and SHa rPrP. Only four sequence variations are in the region 121–231. Whereas three appear to be conservative with no apparent structural effect, we note that Thr^{215} in the SHa sequence is Val in the mouse-A and Ile in the human PrP. Although it is conceivable that this may account for the differences in the length of helix C, it seems unlikely.

The α-proton and α-carbon chemical shifts for residues 90–127 are consistent with the region having α-helical content, but the extent of the chemical shifts relative to that of random coil values was generally not enough to indicate α-helix formation via tripartite chemical shift indices. Insufficient NOE connectivities exist to conclude that an α-helix is formed. The few medium-range connectivities in the segment 90–112 demonstrate sparse elements of structure. For example, for residues 95–100, we have so far identified nine nonsequential NOE connectivities. This implies that some structure exists at least transiently. The small number of long-range connectivities for the N-terminal segment 90–112 implies that it is largely disordered.

We have so far identified 36 long-range NOE crosspeaks involving side-chain resonances for the hydrophobic residues in the segment 113–125. An uncommon combination of glycines and hydrophobic residues leads to an unusual and dynamic structural feature. Most of the NOE connectivities indicate that these residues form a hydrophobic cluster with substantial backbone reversals permitted by the many glycines; indeed Val^{121}, Val^{122}, and Leu^{125} each exhibit 10 ± 3 long-range connectivities. As seen in Fig. 2*A*, the backbone for this cluster is not well defined in spite of the many connectivities. This may reflect the true dynamic nature of such a hydrophobic cluster, as the ^{15}N HSQC spectral linewidths for these residues were also about 6 Hz smaller than for the core of the protein (ca. 18 vs. 24–25 Hz). Apparently, the combination of glycines with hydrophobic residues permits many alternative conformations with comparable free energies.

Some long-range connectivities place the hydrophobic cluster adjacent to the β-sheet in contact with the S1 strand (Fig. 2*B*). The weak, broadened ^{15}N HSQC spectral signals for S1 residues Met^{129} (32 Hz), Leu^{130} (32 Hz), and Gly^{131} (44 Hz), as well as for S2 residues Tyr^{162} (33 Hz) and Arg^{164} (33 Hz), may well reflect conformational exchange effects in the interacting hydrophobic cluster pervading the adjacent irregular β-sheet. Taken together, these results suggest that the hydrophobic cluster and adjacent β-strands constitute a domain with marginally stable polymorphic structure.

DISCUSSION

The apparent conformational heterogeneity of the N-terminal region of rPrP may reflect the process by which PrP^C is converted into PrP^{Sc}. Transgenetic studies suggest that PrP^{Sc} formation requires the substrate PrP^C to bind to the product PrP^{Sc} at an intermediate stage of the conversion process (35). PrP^C is thought to be in equilibrium with a metastable intermediate, designated PrP*, which binds to PrP^{Sc} in the conversion process (36). In fact, destabilization of PrP^C has been shown to be necessary for it to bind to PrP^{Sc} *in vitro* (37–39). Further evidence for the conformational plasticity of PrP comes from unfolding studies of rPrP using guanidinium chloride (22). The free energy difference ΔG_2 of 6.5 ± 1.2 kcal/mol between an intermediate state and the unfolded state was found to be comparable to literature values (5–15 kcal/mol) for protein unfolding (40, 41). However, the completely refolded rPrP, as used for the present NMR studies, is only marginally more stable (ΔG_1 = 1.9 ± 0.4 kcal/mol) than the folding intermediate. This is consistent with the extensive

planes of the unresolved Val^{166} methyl resonances and the Ser^{222} resonances (*a*–*d*) and the ^{15}N plane showing the Tyr^{225} amide interaction with Val^{166} (*e*). The diagonal peaks and mirrored crosspeaks for each ^1H-^1H connectivity are shown. The solid lines connecting peaks designate NOE connectivities.

conformational flexibility evident in the current NMR studies for part of the protein.

The NMR results for rPrP, compared with the structure reported for MoPrP(121–231) (20), support the notion that the core of the PrP^C structure is formed by parts of helices B and C, corresponding largely to the predicted H3 and H4 regions (10), and is stabilized by the disulfide, which is essential for α-helical folding (18, 22). As seen in Fig. 2, helices B and C essentially form one side of the protein structure. This core is further stabilized by helix A, which lies across helix C with side chains interacting between the two helices (Fig. 2*C*). Strand S2 also lies on this side of the protein and interacts predominantly with helices B and C as well as S1. With or without S2 and S1, we presume this relatively stable folding core is associated with the second unfolding transition. Attempts to prepare MoPrP(108–231) resulted in proteolytic cleavage producing MoPrP(121–231) (20), indicative of a stable core beginning with residue 121 (41). Conclusions about the "stable core" of MoPrP(121–231), however, must be considered within the context of the unstructured loop (165–171) and the shortened helices B and C. It is likely that the structure of MoPrP(121–231) corresponds to that of PrP^C-II, which is formed in caveolae during the initial degradation of PrP^C (9, 42). Whether the ineligibility of PrP^C-II for conversion into PrP^{Sc} is determined by the disordered structure assumed by the loop (165–171) as well as by the unraveling of helices B and C remains to be determined (43).

The presence of the additional 31 N-terminal residues of rPrP, relative to MoPrP(121–231), induces substantial changes in the structure of PrP, which include alterations in the C terminus. Helix C is extended by at least nine residues, helix B is up to seven residues longer, and the loop comprising residues 165–171 is sufficiently ordered that many long-range restraints can be observed. The hydrophobic cluster (residues 113–125) predominantly interacts with S1 in the β-sheet (Fig. 2) and may serve to stabilize the observed extension of helix B from 179 in MoPrP(121–231) to 172 in rPrP. Stability also may be conferred by hydrophobic interactions of Tyr^{128} with Tyr^{163} in the β-sheet, which, in turn, interact with Val^{176}. The relative stability of the 165–171 loop and the three additional helical turns in helix C presumably are connected to stabilization of the other structural elements.

Strains of prions exhibit different incubation times before symptoms of disease appear and different patterns of PrP^{Sc} accumulation. Recent work indicates that the properties of prion strains might be manifestations of different conformers of PrP^{Sc} (44, 45). Studies on the transmission of human prions to transgenic mice suggest that a species-specific factor, provisionally designated protein X, might function like a molecular chaperone in PrP^{Sc} formation (46). Our current working hypothesis is that protein X forms a transient complex with the metastable intermediate PrP^*, diminishing the activation energy barrier between PrP^C and PrP^{Sc} and facilitating formation of PrP^{Sc} (36, 46). Our analysis comparing the full-length helix C and ordering of the 165–171 loop in rPrP with the truncation of helix C at Gln^{217} in MoPrP(121–231) is consistent with this concept. Recent work suggests SHa residues Gln^{168}, Gln^{172}, Thr^{215}, and Gln^{219} are at the site of protein X binding (47); the glycosylation sites, Asn^{181} and Asn^{197}, are apparently quite distant from this putative binding site (Fig. 2*E*). As seen in Fig. 2*D*, Thr^{215} and Gln^{219} lie in register one turn apart on helix C and interact with the residues in the 165–171 loop. SHa residue 168 is a Gln in most species and corresponds to sheep PrP codon 171, which is polymorphic, encoding either Gln or Arg. Almost all Suffolk sheep with scrapie were found to be Gln/Gln, indicating that heterozygosity for Arg conferred resistance (48–56). Equally important is the observation that $\approx$12% of PrP alleles in Japanese encode Lys instead of Glu at position 219 (57). No cases of Creutzfeldt–Jakob disease have been found in people with Lys^{219}, which, like Arg, is basic. These findings and data on the conversion of mutagenized PrP into PrP^{Sc} in ScN2a cells suggest that protein X binds to a discontinuous epitope, incorporating residues 168, 172, 215, and 219 in rPrP that is disordered in MoPrP(121–231).

Residues where point mutations lead to human diseases are highlighted in Fig. 2*E*. The D178N point mutation in the PrP gene causes fatal familial insomnia if residue 129 is Met (4). A potentially important difference between the structures of rPrP and MoPrP(121–231) lies in the proximity of residues 178 and 129. The side chains of these residues determine the phenotypes of two inherited human prion diseases (58). In rPrP, residue 178 lies within helix B and is located opposite residue 129 with strand S2 partially intervening. Such geometry suggests that the D178N mutation destabilizes PrP through partially unraveling helix B and that the conformation of mutant PrP^{Sc} is modulated by the side chain of residue 129. The particular conformation adopted by mutant PrP^{Sc} might determine in which regions of the central nervous system PrP^{Sc} is deposited, and thus, be responsible for whether patients present with insomnia or dementia (58). When residue 129 is Val, then patients present with a dementing illness called familial Creutzfeldt–Jakob disease. In MoPrP(121–231), residues 178 and 129 are apparently distant from each other; in fact, residue 178 does not even form part of helix B.

Our structural studies of rPrP underscore the conformational plasticity evident in the N-terminal region (19) and define important structural features not evident in a smaller C-terminal fragment (20). Previous studies, including those most recently performed with rFabs, indicate that the region corresponding to the N-terminal 30–40 residues of rPrP undergoes a profound conformational change during formation of PrP^{Sc} (17). This conformational change seems to be mediated by protein X, whose binding site on PrP^C was delineated by the structure of rPrP reported here and by site-directed mutagenesis (47).

We are especially grateful to P. E. Wright and H. J. Dyson for support and for use of the Skaggs NMR Facility. For help with some of the initial spectra, we thank V. J. Basus, M. A. Kennedy, D. L. Mattiello, S. Mayo, S. Ross, and G. M. Wolfe. We thank C. Kojima for helpful discussions and the University of California, San Francisco Computer Graphics Laboratory for use of its facilities. This work was supported by National Institutes of Health Grants AG10770 and GM39247 as well as by gifts from the Leila and Harold G. Mathers, Sherman Fairchild, and the Bernard Osher foundations.

1. Prusiner, S. B. (1996) *Trends Biochem. Sci.* **252**, 482–487.
2. Gajdusek, D. C. (1977) *Science* **197**, 943–960.
3. Masters, C. L., Gajdusek, D. C. & Gibbs, C. J., Jr. (1981) *Brain* **104**, 559–588.
4. Medori, R., Tritschler, H.-J., LeBlanc, A., Villare, F., Manetto, V., Chen, H. Y., Xue, R., Leal, S., Montagna, P., Cortelli, P., Tinuper, P., Avoni, P., Mochi, M., Baruzzi, A., Hauw, J. J., Ott, J., Lugaresi, E., Autilio-Gambetti, L. & Gambetti, P. (1992) *N. Engl. J. Med.* **326**, 444–449.
5. Anderson, R. M., Donnelly, C. A., Ferguson, N. M., Woolhouse, M. E. J., Watt, C. J., Udy, H. J., MaWhinney, S., Dunstan, S. P., Southwood, T. R. E., Wilesmith, J. W., Ryan, J. B. M., Hoinville, L. J., Hillerton, J. E., Austin, A. R. & Wells, G. A. H. (1996) *Nature (London)* **382**, 779–788.
6. Chazot, G., Broussolle, E., Lapras, C. I., Blättler, T., Aguzzi, A. & Kopp, N. (1996) *Lancet* **347**, 1181.
7. Will, R. G., Ironside, J. W., Zeidler, M., Cousens, S. N., Estibeiro, K., Alperovitch, A., Poser, S., Pocchiari, M., Hofman, A. & Smith, P. G. (1996) *Lancet* **347**, 921–925.
8. Stahl, N., Baldwin, M. A., Teplow, D. B., Hood, L., Gibson, B. W., Burlingame, A. L. & Prusiner, S. B. (1993) *Biochemistry* **32**, 1991–2002.
9. Taraboulos, A., Scott, M., Semenov, A., Avrahami, D., Laszlo, L. & Prusiner, S. B. (1995) *J. Cell Biol.* **129**, 121–132.
10. Huang, Z., Gabriel, J.-M., Baldwin, M. A., Fletterick, R. J., Prusiner, S. B. & Cohen, F. E. (1994) *Proc. Natl. Acad. Sci. USA* **91**, 7139–7143.

11. Huang, Z., Prusiner, S. B. & Cohen, F. E. (1996) *Folding Design* **1,** 13–19.
12. Prusiner, S. B., Bolton, D. C., Groth, D. F., Bowman, K. A., Cochran, S. P. & McKinley, M. P. (1982) *Biochemistry* **21,** 6942–6950.
13. Rogers, M., Yehiely, F., Scott, M. & Prusiner, S. B. (1993) *Proc. Natl. Acad. Sci. USA* **90,** 3182–3186.
14. Fischer, M., Rülicke, T., Raeber, A., Sailer, A., Moser, M., Oesch, B., Brandner, S., Aguzzi, A. & Weissmann, C. (1996) *EMBO J.* **15,** 1255–1264.
15. Williamson, R. A., Peretz, D., Smorodinsky, N., Bastidas, R., Serban, H., Mehlhorn, I., DeArmond, S. J., Prusiner, S. B. & Burton, D. R. (1996) *Proc. Natl. Acad. Sci. USA* **93,** 7279–7282.
16. Peretz, D., Williamson, A., Matsunaga, Y., Burton, D. R. & Prusiner, S. B. (1997) *J. Allergy Clin. Immunol.* **99,** S222.
17. Peretz, D., Williamson, R. A., Matsunaga, Y., Serban, H., Pinilla, C., Bastidas, R., Rozenshteyn, R., James, T. L., Houghten, R. A., Cohen, F. E., Prusiner, S. B. & Burton, D. R. (1997) *J. Mol. Biol.*, in press.
18. Mehlhorn, I., Groth, D., Stöckel, J., Moffat, B., Reilly, D., Yansura, D., Willett, W. S., Baldwin, M., Fletterick, R., Cohen, F. E., Vandlen, R., Henner, D. & Prusiner, S. B. (1996) *Biochemistry* **35,** 5528–5537.
19. Zhang, H., Kaneko, K., Nguyen, J. T., Livshits, T. L., Baldwin, M. A., Cohen, F. E., James, T. L. & Prusiner, S. B. (1995) *J. Mol. Biol.* **250,** 514–526.
20. Riek, R., Hornemann, S., Wider, G., Billeter, M., Glockshuber, R. & Wüthrich, K. (1996) *Nature (London)* **382,** 180–182.
21. Turk, E., Teplow, D. B., Hood, L. E. & Prusiner, S. B. (1988) *Eur. J. Biochem.* **176,** 21–30.
22. Zhang, H., Stöckel, J., Mehlhorn, I., Groth, D., Baldwin, M. A., Prusiner, S. B., James, T. L. & Cohen, F. E. (1997) *Biochemistry* **36,** 3543–3553.
23. Muhandiram, D. R. & Kay, L. E. (1994) *J. Magn. Reson. B* **103,** 203–216.
24. Logan, T. M., Olejniczak, E. T., Xu, R. X. & Fesik, S. W. (1993) *J. Biomol. NMR* **3,** 225–231.
25. Kay, L. E., Xu, G.-Y., Singer, A. U., Muhandiram, D. R. & Forman-Kay, J. D. (1993) *J. Magn. Reson. B* **101,** 333–337.
26. Marion, D., Driscoll, P. C., Kay, L. E., Wingfield, P. T., Bax, A., Gronenborn, A. M. & Clore, G. M. (1989) *Biochemistry* **28,** 6150–6156.
27. Muhandiram, D. R., Farrow, N. A., Xu, G. Y., Smallcombe, S. H. & Kay, L. E. (1993) *J. Magn. Reson. B* **102,** 317–321.
28. Delaglio, F., Grzesiek, S., Vuister, G. W., Zhu, G., Pfeifer, J. & Bax, A. (1995) *J. Biomol. NMR* **6,** 277–293.
29. Kneller, D., Kuntz, I. D. & Goddard, T. (1996) SPARKY (University of California, San Francisco).
30. Güntert, P., Braun, W. & Wüthrich, K. (1991) *J. Mol. Biol.* **217,** 517–530.
31. Pearlman, D. A., Case, D. A., Caldwell, J., Ross, W. S., Cheatham, T.E., III, T. E., Ferguson, D. N., Seibel, G. L., Singh, U. C., Weiner, P. K. & Kollman, P. A. (1995) AMBER 4.1. (University of California, San Francisco).
32. Pan, K.-M., Baldwin, M., Nguyen, J., Gasset, M., Serban, A., Groth, D., Mehlhorn, I., Huang, Z., Fletterick, R. J., Cohen, F. E. & Prusiner, S. B. (1993) *Proc. Natl. Acad. Sci. USA* **90,** 10962–10966.
33. Wishart, D. S., Sykes, B. D. & Richards, F. M. (1992) *Biochemistry* **31,** 1647–1651.
34. Schätzl, H. M., Da Costa, M., Taylor, L., Cohen, F. E. & Prusiner, S. B. (1995) *J. Mol. Biol.* **245,** 362–374.
35. Prusiner, S. B., Scott, M., Foster, D., Pan, K.-M., Groth, D., Mirenda, C., Torchia, M., Yang, S.-L., Serban, D., Carlson, G. A., Hoppe, P. C., Westaway, D. & DeArmond, S. J. (1990) *Cell* **63,** 673–686.
36. Cohen, F. E., Pan, K.-M., Huang, Z., Baldwin, M., Fletterick, R. J. & Prusiner, S. B. (1994) *Science* **264,** 530–531.
37. Kocisko, D. A., Come, J. H., Priola, S. A., Chesebro, B., Raymond, G. J., Lansbury, P. T., Jr. & Caughey, B. (1994) *Nature (London)* **370,** 471–474.
38. Kaneko, K., Peretz, D., Pan, K.-M., Blochberger, T., Wille, H., Gabizon, R., Griffith, O. H., Cohen, F. E., Baldwin, M. A. & Prusiner, S. B. (1995) *Proc. Natl. Acad. Sci. USA* **32,** 11160–11164.
39. Kaneko, K., Wille, H., Mehlhorn, I., Zhang, H., Ball, H., Cohen, F. E., Baldwin, M. A. & Prusiner, S. B. (1997) *J. Mol. Biol.* **270,** 574–586.
40. Pace, C. N. (1995) *Methods Enzymol.* **259,** 538–554.
41. Hornemann, S. & Glockshuber, R. (1996) *J. Mol. Biol.* **262,** 614–619.
42. Pan, K.-M., Stahl, N. & Prusiner, S. B. (1992) *Protein Sci.* **1,** 1343–1352.
43. Muramoto, T., Scott, M., Cohen, F. & Prusiner, S. B. (1996) *Proc. Natl. Acad. Sci. USA* **93,** 15457–15462.
44. Bessen, R. A. & Marsh, R. F. (1992) *J. Virol.* **66,** 2096–2101.
45. Telling, G. C., Parchi, P., DeArmond, S. J., Cortelli, P., Montagna, P., Gabizon, R., Mastrianni, J., Lugaresi, E., Gambetti, P. & Prusiner, S. B. (1996) *Science* **274,** 2079–2082.
46. Telling, G. C., Scott, M., Mastrianni, J., Gabizon, R., Torchia, M., Cohen, F. E., DeArmond, S. J. & Prusiner, S. B. (1995) *Cell* **83,** 79–90.
47. Kaneko, K., Zulianello, L., Scott, M., Cooper, C. M., Wallace, A. C., James, T. L., Cohen, F. E. & Prusiner, S. B. (1997) *Proc. Natl. Acad. Sci. USA* 10069–10074.
48. Hunter, N., Goldmann, W., Benson, G., Foster, J. D. & Hope, J. (1993) *J. Gen. Virol.* **74,** 1025–1031.
49. Goldmann, W., Hunter, N., Smith, G., Foster, J. & Hope, J. (1994) *J. Gen. Virol.* **75,** 989–995.
50. Westaway, D., Zuliani, V., Cooper, C. M., Da Costa, M., Neuman, S., Jenny, A. L., Detwiler, L. & Prusiner, S. B. (1994) *Genes Dev.* **8,** 959–969.
51. Belt, P. B. G. M., Muileman, I. H., Schreuder, B. E. C., Ruijter, J. B., Gielkens, A. L. J. & Smits, M. A. (1995) *J. Gen. Virol.* **76,** 509–517.
52. Clousard, C., Beaudry, P., Elsen, J. M., Milan, D., Dussaucy, M., Bounneau, C., Schelcher, F., Chatelain, J., Launay, J. M. & Laplanche, J. L. (1995) *J. Gen. Virol.* **76,** 2097–2101.
53. Ikeda, T., Horiuchi, M., Ishiguro, N., Muramatsu, Y., Kai-Uwe, G. D. & Shinagawa, M. (1995) *J. Gen. Virol.* **76,** 2577–2581.
54. Hunter, N., Moore, L., Hosie, B. D., Dingwall, W. S. & Greig, A. (1997) *Vet. Rec.* **140,** 59–63.
55. Hunter, N., Cairns, D., Foster, J. D., Smith, G., Goldmann, W. & Donnelly, K. (1997) *Nature (London)* **386,** 137.
56. O'Rourke, K. I., Holyoak, G. R., Clark, W. W., Mickelson, J. R., Wang, S., Melco, R. P., Besser, T. E. & Foote, W. C. (1997) *J. Gen. Virol.* **78,** 975–978.
57. Kitamoto, T. & Tateishi, J. (1994) *Philos. Trans. R. Soc. London B* **343,** 391–398.
58. Goldfarb, L. G., Petersen, R. B., Tabaton, M., Brown, P., LeBlanc, A. C., *et al.* (1992) *Science* **258,** 806–808.
59. Wishart, D. S., Bigam, C. G., Yao, J., Abildgaard, F., Dyson, H. J., Oldfield, E., Markley, J. L. & Sykes, B. D. (1995) *J. Biomol. NMR* **6,** 135–140.
60. La Rosa, E., Stern, A. & Hoch, J. (1996) VINCE (Rowland Institute for Science, Cambridge, MA).

THE JOURNAL OF BIOLOGICAL CHEMISTRY
Vol. 275, No. 48, Issue of December 1, pp. 38081–38087, 2000
Printed in U.S.A.

A Monomer-Dimer Equilibrium of a Cellular Prion Protein (PrP^C) Not Observed with Recombinant PrP*

Received for publication, August 7, 2000
Published, JBC Papers in Press, August 30, 2000, DOI 10.1074/jbc.M007114200

Rudolf K. Meyer‡§, Ariel Lustig¶, Bruno Oesch‖, Rosmarie Fatzer‡, Andreas Zurbriggen‡, and Marc Vandevelde‡

From the ‡TSE Reference Center, Institute of Animal Neurology, University of Bern, Bremgartenstrasse 109a, CH-3012 Bern, ¶Biocenter, University of Basel, Klingelbergstrasse 70, 4056 Basel, and ‖Prionics Ltd., University of Zürich, Winterthurerstrasse 190, CH-8057 Zürich, Switzerland

Both the purified normal (protease-sensitive) isoform of the prion protein (PrP^C) (Pergami, P., Jaffe, H., and Safar, J. (1996) *Anal. Biochem.* 236, 63–73) and recombinant prion protein (PrP) have been found to be in monomeric form (Mehlhorn, I., Groth, D., Stockel, J., Moffat, B., Reilly, D., Yansura, D., Willet, W. S., Baldwin, M., Fletterick, R., Cohen, F. E., Vandlen, R., Henner, D., and Prusiner, S. B. (1996) *Biochemistry* 35, 5528–5537; and this paper), and therefore PrP^C-PrP^C interactions were previously unknown. In this report we confirm recombinant PrP to be a monomer by analytical ultracentrifugation. However, by three lines of evidence (enzyme-linked immunosorbent assay (ELISA), cross-linking experiments, and size exclusion chromatography) we could also demonstrate that, under native conditions, at least part of the native bovine PrP^C exists as a monomer-dimer equilibrium. A bovine PrP^C-specific immunosandwich ELISA was developed and calibrated with recombinant PrP (Meyer, R. K., Oesch, B., Fatzer, R., Zurbriggen, A., and Vandevelde, M. (1999) *J. Virol.* 73, 9386–9392). By this ELISA we identified a distinct PrP^C fraction and partially purified this protein. When serial dilutions of brain homogenate or partially purified PrP^C were measured, using the peptide antibody C15S, a nonlinear dose-response curve was obtained. This nonlinearity was shown not to be due to an artifact of the procedure but to a monomer-dimer equilibrium of PrP^C with preferential binding of the antibody to the dimer. From the curvature we could deduce the association constant ($3.9 \times 10^8\ M^{-1}$ at 37 °C). Accordingly, $\Delta G°$ of the reaction was calculated (-48.6 kJ M^{-1}), and $\Delta H°$ (9.5 kJ M^{-1}) as well as $\Delta S°$ (0.2 kJ $K^{-1}\ M^{-1}$) were extrapolated from the van't Hoff plot. When serial dilutions of monomeric recombinant PrP were tested, only a straight line was obtained, supporting our hypothesis. Additional evidence of dimer formation was revealed by Western blotting of partially purified PrP^C cross-linked by the homobifunctional cross-linker BS^3. Finally, size exclusion chromatography of partially purified PrP^C fractions revealed an additional shoulder not observed with recombinant PrP. The difference in respect of dimer formation between native PrP^C and recombinant PrP could be explained by the lack of glycosylation of the latter.

The prion protein (PrP)[1] was detected in attempts to identify the infective agent of transmissible spongiform encephalopathies (4). Later, several isoforms of this protein were described and named, in particular PrP^C (5), either membrane bound (6) or soluble (7, 8), and PrP^{Sc} (9). All of these isoforms have essentially the same amino acid sequence but different biochemical characteristics. They are sialoglycoproteins (10) with two possible glycosylation sites, leading to diglycosylated, monoglycosylated, and nonglycosylated forms (11). Membrane-bound PrP^C has a phosphatidylinositol anchor by which it is bound to the cell membrane (12). Most of the biochemistry of PrP^C is known from recombinant PrP, because PrP^C is comparatively rare even in the brain, and only a few micrograms have yet been purified (1, 13). Recombinant PrP is a monomer (2); its structure has been elucidated by nuclear magnetic resonance (14). Membrane interaction (15), copper binding (16), and superoxide dismutase activity (17) have all been described. However, all recombinant PrPs have been cloned and expressed in bacterial expression systems. Therefore, they lack both glycosylation and a phosphatidylinositol anchor. The influence of these two posttranslational modifications on structure and function is largely unknown.

PrP^{Sc} is part of, or even identical to, the prion, the infective agent of transmissible spongiform encephalopathies (18). It is not very soluble and mostly aggregated in prion rods or amyloid deposits (19). Whereas PrP^C has a high α-helix content, β-sheets predominate in PrP^{Sc} (20). Prions, including PrP^{Sc}, are remarkably heat- and protease-stable, making infectivity difficult to destroy (21, 22). In spongiform encephalopathies, PrP^C is converted into PrP^{Sc} by an unknown process (20, 23). Some prion diseases, such as familial Creutzfeldt-Jakob disease (24), Gerstmann-Sträussler-Scheinker disease (25), and fatal familial insomnia (26) of humans, are caused by germline mutations of the PrP gene, which facilitate conversion into the pathological isoform. Others, such as variant Creutzfeldt-Jakob disease and bovine spongiform encephalopathy, have been caused by accidental transmission of prions with contaminated food (27, 28). The conversion of PrP^C into PrP^{Sc} in infected animals involves a conformational change within the N-terminal segment of the protein (29, 30). This conformational change is induced by the presence of PrP^{Sc} (31). Several hypotheses exist about the mechanism of this interaction (20). A seeding model was proposed, in which a spontaneous, reversible thermodynamically controlled conformational change of

* This work was supported by a grant from the Swiss Federal Veterinary Office and by the Swiss Federal Office for Education and Science (Fair5-CT97-3311). The costs of publication of this article were defrayed in part by the payment of page charges. This article must therefore be hereby marked "*advertisement*" in accordance with 18 U.S.C. Section 1734 solely to indicate this fact.

§ To whom correspondence should be addressed. E-mail: rudolf.meyer@itn.unibe.ch.

[1] The abbreviations used are: PrP, prion protein; PrP^C, normal (protease-sensitive) isoform of the prion protein; PrP^{Sc}, pathological (protease-resistant) isoform of the prion protein; ELISA, enzyme-linked immunosorbent assay; PBS, phosphate-buffered saline containing 137 mM NaCl.

PrP^C to PrP^{Sc} was postulated. PrP^{Sc} is stabilized only when bound to a crystal-like seed or aggregate of PrP^{Sc}. Seed formation is extremely slow, but once a seed is present monomers can be added rapidly (20). However, increasing experimental evidence argues for a more specific interaction of PrP^C with PrP^{Sc} (32). The conversion of PrP^C to PrP^{Sc} was inhibited by antibody binding to PrP^C *in vitro* and was interpreted as steric blocking of a binding site to PrP^{Sc} (33). The site of this interaction was located on amino acid positions 91–146 using synthetic peptides (34). Such protein-protein interactions were absent in bovine recombinant PrP (34), and highly purified PrP^C has not been shown by others to form dimers *in vitro* (1). Because both purified PrP^C and recombinant PrP were found to be present in a monomeric form, the PrP^C-PrP^{Sc} interaction was thought to require additional factors. It was postulated that in an uninfected cell PrP^C should exist in equilibrium in its monomeric α-helical state or bound to a hypothetical protein X (35). The hypothetical protein X, a PrP-binding protein present in brain homogenates, would enable dimerization (35, 36) and could be a requirement for PrP^C-PrP^{Sc} interaction. The PrP^C-protein X complex would then bind PrP^{Sc}, creating a replication-competent assembly (36).

By antibody studies to monitor protein expression in native bovine brain tissues, we obtained convincing evidence of a monomer-dimer equlibrium of at least a fraction of PrP^C. This evidence was further confirmed by cross-linking and by size exclusion chromatography of partially purified PrP^C. Such protein-protein interactions were absent in recombinant protein, showing for the first time a biochemical difference in respect to the native, glycosylated form.

MATERIALS AND METHODS

Preparation of Brain Homogenates—Brain material (thalamus) was derived from normal Swiss cattle. Brain tissue from the fish *Salmo truta* and from PrP null mice was used as a negative control and for preparing dilutions. Fragments of brain tissue (≥0.5 g) were homogenized in 10 ml of a 320 mM sucrose solution per g (wet weight) with an Ultra-Turrax T25 (Janke and Kungel, Staufen, Germany). The homogenate was cleared by a short (5 min) centrifugation at 7000 × *g*.

Recombinant PrP—Recombinant PrP was obtained from Prionics Ltd. (Zürich, Switzerland). Recombinant bovine PrP open reading frame was amplified by polymerase chain reaction from genomic DNA using the primers 5′-GGGAA TTCCA TATGA AGAAG CGACC AAAAC CTTG and 5′-CGGGA TCCTA TTAAC TTGCC CCTCG TTGGTA. The resulting product was cloned into pET11a (Novagen). The resulting plasmid (pBPrP3) was transfected into *Escherichia coli* BL21 (DE3). Recombinant bovine PrP was purified from inclusion bodies, after solubilization in 8 M urea, 10 mM 3-(*N*-morpholino)propanesulfonic acid, first on a carboxymethyl-Sepharose column and then by reverse-phase high pressure liquid chromatography (C4 protein column, Vydac). The sequence was as follows: MKKRP KPGGG WNTGG SRYPG QGSPG GNRYP PQGGG GWGQP HGGGW GQPHG (50) GGWGQ PHGGG WGQPH GGGWG QPHGG GGWGQ GGTHG QWNKP SKPKT NMKHV (100) AGAAA AGAVV GGLGG YMLGS AMSRP LIHFG SDYED RYYRE NMHRY PNQVY (150) YRPVD QYSNQ NNFVH DCVNI TVKEH TVTTT TKGEN FTETD IKMME RVVRQ (200) MCITQ YQRES QAYYQ RGAS (219).

Analytical Ultracentrifugation—The sedimentation velocity and sedimentation equilibrium of recombinant PrP were determined in RPB buffer (13.7 mM NaCl, 2.7 mM KCl, 1.4 mM KH_2PO_4, 8.1 mM Na_2HPO_4, pH 7.3) using a Beckman model XLA analytical ultracentrifuge equipped with absorption optics. A sedimentation velocity run was made at 20 °C and 56,000 rpm using 0.15 mg/ml recombinant PrP in a 12-mm DS Epon cell. Scans were taken at 230 nm during 213 min.

Two sedimentation equilibrium runs were carried out at 0.15 and 0.05 mg/ml in the same cell as mentioned above. Both runs were performed at 20 °C and 22,000 rpm. Records were taken at 230 nm. The molecular mass was calculated using a floating baseline computer program that adjusted the baseline absorbance to obtain the best linear fit of absorbance *versus* the square of the radial distance. For calculations, a partial specific volume of 0.714 ml/g, a buffer viscosity of 1.001 centipoise, and a buffer density of 1.001 g/ml were used.

Anti-PrP Antibodies—For detection of PrP in Western blots and for ELISA, two different anti-PrP antibodies were used, one monoclonal antibody (6H4) and a rabbit antiserum (C15S). C15S was raised against a peptide of the bovine PrP sequence (37) (GQGGT HGQWN KPS). Both antibodies, 6H4 (30) and C15S, are described in detail elsewhere (3). Both could detect PrP^C and PrP^{Sc} in immunocytochemistry and Western blot (3).

Western Blotting—Samples were first separated on either 10 or 12% sodium dodecyl sulfate polyacrylamide gels and then blotted on polyvinylidene difluoride membranes (Millipore). The membranes were then blocked for 1 h in PBS-Tween (137 mM NaCl, 2.7 mM KCl, 1.4 mM KH_2PO_4, 8.1 mM Na_2HPO_4, 0.01% Tween 20, pH 7.3) containing 10% dry milk. First and second antibodies were diluted 1:1000 to 1:5000 in PBS-Tween containing 3% dry milk and successively incubated with the membranes after thorough washing with PBS-Tween. Second antibodies were either swine anti-rabbit immunoglobulins or rabbit anti-mouse immunoglobulins (Dako, Glostrup, Denmark) labeled with horseradish peroxidase. Detection was carried out with ECL (Amersham Pharmacia Biotech) according to the provider.

ELISA for PrP—ELISA plates were coated by overnight incubation with 0.1 ml of carbonate buffer (15 mM Na_2CO_3, 35 mM $NaHCO_3$, 0.02% NaN_3, pH 9.6) containing 1 μg of monoclonal antibody 6H4 at 4 °C per well. The plates were blocked with 0.2 ml of RPB containing 0.01% Tween 20 (RPB-Tween) and 10% dry milk per well for 1 h at 37 °C. The samples were prepared by diluting bovine brain homogenate (*e.g.* 200, 165, 130, 95, 60, and 25 μl) or partially purified PrP to 400 μl with RPB-Tween additionally containing either 5% dry milk or 1:2 diluted PrP null mouse or fish brain homogenate as indicated. All samples were incubated at 4, 25, or 37 °C for 45–60 min, except the standard, which was incubated solely at 25 °C. Samples were loaded in triplicates to the plates (0.1 ml/well). Incubation was for 1 h at the temperature used for sample incubation (if required a standard was run on a separate plate). After washing with RPB-Tween, the bound PrP was quantified by successive incubation with two other antibodies (1 h each at 37 °C). One was C15S, and the other was a horseradish peroxidase-conjugated swine anti-rabbit antibody (Dako). The rabbit PrP antiserum was diluted 1:500 in RPB-Tween containing 3% dry milk, and the swine anti-rabbit antibody was diluted 1:300 in the same buffer. 0.1 ml/well was applied. After incubation the plates were washed with PBS-Tween. 0.2 ml of 2,2′-azinobis (3-ethylbenzthiazolinesulfonic acid) solution (Roche Molecular Biochemicals) per well was added for reaction with horseradish peroxidase. The plate was then measured at 405 nm in an ELISA reader. The calibration procedure with recombinant PrP is described elsewhere (3). To create a standard, bovine brain homogenate was diluted with fish brain homogenate to a concentration corresponding to 75 ng/ml. A 0.1-ml concentration per well of a 1:2 dilution in RPB-buffer of this standard was included in each plate to determine the length of the horseradish peroxidase reaction. The *A* of the plates was read when the standard reached an *A* between 0.900 to 1.100. To allow comparison of the results of different plates, zero values were subtracted first, and then all results were divided by the value of the standard. Its optical density (75 ng of PrP/ml) became 1.000 at this step.

Partial Purification of PrP^C—Pieces of brain tissue (about 10 g) were homogenized in 10 ml of a 320 mM sucrose solution per g (wet weight) with an Ultra-Turrax T25 (Janke and Kungel). The homogenate was cleared by a short (5 min) centrifugation at 7000 × *g*. The supernatant was separated from the pellet and diluted with RPB-Tween and guanidine thiocyanate to 0.1 M guanidine thiocyanate. The solution was transferred to a 200-ml glass bottle with an airtight metal cap. The bottle was incubated in a laboratory oven set at 150 °C (actual temperature, 150–160 °C) for 20 min. After cooling to room temperature, the homogenate was centrifuged again for 15 min at 7000 × *g*. The supernatant was dialyzed overnight against RPB-Tween diluted 1:5 with distilled water. Finally, the dialysate was concentrated in a vacuum evaporator to about one-tenth to one-fifteenth of the starting volume. Protein concentration was measured by the bicinchoninic acid (BCA) reagent kit obtained from Pierce, and the concentration of PrP^C was measured by ELISA.

Dot Plot Assay—The assay was adapted according to a procedure published elsewhere (38). Recombinant PrP, partially purified PrP^C, and thalamus homogenate were serially diluted in RPB-Tween containing 5% dry milk. Samples of 5 μl were applied to nitrocellulose membranes (Bio-Rad) and air dried. The membranes were transferred to RPB-Tween containing 5% dry milk and incubated for 1 h at room temperature. 6H4 and rabbit anti-mouse immunoglobulins (Dako), labeled with horseradish peroxidase, were diluted 1:1000 to 1:5000 in PBS-Tween containing 3% dry milk and then incubated with the membranes for 1 h after thorough washing with PBS-Tween. Detection was carried out with ECL (Amersham Pharmacia Biotech) according to the

THE JOURNAL OF BIOLOGICAL CHEMISTRY jbc

TABLE I
Partial purification of PrP^C

	Volume	Total protein[a]	PrP^C[b]	Purification of PrP^C[c]
	ml	*mg/ml*	*ng/ml*	
Homogenate	110	2.4	43	1.0
Supernatant after heat treatment and centrifugation	90	0.6	37	3.4
Dialysate	115	0.3	34	6.3
Dialysate after vacuum evaporation	8	2.2	262	6.7

[a] As measured by the BCA-assay.
[b] As measured by the ELISA.
[c] In respect to total protein.

provider.

BS^3 Cross-linking—The homobifunctional cross-linker bis(sulfosuccinimidyl)-suberate (BS^3) was obtained from Pierce. A solution of 5 mM BS^3 in 5 mM sodium citrate buffer (pH 5.0) was freshly prepared. Four 50-μl samples of partially purified PrP^C were diluted with 0, 1.9, 9.5, and 38.0 μl of 5 mM BS^3 and water to 95 μl. After 20 min 5 μl of 1.5 M Tris buffer pH 6.8 was added to all samples to stop the reaction. Fifteen min later the samples were mixed 1:2 with sample buffer and analyzed on Western blots.

Size Exclusion Column Chromatography—A 30-cm column having a diameter of 1 cm was filled with Macro-Prep S.E. 1000/40 (Bio-Rad) according to the instructions of the provider. The column was washed and run with RPB-Tween. The typical flow rate was 0.47 ml/min. Fractions of 0.75 ml were collected. Calibration was done by running reconstituted gel filtration standards (Bio-Rad). For PrP analysis samples of 0.75 ml of partially purified PrP^C were loaded. All 35 fractions collected were analyzed for protein by the BCA reagent kit (Pierce) and for PrP by ELISA.

Calculations—For calculations Microsoft Excel was used, and for statistics Statistix Analytical software was used. For calculation the molecular weight of both the recombinant PrP and PrP^C was assumed to be 24,000.

RESULTS

A Native PrP^C Fraction Detected by ELISA

A bovine PrP^C-specific immuno-sandwich ELISA was developed and calibrated with recombinant PRP (3). To learn more about the nature of PrP^C detected by this assay, PrP^C was partially purified from normal bovine brain thalamus using the ELISA as a purification guide (Table I). In a first step, heat-labile proteins were precipitated by heat treatment. Most proteins, but little of the PrP under consideration, were precipitated by this procedure. After removing the precipitate by centrifugation, the supernatant was dialyzed and finally concentrated by vacuum evaporation. A Western blot of relevant samples is shown in Fig. 1. Bands having approximate molecular weights of 25,000 and 28,000–35,000 were observed in untreated brain homogenate. In partially purified fractions the patterns of the bands at 28,000–35,000 remained mainly unchanged by the heat treatment (compare *lanes a* and *c* in Fig. 1). However, their intensity was markedly reduced (compare *lanes a* and *b* in Fig. 1), and an at least 7-fold concentration was needed to restore it.

Quantification of the PrP bands of homogenates in Western blots (Fig. 1*a*) revealed no correspondence with the quantitative results obtained by the ELISA (Table I), suggesting that not all PrP^C was detected. For further quantification, a dot plot assay was used (38). Recombinant PrP, partially purified PrP^C, and thalamus homogenate were serially diluted, adsorbed to nitrocellulose membranes, and tested for PrP^C by immunological methods using 6H4 as the detecting antibody (see "Materials and Methods"). The relative amount of PrP in the different samples was compared with the known amount of recombinant PrP. In brain homogenate, about 10 times more PrP^C was detected with the dot blot assay than with the ELISA. But the amount of partially purified PrP^C detected both by the dot plot assay and by the ELISA corresponded well with each other

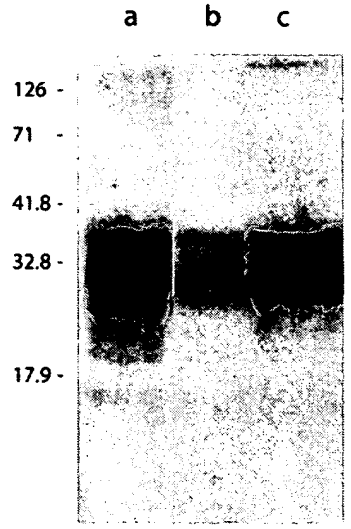

FIG. 1. **Western blot of partially purified PrP^C (see Table I) on a 12% acrylamide slab gel.** *Lane a*, brain homogenate. Western blot staining intensity does not correlate in this fraction with the 43 ng/ml PrP^C detected by the ELISA. *Lane b*, supernatant of the heat-treated and centrifuged brain homogenate. 37 ng/ml PrP^C were detected by the ELISA in this fraction, and Western blot staining intensity does correlate. *Lane c*, the same as in *lane b* but concentrated by vacuum evaporation to 262 ng/ml PrP^C. The position and molecular weight (×1000) of standards are given on the *left*. The bands were developed with 6H4 diluted 1:500.

(Fig. 2). In conclusion, the ELISA detected only about 10% of the PrP^C present in untreated thalamus homogenate, and only this fraction was actually partially purified. The nature of the remaining PrP^C, not detected by the ELISA, was not analyzed further.

Dose-response Curve

When serial dilutions of PrP^C were measured with the ELISA, a quadratic dose-response curve was obtained (Fig. 3). The shape of the curve did not depend on the concentration of the antibody used nor on the composition of the diluting agent. The dose response was linear when the concentration of the first, second, or third antibody (1:1000 to 1:100) was varied and the PrP^C concentration was kept constant. With no difference in the result, fish brain homogenate, nonfat dry milk (10%), and brain homogenate of PrP null mice were tested as diluting agents. The bovine brain homogenate could be diluted even without added proteins. However, the results were quite inconsistent, and therefore the dilutions were routinely done with proteins included in the diluting buffer.

The dose-response curves of PrP^C in untreated brain homogenate and partially purified PrP^C were indistinguishable when tested at the same concentration range. But the size and curvature of the dose-response curve did depend on the temperature of the samples at the point of time when they were loaded to the ELISA plates (4, 25, and 37 °C were tested; see Fig. 3). We concluded that the nonlinear dose response was a property of PrP^C and not an artifact of the assay.

The quadratic nature of the dose-response curve suggested a monomer-dimer equilibrium of PrP^C, with mostly dimers contributing to the measured *A*. To prove this hypothesis, we attempted to fit the experimentally obtained *A* by mathematical modeling based on the law of thermodynamics and of mass action.

Accordingly, six different PrP^C concentrations between 0.2 and 1.6 nM were selected. A sample of each was incubated at three different temperatures, 0, 25, and 37 °C, and measured in the ELISA. The averaged results of the optical density of at

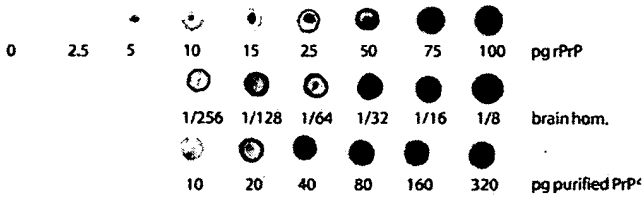

FIG. 2. **Semiquantitative dot plot assay of serial dilutions of recombinant PrP (*rPrP*), bovine brain homogenate (thalamus), and partially purified PrP^C.** 5 μl of each solution were pipetted at each spot. All dilutions were done in 5% dry milk. The concentration of purified PrP^C stock solution was 262 ng/ml (Table I). According to ELISA measurements the respective concentration was 86 ng/ml in the brain homogenate (*brain hom.*). The plot was developed with 6H4 diluted 1:500.

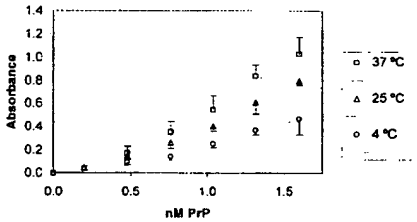

FIG. 3. **Nonlinear dose-response curves of PrP^C in respect to sample incubation temperature.** The diluted samples were incubated at 4, 25, or 37 °C before loading to the ELISA plates. For each point the average and the standard deviation of at least three independent experiments are shown. The *lines* represent calculated values. Calculations were done according to a dimer-monomer equilibrium model of PrP^C, with $A = \alpha[PrP_2]$. For the calculation of $[PrP_2]$ see "Results".

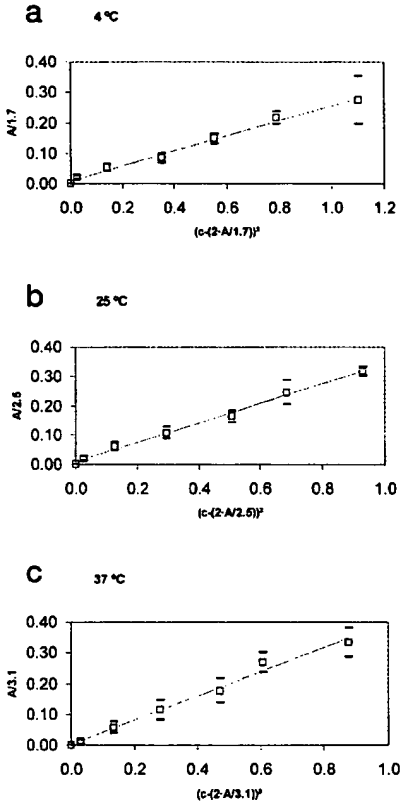

FIG. 4. **To find the values of the dissociation constant K for each of the three temperatures tested (4 (*a*), 25 (*b*), or 37 °C (*c*)), the respective A was divided by a selected value of α (*y* axis) and plotted against $(c - (2\cdot(A/\alpha)))^2$ (*x* axis).** The value of α (1.7 nM^{-1} at 4 °C, 2.5 nM^{-1} at 25 °C, and 3.1 nM^{-1} at 37 °C) was chosen such that the resulting values could be connected by a straight line by linear regression with the slope K (0.25 nM^{-1} at 4 °C, 0.33 nM^{-1} at 25 °C, and 0.39 nM^{-1} at 37 °C).

least three independent experiments were used for subsequent calculations (Fig. 3). In this respect, the total concentration (nM) of soluble PrP^C in each of the samples was designated "*c*", the monomer concentration was designated "[PrP]," and the hypothetical dimer concentration was designated "$[PrP_2]$."

$$c = [PrP] + 2\cdot[PrP_2] \quad \text{(Eq. 1)}$$

According to our hypothesis, A should obey equation 2,

$$A = \alpha\cdot[PrP_2] \quad \text{(Eq. 2)}$$

where α is a proportionality constant representing the efficiency of PrP^C binding to 6H4, of C15S binding to PrP^C, of the swine antibody binding to the rabbit antibody, and finally the horseradish peroxidase color reaction.

In addition, [PrP] and $[PrP_2]$ are connected by the law of mass action with the association constant K (equation 3).

$$[PrP_2] = K\cdot[PrP]^2 \quad \text{(Eq. 3)}$$

With known K, both [PrP] and $[PrP_2]$ can be calculated for each dilution c by first solving the quadratic equation 4 (a combination of equations 1 and 3) for [PrP] and then introducing the results into equation 1 or 3.

$$2\cdot K\cdot[PrP]^2 + [PrP] - c = 0 \quad \text{(Eq. 4)}$$

With [PrP] and $[PrP_2]$ known, α can be calculated by fitting the results with the experimental values. To get an estimate for appropriate K values, we combined equations 1, 2, and 3 to create equation 5.

$$A/\alpha = K\cdot(c - (2\cdot(A/\alpha)))^2 \quad \text{(Eq. 5)}$$

Using each set of A values obtained at the three different incubation temperatures, we searched for values of α for which a plot of A/α *versus* $(c - (2\cdot(A/\alpha)))^2$ yielded a straight line through the origin with the slope K (Fig. 4). For most values of α, bizarre nonlinear plots were obtained. However, when using 1.7 nM^{-1} (4 °C), 2.5 nM^{-1} (25 °C), and 3.1 nM^{-1} (37 °C) for α, straight lines were obtained having slopes (K) of 0.25, 0.33, and 0.39 nM^{-1}, respectively (Fig. 4). As shown in Fig. 5, a plot of ln α_T *versus* $1/T$ yielded a straight line. In Fig. 3 the calculated dose-response curves are superimposed to the average of the experimental values.

When freshly prepared dilutions were incubated less than 30 min at the selected temperature before loading to the plates, the resulting A was usually higher than calculated (data not shown).

Calculation of the Change in Free Energy of the PrP Monomer-Dimer Equilibrium

The formula $\Delta G° = -RT \ln K$ was used to calculate the free energy of the dimerization reaction. The result was a change in free energy of $\Delta G° = -48.6$ kJ M^{-1} (with $K = 0.33$ nM^{-1} at 25 °C). To obtain the change in enthalpy ($\Delta H°$) and entropy ($\Delta S°$) of the equilibrium reaction, ln K_T *versus* $1/T$ was plotted (van't Hoff plot) (Fig. 6). The respective values were calculated form the slope and the intercept of the linear regression. The values obtained were 9.5 kJ M^{-1} for $\Delta H°$ and 0.2 kJ K^{-1} M^{-1} for $\Delta S°$.

Other Experiments Supporting PrP Dimer Formation

Recombinant PrP—Recombinant PrP has been reported to be a monomer by others (2, 39, 40). For verification, we investigated the aggregation of recombinant PrP by sedimentation velocity and sedimentation equilibrium. Both the resulting mo-

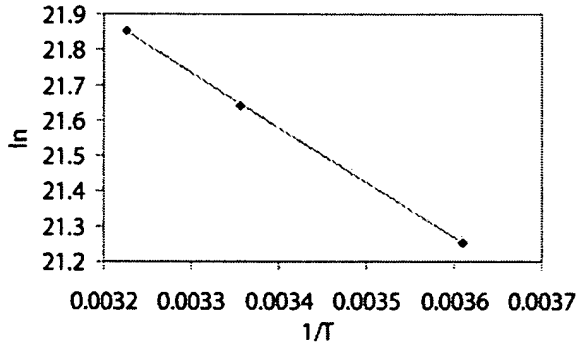

FIG. 5. **The values of ln α (with α = 1.7 nM^{-1} at 4 °C, 2.5 nM^{-1} at 25 °C, 3.1 nM^{-1} at 37 °C) are plotted against the inverse of the absolute temperature.** A straight line is obtained.

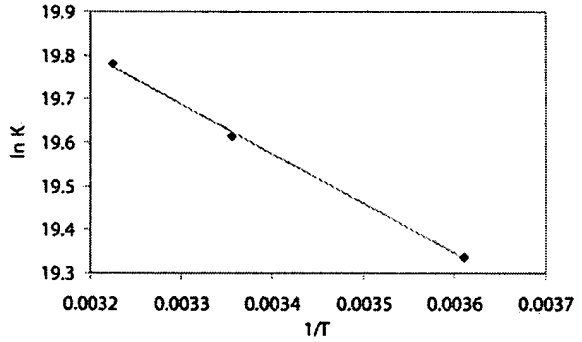

FIG. 6. **van't Hoff plot of ln K (with K = 0.25 nM^{-1} at 4 °C, 0.33 nM^{-1} at 25 °C, and 0.39 nM^{-1} at 37 °C) against the inverse of the absolute temperature.**

lecular weight of 25,000 and the sedimentation coefficient of $s_{20,w}$ = 2.1 gave no proof of dimerization or aggregation. When serial dilutions of recombinant PrP were tested in the ELISA, a linear, comparatively weak signal was observed (Fig. 7, *rectangles*). With PrP^C these assay conditions resulted in a quadratic dose-response curve (Figs. 3 and 7), suggesting that mostly dimers contribute to the signal (equation 2). Because dimers were not present in recombinant PrP, equation 2 was adapted to equation 6.

$$A_{rPrP} = \gamma \cdot c_{rPrP} = \gamma \cdot [rPrP] \quad \text{(Eq. 6)}$$

From the slope of the linear regression, the proportionality constant γ was calculated to be 0.1 nM^{-1} at 25 °C. All the results with (bovine) recombinant PrP described above did not depend on the protein composition of the diluent in which the protein was dissolved. The same outcome was observed when either 10% dry milk or brain homogenate from fish or PrP null mice was used.

Size Exclusion Column Chromatography and Cross-linking of PrP^C—To get additional evidence of the dimerization reaction besides dose-response curves, partially purified PrP^C was cross-linked by adding the homobifunctional cross-linker BS^3 and analyzed on Western blots. No high molecular weight bands were observed without the cross-linker (Fig. 8, *lane a*). Additional bands at the molecular weight of PrP^C dimers became visible when the samples had been incubated with the cross-linker (Fig. 8, *lanes b–d*). The distribution and intensity of those bands was varied with the effective BS^3 concentration. In the untreated sample PrP bands were observed at molecular weights of about 28,000, 33,000, and 35,000. When 0.1 mM BS^3 was added one additional band appeared at M_r 63,000. With 0.5 mM BS^3 two additional bands appeared, at M_r 63,000 and 76,000. With 2.0 mM BS^3 four additional bands at M_r 63,000,

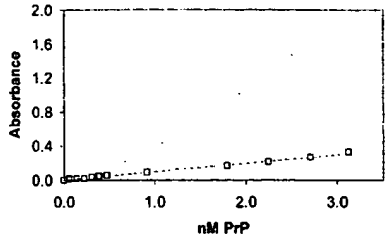

FIG. 7. **Dose-response curves of recombinant PrP.** The values (*rectangles*) are connected by a straight line having the slope of 0.1 nM^{-1}. The calculated A obtained with PrP^C under the same conditions is also shown.

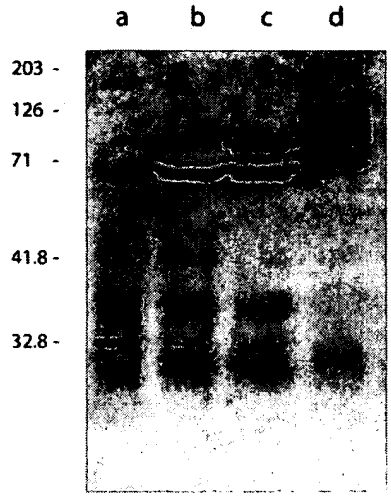

FIG. 8. **Western blot of partially purified PrP^C (see Table I) on a 10% polyacrylamide slab gel without (*lane a*) and with the cross-linker BS^3 added (*lanes b–d*).** Samples of partially purified PrP^C were diluted with 5 mM BS^3 in sodium citrate. After 20 min 1.5 M Tris buffer was added to the samples to stop the reaction. The samples were then mixed with sample buffer and analyzed. *Lane a*, partially purified PrP^C, no BS^3 added; *lane b*, 0.1 mM BS^3 added; *lane c*, 0.5 mM BS^3 added; *lane d*, 2.0 mM BS^3 added. The positions of molecular weight standards are given on the *left*.

76,000, 97,000, and at the top of the gel were observed with a significant reduction of the staining intensity of the PrP bands of lower molecular weight.

For additional verification of the PrP monomer-dimer equilibrium, size exclusion column chromatography was performed on a Bio-Rad Macro-Prep S.E. 1000/40 column. The column was calibrated with protein standards. Partially purified PrP^C was run over the column, and each fraction was analyzed both for protein by BCA and for PrP by ELISA. As shown in Fig. 9, the main peak of PrP was between the position of ovalbumin (M_r 44,000) and myoglobin (M_r 17,000). However, about 30% of the PrP detected ran as a shoulder in front of the M_r 44,000 marker but behind gamma globulin (M_r 158,000), indicating the presence of PrP polymers. The PrP^C fractions eluted from the column still behaved like a monomer-dimer equlibrium, as judged from the results of ELISA dose-response experiments. The size exclusion column profile with recombinant PrP was as published elsewhere (40), with no shoulder observed.

DISCUSSION

In the present study we used an antibody binding assay, cross-linking experiments, and column chromatography to investigate a monomer-dimer equilibrium of bovine brain PrP^C. Such protein-protein interactions were absent in bovine recombinant PrP, indicating that this protein does not reflect all aspects of PrP^C in animal tissues.

A distinctive PrP^C fraction was identified by our PrP-specific

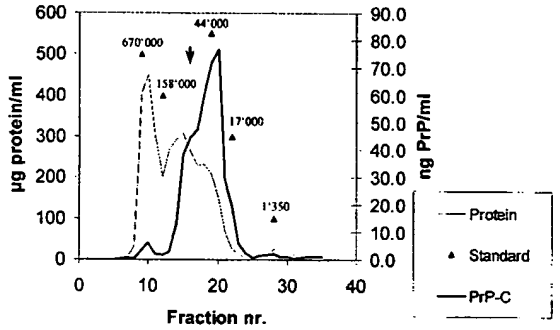

FIG. 9. **Size exclusion column chromatography of partially purified PrP^C.** Each fraction was measured for protein by the BCA protein assay (*dotted line*) and for PrP by the ELISA (*solid line*). The peak fractions of the molecular weight markers thyroglobulin (670,000), gamma globulin (158,000), ovalbumin (44,000), myoglobin (17,000), and vitamin B-12 (1350) are shown by *triangles*. *Arrow*, high molecular weight fraction of PrP^C.*nr.*, number.

ELISA procedure. The PrP^C in question could be separated from other PrP^C by heat treatment in the presence of 0.1 M guanidine thiocyanate and subsequent centrifugation. The use of bovine brain, instead of *e.g.* mouse brain, had the advantage that large amounts of precisely specified tissue (thalamus) were available. The quantitative difference in PrP^C content between untreated and partially purified samples was revealed by a semiquantitative dot plot assay (Fig. 2) and by Western blots (Fig. 1). Accordingly, only about 10% of total PrP^C was selectively purified by the heat treatment method, and only this fraction was detected by the ELISA in brain homogenates (Table I). The remaining PrP^C was removed together with membranes, cellular fragments, and other proteins. Most likely the purified PrP^C was soluble, either secreted (41, 42) or released during homogenization. A soluble form of PrP^C was described for human cerebrospinal fluid (8). In our Western blots the main difference after purification was a missing band at M_r 25,000 (Fig. 1). This band probably represents the unglycosylated PrP^C usually enclosed in the cell lumen (11, 43) and was precipitated together with other intracellular proteins. It is difficult to discriminate between native and denatured PrP^C in the absence of an accepted assay for PrP function, but usually in the absence of added detergents proteins remaining in solution are not denatured. Therefore the PrP^C detected seems not to be denatured by the treatment, and its heat stability was comparable with that of the infective PrP isoform PrP^{Sc} (21, 22).

Quantification of ELISA results is difficult with nonlinear dose-response curves. We observed such a curve in our PrP^C-specific ELISA (Fig. 3). We thoroughly investigated the cause of this nonlinearity. In a first series of experiments we excluded artifacts caused by protease digestion, by the diluting agent, or by other experimental procedures. We verified that it was not connected to the antibody concentration. We finally concluded it had to be an intrinsic property of the detected PrP^C. The quadratic nature of the curve suggested a monomer-dimer equilibrium of PrP^C as the most likely explanation, with most of the antibody binding to the dimeric form. Based on this hypothesis, we were able to describe the nonlinear dose-response curve by the law of mass action and by the law of thermodynamics. We predicted, for example, that according to the law of thermodynamics both the intensity and curvature of the results should be dependent on the temperature of the sample at the time of its incubation on the plates. This actually was observed and was a main argument for further investigations.

The conclusion was further supported by a linear dose-response curve obtained when recombinant PrP was tested under the same conditions (Fig. 7). If the nonlinear dose response was evidence of PrP^C dimerization, then the linear dose response of recombinant PrP should be evidence of a monomeric form. We have shown by equilibrium centrifugation that recombinant PrP is indeed present as a monomer, as suggested by others (39, 40). In addition, with recombinant PrP the proportionality constant (γ in equation 6) was only 4% of that observed with tissue-derived PrP^C (α in equation 2). Therefore, the affinity of the antibody to PrP monomers was only about 4% as compared with PrP dimers, allowing monomers to be omitted in equation 2. We do not know why C15S would preferentially bind to dimers. The most logical explanation for this phenomenon is that both antibody-binding sites are used because of the close proximity of two epitopes. Such a constellation would be present in a dimeric form of PrP^C.

Mathematical replication of the quadratic dose-response curve revealed the dissociation constant K of the monomer-dimer equilibrium reaction of PrP^C. This value should be regarded as an approximation because the experimental error of the data was up to 15% (3). However, the value could be fitted accurately in a van't Hoff plot (Fig. 6). The calculation of the free energy ($\Delta G° = -48.6$ kJ M^{-1}), enthalpy ($\Delta H° = 9.5$ kJ M^{-1}), and entropy ($\Delta S° = 0.2$ kJ K^{-1} M^{-1}) of the equilibrium reaction revealed ranges not unusual for protein-protein interactions. The temperature dependence of the proportionality constant α (equation 2) represented the temperature-dependent binding of PrP to 6H4. Only at this step the temperature of sample and incubation was varied, and the affinity of all other antibodies was not supposed to change therefore. Accordingly, α increased with increasing temperature and obeyed van't Hoff equations. A plot of $1/T$ *versus* ln α yielded a straight line (Fig. 5).

The hypothesis of a monomer-dimer equilibrium of PrP^C was further confirmed by cross-linking experiments and size exclusion chromatography. Addition of the cross-linker BS^3 to partially purified PrP^C resulted in additional bands having the molecular weight of PrP dimers (Fig. 8). Without the cross-linker added such bands were not visible in Western blots (Fig. 8, *lane a*), probably because the samples are denatured by mixing with sodium dodecyl sulfate and heating before electrophoresis. Detergents and denaturation obviously inhibit dimer formation because previously purified PrP^C was in monomeric form (1). BS^3 is a homobifunctional cross-linker, which cross-links primary amines. In proteins this is predominantly lysine (Pierce, product description). Bovine PrP has 11 lysines, with only one of them located within the signal sequence, *i.e.* there are ample possibilities for BS^3 cross-linking. With a spacer length of 11.5 Å, only proteins rather close to each other are cross-linked. Even in the partially purified fractions, PrP^C is outnumbered by more than 8000 (by weight) by unrelated proteins (Table I), thus arguing against unspecific cross-linking of PrP molecules simply by chance. With increasing BS^3 concentration, additional bands appeared, with the concomitant disappearance of the monomeric PrP. But even with a rather high BS^3 concentration (2 mM), PrP monomers were still observed, as would be expected for a monomer-dimer equilibrium, which always has some unbound monomers (Fig. 8, *lane d*).

We also performed size exclusion chromatography with partially purified PrP^C on a calibrated column. The advantage of this technique is that it reveals the molecular weights of the native proteins. The shortcoming is a rather steep exponential molecular weight gradient. As expected, the peak of soluble PrP^C appeared just behind ovalbumin (M_r 44,000), as did recombinant PrP (40). But as much as 30% of loaded PrP^C appeared in a broad shoulder located between gamma globulin (M_r 158,000) and ovalbumin (Fig. 9). This shoulder was never

observed with recombinant PrP. Because of the monomer-dimer equilibrium, faster-moving dimers will dissociate when they separate from the monomer pool, resulting in a deformation of the monomer peak toward higher molecular weights and not necessarily in the formation of an additional peak. Therefore, the existence of a PrP^C monomer-dimer equlibrium was supported by two additional and independent experiments.

The most obvious difference between tissue-derived PrP^C and recombinant PrP is the lack of glycosylation of the latter. Probably, a specific PrP conformation is induced by carbohydrate addition, exposing the amino acids responsible for the dimerization reaction (33). However, highly purified PrP^C has not been shown by others to form dimers *in vitro* (1). This obvious lack of dimerization could be explained either by denaturation during the purification process due to the use of high detergent concentrations. A PrP^C dimerization has been described for neuroblastoma cells (44), but the PrP dimer observed by these authors was covalently cross-linked. We speculate that the cross-linking was enzymatically induced by the tissue culture cells used.

Our results showing a spontaneous PrP^C monomer-dimer equilibrium support the concept of PrP dimer and heterodimer formation in prion propagation (32). Knowledge of the components involved in PrP interactions may not only allow the prediction of interspecies transmission of prion diseases but will also reveal possible points of intervention to interrupt the process of prion propagation.

Acknowledgment—We kindly thank Dr. A. Raeber, Institute of Neuropathology, University of Zürich, Switzerland for providing PrP null mice.

REFERENCES

1. Pergami, P., Jaffe, H., and Safar, J. (1996) *Anal. Biochem.* **236,** 63–73
2. Mehlhorn, I., Groth, D., Stockel, J., Moffat, B., Reilly, D., Yansura, D., Willet, W. S., Baldwin, M., Fletterick, R., Cohen, F. E., Vandlen, R., Henner, D., and Prusiner, S. B. (1996) *Biochemistry* **35,** 5528–5537
3. Meyer, R. K., Oesch, B., Fatzer, R., Zurbriggen, A., and Vandevelde, M. (1999) *J. Virol.* **73,** 9386–9392
4. Bolton, D. C., McKinley, M. P., and Prusiner, S. B. (1982) *Science* **218,** 1309–1311
5. Oesch, B., Westaway, D., Wälchli, M., McKinley, M. P., Kent, S. B. H., Aebersold, R., Barry, R. A., Tempst, P., Teplow, D. B., Hood, L. E., Prusiner, S. B., and Weissmann, C. (1985) *Cell* **40,** 735–746
6. Meyer, R. K., McKinley, M. P., Bowman, K. A., Braunfeld, M. B., Barry, R. A., and Prusiner, S. B. (1986) *Proc. Natl. Acad. Sci. U. S. A.* **83,** 2310–2314
7. Borchelt, D. R., Scott, M., Taraboulos, A., Stahl, N., and Prusiner, S. B. (1990) *J. Cell Biol.* **110,** 754–752
8. Tagliavini, F., Prelli, F., Porro, M., Salmona, M., Bugiani, O., and Frangione, B. (1992) *Biochem. Cell Biol.* **184,** 1398–1404
9. Prusiner, S. B., Groth, D., Bolton, D. C., Kent, S. B., and Hood, L. E. (1984) *Cell* **38,** 127–134
10. Bolton, D. C., Meyer, R. K., and Prusiner, S. B. (1985) *J. Virol.* **53,** 596–606
11. Haraguchi, T., Fisher, S., Olofsson, S., Endo, T., Groth, D., Tarentino, A., Borchelt, D. R., Teplow, D., Hood, L., Burlingame, A., Lycke, E., Kobata, A., and Prusiner, S. B. (1989) *Arch. Biochem. Biophys.* **274,** 1–13
12. Stahl, N., Borchelt, D. R., Hsiao, K., and Prusiner, S. B. (1987) *Cell* **51,** 229–240
13. Pan, K.-M., Stahl, N., and Prusiner, S. B. (1992) *Protein Sci.* **1,** 1343–1352
14. Riek, R., Hornemann, S., Wider, G., Billeter, M., Glockshuber, M., and Wüthrich, K. (1996) *Nature* **382,** 180–182
15. Morillas, M., Swietnicki, W., Gambetti, P., and Surewicz, W. K. (1999) *J. Biol. Chem.* **274,** 36859–36865
16. Viles, J. H., Cohen, F. E., Prusiner, S. B., Goodin, D. B., Wright, P. E., and Dyson, J. H. (1999) *Proc. Natl. Acad. Sci. U. S. A.* **96,** 2042–2047
17. Brown, D. R., Wong, B.-S., Hafiz, F., Clive, C., Haswell, S. J., and Jones, I. M. (1999) *Biochem. J.* **344,** 1–5
18. Prusiner, S. B. (1982) *Science* **216,** 136–144
19. Prusiner, S. B., McKinley, M. P., Bowman, K. A., Bolton, D. C., Bendheim, P. E., Groth, D. F., and Glenner, G. G. (1983) *Cell* **35,** 349–358
20. Aguzzi, A., and Weissmann, C. (1997) *Nature* **389,** 795–798
21. Safar, J., Roller, P. P., Gajdusek, D. C., and Gibbs, C. J. (1993) *Protein Sci.* **2,** 2206–2216
22. Brown, P., Rohwer, R. G., Green, E. M., and Gajdusek, D. C. (1982) *J. Infec. Dis.* **145,** 683–687
23. Prusiner, S. B., Scott, M. R., DeArmond, S. J., and Cohen, F. E. (1998) *Cell* **93,** 337–348
24. Gabizon, R., Rosenmann, H., Meiner, Z., Kahana, I., Kahana, E., Shugart, Y., Ott, J., and Prusiner, S. B. (1993) *Am. J. Hum. Genet.* **53,** 828–835
25. Hsiao, K., Baker, H. F., Crow, T. J., Poulter, M., Owen, F., Tewiliger, J., Westaway, D., Ott, J., and Prusiner, S. B. (1989) *Nature* **338,** 342–345
26. Lugaresi, E., Medori, R., Montagna, P., Baruzzi, A., Cortelli, P., Lugaresi, A., Tinuper, P., Zucconi, M., and Gambetti, P. (1986) *N. Engl. J. Med.* **315,** 997–1003
27. Prusiner, S. B. (1998) *Brain Pathol.* **8,** 499–513
28. Prusiner, S. B. (1997) *Science* **278,** 245–251
29. Peretz, D., Williamson, R. A., Matsunaga, Y., Serban, H., Pinilla, C., Bastidas, R. B., Rozenshteyn, R., James, T. L., Houghten, R. A., Cohen, F. E., Prusiner, S. B., and Burton, D. R. (1997) *J. Mol. Biol.* **273,** 614–622
30. Korth, C., Stierli, B., Streit, P., Moser, M., Schaller, O., Fischer, R., Schulz-Schaeffer, W., Kretzschmar, H., Raeber, A., Braun, U., Ehrensperger, F., Hornemann, S., Glockshuber, R., Riek, R., Billeter, M., Wüthrich, K., and Oesch, B. (1997) *Nature* **390,** 74–77
31. Kocisko, D. A., Come, J. H., Priola, S. A., Chesebro, B., Raymond, G. J., Lansbury, P. T., and Caughey, B. (1994) *Nature* **370,** 471–474
32. Prusiner, S. B., Scott, M., Foster, D., Pan, K.-M., Goth, D., Mirenda, C., Torchia, M., Yang, S.-L., Serban, D., Carlson, G. A., Hoppe, P. C., Westaway, D., and DeArmond, S. J. (1990) *Cell* **63,** 673–686
33. Horiuchi, M., and Coughey, B. (1999) *EMBO J.* **18,** 3193–3203
34. Kaneko, K., Peretz, D., Pan, M.-K., Blochberger, T. C., Wille, H., Gabizon, R., Griffith, O. H., Cohen, F. E., Baldwin, M. A., and Prusiner, S. B. (1995) *Proc. Natl. Acad. Sci.* U. S. A. **92,** 11160–11164
35. Kaneko, K., Zulianello, L., Scott, M., Cooper, C. M., Wallace, A. C., James, T. L., Cohen, F. E., and Prusiner, S. B. (1997) *Proc. Natl. Acad. Sci. U. S. A.* **94,** 10069–10074
36. Telling, G. C., Scott, M., Mastrianni, J., Gabizon, R., Torchia, M., Cohen, F. E., DeArmond, S. J., and Prusiner, S. B. (1995) *Cell* **83,** 79–90
37. Goldmann, W., Hunter, N., Martin, T., Dawson, M., and Hope, J. (1991) *J. Gen. Virol.* **72,** 201–204
38. Serban, D., Taraboulos, A., DeArmond, S. J., and Prusiner, S. B. (1990) *Neurology* **40,** 110–117
39. Donne, D. G., Viles, J. H., Groth, D., Mehlhorn, I., James, T. L., Cohen, F. E., Prusiner, S. B., Wright, P. W., and Dyson, H. J. (1997) *Proc. Natl. Acad. Sci. U. S. A.* **94,** 13452–13457
40. Jackson, G. S., Hosszu, L. L. P., Power, A., Hill, A. F., Kenney, J., Saibil, H., Craven, C. J., Waltho, J. P., Clarke, A. R., and Collinge, J. (1999) *Science* **283,** 1935–1937
41. Borchelt, D. R., Rogers, M., Stahl, N., Telling, G., and Prusiner, S. B. (1993) *Glycobiology* **3,** 319–329
42. Hay, B., Prusiner, S. B., and Lingappa, V. (1987) *Biochemistry* **26,** 8110–8115
43. Rogers, M., Taraboulos, A., Scott, M., Groth, D., and Prusiner, S. B. (1990) *Glycobiology* **1,** 101–109
44. Priola, S. A., Caughey, B., Wehrly, K., and Chesebro, B. (1995) *J. Biol. Chem.* **270,** 3299–3305

TULYMENIDOU M.
F-TSE

BMC Infectious Diseases

BioMed Central

Research article

Open Access

A short purification process for quantitative isolation of PrP^{Sc} from naturally occurring and experimental transmissible spongiform encephalopathies

Magdalini Polymenidou[1], Susan Verghese-Nikolakaki[1], Martin Groschup[2], Melanie J Chaplin[3], Mick J Stack[3], Andreas Plaitakis[4] and Theodoros Sklaviadis*[1]

Address: [1]Laboratory of Pharmacology, Department of Pharmaceutical sciences School of Health Sciences, Aristotle University of Thessaloniki, Thessaloniki 54124, Greece, [2]Institute of Novel and Emerging Infectious Diseases, Federal Research Centre for Virus Diseases of Animals, Boddenblick 5a17498 Insel Riems, Mecklenburg-Vorpommern, Germany, [3]Veterinary Laboratories Agencies, Weybridge, UK and [4]Department of Neurology, University of Crete, School of Health Sciences, Heraklion, Crete, Greece

E-mail: Magdalini Polymenidou - Magdalini.Polymenidou@pty.usz.ch; Susan Verghese-Nikolakaki - sverg@pharm.auth.gr; Martin Groschup - mrtin.groschup@rie.bfav.de; Melanie J Chaplin - Melanie.M.J.Chaplin@vla.defra.gsi.gov.uk; Mick J Stack - m.j.stack@vla.defra.gsi.gov.uk; Andreas Plaitakis - plaitakis@med.uch.gr; Theodoros Sklaviadis* - sklaviad@auth.gr

*Corresponding author

Published: 8 October 2002

BMC Infectious Diseases 2002, 2:23

Received: 27 June 2002
Accepted: 8 October 2002

This article is available from: http://www.biomedcentral.com/1471-2334/2/23

Abstract

Background: Transmissible spongiform encephalopathies (TSEs) are neurodegenerative diseases affecting both humans and animals. They are associated with post-translational conversion of the normal cellular prion protein (PrP^{C}) into a heat- and protease-resistant abnormal isoform (PrP^{Sc}). Detection of PrP^{Sc} in individuals is widely utilized for the diagnosis of prion diseases.

Methods: TSE brain tissue samples have been processed in order to quantitatively isolate PrP^{Sc}. The protocol includes an initial homogenization, digestion with proteinase K and salt precipitation.

Results: Here we show that over 97 percent of the PrP^{Sc} present can be precipitated from infected brain material using this simple salting-out procedure for proteins. No chemically harsh conditions are used during the process in order to conserve the native quality of the isolated protein.

Conclusion: The resulting PrP^{Sc}-enriched preparation should provide a suitable substrate for analyzing the structure of the prion agent and for scavenging for other molecules with which it may associate. In comparison with most methods that exist today, the one described in this study is rapid, cost-effective and does not demand expensive laboratory equipment.

Background

Scrapie, bovine spongiform encephalopathy (BSE) and Creutzfeldt-Jakob disease (CJD) are all related transmissible spongiform encephalopathies, the common major causative agent of which is believed to be a protease- and heat-resistant, beta-sheet rich isoform (PrP^{Sc}) of the normal cellular prion protein (PrP^{C}) [1]. The patho-physiological identity of the infectious agent has not been

understood so far, although there is sufficient proof that the conversion of PrP^{C} to PrP^{Sc} plays a crucial role during pathogenesis [2]. Clinically, the disease is characterized by long incubation periods which, as in the recent crossover of the bovine spongiform encephalopathy (BSE) agent to humans, may be prolonged further when the disease is transmitted from one species to another. Necropsy findings from TSE cases generally show accumulation of PrP^{Sc} in the brain, accompanied by extensive neurodegeneration, which is also the major cause of fatality. Similar deposits have been demonstrated as well, in some of the peripheral organs and the lymphoreticular compartment in certain species [3,4]. Today, the ultimate confirmation of the disease comes only after post-mortem examination of the brain, even though extensive research being carried out in the field offers hope for pre-clinical diagnosis through the detection of PrP^{C} in tonsils or body fluids.

Clinical signs of neurodegeneration, supported by the presence of characteristic microscopic lesions and PrP^{Sc} in the brain [5] are signs that eventually lead to the diagnosis of TSEs. As well, the clinical indications, histopathological symptoms and glycoform pattern of PrP^{Sc} isolated from experimental animals are typical of the 'strain' or species origin of the inoculums [6]. A number of *in vitro* assays have been reported for the detection of PrP^{Sc} in the tissue, including the dot-blot immunoassay, enzyme-linked immunosorbent assay (ELISA), immunocytochemistry, Western blot analysis, and recently, capillary electrophoresis [7–12]. At present, the template source of PrP^{Sc} for all these procedures is either the crude brain homogenate or a harshly processed preparation called scrapie associated fibrils (SAF). While these procedures take relatively less time to perform, *in vivo* bioassays requiring the inoculation of laboratory animals such as mice or hamsters with the infected material have been used over the years for the detection of prion diseases. The main disadvantage of the bioassay technique however, lies in the lengthy incubation period that incurs between inoculation and appearance of clinical symptoms, compounded by the expense of maintaining large animal colonies. Therefore, scientists working in the field of prion diseases most often prefer *in vitro* methods of diagnosis when there is no absolute requirement to use laboratory animals.

In order to routinely detect PrP^{Sc} in specimens, reliable, quantitative and yet relatively simple protocols are necessary for its isolation. Here we report that over 97% of total PrP^{Sc} in a brain sample may be detected *in vitro* following an exceptionally short and simple precipitation method of enrichment for the protein. The method was validated within a European Union consortium of several laboratories for standardization of the diagnosis of BSE and scrapie by estimating the limiting dilution of detection of PrP^{Sc} from infected brain. Using multiple preparations from five different species, we also showed that the method described herein concentrated PrP^{Sc} without altering the PrP^{Sc} glycoform pattern, a quality that makes this protocol suitable for glycotype analyses for species or strain identification of the infectious agent.

Methods

Experimental material

Infected brain tissues from mouse scrapie, strain ME7, were obtained from FRCVD, Tubingen, Germany and mouse BSE, strain 301 V from VLA, Weybridge, UK. Brain tissues from sheep with natural scrapie or normal sheep were obtained from the School of Veterinary Medicine, Aristotle University, Thessaloniki (courtesy Prof. O. Papadopoulos). BSE brain samples were obtained from VLA, Weybridge, UK and the human CJD brain samples came from recently reported cases of sporadic CJD (sCJD) from within Greece [13]. All tissues were stored at -70°C until use. Autolytic deterioration was observed only in tissues from the BSE cases due to handling during transportation etc. Area of choice of the tissue for each species depended on relevant data from our own and other laboratories.

Homogenization

A 10% homogenate of the tissue was prepared in cold homogenization buffer (0.5% IGEPAL CA-630 (NP-40) and 0.5% sodium deoxycholate in phosphate buffered saline, pH 7.4) using a polytron homogenizer (Kinematica, Switzerland) at setting 4, twice for 6 seconds each. For limiting dilution experiments, the polytron was replaced with the OmniGLH homogenizer (CAMLAB, UK) which worked equally well with disposable probes, a very useful factor to be considered while attempting multiple homogenizations with large number of samples. All homogenates were stored in aliquots at -70°C until use and thawed only once.

Proteinase K treatment

On the day of use, 100 µl of homogenate was diluted with an equal volume of the homogenization buffer and incubated with proteinase K (Sigma-Aldrich) for 1 hour at 37°C with mild rocking. Concentrations of proteinase K used varied with the species and are provided separately with each figure. The reaction was stopped by the addition of 5 mM PMSF (Sigma-Aldrich), a protease inhibitor.

Precipitation of PrP^{Sc}

The proteinase K digestion mixture was diluted with 300 µl phosphate buffered saline (PBS) pH 7.4 and brought to 10% NaCl by the addition of an equal volume of 20% NaCl in PBS containing 0.1% sarkosyl. The tube was kept in ice for 10 minutes with occasional shaking. After centrifugation at 16,000 g for 10 minutes at room temperature, the pellet was washed once with 25 mM Tris-HCl buffer, pH 8.8 containing 0.05% sarkosyl (w/v) and cen-

trifuged again at 16,000 g for 10 minutes. The final, enriched pellet was then resuspended in 2.5× loading buffer 10% v/v glycerol, 50 mM Tris pH 6.8, 2% w/v SDS, 3% β-mercaptoethanol and used for detecting PrP^{Sc} by western blotting. Normally, for a starting volume of 100 µl homogenate (10 mg brain equivalent) the final pellet was resuspended in the same volume (i.e. 100 µl) of loading buffer, of which 30 µl (3 mg brain equivalent) was loaded per lane for the western blot analysis.

In order to estimate any loss of PrP^{Sc} during the extraction procedure, total proteins in the supernatants from both the precipitation step and the wash step were precipitated with 9 volumes of methanol overnight at -70°C. After centrifugation at 16,000 g, the supernatants were discarded and the pellets resuspended in loading buffer (see above) and used for western blot detection of PrP^{Sc} as described below.

Polyacrylamide gel electrophoresis and western blotting of PrP^{Sc}

Proteins were subjected to electrophoresis using a 12 or 15% Laemmli sodium dodecyl sulfate polyacrylamide gel (SDS-PAGE) and transferred to a PVDF membrane (Sigma-Aldrich) and incubated with the primary antibody for 1 hr. This was followed by washes with PBS, pH 7.4 and a further incubation for 35 minutes with the corresponding secondary antibody. All incubations and washes were done at room temperature. The primary antibodies were SAL1 (manuscript in preparation), or 6H4 (Prionics AG, Switzerland) depending on the species being tested. Details of the use of primary and secondary antibodies is given in the figure legends. Following three washes of 15 min each, the reaction was visualized using the CDP star (New England Biolabs) chemiluminiscence detection technique according to manufacturer's instructions. The membranes were exposed to X-OMAT (Kodak) X-ray films for between 5 seconds to 5 minutes depending on the degree of positivity in the starting material.

The films were scanned (Hewlett Packard ScanJet 6300C) and the positive signal analyzed and expressed as integrated optical density (IOD) using the Gel-Pro Analyzer 3.0 software. The percentage recovery of PrP^{Sc} in the final pellet (P) was then calculated using the formula:

$$\text{Percentage recovery of } PrP^{Sc} = \frac{IOD(P)\times 100}{IOD(W1)+IOD(W2)+IOD(P)}$$

Where P is the final pellet, W1 is the supernatant after salt-precipitation and W2 is the supernatant after the final wash.

Silver staining for total proteins

The initial crude homogenate, pellet after the final wash, and the supernatants after salt precipitation and the final wash, the latter two precipitated in 9 volumes of methanol at -70°C, were subjected to electrophoresis using an SDS-PAGE system as described earlier. To avoid overloading the gel, ten times less brain equivalent (0.3 mg) was loaded for the crude homogenate than for the other samples (3 mg each). The procedure used for staining was a standard method [27]. In short, the gel was fixed in 50% methanol and 12% (v/v) acetic acid for 1 hour, followed by incubation in 10% ethanol and 5% acetic acid (v/v) for another hour. This was followed by treatment with 3.4 mM potassium dichromate in 2.8 mM nitric acid after which the gel was washed with distilled water and incubated for 30 min with shaking in 20% (w/v) silver nitrate. The reaction was developed in 3% sodium carbonate containing 0.5 ml formaldehyde 37% (paraformaldehyde) per liter and stopped by the addition of 2.3 M citric acid when the bands were clearly visible. Intensities of the lanes due to total proteins were estimated as described above.

Estimation of the degree of brain positivity for scrapie and BSE

Pooled homogenates of cerebellum from scrapie positive sheep (P1) or brain stems from BSE positive cattle (P2) were prepared as described above. Similarly, homogenates were also prepared from healthy sheep (N1) or healthy cattle (N2). In order to achieve different degrees of tissue positivity, P1 and P2 were initially diluted up to 50% or 6.25% with N1 and N2, respectively, and the resulting mixtures then used for precipitating PrP^{Sc} as described in the steps above. Undiluted P1 and P2 served as positive controls (100% positivity) whereas N1 and N2 served as negative controls for these experiments. Prior to loading on the NuPage (Invitrogen) western blotting system, the final pellet from each sample was subjected to eleven 2-fold serial dilutions with loading buffer. The 6H4 monoclonal antibody was used to detect PrP^{Sc} on a PVDF membrane and the positive signal was analyzed on a Bio-Rad Fluor-S multiImager (Bio-Rad, USA).

Precipitation of PrP^{Sc} from different species

The validity of the current protocol to enrich for PrP^{Sc} from different species and its use in glycotyping, the technique currently employed for species and strain identification, was examined using both experimental and native TSEs. Homogenates of mouse scrapie or mouse BSE whole brain, native sheep scrapie cerebellum, BSE brain stem or sporadic CJD cortex were used for this purpose. PrP^{Sc} was precipitated from all species using 10% sodium chloride as described above and detected on a western blot using the polyclonal antibody SAL1. In order to perform glycoform analysis, band intensities of the double-, mono- or

non-glycosylated isoforms were determined in each sample and each glycoform was expressed as a percentage of the total signal obtained.

Results

Percentage recovery of PrP^{Sc} in the final pellet

The migration pattern of PrP^{Sc} in the final enriched pellet (P) and in the supernatants from the salt-precipitation (W1) and wash (W2) steps from a sheep scrapie sample is shown in Figure 1a. Loss of PrP^{Sc} in the discarded supernatants in the two preceding steps was estimated to allow the calculation of the degree of its recovery at the end of the procedure. PrP^{Sc}-specific signal was discerned as the classical three-band pattern representing the double-, mono- and non-glycosylated isoforms, each of which was typical of the individual species studied. The sum of the signals obtained from P, W1 and W2 accounted for total PrP^{Sc} in the starting material, and the percentage recovery of PrP^{Sc} was calculated as described in Methods. As shown in the inset table, as much as 97.4% of PrP^{Sc} was found in the pellet with minimal loss in the supernatants, either from the precipitation (2.08%) or the final wash step (0.5%). These calculations are indicative from this particular experiment, whereas variability of the recoveries is approximately 2%.

Estimation of total proteins using silver stain and estimation of the degree of purification of PrP^{Sc}

Figure 1b shows staining for total proteins in the crude homogenate (H) and in the fractions P, W1 and W2 that were produced through the sodium salt precipitation procedure, each expressed as integrated optical densities (IOD). Most cellular proteins remaining after protease K digestion were present in supernatant W1 that was discarded after salt precipitation, leaving relatively few proteins in W2, the supernatant from the wash, and in the final pellet, P. Intensity in lane H represents signal due to total proteins in 0.3 mg brain equivalent of the initial crude homogenate (the brain equivalent amount loaded with the total homogenate was ten times less in order to enable smooth running of the gel). All other lanes contain 3 mg brain equivalents each. The inset table shows values for intensities in lanes H and P, and gives the degree of purification of PrP^{Sc} in lane P as a result of enrichment. As may be seen, the IOD value in P (31.89) is 2 logs less than in H (3121.5) indicating an 100-fold reduction in total proteins in P. In conjunction with Figure 1a, where 97.4% of the total PrP^{Sc} is shown to be present in P, it is clear that the degree of purification of PrP^{Sc} in the final pellet was a hundred times that of the initial homogenate, H.

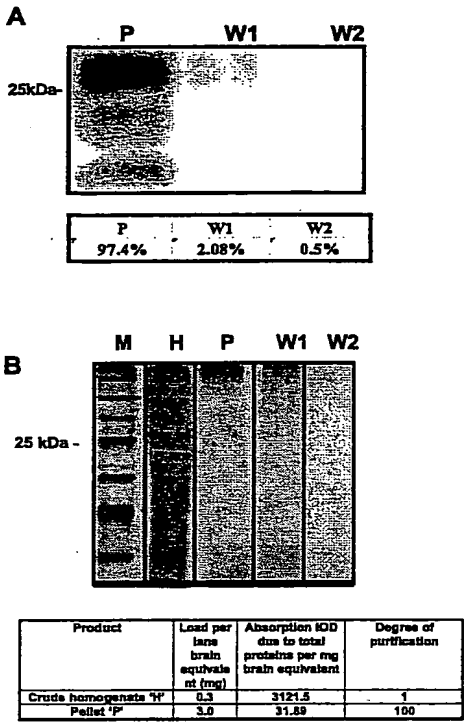

Figure 1

Comparison of PrP^{Sc} and total protein during the enrichment process. A) Western blots depicting the migration pattern of PrP^{Sc} in the final enriched pellet (P) and in the supernatants after the precipitation (W1) and the wash (W2) steps in native sheep scrapie. Total proteins in W1 and W2 were precipitated with 9 volumes of methanol over night at -70°C. SAL1 (1:3000) was used as the primary antibody and alkaline phosphatase labeled goat anti-rabbit IgG (1:1500, Roche) as the secondary antibody. Each lane contains 3 mg brain equivalent. The table shows percentage recoveries of PrP^{Sc} in P, W1 and W2. The estimations were made by first determining the values for integrated optical density (IOD) due to PrP^{Sc} for each lane. The sum of the values in P, W1 and W2 was then taken to be one hundred percent total PrP^{Sc} in the starting material. Values due to PrP^{Sc} in each of P, W1 and W2 were then deduced as percentages of the sum total as described in *Materials and Methods*. Proteinase K used was 30 μg per ml homogenate. B) Silver staining of H (starting undigested homogenate), P, W1 and W2 run on a SDS-PAGE system. All lanes contain 3 mg brain equivalent loads except for lane H which contains 0.3 mg of the same. Molecular weight markers are shown in lane M. It may be noticed that the some of the proteins present in H are also present in W1, in the discarded supernatant after the precipitation step. Lanes P and W2 contain few detectable proteins. The table provides a quantitative estimation of the degree of purification of PrP^{Sc} in P after taking into account, signals due to total proteins in lanes H and P respectively.

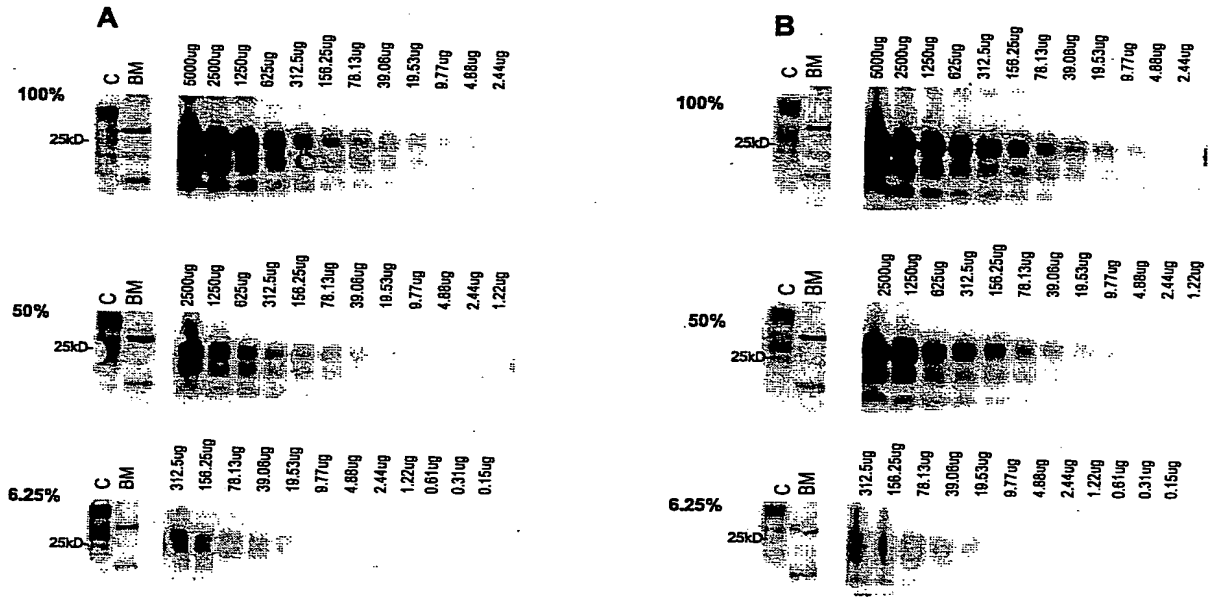

Figure 2
Comparison of signal detection after blending PrP^{Sc} positive and negative homogenates in different ratios in A) sheep scrapie and B) BSE. In each case, western blot analysis is shown for 100% positive tissue (top panels); 50% positive tissue (middle panels); and 6.25% positive tissue (bottom panels). Antibodies used were 6H4 (1:5000) and alkaline phosphatase labeled rabbit anti-mouse (1:5000), both from Prionics. Lanes show: C – 10% negative brain homogenate, unprocessed and without proteinase K digestion; BM – molecular weight marker. Amounts listed above other lanes indicate the amount of positive tissue equivalents loaded. Staining seen in the negative sample was considered to be due to improper digestion of the tissue. Amount of proteinase K used was 100 μg per ml homogenate in each case. The negative control and all test samples were processed by the described salt precipitation protocol. The signal seen in lane C may be attributed to cellular prion protein, PrP^{C}, present in normal brain tissue.

Estimation of degree of positivity in the tissue

Low limits of PrP^{Sc} detection are essential for a method to be successfully applied to the determination of animals in the pre-clinical stages of the TSE disease. It was therefore considered mandatory to test the capability of the current protocol for determining minimum positive tissue equivalents in normal tissue homogenates spiked to various degrees with infected tissue. The lower limit of detection of PrP^{Sc} using the current protocol was estimated using pooled brain homogenates in order to avoid sample to sample variations. Thus, pooled homogenates of cerebellum from scrapie positive sheep (P1) or brain stems from BSE positive cattle (P2) were used and similar homogenates from healthy sheep (N1) or healthy cattle (N2) served as negative controls. For both scrapie and BSE, the positive (100% positivity) and negative (0% positivity) homogenates were blended in ratios that provided final mixtures containing 100%, 50%, or 6.5 % positive tissue material. PrP^{Sc} was then precipitated from each of these and the lowest limits of detection were determined using western blot analysis. For both scrapie (Figure 2a) and BSE (Figure 2b) samples, the lowest detection limit ranged between 5–10 μg brain equivalents.

Precipitation of PrP^{Sc} from different species

Since TSEs affect a variety of species, we also tested the efficiency of the sodium chloride method of PrP^{Sc} enrichment on brain tissues of animals with natural and experimental forms of TSEs. This was considered important because of the species-related differences in the tissue distribution and glycoform patterns of PrP^{Sc}. Brain equivalents of 3 mg each in cases of scrapie, BSE and CJD, and 2 mg each in cases of mouse scrapie and mouse BSE were loaded into each lane of an SDS-PAGE gel for western blot

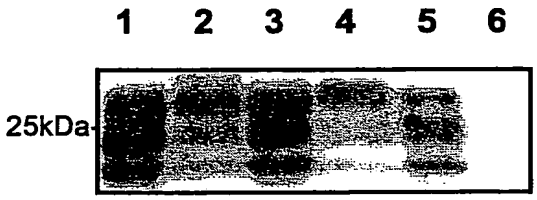

Figure 3
Detection of PrP^{Sc} in TSEs from different host species. Lanes show: 1 – mouse scrapie ME7, 2 – sheep scrapie, 3 – mouse BSE, 4 – BSE, 5 – sporadic CJD, 6 – normal sheep. Lanes 1 and 3 contain 2 mg and lanes 2, 4, 6 contain 3 mg brain equivalent load each. SAL 1 (1:3000) and alkaline phosphatase labeled goat anti-rabbit IgG (1:1500, Roche) were the primary and the secondary antibodies respectively. Amounts of proteinase K used per ml homogenate were 30 μg in the cases of mouse scrapie, sheep scrapie and BSE and 50 μg in the case of sCJD.

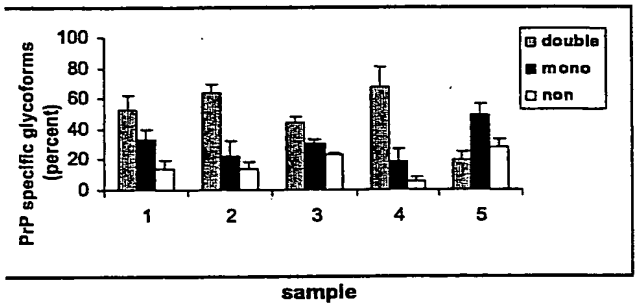

Figure 4
Glycoforms of PrP^{Sc} isolated from different species. Samples 1–5 represent ME7, sheep scrapie, mouse BSE, BSE and sporadic CJD respectively. Percentages of specific glycoform are shown as average + standard error for each species. Values shown were obtained from independent experiments with 7 ME7 samples, 8 sheep samples, 2 mouse BSE samples, 5 BSE samples and 5 sCJD samples. Bars represent percentage glycoforms of double, mono and non-glycosylated bands according to the insert.

analysis. It has been observed during routine laboratory practice, however, that with animals suspected to have TSEs or with doubtful positive signal for PrP^{Sc}, the load per lane could be increased up to 10 mg brain equivalents, thereby increasing the probability of detecting PrPSc. This is accomplished by resuspending the final pellet in a smaller volume of loading buffer. Mouse samples were particularly useful as standard controls for glycoform analyses as total brain homogenates were used in these cases and thus uniform patterns, uninfluenced by the choice of a certain area of the brain, were obtained on the western blot. Banding patterns representative of each species are shown in Figure 3. All samples were processed and electrophoresed simultaneously. The sporadic CJD (sCJD) case in lane 5 was of sporadic type 2 from Greece [13]. Quantitative estimations of the glycoforms for each species are given in the histogram in Figure 4. Average values and their standard errors were obtained for each species after analyzing multiple samples in each case. In all cases, the glycoform patterns presented by PrP^{Sc} matched those previously reported in the literature [14–16] and was not affected otherwise by the current method of enrichment.

Discussion

The first cases of BSE were reported in the United Kingdom [17] and since that time the cattle disease has been implicated as a causative agent for new variant CJD in humans [18,19]. Fears have also been raised that BSE may have crossed back into sheep [20,21] in the guise of sheep scrapie. Given this scenario, two aspects of prion disease monitoring need immediate attention. One is the pressing need for the establishment of reliable, rapid and, at the same time, sensitive protocols for the detection of TSEs from both animal and human sources. The other is that these methods should be easy to perform and cost-effective with minimal requirement for expensive equipment.

PrP^{Sc} remains the ultimate and sole determinant for a confirmatory diagnosis of TSE. Given this fact, it seems obvious that the successful, efficient extraction of this molecule is of utmost importance. We have shown here that it is now possible to enrich for PrP^{Sc} using sodium chloride precipitation and obtain an end product containing up to 97.4% of the total PrP^{Sc} in the tissue. Loss of PrP^{Sc} in the two wash steps during the procedure was negligible and might well be attributed to the handling of the material. The high degree of purification of PrP^{Sc} in the pellet at the end of the method was indicated by a general reduction in total proteins in the final enriched pellet (Figure 1b) suggesting a 100-fold purification for PrP^{Sc} in the latter. PrP^{Sc} could be extracted even more efficiently from mouse species with a recovery of 99.7% (data not shown), probably due to the uniform and homogeneous constitution of the tissue involved. The method was also

tested in more than one species to establish that the electrophoretic mobility of PrP^{Sc} thus obtained was not distorted as reported recently with sodium phosphotungstate salt [4]. Thus, PrP^{Sc} precipitated with sodium chloride salt in this manner would be well suited for TSE strain and species type analyses.

Early in the development of this protocol we noticed that the low speed debris usually discarded during most PrP^{Sc} purification procedures contained as much as 20–30% of the total protein in the tissue (personal observation). It was therefore considered useful to include tissue debris in the extraction procedure described in this study and not to use the common practice of 'clearing' tissue homogenates. As would be expected, and as was indeed seen by silver staining (Figure 1b), other molecules also were precipitated along with PrP^{Sc}. Although considered contaminants in the present preparation, these molecules could become suitable candidates when searching for other components including proteins, non-proteins or nucleic acids [22] that participate with PrP^{Sc} [23,24] in prion pathogenesis in the different intermolecular interactions during the course of the disease. The above protocol could be safely recommended as an alternative confirmatory protocol of the commercially available protocols taking into account the achieved concentration was at least 20 times higher. Though less popular than it was once, the SAF procedure also precipitates PrP^{Sc} by aggregating it into fibrils, through a rather harsh treatment with sarkosyl [25,26] and high-speed centrifugation. Although it was the method of choice a few years ago, and still is considered as a confirmatory diagnosis for TSEs by International Office of Epizootics (IOE), SAF preparations are used less today because the method is tedious to perform and requires larger quantities of starting tissue to offset heavy losses throughout (with only 20% recovery of PrP^{Sc}). The low recovery is indeed a problem, particularly with samples such as BSE and CJD where there is a constant dearth of available material. In our hands, at least fifty times the amount of tissue reported in the present sodium chloride precipitation procedure was required for the detection of PrP^{Sc} as SAFs [10]. When the salt precipitated material was examined for the presence of SAF's there weren't clearly detectable fibrilar structures thus making this protocol improper for the detection of them.

The salt precipitation method described here gave satisfactory results with all species of natural or experimental forms of TSEs tested. The finding that the species origin of the tissue did not affect the validity makes the procedure universally applicable for enriching PrP^{Sc} in samples intended both for diagnoses of prion diseases and for characterization of the infectious agent. Additionally, the observation that the glycoform pattern of PrP^{Sc}[14–16] was not distorted after digestion with Proteinase K indicates that the electrophoretic mobility of PrP^{Sc} was not affected. This is an important issue to consider while choosing any purification method for PrP^{Sc} because glycotyping has become a useful tool for strain typing TSEs.

Conclusions

This study is the first where an attempt has been made to estimate the recovery of PrP^{Sc} after its precipitation from brain tissue. The major advantages of the procedure include speed, low cost, simplicity and reproducibility unaffected by species origin. The ability to concentrate PrP^{Sc} through precipitation should make it a putative protocol of choice for detecting low amounts of PrP^{Sc}, as would be present in preclinical cases. Several TSE testing laboratories have applied succefully this protocol as a confirmatory technique for PrP^{Sc} detection (Personal communications). Future experiments to be undertaken include estimations of infectious titers in the PrP^{Sc} enriched pellet and validation of the method in the detection of PrP^{Sc} from non-neural tissues.

Authors' contributions

MP performed the precipitations and immunoblots for determination of the degree of purity of PrP^{Sc} and the applicability of the protocol to different species. SV-N. participated in the analysis of the data, and drafted the manuscript. MJC and MJS determined the limits of detection for the protocol with scrapie and BSE and they provided the P1 and P2 tissue homogenates. AP provided human brain tissue. MG provided mouse brain material and performed standardization experiments for immunostaining. TS conceived of the study and participated in its design and coordination.

Competing interests

None declared.

Acknowledgements

The authors wish to thank the European Union for partial funding of this study through FAIR PL 987021 and BMH4-98-6040. They also thank Dr C.H. Panagiotidis for her revisions and her help for preparation of the manuscript. The authors are also thankful for the support from the Greek Ministry of Health through the Center for Control of infectious diseases KEEL.

References

1. Prusiner SB: **The prion diseases.** *Brain Pathol* 1998, 8:499-513
2. Telling GC, Scott M, Mastrianni J, Gabizon R, Torchia M, Cohen FE, Dearmond SJ, Prusiner SB: **Prion propagation in mice expressing human and chimeric prp transgenes implicates the interaction of cellular Prp with another protein.** *Cell* 1995, 83:79-90
3. Jeffrey M, Ryder S, Martin S, Hawkins SA, Terry L, Berthelin Baker C, Bellworthy SJ: **Oral inoculation of sheep with the agent of bovine spongiform encephalopathy (BSE). 1. Onset and distribution of disease-specific prp accumulation in brain and viscera.** *J Comp Pathol* 2001, 124:280-289
4. Wadsworth JD, Joiner S, Hill AF, Campbell TA, Desbruslais M, Luthert PJ, Collinge J: **Tissue distribution of protease resistant prion protein in variant Creutzfeldt-Jakob disease using a highly sensitive immunoblotting assay.** *Lancet* 2001, 358:171-180

5. Van Keulen LJM, Screuder BE, Meloen RH, Mooij-Harkes G, ME Vromans, Langeveld JP: **Immunohistochemical detection of prion protein in lymphoid tissues of sheep with natural scrapie.** *J Clin Microbiol* 1996, **34**:1228-1231
6. Bruce M, Chree A, McConnell I, Foster J, Pearson G, Fraser H: **Transmission of bovine spongiform encephalopathy and scrapie to mice: strain variation and the species barrier.** *Philos Trans R Soc Lond B Biol Sci* 1994, **343**:405-411
7. Serban D, Taraboulos A, Dearmond SJ, Prusiner SB: **Rapid detection of Creutzfeldt-Jakob disease and scrapie prion proteins.** *Neurology* 1990, **40**:110-117
8. Beekes M, Baldauf E, Cassens S, Diringer H, Keyes P, Scott AC, Wells GA, Brown P, Gibbs CJ, Gajdusek DC: **Western blot mapping of disease-specific amyloid in various animal species and humans with transmissible spongiform encephalopathies using a high-yield purification method.** *J Gen Virol* 1995, **76**:2567-76
9. Grathwohl KU, Horiuchi M, Ishiguro N, Shinagawa M: **Sensitive Enzyme-Linked Immunosorbent assay for detection of PrP(Sc) in crude tissue extracts from scrapie-affected mice.** *J Virol Methods* 1997, **64**:205-216
10. Farquhar CF, Somerville RA, Ritchie LA: **Post-mortem immunodiagnosis of scrapie and bovine spongiform encephalopathy.** *J Virol Methods* 1989, **24**:215-221
11. Schmerr MJ, Jenny AL, Bulgin MS, Miller JM, Hamir AN, Cutlip RC, Goodwin KR: **Use of capillary electrophoresis and fluorescent labeled peptides to detect the abnormal prion protein in the blood of animals that are infected with a transmissible spongiform encephalopathy.** *J Chromatogr A* 1999, **853**:207-214
12. Manousis T, Verghese-Nikolakaki S, Keyes P, Sachsamanoglou M, Dawson M, Papadopoulos O, Sklaviadis TK: **Characterization of the murine BSE infectious agent.** *J Gen Virol* 2000, **81**:1615-1620
13. Plaitakis A, Viskadouraki AK, Tzagournissakis M, Zaganas I, Verghese-Nikolakaki S, Karageorgis V, Panagiotidis I, Kilindireas C, Patsouris E, Haberler C, Budka H, Sklaviadis T: **Increased incidence of sporadic Creutzfeldt-Jakob disease on the island of Crete associated with a high rate of Prnp 129-methionine homozygosity in the local population.** *Ann Neurol* 2001, **50**:227-233
14. Kuczius T, Haist I, Groschup MH: **Molecular analysis of bovine spongiform encephalopathy and scrapie strain variation.** *J Infect Dis* 1998, **178**:693-699
15. Madec JY, Groschup MH, Buschmann A, Belli P, Calavas D, Baron T: **Sensitivity of the western blot detection of prion protein Prpres in natural sheep scrapie.** *J Virol Methods* 1998, **75**:169-177
16. Sweeney T, Kuczius T, McElroy M, Gomez Parada M, Groschup MH, Parada MG: **Molecular analysis of Irish sheep scrapie cases** *J Gen Virol* 2000, **81**:1621-1627
17. Wells GA, Scott AC, Johnson CT, Gunning RF, Hancock RD, Jeffrey M, Dawson M, Bradley R: **A novel progressive spongiform encephalopathy in cattle** *Veterinary Record* 1987, **121**:419-420
18. Hill AF, Desbruslais S, Joiner S, Sidle KCL, Gowland L, Collinge J: **The same prion strain causes vCJD and BSE.** *Nature* 1997, **389**:448-450
19. Bruce ME, Will RG, Ironside JW, Mcconnell I, Drummond D, Suttie A, Mccardle L, Chree A, Hope J, Birkett C, Cousens S, Fraser H, Bostock CJ: **Transmissions to mice indicate that 'new variant' CJD is caused by the BSE agent.** *Nature* 1997, **389**:498-501
20. Hill AF, Sidle KCL, Joiner S, Keyes P, Martin TC, Dawson M, Collinge J: **Molecular screening of sheep for Bovine Spongiform Encephalopathy.** *Neuroscience Letters* 1998, **255**:159-162
21. Hope J, Wood SC, Birkett CR, Chong A, Bruce ME, Cairns D, Goldmann W, Hunter N, Bostock CJ: **Molecular analysis of ovine prion protein identifies similarities between BSE and an experimental isolate of natural scrapie, CH1641.** *J Gen Virol* 1999, **80**:1-4
22. Gabus C, Derrington E, Leblanc P, Chnaiderman J, Dormont D, Swietnick W, Morillas M, Surewicz WK, Marc D, Nandi P, Darlix JL: **The prion protein has RNA binding and chaperoning properties characteristic of nucleocapsid protein NCP7 of HIV-1.** *J Biol Chem* 2001, **276**:19301-19309
23. Telling GC, Parchi P, Dearmond SJ, Cortelli P, Montagna P, Gabizon R, Mastrianni J, Lugaresi E, Gambetti P, Prusiner SB: **Evidence for the conformation of the pathologic isoform of the prion protein enciphering and propagating prion diversity.** *Science* 1996, **274**:2079-2082
24. Maissen M, Roeckl C, Glatzel M, Goldmann W, Aguzzi A: **Plasminogen binds to disease-associated prion protein of multiple species.** *Lancet* 2001, **357**:2026-2028
25. Diringer H, Gelderblom H, Hilmert H, Ozel M, Edelbluth C, Kimberlin RH: **Scrapie infectivity, fibrils and low molecular weight protein.** *Nature* 1983, **306**:476-478
26. Sklaviadis T, Manuelidis L, Manuelidis EE: **Characterization of major peptides in Creutzfeldt-Jakob disease and scrapie.** *Proc Natl Acad Sci USA* 1986, **83**:6146-6150
27. Merril CR, Goldman D, Sedman SA, Ebert MH: **Ultrasensitive stain for proteins in polyacrylamide gels shows regional variation in cerebrospinal fluid proteins.** *Science* 1981, **211**:1437-1438

Pre-publication history

The pre-publication history for this paper can be accessed here:

http://www.biomedcentral.com/1471-2334/2/23/prepub

Eight prion strains have PrP^{Sc} molecules with different conformations

JIRI SAFAR[1], HOLGER WILLE[1], VINCENZA ITRI[1], DARLENE GROTH[1], HANA SERBAN[1], MARILYN TORCHIA[1], FRED E. COHEN[2-4] & STANLEY B. PRUSINER[1,2]

Department of [1]Neurology, [2]Biochemistry and Biophysics, [3]Medicine and [4]Cellular and Molecular Pharmacology, University of California, San Francisco, California 94143-0518, USA
Correspondence should be addressed to S.B.P.

Variations in prions, which cause different incubation times and deposition patterns of the prion protein isoform called PrP^{Sc}, are often referred to as 'strains'. We report here a highly sensitive, conformation-dependent immunoassay that discriminates PrP^{Sc} molecules among eight different prion strains propagated in Syrian hamsters. This immunoassay quantifies PrP isoforms by simultaneously following antibody binding to the denatured and native forms of a protein. In a plot of the ratio of antibody binding to denatured/native PrP graphed as a function of the concentration of PrP^{Sc}, each strain occupies a unique position, indicative of a particular PrP^{Sc} conformation. This conclusion is supported by a unique pattern of equilibrium unfolding of PrP^{Sc} found with each strain. Our findings indicate that each of the eight prion strains has a PrP^{Sc} molecule with a unique conformation and, in accordance with earlier results, indicate the biological properties of prion strains are 'enciphered' in the conformation of PrP^{Sc} and that the variation in incubation times is related to the relative protease sensitivity of PrP^{Sc} in each strain.

Creutzfeldt-Jakob disease (CJD) of humans and bovine spongiform encephalopathy and scrapie of animals are neurodegenerative diseases caused by prions[1]. Studies of scrapie in goats and later in mice demonstrated reproducible variations in disease phenotype with the passage of prions in genetically inbred hosts[2]. The distinct varieties or isolates of prions were called 'strains', because for many years scrapie and CJD were thought to be caused by slow viruses[3,4]. The existence of these strains became the strongest argument for a scrapie-specific nucleic acid[5-7].

The only known component of the infectious prion is an abnormal, disease-causing isoform of the prion protein (PrP), called PrP^{Sc}. During a post-translational process, PrP^{Sc} is formed from the normal, cellular PrP isoform (PrP^{C}). Each prion strain produces a specific phenotype of prion disease as manifest by the length of the incubation time, the topology of PrP^{Sc} accumulation and the distribution of pathological lesions[8-11]. Strains replicate with a high degree of fidelity, which demands a mechanism that can account for this phenomenon. PrP^{Sc} might exist in multiple conformations, which would account for the strains, but supporting evidence for this was initially lacking[12,13]. Subsequently, isolation of prion strains from mink by passage in hamsters[14] and passage of inherited human prion diseases to transgenic mice[15] indicated that the properties of prion strains are 'enciphered' in the conformation of PrP^{Sc}.

In those studies of prion strains, the size of the protease-resistant PrP^{Sc} fragment (PrP 27-30) was used to distinguish between strains with different biological properties. Because PrP^{C} and PrP^{Sc} have the same covalent structure[16], differences in protection against proteolytic degradation must reflect alterations in the tertiary structure of PrP^{Sc}. The diminished protease resistance of PrP^{Sc} from the Drowsy (DY) prion strain did not correlate with prolonged incubation times, as several scrapie strains with similar incubation times did not have the same decreased protease resistance[11]. Because seven of the eight prion strains investigated have similar patterns of protease resistance, we sought a more sensitive technique to study the conformations of PrP^{Sc} of these strains. Having developed a highly sensitive conformation-dependent immunoassay that measures the relative amounts of β-sheet and α-helical content, we analyzed eight prion strains to determine whether the secondary structure of each PrP^{Sc} was distinct and thus, strain-specific. In graphs of the ratio of antibody binding to denatured/native PrP plotted as a function of the concentration of PrP^{Sc}, each strain occupies a unique position. These findings, with the results of earlier studies, indicate that the biological properties of prion strains are 'enciphered' in the conformation of PrP^{Sc} and that the variation in incubation times is related to the relative protease sensitivity of PrP^{Sc} in each strain.

Development of a PrP^{Sc} conformation-dependent immunoassay

In contrast to PrP^{C}, the immunoreactivity of PrP^{Sc} is greatly enhanced by denaturation[17]. Studies with anti-PrP monoclonal antibodies and recombinant antigen-binding fragments showed that transformation of PrP^{C} into PrP^{Sc} is accompanied by the burial of epitopes near the N terminus of PrP, whereas C-terminal epitopes remain exposed [18]. If some monoclonal antibodies directed against the N terminus of PrP have sufficiently different affinities for the α-helical and β-sheet conformations of PrP, then the difference between these affinities could be a quantitative 'signature' of the native conformation. The affinity of denatured PrP was arbitrarily designated as a reference point.

Recombinant Syrian hamster (SHa) PrP containing residues 90–231 (SHaPrP(90-231)) was refolded into predominantly α-helical or β-sheet forms, which share structural features with PrP^{C} and PrP^{Sc}, respectively[19]. We used these structurally defined recombinant proteins in our initial studies with the monoclonal antibody 3F4 (ref. 20). To measure the binding of antibodies to

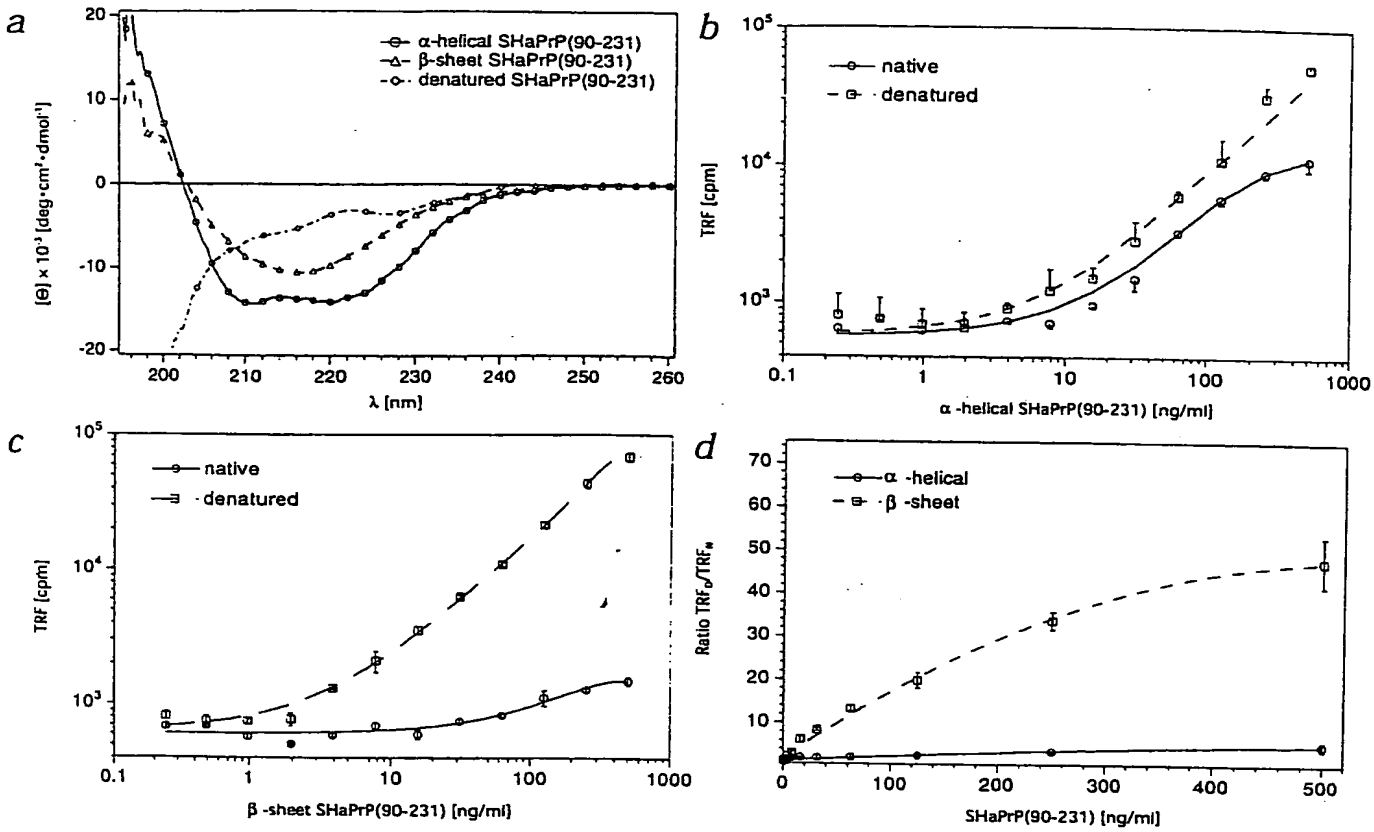

Fig. 1 Development of a conformation-dependent immunoassay for recombinant SHaPrP(90-231) purified from *E. coli* and folded into different conformations. ***a***, Conformation of recombinant SHaPrP(90-231) as determined by circular dichroism (CD) spectroscopy. ***b*** and ***c***, Calibration of conformation-dependent immunoassay with recombinant SHaPrP(90-231) in α-helical (*b*) and in β-sheet (*c*) conformation. ***d***, Ratios between signals of denatured/native recombinant SHaPrP(90-231) in α-helical and β-sheet conformations. Two major bands in the CD spectrum with minima at 208 and 222 nm indicate an α-helical conformation; a single negative band with minimum at 217 nm is characteristic of predominantly β-sheet conformation; a negative trough towards 197 nm documents random-coil conformation. The calibration of the conformation-dependent immunoassay was done in the presence of $Prnp^{0/0}$ mouse brain homogenate. Data represent average ± s.e.m. obtained from four independent measurements.

PrP, we adapted a direct ELISA-formatted, dissociation-enhanced time-resolved fluorescence (TRF) detection system[21]. The sensitivity limit of detecting denatured SHaPrP(90-231) with europium (Eu)-labeled anti-PrP 3F4 monoclonal antibody IgG (ref. 20) was less than or equal to 5 pg/ml with a dynamic range of over 5 orders of magnitude (data not shown).

To simulate physiological conditions, we 'spiked' 5% (weight/volume) brain homogenate obtained from PrP-deficient ($Prnp^{0/0}$) mice[22] with purified recombinant SHaPrP(90-231) in either an α-helical or β-sheet conformation. The conformation of the refolded proteins were verified by circular dichromism (CD) spectroscopy (Fig. 1*a*). SHaPrP(90-231) was unfolded by 4 M guanadine hydrochloride (GdnHCl)for 5 minutes at 80 °C, diluted 20-fold, and stored for 16 hours at 5 °C before its conformation was determined by CD spectroscopy. The results (Fig. 1*a*) confirmed that the protein did not refold under the conditions used for cross-linking to the activated plastic ELISA plate.

When Eu-labeled 3F4 IgG was used in the presence of 5% (weight/volume) $Prnp^{0/0}$ mouse brain homogenate, the detection limit of denatured SHaPrP(90-231) was less than or equal to 2 ng/ml and the dynamic range was over 3 orders of magnitude. The input/output calibration for denatured SHaPrP(90-231) in both α-helical and β-sheet conformations and with purified infectious PrP^{Sc} gave sensitivity and linearity within the same range (data not shown). The interassay variation coefficient (100*standard deviation/average) was within the assay range of less than or equal to 6.6%.

The data obtained with SHaPrP(90-231) in an α-helical conformation (Fig. 1*b*) indicated a relatively small difference between signals of α-helical and denatured proteins. In contrast, the reactivity with the native β-sheet form of SHaPrP(90-231) only marginally exceeded background (Fig. 1*c*). When the results were expressed as a ratio between binding of 3F4 monoclonal antibody to native conformations compared with that of denatured conformations of PrP, the ratio for α-helical SHaPrP(90-231) was less than or equal to 5 and for the β-sheet conformation, it was greater than 5 (Fig. 1*d*). Thus, the ratio of 3F4 monoclonal antibody binding to denatured/native PrP was a sensitive indicator of the original native PrP conformation for which a value greater than 5 in the presence of $Prnp^{0/0}$ brain homogenate indicated the presence of β-sheet conformers of recombinant SHaPrP(90-231).

Measurement of $SHaPrP^{Sc}$ in brain homogenates

Fluorescence signals for native and denatured samples of normal SHa brain homogenate containing PrP^{C} were similar, and the ratio of antibody binding to denatured/native PrP was less than

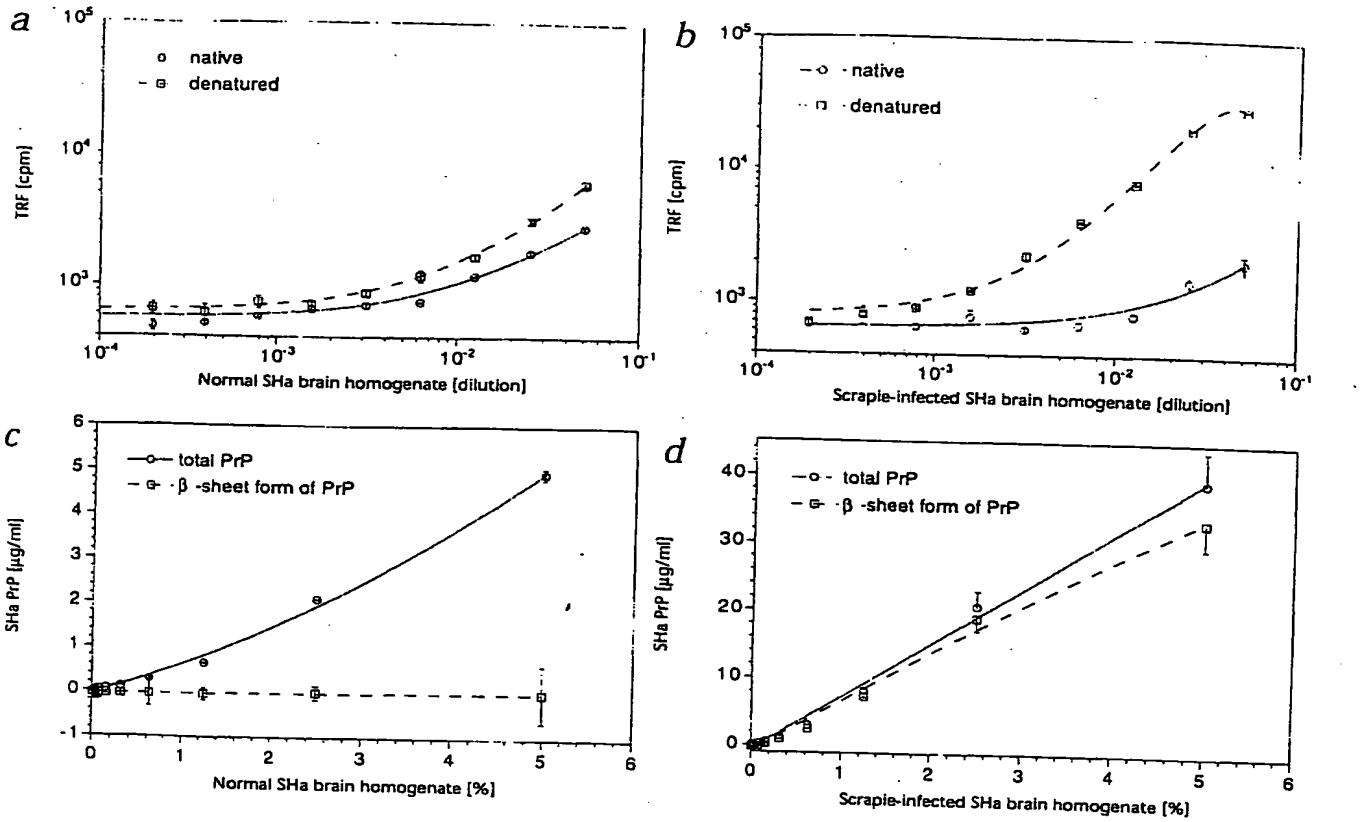

Fig. 2 Conformation-dependent immunoassays of PrPs in homogenates prepared from SHa brains. *a*, PrP^{C} in normal SHa brain homogenates. *b*, PrP^{C} and PrP^{Sc} in homogenates from the brains of Syrian hamsters showing signs of CNS dysfunction about 70 d after inoculation with Sc237 prions. *c*, Normal SHa brain homogenates; total amount of PrP and the amount of PrP in the β-sheet form. *d*, Homogenates from the brains of Syrian hamsters inoculated with Sc237 prions; total amount of PrP and the amount of PrP in the β-sheet form. The concentration of SHaPrP on the ordinate was calculated from equation 1. The samples of brain homogenates obtained from normal or scrapie-infected Syrian hamsters were serially diluted into $Prnp^{0/0}$ mouse homogenate. Data represent average ± s.e.m. obtained from four independent measurements.

or equal to 1.8 (Fig. 2*a*). In contrast, the ratio for a serial dilution of scrapie-infected SHa brain homogenate containing a mixture of PrP^{C} and PrP^{Sc} was greater than 2 (Fig. 2*b*). In general, the data on serially diluted normal and scrapie-infected SHa brain homogenate followed the pattern described for α–helix and β-sheet conformations of recombinant PrP(90-231). A ratio of antibody binding to denatured/native PrP greater than 1.8 indicated the presence of $SHaPrP^{Sc}$.

From the signal of denatured and native samples developed with Eu-labeled 3F4 IgG, the concentration of PrP^{Sc} may be directly calculated by equation 1 (Methods) (Fig. 2*c,d*). The correlation function f_α for $SHaPrP^{C}$ of brain origin in equation 1 was obtained by dilution experiments with normal SHa brain homogenate containing only PrP^{C}. Identical values of f_α were obtained with PrP^{C} purified from SHa brains. The correlation function for brain PrP^{C} did not exceed 1.8 and was used for all experiments with SHa brains described here. As expected, the normal brain homogenate contained only PrP^{C} in an α-helical conformation. In contrast, the data show that an approximately fivefold increase in total PrP in the brains of scrapie-infected Syrian hamsters was caused by accumulation of PrP^{Sc} in a β-sheet conformation (Fig. 2*d*).

Evidence for different conformations of PrP^{Sc} in eight prion strains

Using the highly sensitive conformation-dependent immunoassay for measurement of PrP^{Sc} in tissue homogenates, we analyzed eight different prion strains passaged in Syrian hamsters. Brains from Syrian hamsters were collected when the animals displayed signs of neurologic dysfunction; the incubation times for the prion strains varied from 70 to 320 days. Most of the PrP in the brains of Syrian hamsters with signs of neurologic disease was PrP^{Sc} as defined by the β-sheet conformation. The level of PrP^{Sc} in the brains of these clinically ill animals exceeded that of PrP^{C} by threefold to tenfold (Fig. 3*a*). The highest levels of PrP^{Sc} were found in the brains of Syrian hamsters infected with the Me7-H strain; in contrast, the lowest levels were found in the brains of Syrian hamsters inoculated with the SHa(Me7) strain (Fig. 3*a*). The Me7-H and SHa(Me7) strains, which were both derived from Me7 passaged in mice, had similar denatured/native PrP ratios, but they accumulated PrP^{Sc} to very different levels (Fig. 3*a,b*). The highest denatured/native PrP ratio of all tested strains was SHa(RML). There seemed to be no relationship between incubation time and either the concentrations of PrP^{Sc} or the ratio of denatured/native PrP.

The apparent independence of the ratio of denatured/native PrP from the concentration of PrP^{Sc} became obvious after plotting both parameters in a single plot (Fig. 3*b*). Each strain occupied a unique position, indicating differences in the conformation of accumulated PrP^{Sc}. Because the PrP^{C} concentration in each strain was less than or equal to 5 µg/ml and the PrP

ratio for PrP^C was less than or equal to 1.8, the expected effect of the presence of PrP^C on the final PrP ratio was less than or equal to 15%.

Because only the most tightly folded conformers of PrP^{Sc} are likely to be protease resistant, we digested each of the brain homogenates with proteinase K before measuring the ratio of denatured/native PrP (Fig. 3*c*). The positions of many strains changed when the protease-sensitive conformers of PrP^{Sc} were enzymatically hydrolyzed (Fig. 3*c*). The DY strain, which was readily detectable before limited proteolysis by immunoassay (Fig. 3*b*), became almost undetectable after digestion (Fig. 3*c*), in accordance with earlier western blot studies[14,23]. Strains such as Sc237 and Hyper (HY) were not well separated before proteinase K digestion (Fig. 3*b*) but became very distinct afterwards (Fig. 3*c*). These findings indicate that Sc237 and HY are distinct strains even though they have similar incubation times of about 70 days when passaged in Syrian hamsters[11]. Limited proteolysis of PrP^{Sc} from Sc237- and HY-infected brains produced PrP 27-30 proteins that were indistinguishable by migration in SDS-PAGE as detected by western immunoblotting[11]. As with PrP^{sc}, there was no relationship between incubation time and either the concentration of PrP 27-30 or the ratio of denatured/native PrP.

To assess the fraction of PrP^{Sc} that is sensitive to proteolysis during limited digestion with proteinase K, we subtracted the protease-resistant PrP 27-30 fraction (Fig. 3*c*) from the total PrP^{Sc} (Fig. 3*b*) for each of the eight prion strains. We asked whether the proteinase K-sensitive fraction of PrP^{Sc} ($[PrP^{Sc}]-[PrP\ 27\text{-}30]$) might reflect those PrP^{Sc} molecules that are most readily cleared by cellular proteases. The clearance of PrP^{Sc} is of interest for control of the length of the incubation time and other phenotypic features of prion strains[24]. When the $[PrP^{Sc}]-[PrP\ 27\text{-}30]$ fraction was plotted as a function of the incubation time, a linear relationship was found with an excellent correlation coefficient ($r = 0.94$) (Fig. 3*d*).

Equilibrium dissociation and unfolding of PrPs by GdnHCl

To extend these studies on the Sc237 and HY strains, we monitered equilibrium dissociation and unfolding of the PrP^{Sc} molecules in GdnHCl by Eu-labeled 3F4 IgG (Fig. 4). Data for PrP^C and the DY strain were also accumulated. After equilibrium unfolding, the proteins were rapidly diluted to the same protein and GdnHCl concentrations and then cross-linked to the glutaraldehyde-activated plate. The binding of 3F4 IgG was expressed as the ratio of antibody binding to denatured/native PrP (Fig. 4*a*) or as the fractional change in the transition from the native (~0) to fully unfolded (~1) state (Fig. 4*b*). The PrP ratios in-

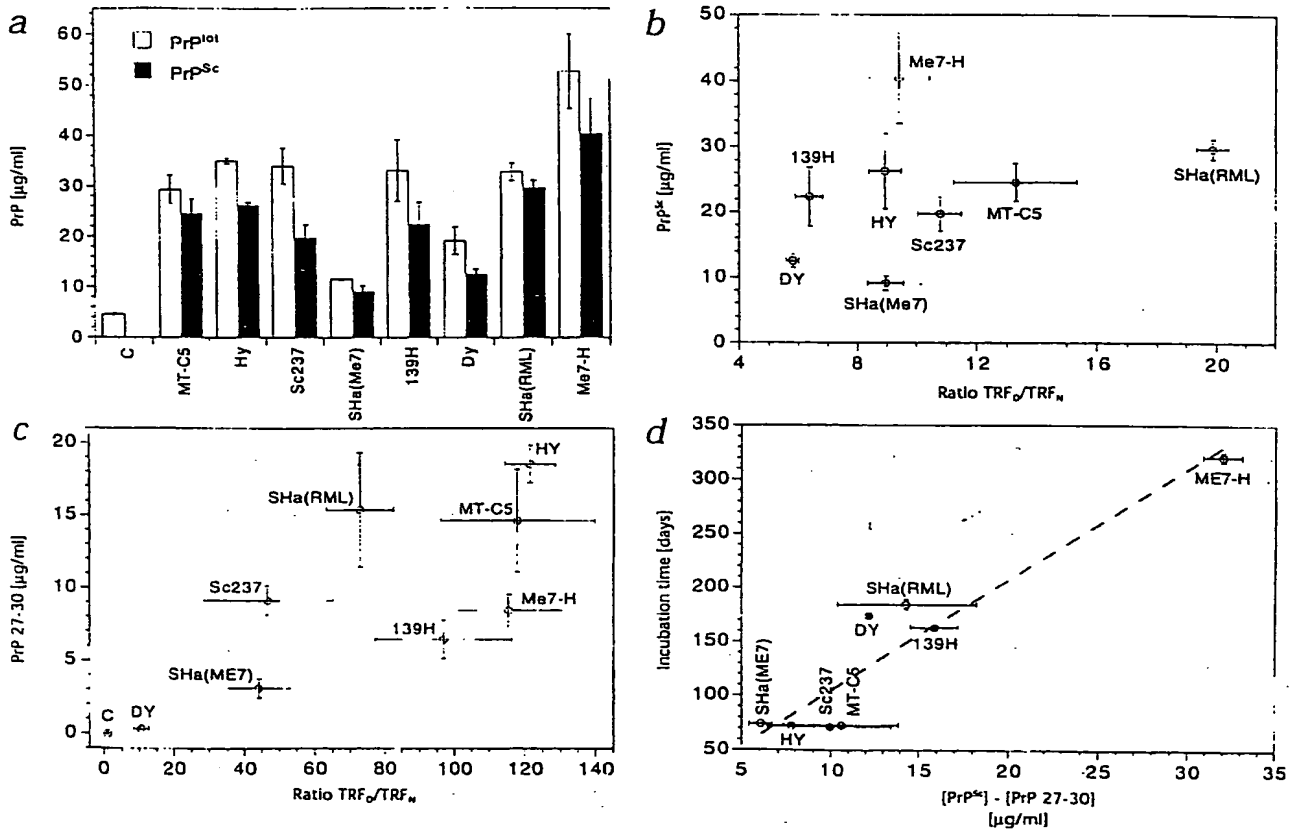

Fig. 3 Eight prion strains distinguished by the conformation-dependent immunoassay. *a*, Concentration of total PrP and PrP^{Sc}. Data represent the average ± s.e.m. obtained from three different brains of LVG/LAK Syrian hamsters infected with different prion strains and measured in three independent experiments. *b*, Ratio of antibody binding to denatured/native PrP and a function of concentration of PrP^{Sc} in the brains of Syrian hamsters infected with different prion strains. Concentration of PrP^{Sc} (equation 1) and the ratio of antibody binding to denatured/native PrP were measured by the conformation-dependent immunoassay. *c*, Brain homogenates of Syrian hamsters inoculated with different scrapie strains and uninoculated controls (C) were digested with proteinase K before the conformation-dependent immunoassay. *d*, Incubation time plotted as a function of the concentration of the proteinase K-sensitive fraction of PrP^{Sc} ($[PrP^{Sc}]-[PrP\ 27\text{-}30]$).

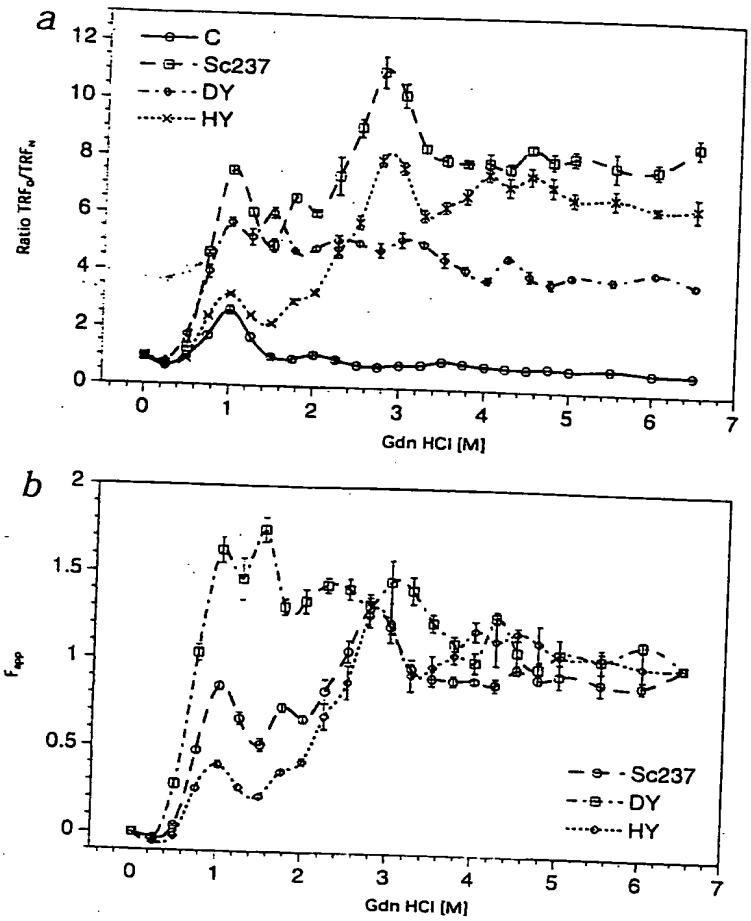

Fig. 4 Equilibrium dissociation and unfolding of PrP^C and PrP^{Sc} in three prion strains. Ratio of antibody binding to denatured/native PrP and apparent fractional change of unfolding of prion proteins during equilibrium dissociation and unfolding. *a*, The brains of uninoculated controls and Syrian hamsters infected with Sc237, DY or HY strains of prions were analyzed by the conformation-dependent immunoassay; the ratio of antibody binding to denatured/native PrP is plotted as a function of the GdnHCl concentration. *b*, The apparent fractional change of unfolding (F_{app}) of PrP^{Sc} from the Sc237, DY or HY (diamonds with dotted line) strains. Data represent the average ± s.e.m. obtained from four different measurements.

creased with increasing GdnHCl concentrations, indicating continued unfolding. The unfolding patterns of the ratio of antibody binding to denatured/native PrP for PrP^C in normal brain were distinctly different from the unfolding patterns for the PrPs in scrapie-infected brains. Each strain had a unique ratio of antibody binding to denatured/native PrP and, as a result, a unique unfolding pattern. The peaks indicated the presence of PrP conformers with a higher affinity than at the next-higher or -lower GdnHCl concentrations. The largest inter-strain differences were at ~1 M, ~3 M and 6.5 M GdnHCl (Fig. 4*a*). The ratios of antibody binding to denatured/native PrP for different prion strains at 6.5 M GdnHCl, at which all PrPs were unfolded[25], were close to the values obtained with samples exposed to 4 M GdnHCl and 80 °C for 5 minutes (Figs. 3*b* and 4*a*).

We also compared the relative abundance of different PrP conformers in brains infected with Sc237, DY or HY during the transition from the folded (native ~0) to unfolded state (denatured ~1) (Fig. 4*b*). The data expressed as apparent fractional change (F_{app}) allowed for the comparison of samples with different PrP concentrations. The largest inter-strain differences were at about 1 M GdnHCl; the highest fraction of conformers that were sensitive to such low concentrations of GdnHCl was found in SHa brains infected with the DY strain.

Selective precipitation of PrP^{Sc} by NaPTA

After the utility of our conformation-dependent immunoassay for PrP^{Sc} became apparent, we sought to increase both sensitivity and specificity by enriching for PrP^{Sc} before immunoassay. Although we could easily detect PrP^{Sc} when the concentration of PrP^{Sc} was equal to or exceeded that of PrP^C, we encountered difficulty with measuring PrP^{Sc} when its level was 1% or less that of PrP^C. After testing a number of precipitation procedures, we found that at neutral pH in the presence of Mg^{2+}, sodium phosphotungstate (NaPTA) formed complexes with oligomers and polymers of infectious PrP^{Sc} and PrP 27-30 but not with PrP^C. The resultant dense aggregates were then collected by a single 30-minute low-speed centrifugation. The pellet contained about 99% of the prions but less than 1% of other proteins. PrP 27-30 formed rod-like structures that could be detected directly by electron microscopy without further processing (Fig. 5). The morphology of these rod-like structures resembled in some respects the rods found in highly purified preparations of PrP 27-30 (ref. 26).

After the selective precipitation of PrP^{Sc} by NaPTA was incorporated into the conformation-dependent immunoassay for PrP^{Sc}, it was possible to measure low concentrations of PrP^{Sc} in brain homogenates from prion-infected animals. Scrapie-infected SHa brain homogenate was serially diluted into normal, uninfected SHa brain homogenate to simulate *in vivo* conditions early after initiation of infection, when the levels of PrP^{Sc} are low. The resultant samples contained different levels of infectivity and PrP^{Sc} in the presence of a constant level of PrP^C. The level of PrP^{Sc} could be measured as a function of the ratio of antibody binding to denatured/native PrP over approximately a 10^5-fold range. After scrapie-infected homogenates were diluted about 100,000-fold, the ratio of denatured/native PrP approached 1.8, which is that found when PrP^C alone was measured (Fig. 6*a*). Above a value of 1.8, the ratio of antibody binding to denatured/native PrP reliably indicated the presence of increasing quantities of PrP^{Sc}.

The application of equation 1 allowed direct calculation of the concentration of PrP^{Sc} in a mixture of scrapie-infected and normal brain homogenates (Fig. 6*b*). The sensitivity limit by PTA precipitation followed by immunoassay is less than or equal to 1 ng/ml of PrP^{Sc} in the presence of a 3,000-fold excess of PrP^C. Because the prion titer for Sc237-infected SHa brain homogenate is $10^{8.3}$ ID_{50}/ml, as determined by incubation time assay[27], the sensitivity limit of PrP^{Sc} detection corresponds to an infectivity titer of about 10^3 ID_{50}/ml (Fig. 6).

Discussion

The conformation-dependent immunoassay described here has wide utility. It has not only already greatly increased our understanding of prion strains but also will provide an extremely sensitive and rapid method for detection of animal and human prions. Although the low limit of detection reported here corresponds to about 10^3 ID_{50} units/ml, we have already improved the sensitivity of the immunoassay by 10- to 100-fold using a dual

wavelength, laser-driven fluorometer. We also anticipate that antibodies with a higher affinity for epitopes buried in PrP^{Sc} but exposed upon denaturation[18] should substantially increase the sensitivity of this assay.

The anti-PrP 3F4 monoclonal antibody used in the conformation-dependent immunoassay reacts with an epitope in a region of PrP^{C} (ref. 20), which seems be relatively unstructured, based on NMR spectroscopy of recombinant PrPs produced in *Escherichia coli* and folded into an α-helical conformation[19,28]. The α-helical conformation of recombinant PrPs is thought to approximate that of PrP^{C} isolated from SHa brain[29-31]. Computational studies indicate that during the conversion of PrP^{C} to PrP^{Sc}, the region with the 3F4 epitope acquires a high β-sheet content[32]. This prediction has been verified by using a panel of recombinant antigen-binding fragments that map to a series of epitopes along the PrP polypeptide chain[18].

PrP^{Sc} conformers 'encipher' strain-specific properties

The existence of multiple prion strains was traditionally offered as an argument for the existence of a scrapie-specific nucleic acid[5,6]. Despite many attempts to find such a nucleic acid by a multitude of approaches, and increasing evidence against the existence of a polynucleotide[33-35], an explanation for strains of prions remained a formidable conundrum[36].

Although different conformers of PrP^{Sc} might be responsible for particular prion strains[12], there was no evidence to support this until analysis was done of the two isolates (DY and HY) from mink that had been passaged in Syrian hamsters[14,23]. However, the HY strain was indistinguishable from the Sc237, SHa(Me7) and MT-C5 strains in incubation times (Fig. 3*d*) and the size of the PrP 27-30 fragment on SDS-PAGE. Moreover, the diminished resistance of DY to limited proteinase K digestion did not correlate with other isolates that produced similar incubation times such as 139H and SHa(RML)(ref. 11). The obscure origin of HY and DY in mink, and a lack of correlation with the properties of other biologically similar strains, made these mink strains difficult to reconcile. Only when prion strains generated *de novo* in humans with inherited prion diseases were passaged in transgenic (MHu2M) mice could a strong case be made for the 'enciphering' of the biological properties of prion strains in the conformation of PrP^{Sc} (refs. 1,15). These studies were fortuitous in that familial CDJ caused by the E200K mutation of the PrP gene [fCJD(E200K)] and fatal familial insomnia caused by the D178N mutation (FFI) gave different sizes of PrP 27-30 fragments after limited proteinase K digestion.

Here, a conformation-dependent immunoassay allowed us to distinguish all eight strains analyzed by plotting the ratio of denatured/native PrP as a function of PrP^{Sc} concentration before and after limited digestion with proteinase K (Fig. 3*b*,*c*). In contrast to the data here, only the DY strain could be distinguished from the other seven strains by western blotting after limited proteolysis; moreover, the relatively increased protease sensitivity of PrP^{Sc} in DY prions can produce an underestimation of its level by immunoblotting[11]. Only the Me7-H strain had a unique incubation time; the remaining seven strains clustered into two groups (Fig. 3*d*).

Many conformations of PrP^{Sc}

Our results demonstrate that eight different strains have at least eight different conformations (Figs. 3*b* and *c* and 4*b*). In fact, our data indicate that each strain is composed of a spectrum of conformations as demonstrated by the limited-protease-digestion and GdnHCl-denaturation studies (Figs. 3 and 4). These findings contrast with the idea that the primary structure of a protein determines a single tertiary structure[37].

How many formations can PrP^{Sc} adopt? The conformation-dependent immunoassay described here provides a rapid tool capable of discriminating the secondary and tertiary structures of many PrP^{Sc} molecules.

Our results indicate that PrP^{Sc} must act as a template in the replication of nascent PrP^{Sc} molecules. It seems likely that the binding of PrP^{C} or a metastable intermediate PrP^{*} to protein X is the initial step in PrP^{Sc} formation and that this is also the rate-limiting step in prion replication[24,38,39]. PrP^{Sc} interacts with PrP^{C} but not with protein X in the PrP^{C}-protein X complex. When PrP^{C} or PrP^{*} is converted into a nascent PrP^{Sc} molecule, protein X is released. Presumably, protein X functions as a molecular chaperone in the formation of PrP^{Sc}.

Thus, the different incubation times of various prion strains should arise mostly from distinct rates of PrP^{Sc} clearance rather than from different rates of PrP^{Sc} formation[24]. Prion strains that are readily cleared, therefore, should have prolonged incubation times, whereas those that are poorly cleared should have abbreviated incubation periods. We investigated this by relying upon the difference in brain PrP^{Sc} concentrations before and after proteinase K treatment as a surrogate for *in vivo* clearance of each prion strain. When clearance, as approximated by [PrP^{Sc}]–[PrP 27-30], was plotted as a function of the incubation time for eight strains, a linear relationship was found (Fig. 3*d*). Proteinase K sensitivity is an imperfect model for *in vivo* clearance, however, and only one strain with a long incubation time exceeding 300 days has been studied.

Asn-linked complex-type carbohydrates (CHOs) may specify prion strains[40], but this is difficult to reconcile with the addition of high-mannose oligosaccharides to Asn-linked consensus sites on PrP in the ER and subsequent remodeling of the sugar chains in the Golgi[41]. Modification of the complex CHOs attached to PrP^{C} is completed before the PrP^{C} is redistributed to the cell surface[42,43], which indicates that the Asn-linked CHOs of PrP^{Sc} do not 'instruct' the addition of such complex-type sugars to PrP^{C}.

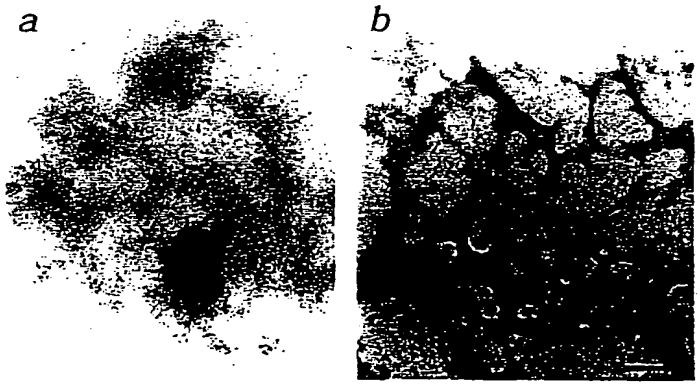

Fig. 5 Electron micrographs of pellets from control and prion-infected SHa brain homogenates precipitated by NaPTA and $MgCl_2$. *a*, Pellet obtained from normal SHa brain homogenate shows only diffuse patches of membrane lipids and detergent, and a few presumably proteinaceous particles of unknown composition. *b*, Pellet from a brain homogenate obtained from Syrian hamsters inoculated with Sc237 prions contains large aggregates that retain NaPTA. The aggregates resemble polymers of PrP 27-30 obtained by an alternative purification protocol[51]. Scale bar represents 100 nm.

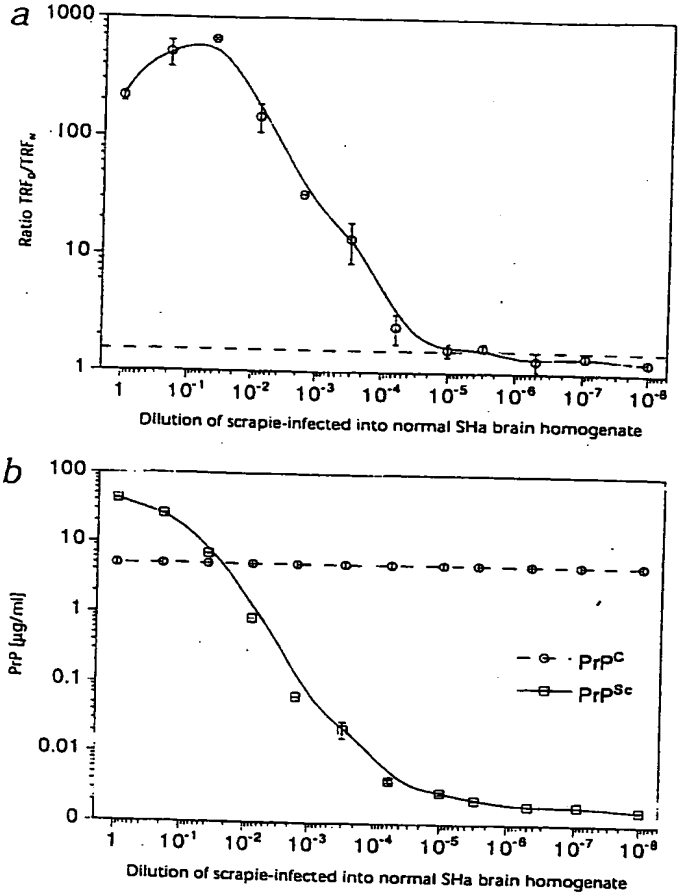

Fig. 6 Dynamic range and sensitivity of the ratio of antibody binding to PrP in denatured and native states. Homogenates prepared from the brains of Syrian hamsters showing signs of CNS dysfunction about 70 d after inoculation with Sc237 prions were serially diluted into normal SHa brain homogenate, and the presence of PrP^{Sc} was measured after NaPTA precipitation by the conformation-dependent immunoassay. *a*, The ratio of the fluorescence signals of denatured and native aliquots plotted as a function of the dilution of scrapie-infected brain homogenate. *b*, The absolute amount of PrP^C and PrP^{Sc} was calculated from equation 1 and plotted as a function of the dilution of scrapie-infected brain homogenate. Data represent average ± s.e.m. obtained from four independent measurements.

Mutagenesis of the complex-type sugar attachment sites seemed to increase PrP^{Sc} formation in cultured cells[44] but resulted in prolonged incubation times in transgenic mice and differences in the patterns of PrP^C distribution and PrP^{Sc} deposition in mice expressing mutant PrPs (ref. 45). These studies indicate that Asn-linked glycosylation might alter the stability of PrP, and in particular PrP^{Sc}, which results in various patterns of PrP^{Sc} deposition. Thus, different clearance rates of PrP^{Sc} may be important in determining not only strain-specific neuropathology but also the length of the incubation time[24].

Assessing prion sterility

When the sensitivity of the conformation-dependent immunoassay is sufficient to measure less than 1 ID_{50} unit, it may be feasible to use the assay to establish the sterility of products derived from both animals and humans. There is considerable concern that bovine prions may have been transmitted to humans who have developed new variant CJD (ref. 46). It should be possible to adapt our immunoassay to a high-throughput system and, thus, to certify whether meat, gelatin, collagen, pharmaceuticals and other bovine products are free of prions. Our immunoassay also might be adapted to ensure that pharmaceuticals manufactured from human blood or plasma or produced in mammalian cells are free of prions[47].

The calibration of any prion immunoassay system is crucial with respect to the number of PrP^{Sc} molecules per 1 ID_{50} unit. At present the only available data is from highly purified prion preparations in which the PrP^{Sc}/ID_{50} unit ratio is about 10^5 (refs 26,48). Using our conformation-dependent immunoassay in conjunction with transgenic mice capable of detecting 1 ID_{50} unit of human or bovine prions[49,50], it should be possible to determine the PrP^{Sc}/ID_{50} unit ratios for prions propagated in different tissues from humans and cattle. The calibration of prion immunoassays using transgenic mice is essential if such assays are to be used to assess the presence or absence of prions in foods, drugs, or other products, as well as to establish the diagnosis of prion disease in living patients.

New approaches arising from this research

The conformation-dependent immunoassay for PrP^{Sc} described here not only discriminates among a wide variety of prion strains but is also capable of measuring very low levels of PrP^{Sc}. This immunoassay provides important information about the tertiary and secondary structure of PrP^{Sc}, which is strain-dependent. Results from this conformation-dependent immunoassay should be correlated with those from optical spectroscopic techniques such as FTIR and CD. The ability to assay features of the tertiary and secondary structure of PrP^{Sc} in crude homogenates opens several new areas of investigation, including determinations of the structure of PrP^{Sc} in various tissues as well as in different regions of the CNS for a variety of prion strains.

Methods

Prion strains. Syrian hamsters (LVG:Lak) were infected by intracerebral injection of the following hamster-adapted scrapie isolates: Drowsy (DY), 139H, Hyper (HY), Me7-H, MT-C5, Sc237, SHa(Me7) and SHa(RML). The Sc237 strain was originally obtained from R. Marsh[51] and was passaged repeatedly in golden Syrian hamsters (LVG:Lak; Charles River Laboratories, Wilmington, Massachusetts). This strain seems to be indistinguishable from strain 263K (ref. 52). The MT-C5 strain was isolated in Syrian hamsters (LVG:Lak) from a cow infected with a second passage of sheep scrapie[53]. The Me7 hamster isolate was a gift from R. Kimberlin and R. Carp. The DY and HY hamster strains were provided by R. Marsh[54]. The 139A isolate was obtained after more than 20 passages of the Chandler isolate in mice[55]. Passage of mouse 139A prions in LVG:Lak golden Syrian hamsters produced the 139H isolate[56]. 139H prions were provided by R. Kimberlin and R. Carp, after six passages in Syrian hamsters. Strains SHa(Me7) and SHa(RML) were generated in our laboratory by passage of the Me7 strain of scrapie through chimeric transgenic(MH2M) and then twice in Syrian hamsters[11].

The animals were killed in the terminal stages of disease, and their brains were immediately frozen and stored at -70 °C. Brains were homogenized on ice by three 30-second strokes of a PowerGen homogenizer (Fisher Scientific) in PBS (pH 7.4) containing protease inhibitors (5 mM PMSF and aprotinin and leupeptin at 4 µg/ml each). The resultant 10% (weight/volume) homogenates were spun for 5 min at 500*g* in a tabletop centrifuge; supernatant was mixed 1:1 with 4% Sarkosyl in PBS (pH 7.4).

Prion bioassays. The titer of Sc237 prions was determined in 5% (weight/volume) brain homogenate by incubation time assay in groups of four Syrian hamsters as described[27].

Expression, purification and refolding of recombinant SHaPrP(90-231). For development and calibration of conformation-dependent immunoassays, recombinant SHaPrP(90-231) was refolded into α-helical or β-sheet conformations as described[19]. PCR (Perkin-Elmer) was used to amplify the DNA corresponding to different portions of SHaPrP for ligation into *E. coli* secretion vectors. Clones containing the PrP insert were sequenced and transformed into the protease-deficient expression strain 27C7 (ATCC number 55244). For purification, 100 g of *E. coli* 'paste' was resuspended in 1 L of 25 mM Tris-HCl, pH 8.0/5 mM EDTA (buffer A). This was centrifuged at 10,000*g* for 20 min, and the supernatant containing soluble periplasmic proteins was discarded. The pellet was resuspended in 1 L of buffer A, passed through a cell disrupter twice (model MF110, Microfluidics International, Newton, Massachusetts) and centrifuged at 30,000*g* for 1 h, after which the supernatant was discarded and the pellet was washed once in buffer A and centrifuged again at 30,000*g* for 1 h. The pellet was subsequently solubilized in 8 M GdnHCl, 25 mM Tris-HCl (pH 8.0) and 100 mM DTT (buffer B), and aliquots of 6 mL of the supernatant containing about 200 mg total protein were separated by size-exclusion chromatography followed by reversed-phase high performance liquid chromatography using a 25-mm/25-cm C-4 column (Vydac, Hesperia, California); Buffer 1, H_2O and 0.1% TFA; Buffer 2, acetonitrile and 0.09% TFA; flow rate 5 mL/min.

Samples of the reduced protein and the refolded oxidized form were concentrated using a Centricon (Amicon, Houston, Texas) with a molecular weight cutoff of 10,000 Da. The buffer for the reduced protein was 10 mM MES (pH 6.5); the oxidized form was concentrated in the refolding buffer. Circular dichroism (CD) spectroscopy on a Jasco 720 spectropolarimeter, as described[25], confirmed that the reduced protein refolded into a β-sheet conformation, and the oxidized protein refolded into an α-helical conformation.

Purification of $SHaPrP^C$ and $SHaPrP^{Sc}$ from brain. $SHaPrP^C$ was purified as described, with some minor modifications[29]. Protein content was determined by amino-acid analysis. The purity of PrP^C was 95%, as demonstrated by SDS–PAGE followed by silver staining and western blot.

$SHaPrP^{Sc}$ was purified from a standard pool of scrapie strain Sc237-infected hamster brains as described with only minor modifications[57]. The infectivity of this pool was 7.3 ID_{50}/ml, as determined by an incubation time assay on Syrian hamsters after intracerebral inoculation, and specific infectivity was 8.2 ID_{50}/mg of PrP^{Sc}. The preparation was considered homogeneous, with one major band on SDS–PAGE after silver staining and western blotting.

Labeling of antibodies. The data described here were generated with monoclonal antibody 3F4 (ref. 20). The IgG was purified from ascitic fluid by Protein A chromatography on a Pharmacia FPLC column and labeled with europium chelate of N-(p-isothiocyanatobenzyl)-diethylenetriamine-N^1,N^2,N^3,N^3-tetraacetic acid (DTTA) at pH 9.6 for 16 h at room temperature according to manufacturer's protocols (Wallac, Turku, Finland). The final Eu/IgG molar ratio was 13.

Immunoassay for PrP^{Sc} by dissociation-enhanced time-resolved fluorescence spectroscopy (TRF). Each sample was divided into two aliquots: one untreated (native) and another mixed to a final concentration of 4 M GdnHCl and heated for 5 min at 80 °C (denatured). Both samples were immediately diluted 20-fold with H_2O containing protease inhibitors (5 mM PMSF and aprotinin and leupeptin at 4 μg/ml each), and aliquots were loaded on a 96-well polystyrene plate that had been activated for 1 h with 0.2% glutaraldehyde in PBS, pH 7.4. The plates were incubated overnight at 5 °C and then blocked with TBS (pH 7.8) containing 0.5% BSA (weight/volume) and 6% Sorbitol (weight/volume) for 2 h at room temperature. They were then washed three times with TBS (pH 7.8) containing 0.05% (volume/volume) of Tween-20 and incubated at room temperature for 2 h with the Eu-labeled antibodies. The plates were developed after seven washing steps in enhancement solution provided by the europium label supplier (Wallac, Turku, Finland), and the signal was counted on a DELFIA 1234 (Wallac, Turku, Finland) fluorometer.

Calibration of the conformation-dependent immunoassay for PrP. The assay was calibrated for different conformations of PrP in the presence of 5% (weight/volume) brain homogenate obtained from PrP-deficient (*Prnp*$^{0/0}$) mice[22]. The homogenate was 'spiked' with purified recombinant SHaPrP(90-231) in α-helical or β-sheet conformations, as determined by CD spectroscopy, and with PrP^C and PrP^{Sc} purified from SHa brains. The data on antibody binding to denatured recombinant α-helical SHaPrP(90-231) or SHa brain PrP^C were plotted as a function of the binding to the native protein and fit by the least squares regression program to obtain the correlation coefficient f_α.

Antibody binding to denatured/native PrP and quantification of PrP^{Sc}. The ratio between binding of Eu-labeled IgG to PrP in native and denatured conformations measured by TRF was designated TRF_D / TRF_N. We have developed a mathematical model to calculate the content of β-sheet-structured PrP in an unknown sample directly:

$$[PrP_\beta] \sim \Delta TRF_\beta = TRF_D - (TRF_N * f_\alpha) \qquad (1)$$

where ΔTRF_β is the change in the time-resolved fluorescence of PrP in β-sheet conformation during the transition from the native to denatured state; TRF_D, the time-resolved fluorescence of PrP in the denatured state; TRF_N, the time-resolved fluorescence of PrP in the native conformation; and f_α, the correlation coefficient for dependency of TRF_D on TRF_N obtained with serially diluted reduced SHa brain homogenate and with purified SHa PrP^C. The coefficient was obtained by fitting the plot of antibody binding to denatured/native protein by the nonlinear least squares regression program. In this equation, an excess of antibody binding to PrP protein in the transition from native to denatured state more than that expected for α-helical conformation is directly proportional to the amount of PrP protein in β-sheet conformation.

Precipitation of prions by NaPTA. Brain homogenate (5% (weight/volume)) containing 2% Sarkosyl was mixed with stock solution containing 4% sodium phosphotungstate (NaPTA) and 170 mM $MgCl_2$, pH 7.4, to obtain a final concentration of 0.2–0.3% NaPTA. Usually, 1-ml samples were incubated for 16 h at 37 °C on a rocking platform and centrifuged at 14,000*g* in a tabletop centrifuge (Eppendorf) for 30 min at room temperature. The optional treatment with 25 μg/ml of proteinase K for 1 h at 37 °C was done before or after precipitation. The pellet was resuspended in H_2O containing protease inhibitors (0.5 mM PMSF and aprotinin and leupeptin at 2 μg/ml each) and assayed by the conformation-dependent immunoassay.

Equilibrium dissociation and unfolding in GdnHCl. Aliquots of 5% (weight/volume) brain homogenates in PBS (pH 7.4) containing 2% Sarkosyl and protease inhibitor cocktail (5 mM PMSF and aprotinin and leupeptin at 4 μg/ml each) were mixed manually to the final concentration of GdnHCl and constant protein concentration in a sample and equilibrated for 16 h at 23 °C. The concentration of stock solution of 8 M GdnHCl (Pierce, Rockford, Illinois) in TBS (pH 7.4) was controlled by refractometry. Equilibrated samples were diluted 20-fold to the same final protein and GdnHCl concentration and assayed with Eu-labeled 3F4 IgG in conformation-dependent immunoassays.

The raw data from each assay were converted into a ratio of antibody binding to denatured/native PrP or the apparent fractional change of unfolding: F_{app} (refs. 25,58) by $F_{app} = (Y_{obsd}-Y_N)/(Y_U-Y_N)$, where Y_{obsd} is the observed value of the parameter and Y_N and Y_U are the values of the parameters for native and unfolded forms, respectively, at the given GdnHCl concentration[25,58].

Electron microscopy. Samples were prepared on carbon-coated 1,000-mesh copper grids that were glow-discharged before staining. Samples (5 μl) were adsorbed for about 30 seconds and washed with 2 drops of water. Contrast was provided by NaPTA retained as positive staining from the NaPTA precipitation step in the preparation; no additional staining was used. After being dried, samples were viewed in a Jeol 100CX II electron microscope at 80 kV at a standard magnification of 40,000. The magnification was calibrated with negatively stained catalase crystals.

Acknowledgments

The authors thank H. Baron, F. Feldman and P. Fuhge for encouragement and discussions. This work was supported by grants from the National Institutes of

Health (AG02132, AG10770, NS22786, and NS14069) as well as by gifts from the G. Harold and Leila Y. Mathers Foundation, Sherman Fairchild Foundation and Centeon.

RECEIVED 22 JUNE; ACCEPTED 24 AUGUST 1998

1. Prusiner, S.B. Prion diseases and the BSE crisis. *Science* 278, 245–251 (1997).
2. Pattison, I.H. & Millson, G.C. Scrapie produced experimentally in goats with special reference to the clinical syndrome. *J. Comp. Pathol.* 71, 101–108 (1961).
3. Sigurdsson, B. Rida, a chronic encephalitis of sheep with general remarks on infections which develop slowly and some of their special characteristics. *Br. Vet. J.* 110, 341–354 (1954).
4. Gajdusek, D.C. Unconventional viruses and the origin and disappearance of kuru. *Science* 197, 943–960 (1977).
5. Bruce, M.E. & Dickinson, A.G. Biological evidence that the scrapie agent has an independent genome. *J. Gen. Virol.* 68, 79–89 (1987).
6. Dickinson, A.G. & Outram, G.W. in *Novel Infectious Agents and the Central Nervous System. Ciba Foundation Symposium* 135 (eds. Bock, G. & Marsh, J.) 63–83 (John Wiley and Sons, Chichester, England, 1988).
7. Bruce, M.E. & Fraser, H. Scrapie strain variation and its implications. *Curr. Top. Microbiol. Immunol.* 172, 125–138 (1991).
8. Fraser, H. & Dickinson, A.G. The sequential development of the brain lesions of scrapie in three strains of mice. *J. Comp. Pathol.* 78, 301–311 (1968).
9. Bruce, M.E., McBride, P.A. & Farquhar, C.F. Precise targeting of the pathology of the sialoglycoprotein, PrP, and vacuolar degeneration in mouse scrapie. *Neurosci. Lett.* 102, 1–6 (1989).
10. Taraboulos, A. *et al.* Regional mapping of prion proteins in brains. *Proc. Natl. Acad. Sci. USA* 89, 7620–7624 (1992).
11. Scott, M.R. *et al.* Propagation of prion strains through specific conformers of the prion protein. *J. Virol.* 71, 9032–9044 (1997).
12. Prusiner, S.B. Molecular biology of prion diseases. *Science* 252, 1515–1522 (1991).
13. Cohen, F.E. *et al.* Structural clues to prion replication. *Science* 264, 530–531 (1994).
14. Bessen, R.A. & Marsh, R.F. Distinct PrP properties suggest the molecular basis of strain variation in transmissible mink encephalopathy. *J. Virol.* 68, 7859–7868 (1994).
15. Telling, G.C. *et al.* Evidence for the conformation of the pathologic isoform of the prion protein enciphering and propagating prion diversity. *Science* 274, 2079–2082 (1996).
16. Stahl, N. *et al.* Structural analysis of the scrapie prion protein using mass spectrometry and amino acid sequencing. *Biochemistry* 32, 1991–2002 (1993).
17. Serban, D., Taraboulos, A., DeArmond, S.J. & Prusiner, S.B. Rapid detection of Creutzfeldt-Jakob disease and scrapie prion proteins. *Neurology* 40, 110–117 (1990).
18. Peretz, D. *et al.* A conformational transition at the N terminus of the prion protein features in formation of the scrapie isoform. *J. Mol. Biol.* 273, 614–622 (1997).
19. Mehlhorn, I. *et al.* High-level expression and characterization of a purified 142-residue polypeptide of the prion protein. *Biochemistry* 35, 5528–5537 (1996).
20. Kascsak, R.J. *et al.* Mouse polyclonal and monoclonal antibody to scrapie-associated fibril proteins. *J. Virol.* 61, 3688–3693 (1987).
21. Hemmilä, I. & Harju, R. Time-resolved fluorometry. In *Bioanalytical Applications of Labelling Technologies* (eds. Hemmilä, I., Ståhlberg, T. & Mottram, P.) 113–119 (Wallac Oy, Turku, Finland, 1995).
22. Büeler, H. *et al.* Normal development and behaviour of mice lacking the neuronal cell-surface PrP protein. *Nature* 356, 577–582 (1992).
23. Bessen, R.A. & Marsh, R.F. Biochemical and physical properties of the prion protein from two strains of the transmissible mink encephalopathy agent. *J. Virol.* 66, 2096–2101 (1992).
24. Prusiner, S.B., Scott, M.R., DeArmond, S.J. & Cohen, F.E. Prion protein biology. *Cell* 93, 337–348 (1998).
25. Safar, J., Roller, P.P., Gajdusek, D.C. & Gibbs, C.J., Jr. Conformational transitions, dissociation, and unfolding of scrapie amyloid (prion) protein. *J. Biol. Chem.* 268, 20276–20284 (1993).
26. Prusiner, S.B. *et al.* Scrapie prions aggregate to form amyloid-like birefringent rods. *Cell* 35, 349–358 (1983).
27. Prusiner, S.B. *et al.* Measurement of the scrapie agent using an incubation time interval assay. *Ann. Neurol.* 11, 353–358 (1982).
28. James, T.L. *et al.* Solution structure of a 142-residue recombinant prion protein corresponding to the infectious fragment of the scrapie isoform. *Proc. Natl. Acad. Sci. USA* 94, 10086–10091 (1997).
29. Pan, K.-M. *et al.* Conversion of α-helices into β-sheets features in the formation of the scrapie prion proteins. *Proc. Natl. Acad. Sci. USA* 90, 10962–10966 (1993).
30. Pergami, P., Jaffe, H. & Safar, J. Semipreparative chromatographic method to purify the normal cellular isoform of the prion protein in nondenatured form. *Anal. Biochem.* 236, 63–73 (1996).
31. Williamson, R.A. *et al.* Circumventing tolerance to generate autologous monoclonal antibodies to the prion protein. *Proc. Natl. Acad. Sci. USA* 93, 7279–7282 (1996).
32. Huang, Z., Prusiner, S.B. & Cohen, F.E. Scrapie prions: a three-dimensional model of an infectious fragment. *Folding & Design* 1, 13–19 (1995).
33. Meyer, N. *et al.* Search for a putative scrapie genome in purified prion fractions reveals a paucity of nucleic acids. *J. Gen. Virol.* 72, 37–49 (1991).
34. Kellings, K., Prusiner, S.B. & Riesner, D. Nucleic acids in prion preparations: unspecific background or essential component? *Phil. Trans. R. Soc. Lond. B* 343, 425–430 (1994).
35. Kellings, K., Meyer, N., Mirenda, C., Prusiner, S.B. & Riesner, D. Further analysis of nucleic acids in purified scrapie prion preparations by improved return refocussing gel electrophoresis (RRGE). *J. Gen. Virol.* 73, 1025–1029 (1992).
36. Prusiner, S.B. Prions. *Les Prix Nobel* (in the press).
37. Anfinsen, C.B. Principles that govern the folding of protein chains. *Science* 181, 223–230 (1973).
38. Kaneko, K. *et al.* Evidence for protein X binding to a discontinuous epitope on the cellular prion protein during scrapie prion propagation. *Proc. Natl. Acad. Sci. USA* 94, 10069–10074 (1997).
39. Cohen, F.E. & Prusiner, S.B. Pathologic conformations of prion proteins. *Annu. Rev. Biochem.* 67, 793–819 (1998).
40. Collinge, J., Sidle, K.C.L., Meads, J., Ironside, J. & Hill, A.F. Molecular analysis of prion strain variation and the aetiology of "new variant" CJD. *Nature* 383, 685–690 (1996).
41. Endo, T., Groth, D., Prusiner, S.B. & Kobata, A. Diversity of oligosaccharide structures linked to asparagines of the scrapie prion protein. *Biochemistry* 28, 8380–8388 (1989).
42. Borchelt, D.R., Scott, M., Taraboulos, A., Stahl, N. & Prusiner, S.B. Scrapie and cellular prion proteins differ in their kinetics of synthesis and topology in cultured cells. *J. Cell Biol.* 110, 743–752 (1990).
43. Caughey, B. & Raymond, G.J. The scrapie-associated form of PrP is made from a cell surface precursor that is both protease- and phospholipase-sensitive. *J. Biol. Chem.* 266, 18217–18223 (1991).
44. Taraboulos, A. *et al.* Acquisition of protease resistance by prion proteins in scrapie-infected cells does not require asparagine-linked glycosylation. *Proc. Natl. Acad. Sci. USA* 87, 8262–8266 (1990).
45. DeArmond, S.J. *et al.* Selective neuronal targeting in prion disease. *Neuron* 19, 1337–1348 (1997).
46. Will, R.G. *et al.* A new variant of Creutzfeldt-Jakob disease in the UK. *Lancet* 347, 921–925 (1996).
47. Brown, P. in *Transmissible Subacute Spongiform Encephalopathies: Prion Diseases* (eds. Court, L. & Dodet, B.) 447–450 (Elsevier, Paris, 1996).
48. Prusiner, S.B. *et al.* Further purification and characterization of scrapie prions. *Biochemistry* 21, 6942–6950 (1982).
49. Telling, G.C. *et al.* Transmission of Creutzfeldt-Jakob disease from humans to transgenic mice expressing chimeric human-mouse prion protein. *Proc. Natl. Acad. Sci. USA* 91, 9936–9940 (1994).
50. Scott, M.R. *et al.* Identification of a prion protein epitope modulating transmission of bovine spongiform encephalopathy prions to transgenic mice. *Proc. Natl. Acad. Sci. USA* 94, 14279–14284 (1997).
51. Marsh, R.F. & Kimberlin, R.H. Comparison of scrapie and transmissible mink encephalopathy in hamsters. II. Clinical signs, pathology and pathogenesis. *J. Infect. Dis.* 131, 104–110 (1975).
52. Kimberlin, R. & Walker, C. Characteristics of a short incubation model of scrapie in the golden hamster. *J. Gen. Virol.* 34, 295–304 (1977).
53. Gibbs, C.J., Jr., Safar, J., Sulima, M.P., Bacote, A.E. & San Martin, R.A. in *Bovine Spongiform Encephalopathy: The BSE Dilemma* (ed. Gibbs, C.J., Jr.) 84–91 (Springer, New York, 1996).
54. Marsh, R.F., Bessen, R.A., Lehmann, S. & Hartsough, G.R. Epidemiological and experimental studies on a new incident of transmissible mink encephalopathy. *J. Gen. Virol.* 72, 589–594 (1991).
55. Dickinson, A.G. In *Slow Virus Diseases of Animals and Man* (ed. Kimberlin, R.H.) 209–241 (North-Holland Publishing, Amsterdam, 1976).
56. Kimberlin, R.H., Cole, S. & Walker, C.A. Pathogenesis of scrapie is faster when infection is intraspinal instead of intracerebral. *Microb. Pathog.* 2, 405–415 (1987).
57. Turk, E., Teplow, D.B., Hood, L.E. & Prusiner, S.B. Purification and properties of the cellular and scrapie hamster prion proteins. *Eur. J. Biochem.* 176, 21–30 (1988).
58. Safar, J., Roller, P.P., Gajdusek, D.C. & Gibbs, C.J., Jr. Scrapie amyloid (prion) protein has the conformational characteristics of an aggregated molten globule folding intermediate. *Biochemistry* 33, 8375–8383 (1994).

Vol 437|8 September 2005|doi:10.1038/nature03989

nature

LETTERS

The most infectious prion protein particles

Jay R. Silveira[1], Gregory J. Raymond[1], Andrew G. Hughson[1], Richard E. Race[1], Valerie L. Sim[1], Stanley F. Hayes[2] & Byron Caughey[1]

Neurodegenerative diseases such as Alzheimer's, Parkinson's and the transmissible spongiform encephalopathies (TSEs) are characterized by abnormal protein deposits, often with large amyloid fibrils. However, questions have arisen as to whether such fibrils or smaller subfibrillar oligomers are the prime causes of disease[1,2]. Abnormal deposits in TSEs are rich in PrP^{res}, a protease-resistant form of the PrP protein with the ability to convert the normal, protease-sensitive form of the protein (PrP^{sen}) into PrP^{res} (ref. 3). TSEs can be transmitted between organisms by an enigmatic agent (prion) that contains PrP^{res} (refs 4 and 5). To evaluate systematically the relationship between infectivity, converting activity and the size of various PrP^{res}-containing aggregates, PrP^{res} was partially disaggregated, fractionated by size and analysed by light scattering and non-denaturing gel electrophoresis. Our analyses revealed that with respect to PrP content, infectivity and converting activity peaked markedly in 17–27-nm (300–600 kDa) particles, whereas these activities were substantially lower in large fibrils and virtually absent in oligomers of ≤5 PrP molecules. These results suggest that non-fibrillar particles, with masses equivalent to 14–28 PrP molecules, are the most efficient initiators of TSE disease.

In designing strategies to limit TSE infections and their propagation within hosts, it remains important to identify the most infectious particles and their molecular composition. For several protein aggregation diseases, such as Alzheimer's disease and other amyloidoses, recent studies suggest that instead of being pathological, the formation of large amyloid fibrils might be a protective process that sequesters more dangerous subfibrillar oligomers of the amyloidogenic peptide or protein into relatively innocuous deposits[1]. Thus, efforts to disaggregate amyloid deposits might do more harm than good. Although TSE infectivity is associated with a wide range of PrP^{res} aggregate states[6], little is known about the relative levels of infectivity with respect to particle size, PrP content, or other potential constituents. Furthermore, the size of the smallest infectious unit remains under dispute. Reports that sodium dodecyl sulphate (SDS)-solubilized scrapie PrP monomers can be isolated as infectious units[7–9] have not been confirmed[10,11]. Radiation inactivation[12–14] and liposome solubilization studies[15] have suggested that the minimal infectious unit is between 50–150 kDa, which would correspond to 2–6 PrP molecules, but no such small oligomers have been isolated and determined to be infectious. The present study compares the scrapie infectivity and *in vitro* PrP-converting activity associated with particles ranging in size between the ill-defined smallest infectious unit and large amyloid fibrils, and evaluates which are the most active with respect to PrP content. An infectivity bioassay in hamsters was used to measure infectivity directly, whereas much faster *in vitro* PrP conversion assays were used as surrogates and supplements for the bioassay. Previous studies have shown extensive correlation between infectivity and *in vitro* converting activity[6,16].

To break down large PrP^{res} aggregates and create a range of smaller particles for evaluation of these activities, preparations of largely purified PrP^{res} were subjected to treatments with a variety of detergents and sonication. Initial results revealed that relatively small particles with high levels of converting activity were produced when SDS was used at a concentration of ~1% (Supplementary Fig. S1). Subsequent analyses of the alkyl sulphate family of detergents indicated that further optimization was obtained by switching to sodium *n*-undecyl sulphate (SUS) treatment (Supplementary Fig. S2). SUS-treated samples were diluted so that the final SUS concentration (0.1%) was well below the critical micelle concentration, and fractionated according to size using flow field-flow fractionation (FlFFF). Particle molar mass and radius measurements were obtained through in-line light scattering and refractive index detectors. PrP molecules eluted in two major peaks, one spanning fractions 5–8 and another spanning fractions 19–27 (Fig. 1a, filled circles). Dot-blot-based solid-phase conversion assays revealed that converting activity was first observed near fraction 10, rose to a plateau from fractions 12–18, and peaked around fraction 23 (Fig. 1a, open circles). Data obtained from suspension-based conversion assays were consistent with these results, and confirmed that the products observed in the solid-phase conversion assays represented proteinase K-resistant PrP fragments of the expected size[3] (Supplementary Fig. S3a). To assess relative infectivity levels, fraction aliquots were also quickly diluted into normal hamster brain homogenate and inoculated intracerebrally into hamsters. A marked shortening of the incubation period of disease was observed near fraction 9, indicating a substantial increase in infectivity[17], which peaked at fraction 12 and remained relatively steady throughout the rest of the elution (Fig. 1a, red squares). Because titration of both purified PrP^{res} and scrapie brain homogenate stocks produced consistent incubation periods of disease with respect to levels of PrP^{res} (Supplementary Fig. S4a), LD_{50} (dose lethal to 50% of animals tested) values derived from 263K strain scrapie brain homogenates were used to estimate the levels of infectivity in the fractionated material (Supplementary Fig. S4b). This analysis indicated that the 28-day shortening of incubation period between fractions 7 and 12 corresponded to a >600-fold increase in infectivity. Given limits to the resolution of the FlFFF technique, it is likely that the low levels of infectivity and converting activity detected in fractions 5–8 actually represent the leading edge of activities associated with larger particles that peak in fractions ≥9. These results revealed a major discordance between the levels of PrP, converting activity and infectivity with respect to the size of the particles found in preparations of PrP^{res}.

Because PrP is often thought to be the major protein component of the infectious agent, the levels of converting activity and infectivity in the FlFFF fractions were divided by their total PrP content to give relative 'specific converting activity' (Fig. 1b, circles; see also Supplementary Fig. S3b) and 'specific infectivity' values (Fig. 1b, c, red squares). Both of these values peaked near fraction 12 and dropped

[1]Laboratory of Persistent Viral Diseases and [2]Electron Microscopy Core Facility, Rocky Mountain Laboratories, National Institute of Allergy and Infectious Diseases, National Institutes of Health, Hamilton, Montana 59840, USA.

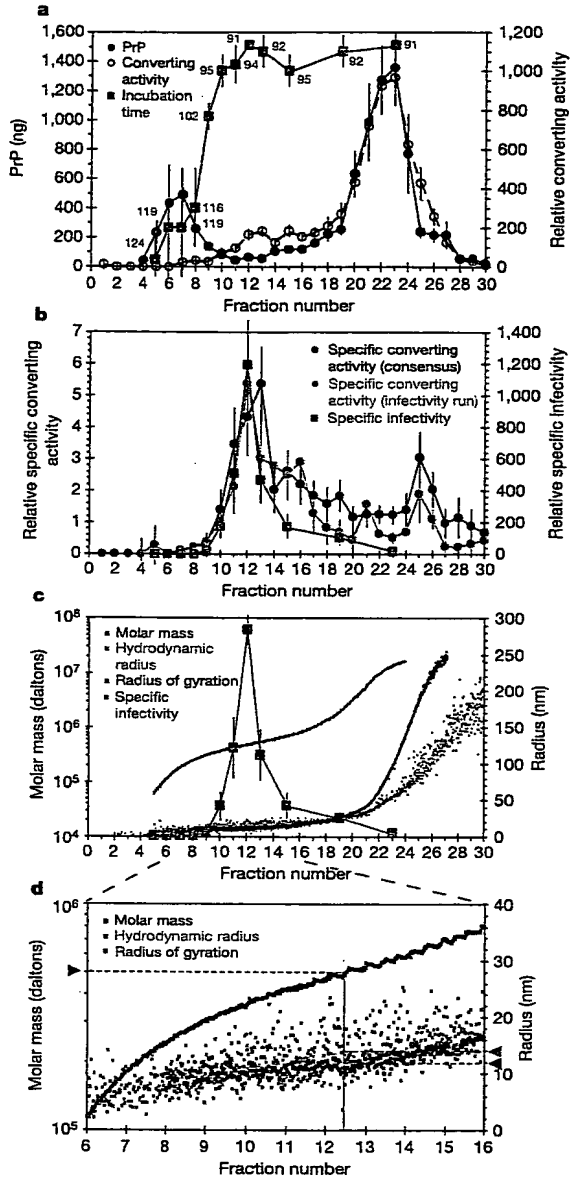

Figure 1 | Analysis of fractionated PrP^{res}. **a**, Quantification of PrP (per 1-ml fractions) by dot immunoblotting with anti-PrP monoclonal antibody 3F4 (n ranged from 3 to 16 from four FlFFF runs), analysis of converting activity by solid-phase conversion assay ($n = 9$ from four FlFFF runs) and scrapie infectivity analysis by incubation time assays in hamsters ($n = 4$ animals from one FlFFF run). Mean incubation periods (days) are indicated by red numbers in the plot. **b**, Calculated specific converting activity for the individual FlFFF run assessed for infectivity ($n = 4$ converting activity analyses), the consensus of all four FlFFF runs ($n = 9$ converting activity analyses) and specific infectivity ($n = 4$ animals). **c**, In-line light scattering analyses of FlFFF runs indicating M_W ($n = 3$), r_h ($n = 4$) and r_g ($n = 4$). The specific infectivity trace from **b** is superimposed. **d**, Expansion of a region of the plot shown in **c**. The solid red line indicates the centre of fraction 12, and the dashed red lines lead to arrowheads, which indicate the mass and radii of particles at this point in the elution. Mean values are shown; error bars represent ±standard error except for incubation time of disease, where they represent ±s.d.

off steeply to each side of the peak. Indeed, the early PrP-containing fraction 7 had ~3,000-fold lower specific infectivity than the peak fraction 12, and the large aggregates in fraction 23 had ~70-fold lower specific infectivity. This analysis revealed a tight correlation between specific infectivity and specific converting activity, and demonstrated that by far the most active particles per unit PrP peaked in fraction 12. Light scattering analyses of these particles indicated that they have apparent weight-average molar masses (M_W) of several hundred kDa (Fig. 1c, d, blue squares) and apparent radii in the 12–14-nm range (Fig. 1c, d, green and violet squares).

Table 1 summarizes the size parameters determined from four independent FlFFF experiments assessed for converting activity, and

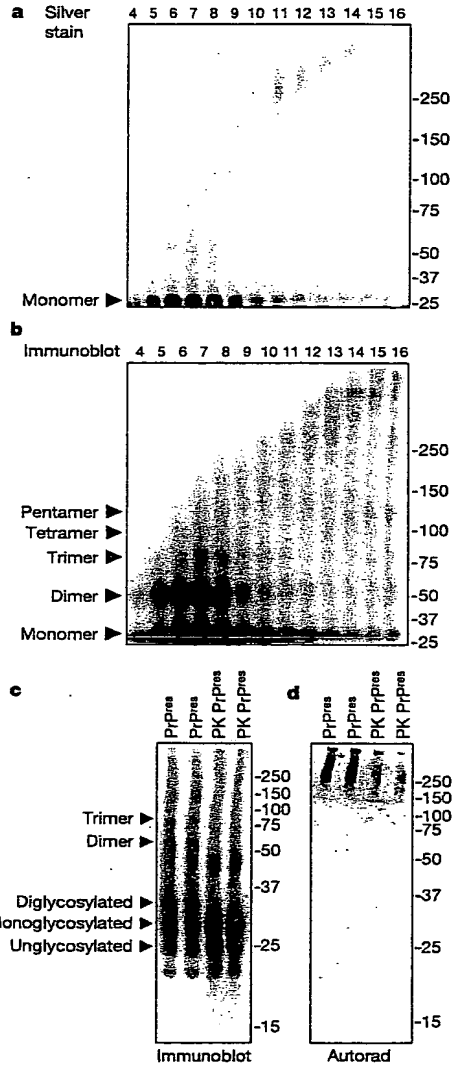

Figure 2 | PAGE analyses of detergent-treated PrP^{res}. **a**, **b**, Samples from FlFFF fractions were subjected to PAGE on 3–8% Tris-acetate gels and analysed by either silver stain (**a**) or immunoblotting with anti-PrP monoclonal antibody 3F4 after transfer to PVDF (**b**). **c**, **d**, Additional samples of purified PrP^{res} were boiled in SDS–PAGE buffer without sonication, subjected to PAGE on 10% Bis-Tris gels, and analysed in duplicate by either immunoblotting (**c**) or solid-phase conversion (**d**). Fraction numbers and types of PrP^{res} used (PK PrP^{res}, proteinase K-digested PrP^{res}) are shown at the top. PrP glycoforms and oligomers are indicated on the left, and molecular weight standards (kDa) are shown on the right.

a single fractionation analysed by infectivity bioassays. The ratio (ρ) of the radius of gyration (r_g) to hydrodynamic radius (r_h) was calculated to estimate the compactness of the particles with peak specific infectivity and converting activity (fraction 12). The values (~0.90) are typical of fairly compact, spherical or ellipsoid shapes[18]. By comparison, much higher ρ values were obtained for fractions 21 and 26, indicating the predominance of highly extended structures. Mean apparent values of ~600 kDa (M_W) and ~13.5 nm (r_h) were determined for the material in fraction 12. These values presumably represent the size of the infectious particles including any bound SUS molecules. Analyses of a set of proteins (bovine serum albumin, ferritin, thyroglobulin) in the presence or absence of SUS showed that observed M_W and r_h values could be increased by as much as 73% and 60% respectively in the presence of SUS (data not shown), suggesting that the particles in fraction 12 may have detergent-subtracted M_W values as low as ~300 kDa and r_h values as low as ~8.5 nm. Thus, these data indicated that the particles with the highest specific infectivity and specific converting activity were approximately 300–600 kDa, roughly spherical-to-elliptical, and 17–27 nm in diameter.

To assess more accurately the oligomeric state of PrP in the early fractions (<9) of the FlFFF separation, samples were subjected to PAGE without further denaturation. Protein (silver) staining (Fig. 2a) and PrP immunoblot (Fig. 2b) analyses of these gels revealed that PrP monomers and a ladder of discrete oligomers up to apparent pentamers (most visible in the immunoblot) peaked in fractions 5–8, which were extremely low in specific infectivity and specific converting activity (Fig. 1b). However, in fractions 11–13, where the highest specific infectivity and specific converting activity were found, monomeric-to-pentameric structures were greatly reduced and larger oligomers above the 250 kDa marker predominated (Fig. 2a, b). The converting activity associated with these oligomers was directly assessed by subjecting detergent-treated PrP^{res} to PAGE as described above, and then electro-blotting the material onto a polyvinylidene difluoride (PVDF) membrane for solid phase conversion analysis. Conversion products were only observed at the bands above the 150–250 kDa markers after SDS (Fig. 2d) or SUS (Supplementary Fig. S5c) treatments, even though the PrP content in the monomer and small oligomer bands was equivalent to, or greatly exceeded, the protein content in the higher bands (Fig. 2c; see also Supplementary Fig. S5a, b). Thus, results obtained from PAGE-based analyses were in excellent agreement with those obtained from dot-blot-based solid-phase conversion analyses (Fig. 1a), and revealed that infectivity and converting activity co-fractionated with structures larger than PrP pentamers, whereas PrP pentamers and smaller oligomers were devoid of converting activity.

To visualize the sizes and shapes of fractionated PrP^{res} particles, samples from representative FlFFF fractions were analysed by transmission electron microscopy (Fig. 3). Consistent with the high ρ values noted in Table 1, fraction 26 contained a preponderance of long fibrils, whereas fraction 21 contained shorter fibrils in conjunction with more amorphous material. Analysis of material from fractions 10 and 15 revealed a collection of smaller amorphous and spherical particles. Although it was unclear whether all of the amorphous/spherical particles contained PrP, the results confirmed that there were no visible fibrils in these fractions. Thus, the size and shape of the particles detected by transmission electron microscopy agreed with the light scattering measurements, indicating that the most infectious particles of PrP^{res} were roughly spherical or ellipsoidal in nature, and ~20–25 nm in diameter.

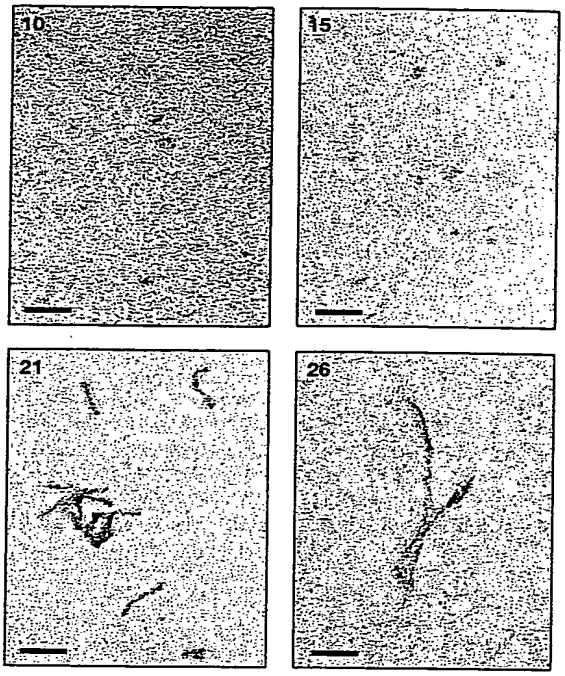

Figure 3 | Transmission electron microscopy analyses of fractionated PrP^{res}. Fraction numbers are indicated in the upper left of each panel. No particles were visible on control grids loaded with buffer alone. Scale bars, 100 nm.

TSE infectious units (prions) are likely to require both biochemical activity as initiators of PrP conversion and stability against degradation in the environment and the host. Whereas large PrP^{res} aggregates might be expected to have greater stability, smaller oligomers (4–15-mers) have been predicted to have greater converting activity and infectivity per unit mass[19,20]. Our present data provide systematic evidence that although the infectivity per particle did not vary by more than approximately twofold between different sizes of infectious aggregates (see Supplementary Discussion), the most infectious units per mass of PrP, or the best apparent compromise between stability and activity, are ~17–27-nm particles of ~300–600 kDa. If these infectious particles are composed solely of PrP molecules averaging ~21.5 kDa each (which may not be the case, see Supplementary Discussion), this would correspond to an

Table 1 | Biophysical parameters of fractionated PrP^{res}

Fraction	M_W (kDa)	$(r_g)_z$ (nm)	$(r_h)_z$ (nm)	ρ
6 (monomer/small PrP oligomers)	155 ± 62	ND	5.0 ± 1.7	ND
12 (peak specific infectivity)	535	12.4	13.4	0.93
12 (peak specific converting activity)	620 ± 331	12.1 ± 2.0	13.5 ± 0.9	0.90
21 (intermediate fibrils)	7,770 ± 4,270	51.9 ± 11.5	37.4 ± 6.7	1.38
26 (largest fibrils)	15,220 ± 9,210	230.1 ± 46.3	90.4 ± 8.1	2.35

Weight-average molar mass (M_W), z-average radius of gyration ($(r_g)_z$) and z-average hydrodynamic radius ($(r_h)_z$) values (mean ± s.d.) were determined from four individual fractionations of PrP^{res}. Values for one fractionation of PrP^{res} assayed for infectivity are also shown. $\rho = r_g/r_h$. ND, not determined.

oligomer of 14–28 PrP molecules. Interestingly, this size range is consistent with the smallest disease-associated PrP aggregates (600 kDa) observed previously[21]. Our observations that the smallest stable unit with PrP converting activity is larger than a 5-mer concur with the results of a previous study that showed that SDS-generated oligomers comprising 4–6 PrP molecules with diameters of ~10 nm are not infectious[22]. Furthermore, we join others in failing to confirm previous reports of the generation of infectious PrP monomers in the presence of alkyl sulphate detergents[7–11]. However, although we screened deliberately for conditions that generate small filterable particles with converting activity, it remains possible that other conditions can stabilize infectious particles that are smaller than PrP hexamers.

The fact that the most infectious units are much smaller than the amyloid fibrils that are often observed in TSE-infected tissues and tissue extracts reinforces concerns that incomplete attempts to destabilize PrP^{res} aggregates for the purposes of therapeutics or decontamination might result in unintended increases in infectivity. Consistent with this possibility, we observed that resonication (in 1% SUS) of large fibrillar PrP^{res} fractions from the FlFFF separation decreased the average fibril length (according to electron microscopy) and increased converting activity by several-fold (data not shown), and others have reported that sonication of PrP^{res} in the presence of phospholipids can increase scrapie infectivity levels[15]. This is not to say that the most infectious particles are necessarily derived from *in vitro* fragmentation of PrP^{res} fibrils. Another strong possibility is that these particles are derived primarily from a distinct non-fibrillar PrP ultrastructure in TSE-infected brain tissue, such as the commonly observed amorphous membrane-associated deposits[23]. Collectively, our observations support the emerging view that with protein folding/aggregation diseases, smaller subfibrillar particles may be much more pathological than larger amyloid fibrils or plaques.

METHODS

Partial disaggregation of PrP^{res}. PrP^{res} was purified from scrapie-infected (263K strain) hamster brain and treated with proteinase K as described previously[24] to produce a product of >90% purity. Unless designated otherwise, the samples were pelleted (20,800*g*, 20 min, 4 °C), re-suspended to 0.1 mg ml^{-1} in 20 mM Tris pH 7.0 containing 1% SUS, sonicated for 1 min in a cup horn at maximum power, frozen in a dry ice/ethanol bath for 5 min, thawed, and incubated at 37 °C for 1 h. Additional FlFFF experiments in which the sonication step was omitted have shown that the intermediate-sized non-fibrillar oligomers with the highest specific converting activity are still generated, and the recovery of converting activity in fractions containing predominantly PrP monomers to pentamers is not enhanced (data not shown). In other designated experiments, samples of PrP^{res} (0.25 mg ml^{-1}) were simply boiled for 2 min in SDS–PAGE buffer (250 mM Tris pH 7.0, 1% SDS, 5% glycerol, 2.5% β-mercaptoethanol, 0.00025% bromophenol blue) without sonication.

Fractionation of PrP^{res}. Samples of partially disaggregated PrP^{res} (50 μg) were filtered through 0.2 μm Nanosep centrifugal devices (Pall Life Sciences) by centrifugation (500*g*, 20 min, 25 °C), and the filtrate was subjected to asymmetrical flow field-flow fractionation[25] on an Eclipse F separation system (Wyatt Technology Europe). The channel was 26.5 cm in length and 350 μm in height, constructed with a trapezoidal spacer of maximal width 21 mm at the inlet, and lined with a 10-kDa cutoff polyethersulphone membrane at the accumulation wall. The sample was loaded in five 100-μl injections, then eluted with 20 mM Tris pH 7.0 containing 0.1% SUS at a channel flow of 1 ml min^{-1} and a cross flow decreasing from 3 ml min^{-1} to 0 ml min^{-1} over 20 min while collecting 1-ml fractions.

Light scattering analyses. Static light scattering, refractive index and dynamic light scattering measurements were carried out on DAWN EOS, Optilab DSP and WyattQELS instruments, respectively (Wyatt Technologies), connected in-line to the FlFFF system. Weight-average molar mass (M_W), *z*-average radius of gyration ($(r_g)_z$) and *z*-average hydrodynamic radius ($(r_h)_z$) values were calculated using ASTRA analysis software (version 4.90.07).

Solid-phase PrP conversion. Samples (50–250 μl) of fractionated PrP^{res} were loaded onto PVDF membranes using a 96-well dot-blot apparatus as described previously[26] or transferred by electro-blotting. Blocking and conversion on membrane sheets (~55 cm^2) were carried out as described[27] under Gdn-free/detergent-free conditions with the following exceptions: conversion reactions (5 ml) on each membrane sheet contained 500,000 counts per min ^{35}S-labelled PrP^{sen}, and 0.1% fetal bovine serum was replaced with 2% BSA. Proteinase K digestion (5 ml; 10 μg ml^{-1}) was terminated by drying the membrane, which was subjected to autoradiography and PhosphorImager analysis. Relative amounts of conversion in dot-blot analyses were obtained by comparison to a series of PrP^{res} standards (1–1,000 ng) loaded onto each membrane sheet.

Incubation time bioassays for scrapie infectivity. Immediately after FlFFF separation, samples of PrP^{res} were diluted fivefold into physiological phosphate buffer containing 1.25% normal hamster brain homogenate and 40 mM sucrose, and 50 μl aliquots were inoculated intracerebrally into Syrian golden hamsters. The incubation period of disease was defined as the number of days from inoculation to euthanization when confirmed to have clinical disease (recumbent animals).

Transmission electron microscopy. Samples of fractionated PrP^{res} (~5 μl) were placed on 400-mesh parlodian-coated nickel grids, incubated for 1 h, washed with H_2O (three times for 10 min), stained with 1% ammonium molybdate for 30 s, dried and visualized on an 80-kV Hitachi H7500 microscope fitted for image capture with a Hamamatsu side-mounted model C4742-95 CCD camera and Advantage HR/HR-B digital image software (AMT). All steps were performed at ambient temperature, and all reagents were passed through 0.02-μm filters within an hour of use.

Received 15 May; accepted 24 June 2005.

1. Caughey, B. & Lansbury, P. T. Protofibrils, pores, fibrils, and neurodegeneration: separating the responsible protein aggregates from the innocent bystanders. *Annu. Rev. Neurosci.* 26, 267–298 (2003).
2. Kayed, R. *et al.* Permeabilization of lipid bilayers is a common conformation-dependent activity of soluble amyloid oligomers in protein misfolding diseases. *J. Biol. Chem.* 279, 46363–46366 (2004).
3. Kocisko, D. A. *et al.* Cell-free formation of protease-resistant prion protein. *Nature* 370, 471–474 (1994).
4. Prusiner, S. B. Prions. *Proc. Natl Acad. Sci. USA* 95, 13363–13383 (1998).
5. Silveira, J. R., Caughey, B. & Baron, G. S. Prion protein and the molecular features of transmissible spongiform encephalopathy agents. *Curr. Top. Microbiol. Immunol.* 284, 1–50 (2004).
6. Caughey, B., Raymond, G. J., Kocisko, D. A. & Lansbury, P. T. Jr Scrapie infectivity correlates with converting activity, protease resistance, and aggregation of scrapie-associated prion protein in guanidine denaturation studies. *J. Virol.* 71, 4107–4110 (1997).
7. Prusiner, S. B. Molecular biology of prion diseases. *Science* 252, 1515–1522 (1991).
8. Brown, P., Liberski, P. P., Wolff, A. & Gajdusek, D. C. Conservation of infectivity in purified fibrillary extracts of scrapie-infected hamster brain after sequential enzymatic digestion or polyacrylamide gel electrophoresis. *Proc. Natl Acad. Sci. USA* 87, 7240–7244 (1990).
9. Safar, J. *et al.* Molecular mass, biochemical composition, and physicochemical behaviour of the infectious form of the scrapie precursor protein monomer. *Proc. Natl Acad. Sci. USA* 87, 6373–6377 (1990).
10. Hope, J. The nature of the scrapie agent: the evolution of the virino. *Ann. NY Acad. Sci.* 724, 282–289 (1994).
11. Morillas, M., Vanik, D. L. & Surewicz, W. K. On the mechanism of α-helix to β-sheet transition in the recombinant prion protein. *Biochemistry* 40, 6982–6987 (2001).
12. Alper, T., Haig, D. A. & Clarke, M. C. The exceptionally small size of the scrapie agent. *Biochem. Biophys. Res. Commun.* 22, 278–284 (1966).
13. Gibbs, C. J. Jr, Gajdusek, D. C. & Latarjet, R. Unusual resistance to ionizing radiation of the viruses of kuru, Creutzfeldt-Jakob disease, and scrapie. *Proc. Natl Acad. Sci. USA* 75, 6268–6270 (1978).
14. Bellinger-Kawahara, C. G., Kempner, E., Groth, D., Gabizon, R. & Prusiner, S. B. Scrapie prion liposomes and rods exhibit target sizes of 55,000 Da. *Virology* 164, 537–541 (1988).
15. Gabizon, R., McKinley, M. P. & Prusiner, S. B. Purified prion proteins and scrapie infectivity copartition into liposomes. *Proc. Natl Acad. Sci. USA* 84, 4017–4021 (1987).
16. Raymond, G. J. *et al.* Molecular assessment of the potential transmissibilities of BSE and scrapie to humans. *Nature* 388, 285–288 (1997).
17. Prusiner, S. B. *et al.* Molecular properties, partial purification, and assay by incubation period measurements of the hamster scrapie agent. *Biochemistry* 19, 4883–4891 (1980).
18. Gast, K., *et al.* in *Laser Light Scattering in Biochemistry* (eds Harding, S. E., Sattelle, D. B. & Bloomfield, V. A.) 209–224 (The Royal Society of Chemistry, Cambridge, 1992).
19. Masel, J., Jansen, V. A. & Nowak, M. A. Quantifying the kinetic parameters of prion replication. *Biophys. Chem.* 77, 139–152 (1999).
20. Masel, J., Genoud, N. & Aguzzi, A. Efficient inhibition of prion replication by PrP-Fc_2 suggests that the prion is a PrP^{Sc} oligomer. *J. Mol. Biol.* 345, 1243–1251 (2005).
21. Tzaban, S. *et al.* Protease-sensitive scrapie prion protein in aggregates of heterogeneous sizes. *Biochemistry* 41, 12868–12875 (2002).

22. Riesner, D. *et al.* Disruption of prion rods generates 10-nm spherical particles having high α-helical content and lacking scrapie infectivity. *J. Virol.* 70, 1714–1722 (1996).
23. Jeffrey, M. *et al.* Correlative light and electron microscopy studies of PrP localisation in 87V scrapie. *Brain Res.* 656, 329–343 (1994).
24. Raymond, G. J. & Chabry, J. in *Techniques in Prion Research* (eds Lehmann, S. & Grassi, J.) 16–26 (Birkhauser, Basel, 2004).
25. Wahlund, K.-G. in *Field-Flow Fractionation Handbook* (eds Schimpf, M., Caldwell, K. & Giddings, J. C.) 279–294 (John Wiley & Sons, New York, 2000).
26. Kocisko, D. A. *et al.* New inhibitors of scrapie-associated prion protein formation in a library of 2000 drugs and natural products. *J. Virol.* 77, 10288–10294 (2003).
27. Maxson, L., Wong, C., Herrmann, L. M., Caughey, B. & Baron, G. S. A solid-phase assay for identification of modulators of prion protein interactions. *Anal. Biochem.* 323, 54–64 (2003).

Supplementary Information is linked to the online version of the paper at www.nature.com/nature.

Acknowledgements We thank C. Y. Huang and D. Follmann (Biostatistics Research Branch, NIH/NIAID) for performing statistical analyses. We thank B. Chesebro, G. S. Baron and S. J. Robertson for critiquing the manuscript. This research was supported in part by the Intramural Research Program of the NIH/NIAID. V.L.S. acknowledges support from the Alberta Heritage Foundation for Medical Research through a clinical fellowship award.

Author Contributions J.R.S. spearheaded the project, developed the critical methods and performed the PrP^{res} disaggregation, fractionation and particle analyses. G.J.R. and A.G.H. purified PrP^{res} and performed bioassays and other supporting experiments. R.E.R. provided bioassay standard curve data. V.L.S. and S.F.H. performed electron microscopy. B.C. helped with project design, data interpretation and writing (primarily with J.R.S.)

Author Information Reprints and permissions information is available at npg.nature.com/reprintsandpermissions. The authors declare no competing financial interests. Correspondence and requests for materials should be addressed to B.C. (bcaughey@nih.gov).

Supplementary Information

The most infectious prion protein particles

Jay R. Silveira[1], Gregory J. Raymond[1], Andrew G. Hughson[1], Richard E. Race[1], Valerie L. Sim[1], Stanley F. Hayes[2], and Byron Caughey[1]

[1]Laboratory of Persistent Viral Diseases and [2]Electron Microscopy Core Facility, Rocky Mountain Laboratories, National Institute of Allergy and Infectious Diseases, National Institutes of Health, Hamilton, Montana 59840, USA

Table of Contents

1. Supplementary Methods

Analysis of filtered converting activity

Samples of purified, PK-digested 263K PrP-res (2 mg/mL) were pelleted (20,800 x g, 20 min, 4°C), and resuspended in an equal volume of 0.25 M Tris pH 7.0. Aliquots (0.5-7.5 uL) were diluted to 0.1 mg/mL in the same buffer containing various detergents, without sonication. Samples were subjected to a 5 min freeze/thaw cycle, incubated at 37°C for one hour, and filtered by centrifugation (14,000 x g, 3 min or 500 x g, 20 min) at 25 °C through 0.2 μm or 300 kDa (~30 nm) Nanosep centrifugal devices. Filtrates of the material were analyzed by solid-phase conversion assay, and the formation of small particles that retained converting activity was assessed by the levels of converting activity in filtrates, which were expressed as a percentage of the level of converting activity detected in untreated, unfiltered PrP-res.

Suspension-based PrP conversion

Samples (20 μL) of fractionated PrP-res were analyzed in suspension-based conversion reactions (40 μL) containing 40,000 CPM ^{35}S-PrP-sen under the same conditions used for solid-phase conversion reactions except for the presence of residual SUS (0.05%) and Tris (10 mM) derived from the samples. PK (20 μg/mL) digestion, SDS-PAGE, and conversion efficiency calculations were performed as described previously[1].

Scrapie infectivity titrations

Groups of Syrian golden hamsters were inoculated intracranially (50 μL/animal) with successive 10-fold dilutions of either 1% brain homogenate or purified PrP-res. Dilutions were made in physiological phosphate buffer containing 2% fetal bovine serum. Homogenates (~10^8 LD_{50}/50 μL) were derived from the brains of hamsters clinically-affected with the 263K strain of hamster scrapie. LD_{50} values were determined as previously described[2], and the incubation period of disease was defined as the number of days from inoculation to euthanization at end-stage clinical disease (recumbent animals).

Determination of specific infectivity, specific converting activity, and statistical analyses

Levels of infectivity (LD_{50}) were first determined from the incubation period of disease for each animal by using the equation fit to the data in Supplementary Figure S4b:

$$LD_{50} = 5.21 \times 10^{51} * T^{-24.097},$$

where T is the incubation period of disease in days.

The mean and standard error (SE) for LD_{50} values, converting activities, and PrP amounts were then determined for each fraction.

The levels of scrapie infectivity and PrP converting activity with respect to PrP amount (specific infectivity and specific converting activity respectively), are defined as:

Specific infectivity = infectivity/PrP amount

Specific converting activity = converting activity/PrP amount

The standard errors of specific infectivity and specific converting activity were derived by using a Taylor series expansion. Note that specific converting activity and specific infectivity are estimated by the ratio of two averages: the average converting activity or infectivity (Y) divided by the average PrP amount (X). The standard error of specific converting activity or specific infectivity (Y/X) can be approximated by:

$$\sqrt{\frac{SE(Y)^2}{E(X)^2} + \frac{E[Y]^2 * SE(X)^2}{E[X]^4}},$$

where E[X] and SE(X) are the mean and the standard error of PrP amount, and E[Y] and SE(Y) are the mean and the standard error of converting activity or infectivity.

2. Filtration of converting activity in SDS-treated samples of PrP-res.

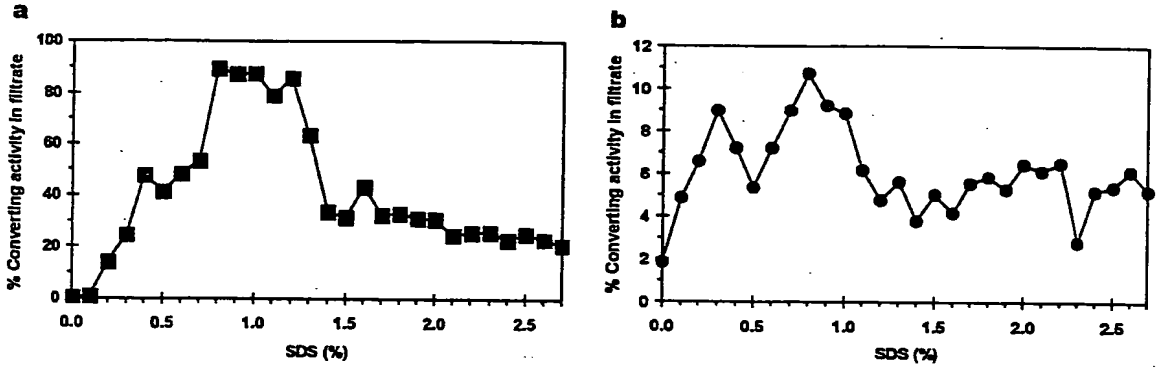

Figure S1 Samples of PrP-res were treated (1 hr, 37° C) with SDS at concentrations from 0 to 2.7% without sonication, passed through either 0.2 μm (**a**) or 300 kDa (**b**) filters, and the filtrate was analyzed for *in vitro* PrP-converting activity by solid-phase conversion assay.

3. 300-kDa filtration of converting activity in alkyl sulfate-treated samples of PrP-res.

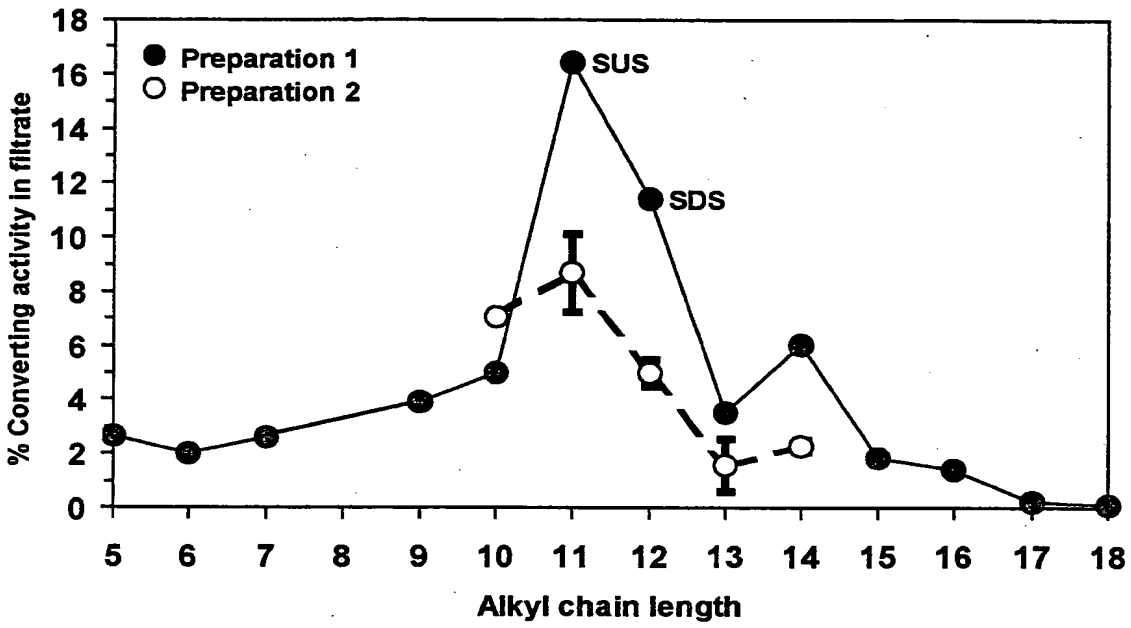

Figure S2 Samples of PrP-res were treated (1 hr, 37° C) with 1% alkyl sulfate solutions without sonication, passed through a 300-kDa filter, and the filtrate was analyzed for *in vitro* PrP-converting activity by solid-phase conversion assay. Values are shown for two different purified stocks of PrP-res, and for preparation #2 represent mean ± range (n = 2). The samples treated with SUS and SDS are indicated for preparation 1.

4. Suspension-based conversion assay of fractionated PrP-res.

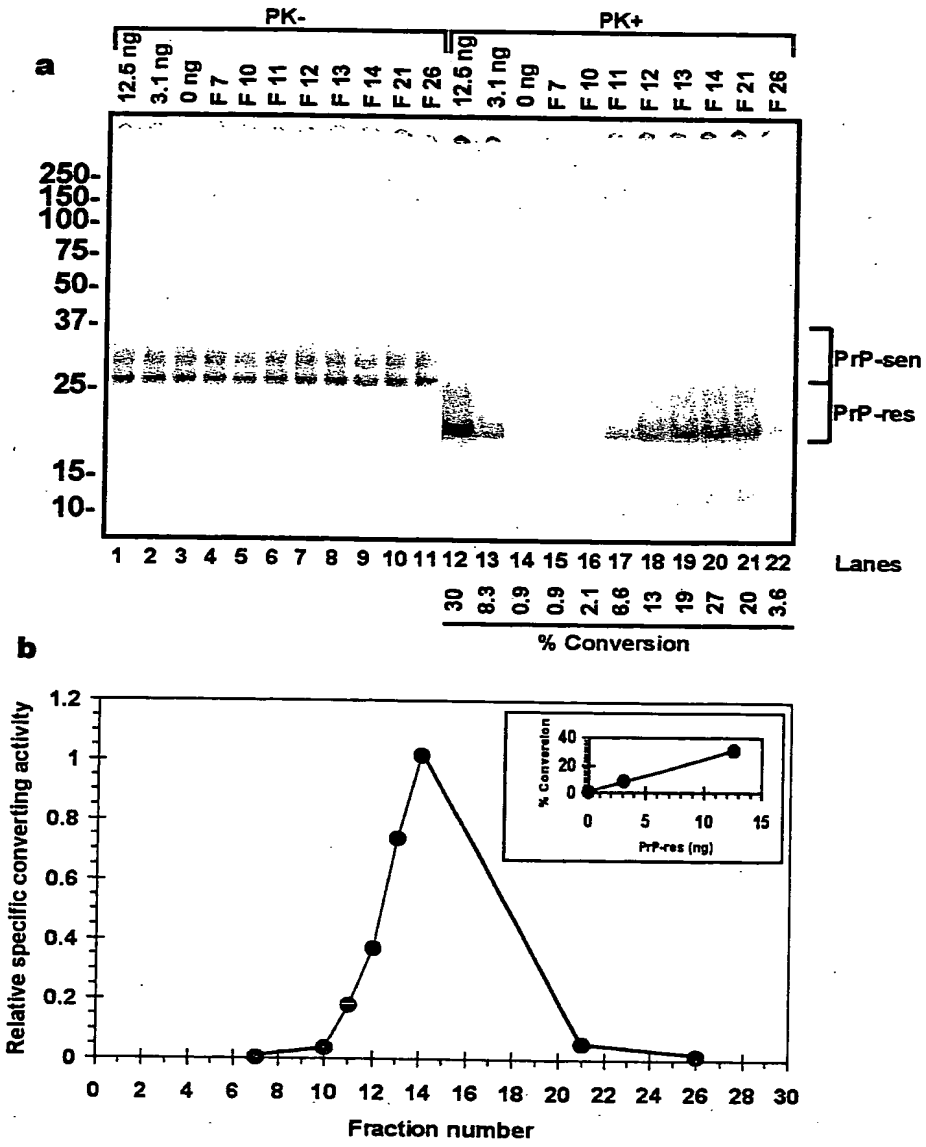

Figure S3 a, autoradiogram of products from suspension-based conversion assay of select FlFFF fractions. Lanes 1-11 represent 1/10 of the ^{35}S-PrP-sen applied to the conversion reactions, and lanes 12-22 represent the remaining 9/10 of the conversion reactions, which were digested with PK. Control reactions with PrP-res (lanes 1-3 and 12-14) were analyzed to relate amounts of PrP-res to percent conversion. Fraction

numbers or amounts of PrP-res (ng) are shown at the top, and the percent conversion (bottom) was calculated using the ^{35}S-PrP bands indicated to the right. Molecular weight standards (kDa) are shown on the left. **b**, Calculated specific converting activity. The relationship between the amount of input PrP-res, and the percent conversion was linear up to at least 12.5 ng PrP-res (inset). The presence of the peak of specific converting activity at fraction 14 was consistent with a slight shift in the elution profile of the PrP-res in this individual analysis and did not represent a notable change in the M_W or size of the particles found at the corresponding peak in solid-phase conversion analyses.

5. Titration of scrapie infectivity.

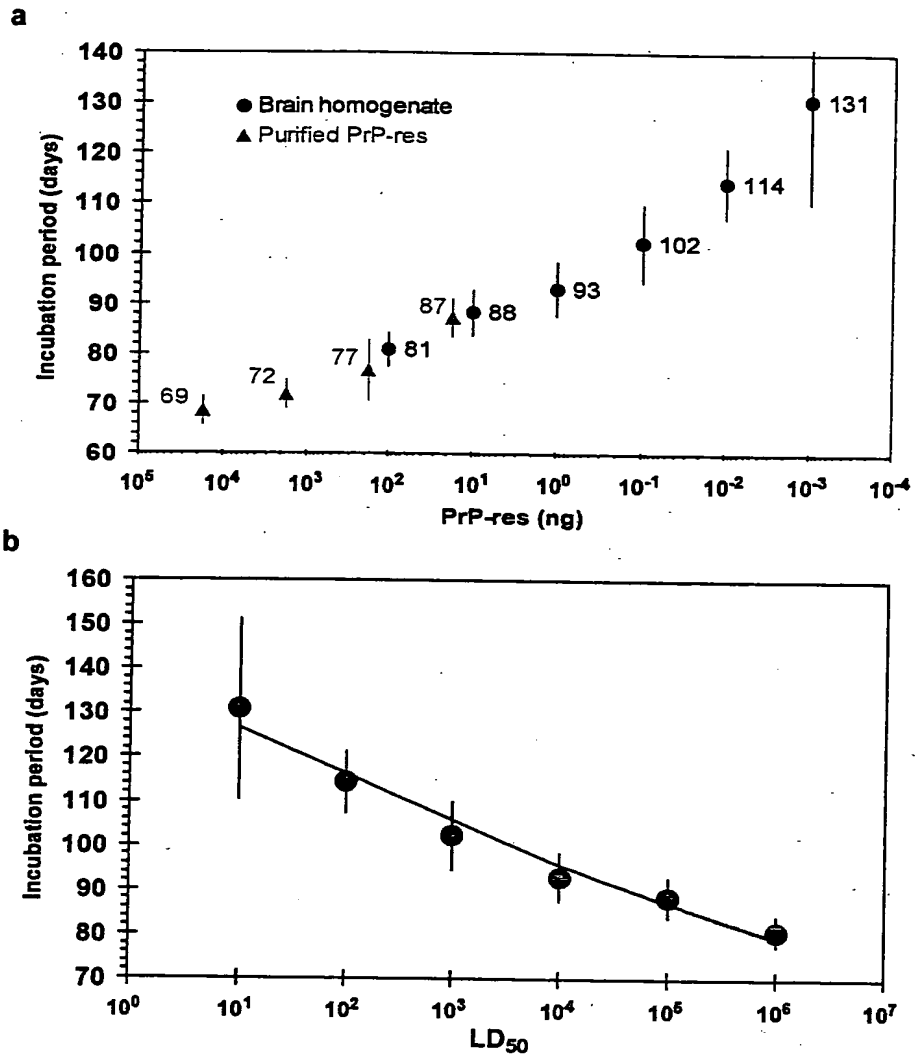

Figure S4 Incubation period of scrapie disease as a function of (**a**) PrP-res derived from either scrapie infected brain homogenates (n ranged from 18 to 28 animals for each dilution) or purified PrP-res (n = 6 for each dilution), or (**b**) LD_{50} (n ranged from 18 to 28 animals for each dilution). Mean incubation periods are indicated by numbers in the plot, error bars represent ± s.d.

6. PAGE analyses of SUS-treated PrP-res.

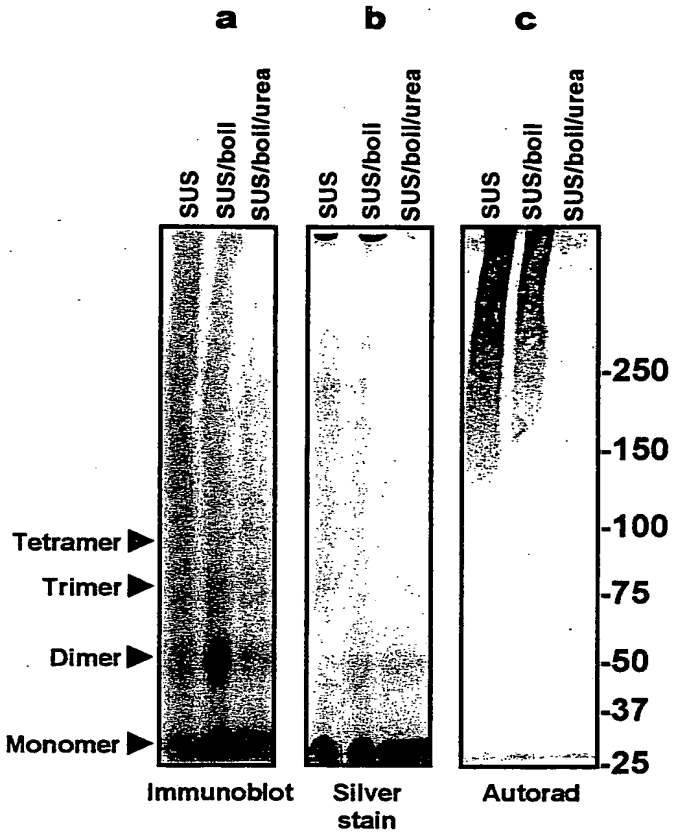

Figure S5 Samples of purified PrP-res were subjected to the SUS disaggregation procedure described in the methods section of the main text, with the addition of 10 min boiling alone, or boiling in urea sample buffer (62.5 mM Tris pH 6.8, 5% glycerol, 5% SDS, 0.02% bromophenol blue, 3 mM EDTA, 4 M urea), separated by PAGE on 3-8% Tris-Acetate gels, and analyzed by either (**a**) immunoblotting, (**b**) silver stain, or (**c**) solid-phase conversion. Note that the lower percentage acrylamide gels used in this figure cannot resolve individual PrP glycoforms, while the higher percentage acrylamide gels used in Fig 2, panels c and d can. PrP oligomers are indicated on the left, and molecular weight standards (kDa) are shown on the right.

7. Denaturing PAGE analyses of fractionated PrP-res.

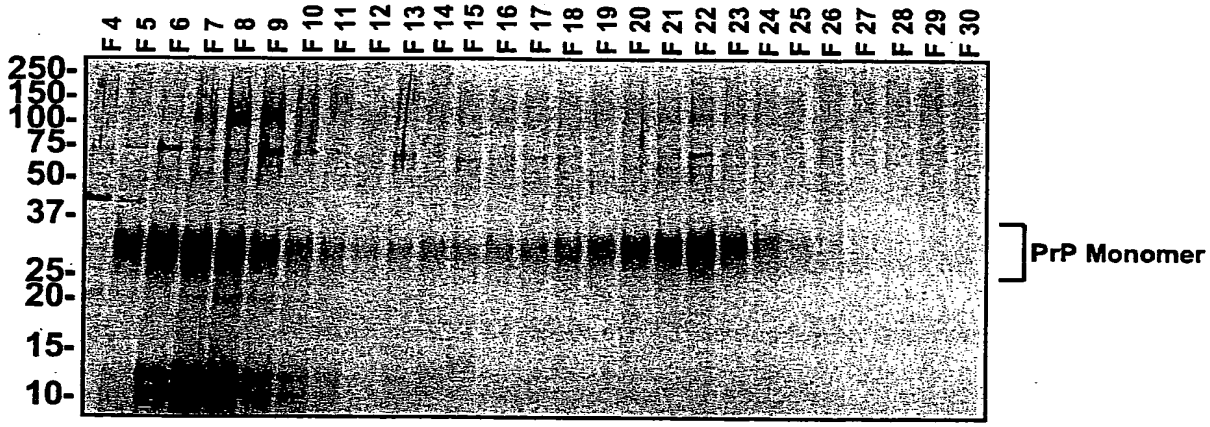

Figure S6 Samples were removed from FlFFF fractions, boiled 10 min in urea sample buffer, subjected to PAGE on 10% Bis-Tris gels, and analyzed by silver stain. Fraction numbers are shown at the top, molecular weight standards (kDa) are shown on the left, and the location of PrP monomer is indicated on the right.

8. Supplementary Discussion

Estimation of infectivity per particle

From our FlFFF data, we can estimate infectivity per particle, rather than per unit PrP. Assuming that most of each particle is PrP (which may not be true for all of the fractions), such calculations suggest that the infectivity per particle values were similar throughout the most infectious FlFFF fractions (10-23 in figure 1), with the smaller non-fibrillar particles (e.g. fraction 12) having values slightly higher, but within 2-fold, of those of large fibrils (e.g. fraction 23) (data not shown). Thus, as long as infectious particles are above a minimum size, particle concentration is a key parameter in determining scrapie infectivity titer.

PrP content of PrP-res aggregates

Based on protein assays and ultra-microbalance measurements, 47±9% of the vacuum-dried weight of the washed, unfractionated SUS-treated PrP-res particles was protein (data not shown), and, according to semi-quantitative western blots (data not shown), >87% of the protein was PrP. Adjusting for the glycan and glycophosphatidylinositol content (~25%) of PK-treated PrP molecules, we estimate that at least 54% of the mass was attributable to PrP molecules. In addition, the silver-stained gel in Supplemental Fig. S6 shows that the vast majority of protein in all of the FlFFF fractions was PrP. However, it is unclear how much of the non-PrP mass of the aggregates is tightly bound SUS versus other molecules (e.g. polysaccharide[3], glycosaminoglycans[4], lipids[5]), or what proportion of the most infectious particles is PrP. We have not been able to separate the unidentified silver-stained molecules migrating below the 15-kDa marker from the FlFFF

fractions with PrP and infectivity (Supplemental Fig. S6). These proteins do not react with our anti-PrP antibodies and, so far, have defied identification by MALDI-mass spectrometry of proteolytic fragments (data not shown). Whether these or other molecules are essential components of the most infectious units remains to be determined. Our demonstration of infectivity in particles of a few hundred kDa establishes this mass as the upper limit for any individual molecular component of infectivity, especially if one is to allow for the presence of PrP molecules as at least part of the minimal particle mass.

9. Supplementary References

1. Maxson, L., Wong, C., Herrmann, L. M., Caughey, B. & Baron, G. S. A solid-phase assay for identification of modulators of prion protein interactions. *Anal. Biochem.* **323**, 54-64 (2003).

2. Hadlow, W. J., Kennedy, R. C. & Race, R. E. Natural infection of Suffolk sheep with scrapie virus. *J. Infect. Dis.* **146**, 657-664 (1982).

3. Appel, T. R., Dumpitak, C., Matthiesen, U. & Riesner, D. Prion rods contain an inert polysaccharide scaffold. *Biol. Chem.* **380**, 1295-1306 (1999).

4. Wong, C. *et al.* Sulfated glycans and elevated temperature stimulate PrPSc-dependent cell-free formation of protease-resistant prion protein. *EMBO J.* **20**, 377-386 (2001).

5. Klein, T. R., Kirsch, D., Kaufmann, R. & Riesner, D. Prion rods contain small amounts of two host sphingolipids as revealed by thin-layer chromatography and mass spectrometry. *Biol. Chem.* **379**, 655-666 (1998).

Eur. J. Biochem. 176, 21–30 (1988)
© FEBS 1988

Purification and properties of the cellular and scrapie hamster prion proteins

Eric TURK[1], David B. TEPLOW[2], Leroy E. HOOD[2] and Stanley B. PRUSINER[1,2]

Departments of [1] Neurology and [2] Biochemistry and Biophysics, University of California, San Francisco
Division of Biology, California Institute of Technology, Pasadena

(Received February 26/May 9, 1988) – EJB 88 0246

During scrapie infection an abnormal isoform of the prion protein (PrP), designated PrP^{Sc}, accumulates and is found to copurify with infectivity; to date, no nucleic acid has been found which is scrapie-specific. Both uninfected and scrapie-infected cells synthesize a PrP isoform, denoted PrP^{C}, which exhibits physical properties that differentiate it from PrP^{Sc}. PrP^{C} was purified by immunoaffinity chromatography using a PrP-specific monoclonal antibody cross-linked to protein-A–Avidgel. PrP^{Sc} was purified by detergent extraction, poly(ethylene glycol) precipitation and repeated differential centrifugation of PrP^{Sc} polymers. Both PrP isoforms were found to have the same N-terminal amino acid sequence which begins at a predicted signal peptide cleavage site. The first 8 residues of PrP^{C} were found to be KKXPKPGG and the first 29 residues of PrP^{Sc} were found to be KKXPKPGGWNTGGSXYPGQGSPGGNRYPP. Arg residues 3 and 15 in PrP^{Sc} and 3 in PrP^{C} appear to be modified since no detectable signals (denoted X) were found at these positions during gas-phase sequencing. Both PrP isoforms were found to contain an intramolecular disulfide bond, linking Cys 179 and 214, which creates a loop of 36 amino acids conthining the two N-linked glycosylation sites. Development of a purification protocol for PrP^{C} should facilitate comparisons of the two PrP isoforms and lead to an understanding of how PrP^{Sc} is synthesized either from PrP^{C} or a precursor.

Scrapie is a neurodegenerative disease of sheep and goats which can be transmitted experimentally to laboratory animals [1–3]. In many respects, scrapie resembles three human neurodegenerative diseases: kuru, Creutzfeldt-Jakob disease and Gerstmann-Sträussler syndrome. These human diseases can also be transmitted to experimental animals after prolonged incubation periods [4–6].

The unusual properties of the infectious particles causing scrapie have been appreciated for many years and have given rise to considerable speculation about the composition of these pathogens [7–10]. Despite intensive efforts to identify a nucleic acid within the scrapie agent, none has been found [9, 11–16]. On the other hand, a protein has been identified which purifies with infectivity and its properties mimic many of those exhibited by the infectious agent [17–19].

To distinguish this novel class of infectious pathogens from viruses and viroids without prejudging their composition, the term 'prion' was introduced [9]. Prions are defined as small proteinaceous infectious particles which resist inactivation by procedures that modify nucleic acids. Subsequently, the prion protein (PrP) from scrapie-infected hamster brains was identified and designated PrP 27–30 [17–19]. Determination of the N-terminal sequence of PrP 27–30 led to the cloning and sequencing of a PrP cDNA [21]. Those studies showed that PrP 27–30 is derived from a larger protein designated PrP^{Sc} and that a cellular PrP isoform designated PrP^{C} is synthesized in both uninfected and scrapie-infected cells [22–24].

The purification of PrP 27–30 was based upon a series of detergent extractions and differential centrifugations, as well as limited protease digestion and discontinuous sucrose gradient sedimentation [18, 25]. Subsequently, other investigators modified this protocol for small-scale purification of PrP 27–30 [26] and for the isolation of PrP^{Sc} by omitting the protease digestion step [27].

The structure and organization of the hamster PrP gene predicted that both PrP isoforms would have the same amino acid sequence [23]. The entire protein coding region is contained within exon II of the PrP gene which is a single-copy chromosomal gene [22, 23]; immunological studies established the relatedness of PrP^{C} and PrP^{Sc} [28, 29]. The differing properties of PrP^{C} and PrP^{Sc}, which include protease sensitivity, ability to form amyloid polymers and association with infectivity [21, 22, 24, 30], are thought to arise from a post-translational event [23]. Whether the difference between PrP^{C} and PrP^{Sc} is solely conformational or arises from a chemical modification remains uncertain. While the function of PrP^{C} is unknown, genetic studies have established that PrP^{Sc} plays a central role in scrapie pathogenesis [31, 32]; biochemical studies suggest that PrP^{Sc} is the major, and possibly the only, component of the infectious particle [17, 19, 20, 33, 34]. In view of the intimate association of infectivity with PrP^{Sc} and the manifest differences between PrP^{C} and PrP^{Sc}, the purification and characterization of PrP^{C} was undertaken with the

Correspondence to S. B. Prusiner, Department of Neurology, HSE-781, School of Medicine, University of California, San Francisco, California, USA-94143-0518

Abbreviations. PrP, prion protein; PrP^{C}, cellular prion protein isoform; PrP^{Sc}, scrapie prion protein isoform; MBB, 4-(*N*-maleimidobutyryl) biocytin; MAb-A-Avidgel, PrP monoclonal antibody cross-linked to protein-A–Avidgel beads; IgG-A-Avidgel, normal mouse IgG cross-linked to protein-A–Avidgel; QA-glass, Whatman GF/F glass-fiber filter derivatized with *N*-trimethoxysilylpropyl-*N*,*N*,*N*-trimethylammonium chloride; KIU, kallikrein inhibitor unit.

aim of eventually establishing the molecular basis for the divergent properties of the two PrP isoforms.

We report here the purification of PrP^C by immunoaffinity procedures using a monoclonal antibody raised against PrP 27–30 and the large-scale purification of PrP^{Sc} using a modified protocol previously developed for PrP 27–30 isolation. Both PrP^{Sc} and PrP^C were shown to have the same N-terminal amino acid sequence, beginning at a site predicted for the cleavage of an N-terminal signal peptide [23, 35]. Both proteins were found to have an intramolecular disulfide bond joining Cys residues predicted from the DNA sequence to occur at positions 179 and 214.

MATERIALS AND METHODS

Materials

All chemicals were of the highest grades commercially available. Sodium dodecyl sarcosinate, sodium cholate, sodium deoxycholate, Triton X-100, poly(ethylene glycol) 8000, aprotinin, phenylmethylsulfonyl fluoride, glycine, Tris, Nonidet P-40, dimethyl pimelimidate dihydrochloride, protein-A–Sepharose and mouse IgG were purchased from Sigma. Molecular mass marker proteins for SDS-PAGE and Western blots were also purchased from Sigma and included α-lactalbumin (M_r 14200), soybean trypsin inhibitor (20100), bovine carbonic anhydrase (31000), rabbit glyceraldehyde-3-phosphate dehydrogenase (36000), ovalbumin (42700), bovine serum albumin (66300) and rabbit phosphorylase *b* (97400). Protein-A–Avidgel was purchased from Bioprobe International (Tustin, CA). SDS was obtained from BDH. Acrylamide and *N,N'*-methylenebisacrylamide were purchased from Bio-Rad Laboratories. Enzyme-grade sucrose and ammonium sulfate were obtained from Schwarz/Mann. *N*-Ethylmaleimide, 4-(*N*-maleimido-butyryl)biocytin (MBB) and Zwittergents 3-14 and 3-16 were purchased from Calbiochem-Behring. Streptavidin–alkaline-phosphatase conjugate was obtained from Zymed. *N*-Trimethoxysilylpropyl-*N,N,N*-trimethylammonium chloride was purchased from Petrarch (Bristol, PA). Trisacryl GF05 was purchased from LKB. Nitroblue-tetrazolium, 5-bromo-4-chloro-3-indolyl phosphate and the alkaline phosphatase conjugates of goat anti-rabbit and goat anti-mouse IgG were purchased from Promega-Biotec. Nitrocellulose sheets were obtained from Hoefer Scientific and guanidinium thiocyanate from Fluka. Colloidal gold conjugate of goat anti-rabbit IgG, Aurodye and silver enhancement reagents were purchased from Janssen.

Source of prion proteins and scrapie bioassay

Syrian golden hamsters (Lak:LVG) were used in our studies. Pregnant females (11-days gestation) were purchased from Charles River Laboratories (Lakeview, NJ). Pups were weaned after four weeks and fed *ad libitum* on Purina rat chow. Those animals to be used for PrP^C purification were sacrificed at one year of age by CO_2 asphyxiation. Forebrains were immediately removed, frozen in liquid N_2 and stored at −80°C.

A hamster-adapted isolate of scrapie prions was kindly provided by Dr Richard Marsh [3]. The passage history of this material has been previously described [36]. Scrapie prion titers were determined by an incubation time interval assay [25, 36]. A 50-µl sample to be assayed was injected intracerebrally into random-bred hamsters (Lak:LVG). The time intervals from inoculation to onset of illness and from inoculation to death were used to estimate the titers of the injected samples.

Weanling hamsters were inoculated intracerebrally with $10^{7.5} \times ID_{50}$ of the scrapie agent [25, 36, 37]. They were sacrificed 60–65 days after inoculation and forebrains were frozen in liquid N_2 for storage at −80°C.

Immobilized antibody

The murine monoclonal antibody 196.13A5 [29] was purified from culture supernates by adsorption on protein-A–Sepharose in the presence of 1.5 M NaCl at pH 8.5 (suggested by Bioprobe International, Tustin, CA) and elution at low pH. Purified monoclonal IgG was then adsorbed to protein-A–Avidgel in the presence of 1.6 M NaCl at pH 8.5 and then cross-linked with dimethyl pimelimidate [38]. Unreacted imidate groups were blocked with ethanolamine. Antibody was coupled at 1 mg/ml bed in this preparation (MAb-A-Avidgel).

Normal mouse IgG was similarly coupled to protein-A–Avidgel at 2 mg/ml bed (IgG-A-Avidgel). The beads were washed with 0.5% acetic acid in 150 mM NaCl, then 0.5 M NaCl, and finally unbuffered 50 mM triethylamine, 0.5% sodium deoxycholate. The three washes were repeated and the beads were stored at 4°C in 0.2 M NaCl, 50 mM Na/Hepes (pH 8 at 5°C), 0.02% NaN_3.

Polyacrylamide gel electrophoresis and Western blotting

Proteins in electrophoresis sample buffer (100 mM Tris/Cl, pH 8.9, at 25°C, 2% SDS, 5% 2-mercaptoethanol, 10% glycerol and 0.002% bromphenol blue) were heated at 100°C for 1–2 min. The proteins were separated by SDS-PAGE (10% monomer) by the method of Laemmli [39]. Transfer of proteins from polyacrylamide gels to nitrocellulose sheets was accomplished overnight at 5 V/cm or for 2 h at 10 V/cm with 0.1% SDS added to the transfer buffer [40].

Immunostaining of Western blots

Rabbit PrP antisera and monoclonal antibody 196.13A5 were produced as described previously [29, 30]. A mono-specific rabbit antiserum raised against the 13 N-terminal amino acids of PrP 27–30 (GQGGGTHNQWNKP) was also used for immunoblotting [28].

Lanes containing molecular mass markers were excised from the nitrocellulose blots and stained with Aurodye as described by the manufacturer (Janssen). The blots were then blocked for 30 min in 5% (mass/vol.) nonfat dry milk in 10 mM Tris/Cl buffer, pH 8.2 at 25°C, 200 mM NaCl, 0.05% Tween 20. Immunoreactive proteins were detected by incubation with diluted rabbit primary antiserum or monoclonal antibody (1–3 µg/ml) in the same buffer for 30–120 min at 23°C, then with alkaline-phosphatase-conjugated secondary antibody for 1–2 h and developing with nitroblue-tetrazolium and 5-bromo-4-chloro-3-indolyl phosphate as suggested by the supplier (Promega Biotec).

Alternatively, colloidal gold-conjugated secondary antibodies were used overnight and the image enhanced with silver as suggested by the manufacturer (Janssen).

Silver staining of polyacrylamide gels

Polyacrylamide gels were stained with silver by a modification [41] of the method of Heukeshoven and Dernick [42].

Amino acid sequencing

Protein samples were suspended in electrophoresis sample buffer supplemented with 10 mM α,α'-dimercaptoadipate and warmed at 60°C for 9 min. Samples of PrP^C were fractionated on 10% polyacrylamide gels by SDS-PAGE and blotted for 7 h at 0.4 A, 3°C, in 25 mM Tris/Cl, pH 8.3 at 23°C, 10 mM glycine, 0.5 mM dithiothreitol, onto a Whatman GF/F glass-fiber disc previously derivatized with *N*-trimethoxysilylpropyl-*N,N,N*-trimethylammonium chloride (QA-glass) [43]. Protein bands were visualized by fluorescence under 254-nm light after the blots were immersed in a 0.01% solution of 3,3'-dipentyl-oxacarbocyanine iodide in 50 mM $NaHCO_3$ and washed in 50 mM $NaHCO_3$. The bands were then excised for N-terminal sequence analysis.

A band of PrP^{Sc} was cut from a gel after SDS-PAGE and protein was eluted in 20 mM Tris/Cl, 0.2% SDS, 1 mM EDTA. PrP^{Sc} was precipitated with 2.3 vol. ethanol, redissolved in anhydrous trifluoroacetic acid, and spotted onto QA-glass for sequencing.

Sequencing was performed using a gas-phase sequenator [44].

Sulfhydryl/disulfide analysis

Analyses of PrP^C and PrP^{Sc} for free sulfhydryls and disulfide bonds was performed using MBB [45]. Substitution of a desalting column for the dialysis steps to remove unreacted *N*-ethylmaleimide, 2-mercaptoethanol and dithiothreitol reduced the time necessary to perform the full sequence of incubations with the sulfhydryl- and disulfide-reactive reagents from 2 days to a few hours. Each sample contained 70 ng PrP^C or 225 µg PrP^{Sc} in phosphate-buffered saline, pH 7.4, supplemented with 0.1% sodium deoxycholate, 1 mM EDTA and blue dextran (referred to as supplemented P_i/NaCl). PrP^{Sc} was solubilized by heating in 2% SDS at 100°C for 1 min. Insoluble residue was removed by centrifugation at 100000 × *g* for 5 min in a Beckman TLA-100.3 rotor. SDS was removed from the supernatant by precipitating PrP^{Sc} with 4 vol. 1% trichloroacetic acid in methanol. PrP^{Sc} was resuspended in unbuffered 150 mM triethylamine, dried in a Savant Speedvac, and dissolved in supplemented P_i/NaCl. Any insoluble residue was removed by ultracentrifugation, as described above. Incubations with MBB, 0.03 mg/ml in supplemented P_i/NaCl, and those in *N*-ethylmaleimide, 10 mg/ml in supplemented P_i/NaCl, were for 1 h at room temperature in a final volume of 50–70 µl. Incubations in 2-mercaptoethanol (2% by vol.), 1 mM dithiothreitol were for 30 min at room temperature. Prior to subsequent incubations, samples were desalted on 4-mm-diameter columns of 0.4 ml Trisacryl GF05 in supplemented P_i/NaCl; addition of blue dextran facilitated collection of fractions containing protein. After the last incubation, all samples were made 2% in 2-mercaptoethanol and 1 mM in dithiothreitol. They were then dried in a Savant Speedvac and the residue dissolved in electrophoresis sample buffer. Proteins were separated on 10% polyacrylamide/SDS gels and blotted onto nitrocellulose. The blots were blocked as described above for immunostaining and then incubated overnight with a 1/1000 dilution of a streptavidin–alkaline-phosphate conjugate in 10 mM Tris/Cl, pH 8.2 at 25°C, 200 mM NaCl, 0.05% Tween 20. After washing in the same buffer, the blots were developed with nitroblue-tetrazolium and 5-bromo-4-chloro-3-indolyl phosphate.

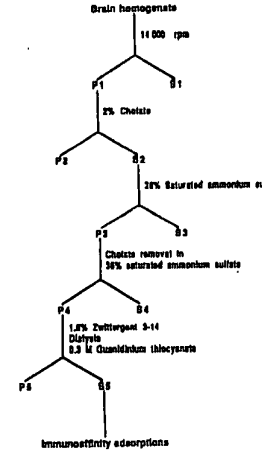

Fig. 1. *Preparative scheme for purification of cellular PrP*

Protein determination

Protein was determined using the bicinchoninic acid/copper assay obtained from Pierce. Protein in amounts > 10 µg was routinely precipitated in 10% trichloroacetic acid after dilution in 0.2 M NaCl, 0.1% SDS and resuspended in 0.1 M NaOH before assay. SDS did not interfere with the acid precipitation of protein [46] and prevented the coprecipitation of detergents. The assay was adapted to quantify as little as 0.1 µg protein from the purest PrP^C fractions. Protein samples were made up to about 40 µl with 0.1% SDS, 0.2 M NaCl in microfuge tubes, previously cleaned in ethanol; 2 µg poly(adenylic acid) was added as carrier and precipitated with the addition of 4 vol. 5% (mass/vol.) trichloroacetic acid in methanol. After 1 h at −20°C, the samples were centrifuged at 40000 rpm in a Beckman TLA-100.3 rotor for 10 min at 2°C. The supernatant fluids were discarded and the pellets dried in a Savant Speedvac; 15 µl 0.1% SDS, 0.2 M NaCl was added to each pellet prior to assay. Bovine serum albumin in 0.1% SDS, 0.2 M NaCl was used as the standard, in amounts ranging over 0.1–10 µg in approximately 1.5-fold increments in a 15-µl final volume. Bicinchoninic acid reagent (250 µl) was added to each tube, mixed, capped and kept at 45°C overnight. (Flip-top microfuge tubes were used; screw-top microfuge caps were avoided due to spurious color development from some compound leaching from the rubber O-ring seal.) Aliquots of 220 µl were transferred to a 96-well microtiter plate and the absorbance at 540 nm measured in a Flow Laboratories Titertek Multiscan. A log/log plot of A_{540} vs µg bovine serum albumin was linear between 0.2–3 µg. A 2-µg polyadenylate blank had an A_{540} of 0.037; 0.1, 1 and 10 µg bovine serum albumin had blank-corrected absorbances of 0.05, 0.4 and 1.7, respectively.

RESULTS

Purification of PrP^C

PrP^C was enriched 3–5-fold using a series of detergent extractions and precipitations prior to immunoaffinity ad-

sorption (Fig. 1). Frozen brains of normal adult hamsters were thawed immediately prior to homogenization with a Brinkmann Polytron in 9 vol. (vol./mass) of 150 mM NaCl, 1 mM EDTA, 20 mM Na/Hepes (pH 8.0 at 5°C) containing 2 mM phenylmethylsulfonyl fluoride (from a 0.2 M stock in dimethyl sulfoxide/1,2-propanediol, 8:2, by vol.) and 20 kallikrein inactivator units (KIU)/ml aprotinin. All manipulations were performed at 4°C and the centrifugations were performed in a Beckman JA-14 rotor unless stated otherwise. The homogenate was then centrifuged at 14000 rpm for 30 min and the pellet (P1) resuspended in 8 vol. (vol./mass brain) of 2% sodium cholate, 150 mM NaCl, 1 mM EDTA prior to centrifugation at 14000 rpm for 10 min. A saturated solution of ammonium sulfate, pH 7.3, was added to the supernatant fluid (S2) to yield a 36% saturated solution. After 10 min without stirring, the suspension was centrifuged at 10000 rpm for 10 min. The pellet (P3) was resuspended in 3.5 vol. (vol./mass brain) of 36% saturated ammonium sulfate, pH 7.3, to remove most of the cholate. The suspension was then centrifuged for 15 min at 9000 rpm and the pellet (P4) resuspended in 0.5 vol. (vol./mass brain) 1 mM dithiothreitol, 40 mM Na/Hepes (pH 8 at 5°C) to lower the concentration of ammonium sulfate before addition of an equal volume of 3% Zwittergent 3-14 (mass/vol.). The suspension was rehomogenized, aprotinin added to a level of 20 KIU/ml and then dialyzed overnight against 0.2 M NaCl.

The dialyzed protein was warmed briefly in a 30°C bath to dissolve detergent crystals. The pH was adjusted to 8.5, the solution made 0.3 M in guanidinium thiocyanate, cooled on ice and centrifuged at 50000 rpm for 30 min in a Beckman 50.2 Ti rotor. The supernatant (S5) was removed, carefully avoiding most of the flocculent material above the pellet, and filtered through a Whatman GF/C glass-fiber filter prior to immunoaffinity purification.

Filtered fraction S5 was incubated with MAb-A-Avidgel (see Materials and Methods) at a concentration of about 5% beads by volume and rocked overnight in the presence of aprotinin, 20 KIU/ml, in a silanized glass bottle at 4°C. The beads were then transferred to a small chromatography column and washed with cold 0.5 M NaCl, 10 mM triethanolamine/acetate pH 8.5, 1 mM EDTA, 0.5% Zwittergent 3-14 (buffer WZ), then with 0.2 M NaCl at 22°C and finally with 50 mM triethylamine/HCl, pH 10.3, 0.2 M NaCl, 0.5% sodium deoxycholate (buffer WE) at 22°C. PrP^C was eluted with 1.5 bed volumes of unbuffered 50 mM triethylamine, 0.5% sodium deoxycholate at 22°C. After adjustment of the eluant (F6) to about 50 mM Hepes, the pH was decreased to 8.6 with 2 M HCl. The solution was further adjusted to 0.2 M NaCl, 1% Zwittergent 3-14, and aprotinin added to 20 KIU/ml.

Proteins which nonspecifically adsorbed to the beads and eluted at pH 11.5 were partially removed by readsorption to beads of protein-A–Avidgel cross-linked to normal mouse IgG (IgG-A–Avidgel; see Materials and Methods). Fraction F6 was incubated with about 6% beads by volume and rocked overnight at 4°C. Nonadsorbed PrP^C was recovered by collecting the liquid phase (F7). The beads were washed in a small chromatography column with two bed volumes of 0.5% Zwittergent 3-14, 0.2 M NaCl, 1 mM EDTA, 50 mM Na/Hepes, pH 8 at 5°C and this wash was added to fraction F7.

The PrP^C in F7 was adsorbed to MAb-A-Avidgel about 12% by volume by incubating overnight at 4°C. The beads were then washed in a small column with buffers WZ and WE described above. PrP^C was eluted (F8) at pH 11.5 with two bed volumes of 50 mM triethylamine in 0.5% sodium deoxycholate, neutralized with 2 M HCl after the addition of Hepes to 50 mM, and concentrated 15-fold by centrifugal ultrafiltration in an Amicon Centricon 30 device.

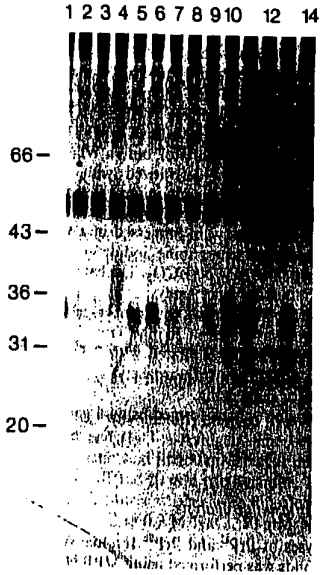

Fig. 2. *Effect of chaotropes and detergents on adsorption of cellular PrP to immobilized monoclonal antibody.* A 10-µl aliquot of fraction P4 (93 µg protein) was incubated overnight with a 10-µl bed of MAb-A-Sepharose in the presence of 1% Nonidet P-40, 0.1 M NaCl and a chaotrope (lanes 1–8) or in the presence of 0.2 M NaCl and a detergent (lanes 9–14). All incubations contained 10 mM Hepes, pH 8.0 at 5°C, and 1 mM EDTA in a final volume of 210 µl. The next day the beads were washed first with 0.5 M NaCl, 50 mM Na/Hepes, pH 8 at 5°C, 1 mM EDTA, 0.5% Nonidet P-40, then with 0.15 M NaCl, 50 mM Na/Hepes, pH 8 at 5°C, 0.5% Nonidet P-40, 0.1% SDS, then with 0.15 M NaCl, 0.5% sodium deoxycholate, and finally with water. The beads were dried and then boiled in 2% SDS, 5% 2-mercaptoethanol, and immunoblotted after SDS-PAGE as described in Materials and Methods. The bands staining darkly at the top of the blot and at about 50 kDa are due to cross-reactivity of the secondary antibody-enzyme conjugate with mouse IgG heavy chain, cross-linked to other proteins and free, respectively, which had been freed from the Sepharose matrix upon boiling. The chaotropes used were triethylammonium trifluoroacetate 0.1 M (lane 1) and 0.4 M (lane 2), dimethylsulfoxide 10% (lane 3) and 50% by vol. (lane 4), guanidinium thiocyanate 0.1 M (lane 5) and 0.5 M (lane 6) and tetramethylurea 0.1 M (lane 7) and 0.5 M (lane 8). Detergents used were 1% Nonidet P-40 (lane 9), 0.5% Zwittergent 3-14 (lane 10), 0.5% Zwittergent 3-16 (lane 11), 0.5% Chaps (lane 12), 0.5% sodium-deoxycholate (lane 13) and 0.5% sodium-cholate (lane 14). Molecular mass is indicated in kDa

The effects of various chaotropes and detergents on the adsorption of PrP^C to immobilized PrP mAbs are illustrated in Fig. 2. The results of these studies were used in developing the purification protocol described above. Addition of trifluoroacetate at 0.1 M or guanidinium thiocyanate at 0.1 M or 0.5 M in the presence of 1% Nonidet P-40 significantly increased PrP^C (≈ 34 kDa) binding to immobilized monoclonal antibody (Fig. 2, lanes 1, 5 and 6) as did the substitution

Table 1. *Purification of PrP^C from hamster brain*
Starting material was 52 g brain. Recovery was estimated by comparison of the immunostaining intensity of fractions on Western blots with that of a dilution series of the homogenate

Recovery fraction	Protein	Purification	Yield
	mg	-fold	%
Homogenate	3080	1	100
P1	1780	1.6	90
Cholate soluble (S2)	1350	1.8	80
$(NH_4)_2SO_4$ pellet (P3/P4)	680	3.4	75
S5	550	4.2	75
First immunoadsorption (F6)	0.67	920	20
Second immunoadsorption (F8)	0.036	3400	4

of deoxycholate for Nonidet P-40 in the absence of chaotropic ions (lane 13). Nonidet P-40 or sodium cholate alone were ineffective for immunoadsorption of PrP^C (lanes 9 and 14). Most striking was the increased binding of PrP^C in the presence of Zwittergent 3-14 or Zwittergent 3-16 (tetradecyl and hexadecyl sulfobetaines, respectively; lanes 10 and 11). The inclusion of 0.3 M guanidinium thiocyanate, pH to 8.5, followed by ultracentrifugation, was found to increase immunoadsorption in the presence of Zwittergent. Presumably, these conditions minimize aggregation of membrane proteins upon their resuspension from the ammonium sulfate pellet (P4).

A summary of PrP^C purification is given in Table 1. Immunostaining variability amongst purified PrP^C preparations complicated our estimates of the degree of purification. This variation was found to be as great as 10-fold and was observed by comparing the apparent antigenicity of purified PrP^C on Western blots relative to protein concentrations measured by the bicinchoninic acid method. We estimate that the extent of PrP^C purification in Table 1 for immunoaffinity fractions F6 and F8 may be as much as 10-fold too low.

The eluates of the first and second immunoaffinity adsorptions were analyzed after SDS-PAGE by silver staining and immunoblotting (Fig. 3). PrP^C is visible by silver staining only after the second immunoadsorption step (Fig. 3A). The protein detected by silver staining and that seen by immunostaining with a PrP monoclonal antibody clearly comigrate (Fig. 3B).

Large-scale purification of PrP^{Sc}

Frozen scrapie-infected hamster brains were homogenized in 9 vol. (vol./mass) of 0.32 M sucrose with a Brinkmann Polytron. All procedures were performed at 4°C unless otherwise stated. The homogenate was clarified by continuous-flow centrifugation in a Beckman JCF-Z rotor at 10000 rpm, loaded at 180 ml/min. The supernatant (S1) was collected and adjusted to a final concentration of 1 mM EDTA and 1 mM dithiothreitol.

Sodium deoxycholate and Triton X-100 were added to supernatant S1 at detergent/S1 protein mass ratios of 3:1 and 3:1 respectively. After each detergent addition, S1 was stirred for 30 min on ice. The solution was then adjusted to 0.1 M NaCl, 20% (by vol.) glycerol, 30 mM Tris/acetate, pH 8.3 at 4°C, and 8% (mass/vol.) poly(ethylene glycol) 8000 and stirred for 90 min. The S1 mixture was precipitated by continuous-flow centrifugation in the JCF-Z rotor at 10000 rpm with loading at 160 ml/min.

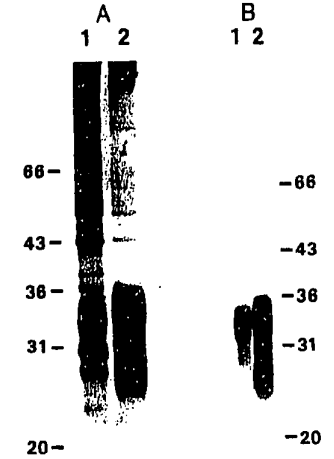

Fig. 3. *Cellular prion protein in purified fractions.* (A) Silver staining after SDS-PAGE of 750 ng protein of fraction F6 (lane 1) and 450 ng of fraction F8 (lane 2). (B) Western blot of PrP^C fractions F6 (lane 1) and F8 (lane 2) immunostained with monoclonal antibody to PrP^C. Molecular mass is indicated in kDa

The pellet (P2) was homogenized in 20 mM Tris/acetate, pH 8.3 at 4°C, 1 mM dithiothreitol, 0.2% Triton X-100 and adjusted to 10 mg protein/ml. The P2 homogenate was then digested with micrococcal nuclease at 12.5 U/ml in the presence of 2 mM $CaCl_2$ for 12 h at 4°C. Sodium cholate was then added to a final concentration of 2% and the digest made 30% saturated in ammonium sulfate by dropwise addition of a saturated solution. The suspension was centrifuged at 19000 rpm in a Beckman type 19 rotor for 90 min. The pellet (P3) was resuspended in 20 mM Tris/Cl, pH 7.4 at 4°C, 1 mM EDTA, 133 mM NaCl, 1 mM dithiothreitol and adjusted to 20 mg protein/ml.

NaCl (0.2 M) was added to P3 and the suspension sonicated in an ice-water bath with a Branson W-350 sonifier, equipped with a microprobe, in 12 7-s bursts. The temperature, monitored by thermistor probe, did not exceed 15°C. After sonication, 5% sodium dodecyl sarcosinate was added and a pellet (P4) was obtained by centrifugation in a Beckman 50.2 Ti rotor at 50000 rpm for 30 min.

The above procedure was repeated twice to yield pellets designated P5 and P6. Aliquots of each pellet were analyzed by SDS-PAGE and the proteins detected by silver staining and immunoblotting (Fig. 4). Apparent dimers and higher multimers of PrP^{Sc} were evident on the immunoblot (Fig. 4B).

N-terminal sequence analysis

The N-terminal amino acid sequences of purified PrP^C and PrP^{Sc} were determined by sequential Edman degradation. Approximately 3 µg PrP^C was subjected to SDS-PAGE and electroblotted to QA-glass. The broad band migrating be-

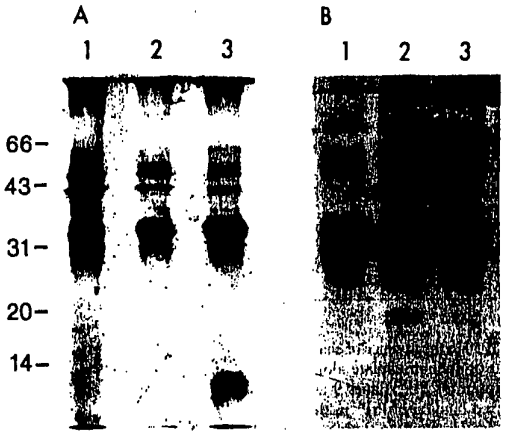

Fig. 4. *Scrapie prion protein in purified fractions.* Silver staining (A) and Western blotting (B) of PrP^{Sc} pellets obtained after sonication in 0.2 M NaCl and subjected to SDS-PAGE. Lanes 1, 2 and 3 correspond to pellets P4, P5 and P6, respectively. Monospecific rabbit antiserum raised to a 13-amino-acid synthetic peptide corresponding to the N-terminus of PrP 27–30 was used for immunostaining. Molecular mass is indicated in kDa

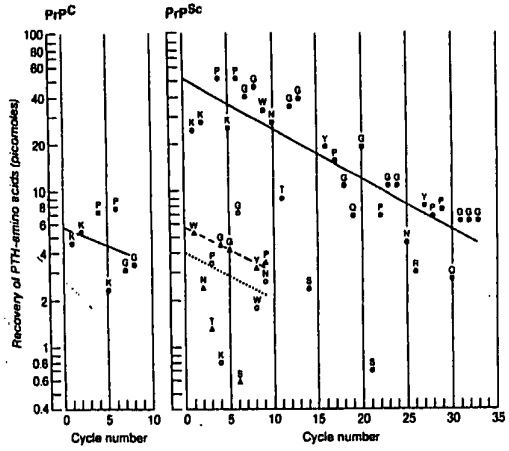

Fig. 5. *N-terminal sequence analyses of cellular and scrapie prion proteins.* Purified PrP^{C} (3 µg) and PrP^{Sc} (24 µg) were adsorbed to QA-glass and subjected to gas-phase sequencing. The signal levels of the identified phenylthiohydantoin amino acid derivatives are presented relative to the Edman degradation cycle number. A single sequence was observed for PrP^{C}. For PrP^{Sc}, three sequences, each corresponding to a portion of the translated PrP gene, were observed. Initial and repetitive yields for each sequence were determined by linear regression analysis, with yields from amino acids with poor recoveries (S, T, R) or from those with spuriously high or low yields excluded from the calculations. The initial yield for PrP^{C} was 5.7 pmol and the repetitive yield was 95%. The initial yield for the major PrP^{Sc} sequence (●——●) was 51 pmol and the repetitive yield was 93%. The initial yields for the two minor PrP^{Sc} sequences (▲——▲, ○·····○) were 5.7 pmol and 4.0 pmol with repetitive yields of 94% and 93%, respectively. The one-letter codes for the amino acids are: C, Cys; G, Gly; K, Lys; N, Asn; P, Pro; Q, Gln; R, Arg; S, Ser; T, Thr; V, Val; W, Trp; Y, Tyr

tween 30–35 kDa was excised and analyzed by gas-phase sequencing. The sequence of seven of the first eight amino acids was determined (Fig. 5); with the exception of an unidentified residue at position 3, it corresponded to the amino acid sequence predicted from the translated DNA sequence beginning at the signal peptide cleavage site (see Fig. 8).

N-terminal sequence analysis of 24 µg PrP^{Sc} gave one major sequence and two minor sequences. The major sequence, like that of PrP^{C}, corresponded to the amino acid sequence predicted from the translated DNA sequence beginning at the signal peptide cleavage site, and accounted for 84% of the total signal. The two minor sequences (detected at 8% and 11% of the major signal) corresponded to polypeptides beginning at two and nine amino acids beyond the signal peptide cleavage site (Fig. 5; see Fig. 8). These two minor components may have arisen as a result of protease activity present during the purification, although it is also possible they exist *in vivo*.

The translated PrP gene open reading frame predicts Arg at codons 25, 37 and 48, corresponding to amino acid residues 3, 15 and 26 after N-terminal signal peptide cleavage. While no Arg was detected in the 3rd and 15th Edman degradation cycles of PrP^{Sc} (Fig. 5), Arg was detected in cycle 26. Like PrP^{Sc}, no Arg was detected in the 3rd Edman degradation cycle of PrP^{C}. The small amount of PrP^{C} available for gas-phase sequencing precluded detection of any signals beyond cycle 8. Since an Arg was detected in PrP^{Sc} at position 26, it seems likely that the missing Arg at positions 3 and 15 may be due to post-translational modification which results in degradation or physical adsorption during gas-phase sequencing. Presumably, Arg at the 3rd position of PrP^{C} is also modified.

Evidence for a PrP disulfide

The translated hamster PrP DNA sequence has two Cys residues after the signal peptide cleavage site [23]; to determine if these Cys exist as the free sulfhydryls or a disulfide, PrP^{C} and PrP^{Sc} were treated with a sulfhydryl-reactive derivative of biotin, MBB, under conditions chosen to allow only free sulfhydryls or alternatively only reduced disulfides to react. MBB was covalently coupled to the PrP isoforms only after exposure of the proteins to reducing conditions (Fig. 6). These results argue for the existence of a disulfide bond in both PrP^{C} and PrP^{Sc}. The use of dithiothreitol during the purifications of PrP^{C} and PrP^{Sc} was not deemed to be a complicating factor since the two PrP Cys residues detected by MBB were found as a disulfide and not in a reduced state. Control samples of PrP^{C} and PrP^{Sc}, which were either not treated with MBB or were treated with *N*-ethylmaleimide after 2-mercaptoethanol prior to exposure to MBB, did not bind streptavidin–alkaline-phosphatase, as expected (Fig. 6).

To determine if the disulfides detected in PrP^{C} and PrP^{Sc} were intra- or intermolecular, PrP^{C} and PrP^{Sc} were subjected to SDS-PAGE in the absence of 2-mercaptoethanol to preserve the putative disulfides. No decrease in the migration rates of PrP^{C} or PrP^{Sc} was observed by silver staining (data not shown); thus, neither PrP^{C} nor PrP^{Sc} was linked to another protein molecule through an intermolecular disulfide bond. Therefore, the disulfide detected in each PrP isoform represents a single intramolecular bond.

The possibility that PrP Cys are acyl thioesters was also considered since sulfhydryl compounds, like 2-mercaptoethanol, are potentially capable of exposing new sulfhydryl groups on proteins not only by reduction of disulfides, but also by transacylation of acyl thioesters of Cys [47]. Thioesters are readily distinguishable from disulfides by their high sensitivity to hydroxylamine, by which thioesters are converted to a free sulfhydryl and an acyl hydroxamate [48, 49]. Treatment of PrP^{C} with hydroxylamine under conditions known to cleave protein thioesters quantitatively failed to expose any measurable sulfhydryl groups (0.25 M NH_2OH, 0.15 M NaCl, 0.1% sodium deoxycholate, 1 mM EDTA, 10 mM Hepes pH 7.7, 10 min at 24 °C).

Purification of p33 – a cross-reactive protein

Since no biological activity has yet been associated with PrP^{C}, all methods for its measurement use PrP antibodies. In the initial phase of the studies reported here, a cross-reactive protein triplet at about 33 kDa on Western blots stained much more intensely with the antisera than did PrP^{C}; thus, we were misled and purified the triplet rather than PrP^{C}. We have designated the triplet p33 (indicating a protein of ≈ 33 kDa).

Attempts to solubilize p33 from brain homogenate revealed that an increase in ionic strength (to 0.4 M NaCl) rendered it soluble in 2% Nonidet P-40. At lower ionic strength, p33 was insoluble in this detergent. Thus, a 10% brain homogenate in 0.32 M sucrose, 2% Nonidet P-40, 0.2 M NaCl was prepared and centrifuged at 20000 rpm in a Beckman JA-20 rotor for 20 min at 4 °C to yield a pellet (P1). P1 was suspended in 2% Nonidet P-40, 0.4 M NaCl and resedimented. The solubilized p33 was precipitated by the addition of one volume of water to the supernatant (S2); after 1 h on ice, centrifugation yielded a pellet (P3). The purification of p33 at this stage was more than 100-fold relative to the initial brain homogenate.

On an immunoblot, the faint staining in fraction S1 with antiserum to PrP 27–30 contrasted with the intense immunoreactivity of p33 in S2 (Fig. 7, lanes 1 and 2). P3 was fractionated by SDS-PAGE. A strip of the polyacrylamide gel was silver-stained to locate p33 (Fig. 7, lane 3). Similar results (not shown) were obtained with monospecific antiserum raised against a synthetic peptide corresponding to the N-terminus of PrP 27–30 [28]. Subsequent immunostaining of S1 and S2 with a different rabbit PrP 27–30 antiserum which had low cross-reactivity to p33 was the first indication that PrP^{C} was actually present in fraction S1, not S2. More importantly, deglycosylation of p33 with trifluoromethane sulfonic acid failed to cause a shift in the mobility of this protein on SDS-PAGE (not shown) while deglycosylation of both PrP^{C} and PrP^{Sc} produced a shift in apparent molecular mass from 33–35 kDa to 25–27 kDa [50].

DISCUSSION

PrP gene structure and transcription

Molecular genetic analyses suggest that the two PrP isoforms are encoded by a single-copy chromosomal gene [22, 23]. The PrP gene was shown to have an unusual structure consisting of two exons interrupted by a single 10-kb intron. The PrP open reading frame lies entirely within the second exon so that it is unlikely that the two PrP isoforms arise by alternative splicing [23]. A single 2.1-kb mRNA was detected in equal amounts in both normal and scrapie-infected rodent brains [22, 51]. The identical N-terminal amino acid sequences of PrP^{C} and PrP^{Sc} reported here constitute the first direct chemical evidence that the two isoforms share the same primary sequence, extending earlier results based on nucleic acid sequence studies and immunoblotting experiments [28, 29].

Immunodetection and primary sequence determination of PrP isoforms

To date, all antibody preparations capable of recognizing PrP^{Sc} on Western blots have also recognized PrP^{C}, including

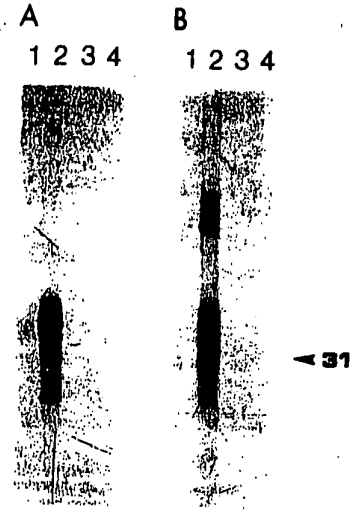

Fig. 6. *Cellular and scrapie PrP isoforms contain a disulfide bond.* Samples of purified PrP^C (A) and PrP^{Sc} (B) were treated as described below, subjected to SDS-PAGE and blotted to nitrocellulose. The blot was blocked, incubated with streptavidin–alkaline-phosphatase conjugate and developed. Lane 1, PrP was directly reacted with MBB; lane 2, PrP was reacted with *N*-ethylmaleimide (10 mg/ml), desalted, reacted with 2% 2-mercaptoethanol, desalted again and finally reacted with MBB; lane 3, PrP was reacted with 2% 2-mercaptoethanol, desalted, reacted with *N*-ethylmaleimide, desalted again, and finally reacted with MBB; lane 4, untreated PrP. Molecular mass of carbonic anhydrase is indicated in kDa

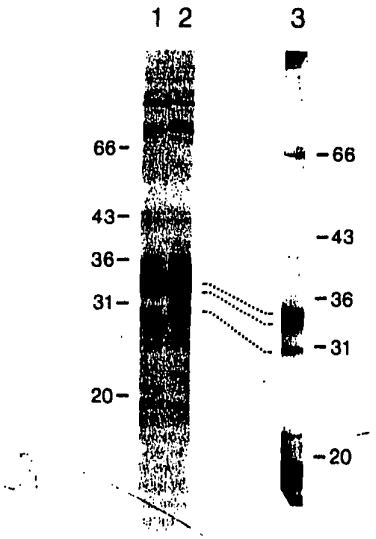

Fig. 7. *Ionic strength fractionation of p33 evaluated by immunoblotting, and silver stain of purified p33.* Lanes 1 and 2, fractions S1 (0.2 M NaCl) and S2 (0.4 M NaCl), respectively, were immunostained on a Western blot with a rabbit anti-(PrP 27–30) antiserum followed by a goat anti-rabbit–colloidal-gold conjugate which was further enhanced with silver; lane 3, pellet P3 was fractionated by SDS-PAGE, the polyacrylamide gel was immersed in transfer buffer containing 16% methanol for 1 h and most proteins in the gel were electrotransferred to nitrocellulose. Protein remaining in the gel was visualized by silver staining. Molecular mass is indicated in kDa

antisera raised against PrP 27–30 [30], monoclonal PrP-antibodies [29] and rabbit antisera raised against synthetic PrP peptides [28, 52]. These data support, but do not prove, the contention that the protein identified as PrP^C on Western blots is the cellular prion protein isoform, encoded by the same mRNA which is a template for PrP^{Sc}. The N-terminal sequences of PrP^C and PrP^{Sc} establish the relatedness of the cellular and scrapie PrP isoforms. As diagrammed in Fig. 8, the N-terminal sequences of purified PrP^C and PrP^{Sc} correspond to that predicted from the PrP genomic DNA after cleavage of a putative signal peptide [23]. The PrP^{Sc} N-terminal sequence reported here agrees with that reported earlier by others [27, 53].

A protein triplet, p33, was mistaken for PrP^C; its strong cross-reactivity on Western blots with two rabbit antisera and its comigration with PrP^C during SDS-PAGE led to its purification. Despite their comigration on polyacrylamide gels and mutual immunostaining with some PrP antisera, PrP^C and p33 were clearly unrelated proteins, as evidenced by their differential solubilities in detergents, electrotransfer behavior, band patterns on immunoblots and silver-stained polyacrylamide gels, and most importantly, susceptibility to chemical deglycosylation. This result serves to underscore the necessity of an independent chemical procedure to corroborate immunological studies. Protein sequencing is clearly the least ambiguous technique.

Problems associated with PrP^C purification

Zwittergent 3-14 was necessary for efficient immunoadsorption of PrP^C (Fig. 2) and 0.3 M guanidinium thiocyanate was required to prevent the formation of protein aggregates (resulting from ammonium sulfate treatment of cholate-solubilized membrane proteins) which precluded antibody-PrP^C interaction.

Proteins which adsorbed nonspecifically during the first immunoaffinity extraction were found to readsorb extensively during a second immunoaffinity step. Use of monoclonal antibody coupled directly to reactive beads without the use of protein A and cross-linker did not obviate nonspecific binding during the second immunoadsorption (not shown). A 'mock' adsorbent, consisting of normal mouse IgG cross-linked to protein-A–Avidgel, was used between the two immunoadsorption steps and found to increase significantly the ultimate purity of PrP^C by removing many of the protein contaminants, which included hamster IgG heavy and light chains (data not shown).

Some purified preparations of PrP^C were unstable. The major component (> 32 kDa) was found to migrate more slowly than expected on SDS-PAGE (Fig. 3, lane 2) and showed a diminished antigenicity on Western blots. This occurred with two of five preparations; these changes were seen to occur in one sample after storage at −20°C for several weeks and thus may be related to denaturation unaffected by

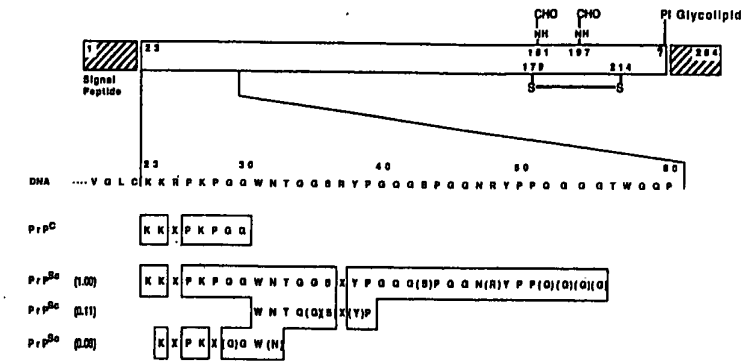

Fig. 8. *Alignment of N-terminal sequences obtained for PrP^C and PrP^{Sc} with the sequence predicted from translated PrP gene.* Analyzed residues concurring with the predicted sequence are boxed. An X indicates no signal was detected at that Edman degradation cycle. The relative signal strengths of the three sequences derived from analysis of PrP^{Sc} are indicated. Residues in parentheses indicate weak but identifiable signals. Post-translational modifications of cellular and scrapie PrP isoforms are also depicted. CHO represents N-linked glycosylation sites and PI denotes phosphatidylinositol. Amino acid residues 1–22 represent an N-terminal signal peptide which is cleaved during maturation of both PrP^C and PrP^{Sc}. Cys residues at 179 and 214 are linked by a disulfide bond. The C-terminal hydrophobic segment of PrP is putatively cleaved upon phosphatidylinositol glycolipid addition

SDS or due to a nonenzymatic chemical alteration. Slower migration on SDS-PAGE is consistent with loss of a diacylglycerol moiety from the phosphatidylinositol glycolipid as was observed with PrP^C from neonatal hamster brain primary cultures after digestion with phosphatidylinositol phospholipase C [54] and with the variant surface glycoprotein of trypanosomes [55].

Post-translational modifications

At least five, and probably six, post-translational modifications of PrP^C and PrP^{Sc} have been identified (Fig. 8). A 22-amino-acid signal peptide is cleaved *in vivo* from the N-terminal of both PrP isoforms [27, 53] (and this paper), in accord with predictions based on the translated DNA sequence [23, 35, 56] and with the results of cell-free translation studies [57]. At least one, and probably both, Asn residues at codons 181 and 197 are glycosylated. Both PrP isoforms exhibit increased migration rates during SDS-PAGE after peptide:*N*-glycosidase F digestion [50]. A phosphatidylinositol glycolipid is attached to each isoform presumably at the C-terminus [54]. The hydrophobic C-terminal domain appears to be removed upon glycolipid addition, although the exact cleavage site is uncertain [22, 54, 58]. Based on amino acid composition data, some investigators have argued that the C-terminal hydrophobic domain of PrP^{Sc} is not cleaved during maturation of the protein [53]. A disulfide bond links Cys residues at codons 179 and 214 of both PrP isoforms. These are the only Cys present in PrP except for a Cys within the signal peptide.

The intramolecular disulfide may be significant in that it creates a 36-amino-acid loop, near the C-terminus, which contains both sites available for N-linked glycosylation. This loop also encompasses one of two PrP amino acid polymorphisms (a Thr→Val variant of codon 189) both of which correlate with the length of scrapie incubation periods in mice [32]. It will be of interest to learn if the disulfide in PrP^{Sc} is essential for infectivity.

Amino acid sequencing studies appear to have identified two more post-translational modifications of PrP^{Sc}. The lack of detectable Arg signals in the 3rd and 15th Edman degradation cycles argues for post-translational modifications of these residues. Other investigators have reported Arg residues in these cycles for hamster PrP^{Sc} [27, 53], raising the possibility that these modifications are variable or labile. Sequencing studies of mouse PrP^{Sc} demonstrate Arg residues in cycles 3 and 15 as well as an unidentified molecule eluting with Thr [59]. It seems doubtful that these putative Arg modifications are important for scrapie infectivity since residues 3 and 15 are not found in PrP 27–30 [21, 23] and PrP^C appears to possess a similar modification of at least Arg 3. While the structures of the Arg modifications in PrP remain to be elucidated, at least seven Arg modifications are known [60].

In summary, purification of both PrP^C and PrP^{Sc} have made possible the direct comparison of their amino acid sequences. Immunodetection on Western blots, heretofore the primary evidence for their relatedness, has demonstrated common epitopes but failed to establish that both proteins are encoded by the same gene. Indeed, our experience with the unrelated protein p33, which comigrates with PrP^C on polyacrylamide gels and is recognized by some PrP antisera, emphasizes the necessity of amino acid sequence determination. Our sequence data and disulfide analyses establish that PrP^C and PrP^{Sc} share identical N-terminal sequences and a disulfide-delimited loop. These data and previous evidence from electrophoretic, immunological and deglycosylation studies argue that PrP^C and PrP^{Sc} are encoded by the same gene and that observed physical differences between them arise through co- or post-translational processing. The availability of purified PrP^C should facilitate the comparative analysis of post-translational modifications with those of PrP^{Sc}.

We are grateful for the technical assistance of J. Valletta, M. Vincent and C. Fan. We thank Drs R. Gabizon, P. Goodman, T. Haraguchi-Hiraoka, M. Scott, N. Stahl, T. Torchia and D. Westaway

for helpful discussions during this work. We also thank A. Turk and L. Gallagher for document production assistance. E. T. was supported by a National Institutes of Health training grant (NS07219). This work was supported by research grants from the National Institutes of Health (AG02132 and NS14069) and a Senator Jacob Javits Center of Excellence in Neuroscience (NS22786) as well as by gifts from the Sherman Fairchild Foundation, RJR/Nabisco, Inc. and the State of California, Department of Health Services (contract 86-89627).

REFERENCES

1. Chandler, R. L. (1961) *Lancet 1*, 1378–1379.
2. Zlotnik, I. & Rennie, J. C. (1965) *J. Comp. Pathol. 75*, 147–157.
3. Marsh, R. F. & Kimberlin, R. H. (1975) *J. Infect. Dis. 131*, 104–110.
4. Gajdusek, D. C., Gibbs, C. J. Jr & Alpers, M. (1966) *Nature (Lond.) 209*, 794–796.
5. Gibbs, C. J. Jr, Gajdusek, D. C., Asher, D. M., Alpers, M. P., Beck, E., Daniel, P. M. & Matthews, W. B. (1968) *Science (Wash. DC) 161*, 388–389.
6. Masters, C. L., Gajdusek, D. C. & Gibbs, C. J. Jr (1981) *Brain 104*, 559–588.
7. Gajdusek, D. C. (1977) *Science (Wash. DC) 197*, 943–960.
8. Dickinson, A. C. & Outram, G. W. (1979) in *Slow transmissible diseases of the nervous system*, vol. 2 (Prusiner, S. B. & Hadlow, W. J., eds) pp. 13–31, Academic Press, New York.
9. Prusiner, S. B. (1982) *Science (Wash. DC) 216*, 136–144.
10. Rohwer, R. G. (1984) *Nature (Lond.) 308*, 658–662.
11. Alper, T. A., Cramp, W. A., Haig, D. A. & Clarke, M. C. (1967) *Nature (Lond.) 214*, 764–766.
12. Diener, T. O., McKinley, M. P. & Prusiner, S. B. (1982) *Proc. Natl Acad. Sci. USA 79*, 5220–5224.
13. McKinley, M. P., Masiarz, F. R., Isaacs, S. T., Hearst, J. E. & Prusiner, S. B. (1983) *Photochem. Photobiol. 37*, 539–545.
14. Bellinger-Kawahara, C., Cleaver, J. E., Diener, T. O. & Prusiner, S. B. (1987) *J. Virol. 61*, 159–166.
15. Bellinger-Kawahara, C., Diener, T. O., McKinley, M. P., Groth, D. F. & Prusiner, S. B. (1987) *Virology 160*, 271–274.
16. Gabizon, R., McKinley, M. P. & Prusiner, S. B. (1987) *Proc. Natl Acad. Sci. USA 84*, 4017–4021.
17. Bolton, D. C., McKinley, M. P. & Prusiner, S. B. (1982) *Science (Wash. DC) 218*, 1309–1311.
18. Prusiner, S. B., Bolton, D. C., Groth, D. F., Bowman, K. A., Cochran, S. P. & McKinley, M. P. (1982) *Biochemistry 21*, 6942–6950.
19. McKinley, M. P., Bolton, D. C. & Prusiner, S. B. (1983) *Cell 35*, 57–62.
20. Prusiner, S. B., McKinley, M. P., Bowman, K. A., Bolton, D. C., Bendheim, P. E., Groth, D. F. & Glenner, G. G. (1983) *Cell 35*, 349–358.
21. Prusiner, S. B., Groth, D. F., Bolton, D. C., Kent, S. B. H. & Hood, L. E. (1984) *Cell 38*, 127–134.
22. Oesch, B., Westaway, D., Wälchli, M., McKinley, M. P., Kent, S. B. H., Aebersold, R., Barry, R. A., Tempst, P., Teplow, D. B., Hood, L. E., Prusiner, S. B. & Weissmann, C. (1985) *Cell 40*, 735–746.
23. Basler, K., Oesch, B., Scott, M., Westaway, D., Wälchli, M., Groth, D. F., McKinley, M. P., Prusiner, S. B. & Weissmann, C. (1986) *Cell 46*, 417–428.
24. Meyer, R. K., McKinley, M. P., Bowman, K. A., Braunfeld, M. B., Barry, R. A. & Prusiner, S. B. (1986) *Proc. Natl Acad. Sci. USA 83*, 2310–2314.
25. Prusiner, S. B., Cochran, S. P., Groth, D. F., Downey, D. E., Bowman, K. A. & Martinez, H. M. (1982) *Ann. Neurol. 11*, 353–358.
26. Hilmert, H. & Diringer, H. (1984) *Biosci. Rep. 4*, 165–170.
27. Hope, J., Morton, L. J., Farquhar, C. F., Multhaup, G., Beyreuther, K. & Kimberlin, R. H. (1986) *EMBO J. 5*, 2591–2597.
28. Barry, R. A., Kent, S. B. H., McKinley, M. P., Meyer, R. K., DeArmond, S. J., Hood, L. E. & Prusiner, S. B. (1986) *J. Infect. Dis. 153*, 848–854.
29. Barry, R. A. & Prusiner, S. B. (1986) *J. Infect. Dis. 154*, 518–521.
30. Bendheim, P. E., Barry, R. A., DeArmond, S. J., Stites, D. P. & Prusiner, S. B. (1984) *Nature (Lond.) 310*, 418–421.
31. Carlson, G. A., Kingsbury, D. T., Goodman, P., Coleman, S., Marshall, S. T., DeArmond, S. J., Westaway, D. & Prusiner, S. B. (1986) *Cell 46*, 503–511.
32. Westaway, D., Goodman, P. A., Mirenda, C. A., McKinley, M. P., Carlson, G. A. & Prusiner, S. B. (1987) *Cell 51*, 651–662.
33. Bolton, D. C., McKinley, M. P. & Prusiner, S. B. (1984) *Biochemistry 23*, 5898–5905.
34. Diringer, H., Gelderblom, H., Hilmert, H., Ozel, M., Edelbluth, C. & Kimberlin, R. H. (1983) *Nature (Lond.) 306*, 476–478.
35. Robakis, N. K., Sawh, P. R., Wolfe, G. C., Rubenstein, R., Carp, R. I. & Innis, M. A. (1986) *Proc. Natl Acad. Sci. USA 83*, 6377–6381.
36. Prusiner, S. B., Groth, D. F., Cochran, S. P., Masiarz, F. R., McKinley, M. P. & Martinez, H. M. (1980) *Biochemistry 19*, 4883–4891.
37. Prusiner, S. B., McKinley, M. P., Bolton, D. C., Bowman, K. A., Groth, D. F., Cochran, S. P., Hennessey, E. M., Braunfeld, M. B., Baringer, J. R. & Chatigny, M. A. (1984) *Methods Virol. 8*, 293–345.
38. Schneider, C., Newman, R. A., Sutherland, D. R., Asser, U. & Greaves, M. F. (1982) *J. Biol. Chem. 257*, 10766–10769.
39. Laemmli, U. K. (1970) *Nature (Lond.) 227*, 680–685.
40. Towbin, H., Staehelin, T. & Gordon, J. (1979) *Proc. Natl Acad. Sci. USA 76*, 4350–4354.
41. Damerval, C., le Guilloux, M., Blaisonneau, J. & de Vienne, D. (1987) *Electrophoresis 8*, 158–159.
42. Heukeshoven, J. & Dernick, R. (1985) *Electrophoresis 6*, 103–112.
43. Aebersold, R. H., Teplow, D. B., Hood, L. E. & Kent, S. B. H. (1986) *J. Biol. Chem. 261*, 4229–4238.
44. Hewick, R. N., Hunkapiller, M. W., Hood, L. E. & Dreyer, W. J. (1981) *J. Biol. Chem. 256*, 7990–7997.
45. Bayer, E. A., Safars, M. & Wilchek, M. (1987) *Anal. Biochem. 161*, 262–271.
46. Schaffner, W. & Weissmann, C. (1973) *Anal. Biochem. 56*, 502–517.
47. Harting, J. & Velick, S. F. (1954) *J. Biol. Chem. 207*, 867–878.
48. Wainfan, E. & Van Bruggen, J. T. (1957) *Arch. Biochem. Biophys. 70*, 43–48.
49. Kaufman, J. F., Krangel, M. S. & Strominger, J. L. (1984) *J. Biol. Chem. 259*, 7230–7238.
50. Haraguchi, T., Groth, D., Barry, R. A., Fisher, S. J., Teplow, D. B., Hood, L. E. & Prusiner, S. B. (1987) *Fed. Proc. 46*, 1319.
51. Chesebro, B., Race, R., Wehrly, K., Nishio, J., Bloom, M., Lechner, D., Bergstrom, S., Robbins, K., Mayer, L., Keith, J. M., Garon, C. & Haase, A. (1985) *Nature (Lond.) 315*, 331–333.
52. Barry, R. A., Vincent, M. T., Kent, S. B. H., Hood, L. E. & Prusiner, S. B. (1988) *J. Immunol. 140*, 1188–1193.
53. Bolton, D. C., Bendheim, P. E., Marmorstein, A. D. & Potempska, A. (1987) *Arch. Biochem. Biophys. 258*, 579–590.
54. Stahl, N., Borchelt, D. R., Hsiao, K. & Prusiner, S. B. (1987) *Cell 51*, 229–240.
55. Cardoso de Almeida, M. L. & Turner, M. J. (1983) *Nature (Lond.) 302*, 349–352.
56. Bazan, J. F., Fletterick, R. J., McKinley, M. P. & Prusiner, S. B. (1987) *Protein Eng. 1*, 125–135.
57. Hay, B., Barry, R. A., Lieberburg, I., Prusiner, S. B. & Lingappa, V. R. (1987) *Mol. Cell Biol. 7*, 914–920.
58. Borst, P. & Cross, G. A. M. (1982) *Cell 29*, 291–303.
59. Hope, J., Multhaup, G., Reekie, L. J. D., Kimberlin, R. H. & Beyreuther, K. (1988) *Eur. J. Biochem. 172*, 271–277.
60. Wold, F. (1981) *Annu. Rev. Biochem. 50*, 783–814.

Purification and characterization of rat-liver cytosolic epoxide hydrolase

Ludwig SCHLADT, Renate HARTMANN, Walter WÖRNER, Helmut THOMAS and Franz OESCH

Institut für Toxikologie, Universität Mainz

(Received February 29/May 5, 1988) – EJB 88 0239

Rat liver cytosolic epoxide hydrolase has been purified and characterized.

The enzyme was purified from tiadenol-induced rat liver 540-fold with respect to *trans*-stilbene oxide as a substrate. Similar purification was obtained with the substrates *trans*-β-ethyl styrene oxide and styrene 7,8-oxide, the specific activities decreasing in the order *trans*-β-ethyl styrene oxide > styrene 7,8-oxide > *trans*-stilbene oxide. The enzyme exerts highest activity at pH 7.4. K_m and V_{max} of the pure enzyme for *trans*-stilbene oxide were 1.7 μM and 205 nmol × min^{-1} × mg $protein^{-1}$ respectively. With *trans*-stilbene oxide as a substrate, the inhibition by organic solvents (2.5% by vol.) increased in the order ethanol < methanol < acetone < isopropanol = *N*,*N*-dimethyl formamide < acetonitrile < tetrahydrofuran. The native enzyme, with a molecular mass of 120 kDa, consists of two 61-kDa subunits.

Digestion of rat liver cytosolic and microsomal epoxide hydrolase by three proteases resulted in markedly different peptide maps.

Western-blot analysis with antiserum against rat liver cytosolic epoxide hydrolase revealed a single band with the purified enzyme, and with liver cytosol from control and clofibrate-induced rats. No cross-reactivity was observed with purified rat microsomal epoxide hydrolase or microsomes.

A positive reaction at the same molecular mass was obtained with liver cytosol of mouse, guinea pig, Syrian hamster and New Zealand white rabbit but not with that of green monkey.

Many natural or man-made toxic substances occur in the environment. They are often lipophilic and tend to accumulate in the lipid fraction of animal tissues. An effective protection mechanism, however, is provided by enzymatic oxidation of these compounds, leading to hydrophilic metabolites which can be eliminated as such or excreted after conjugation to water-soluble carriers. Epoxides have been characterized as the major primary oxidation products formed by cytochrome-P450-dependent monooxygenases from aromatic and olefinic xenobiotics. Epoxides are also generated in the metabolism of leukotrienes [1], by cytochrome-P450-catalyzed oxidation of arachidonic acid [2] and lipid peroxidation. The epoxides formed are electrophilic compounds and can cause toxic, mutagenic or carcinogenic effects [3, 4].

At least three different forms of epoxide hydrolase can be distinguished. The microsomal one, mEH_b, is localized in the endoplasmatic reticulum and has been thoroughly studied since its discovery (for reviews see [3, 6, 7]). It has been shown that it is capable of hydrolyzing a wide variety of epoxides. In routine assays benzo[*a*]pyrene 4,5-oxide and styrene oxide are the most commonly used substrates.

Correspondence to L. Schladt, Institut für Toxikologie der Universität Mainz, Obere Zahlbacher Straße 67, D-6500 Mainz, Federal Republic of Germany

Abbreviations. cEH, cytosolic epoxide hydrolase; mEH_b, microsomal epoxide hydrolase with broad substrate specificity for various xenobiotic epoxides, specifically including benzo[*a*]pyrene 4,5-oxide; *trans*-stilbene oxide, (*E*)-1,2-diphenyloxirane; *trans*-β-ethylstyrene oxide, (*E*)-2-ethyl-1-phenyloxirane; styrene 7,8-oxide, 2-phenyloxirane.

Enzyme. Epoxide hydrolase (EC 3.3.2.3).

Cholesterol epoxide hydrolase is also localized in the microsomes. It differs from mEH_b in many properties, e.g. substrate specificity, inducibility and inhibition [8–10].

In contrast, the third form of epoxide hydrolase (cEH) is mainly localized in the cytosol. Its existence was first demonstrated by Gill et al. [11] using a juvenile hormone analogue as substrate. Today, *trans*-β-ethylstyrene oxide or *trans*-stilbene oxide are routinely used as substrates. While only a few investigations have been done with rabbit, human and monkey liver, most of our knowledge about cEH comes from studies with mice (for reviews see [12–14]).

In contrast to mEH_b little is known about rat cEH. In the present study biochemical and immunochemical properties of rat liver cEH were investigated and compared to those of the microsomal counterpart (mEH_b) and to cEH of other species. A purification scheme for rat liver cEH is presented.

MATERIALS AND METHODS

Chemicals

DEAE-cellulose (DE-52) (Whatman Ltd, Kent, England); phenyl-Sepharose CL-4B, PBE 94, Polybuffer, PD-10 columns, Sephadex G-150, Mono Q-column, blue dextran 2000 (Pharmacia, Freiburg, FRG); hydroxyapatite (Bio-Rad, München, FRG); phosphorylase *b*, bovine serum albumin, fumarase, glyceraldehyde-3-phosphate dehydrogenase, carbonic anhydrase, β-lactoglobulin, dithiothreitol, Lubrol PX, chymotrypsin (treated with tosyllysylchloromethane), trypsin, *Staphylococcus aureus* V8 protease (Sigma, Deisenhofen, FRG); 1-trichloromethyloxirane, benzil (EGA-Chemie, Steinheim, FRG); chalcone (Janssen Chimica, Beerse,

Attorney Docket No. 9013-67 PATENT

IN THE UNITED STATES PATENT AND TRADEMARK OFFICE

In re: Foster et al.
Application No.: 10/518,471
Int'l Filing Date: December 17, 2004
For: ***REMOVAL OF PRION INFECTIVITY***

Confirmation No.: 7924
Group Art Unit: 1746
Examiner: Bibi S. Carrillo

Date: December 8, 2006

Mail Stop RCE
Commissioner for Patents
P.O. Box 1450
Alexandria, VA 22313-1450

Appendix D

Biologicals (1992) 20, 155–158

EEC Regulatory Document

Note for Guidance

Guidelines for Minimizing the Risk of Transmitting Agents Causing Spongiform Encephalopathy via Medicinal Products*

Committee for Proprietary Medicinal Products: Ad Hoc *Working Party on Biotechnology/Pharmacy and Working Party on Safety Medicines*

1. General remarks

Bovine spongiform encephalopathy (BSE) was first recognized in the U.K. in 1986. Since then a large number of cattle and individual herds have been affected. This note for guidance considers the implication of the disease for medicinal products and methods for minimizing the risk of transmission by their use.

The naturally occurring spongiform encephalopathies include scrapie (in sheep and goats), chronic wasting disease (CWD; in mule deer and elk), bovine spongiform encephalopathy (BSE; in cattle) as well as Creutzfeldt-Jakob-Disease (CJD) and Kuru (in humans). Agents causing these diseases replicate in infected individuals without being detectable by diagnostic tests applicable to the living organism. After incubation periods of up to several years the agents cause disease and, finally, lead to a fatal outcome. No means of therapy are known.

Diagnosis is based on clinical signs with post-mortem confirmation of characteristic brain lesions by histopathology or immunological detection of the fibrillary proteins specific for the spongiform encephalopathies. The demonstration of infectivity by the inoculation of suspect tissue into target species or laboratory animals may also be used for confirmation but with an incubation period of months or years. Iatrogenic transmission of spongiform encephalopathies has been reported. In sheep, scrapie has been accidentally transmitted via the application of Louping III vaccine prepared from pooled, formaldehyde-treated ovine brain and spleen in which material from scrapie-infected sheep had been inadvertently incorporated. In humans, cases of transmission of CJD have been reported which have been attributed to the repeated parenteral administration of growth hormone and gonadotropin derived from human cadaveric pituitary glands. Cases of CJD have also been attributed to the use of contaminated instruments in brain surgery and with the transplantation of human meninges and cornea.

There is no evidence that spongiform encephalopathies have been transmitted from animals to humans. However, the possibility of such transmissions, although remote, cannot be dismissed. Therefore due prudence is warranted if biological materials are used for the manufacture of medicinal products from species affected via non-experimental routes by those diseases, primarily ruminants, and among these especially cattle, sheep and goats.

Information on the characteristics of the agents is limited. They are extremely resistant to the chemical and physical procedures that inactivate conventional viruses. They do not induce a detectable immune response. There are natural barriers which limit the interspecies spread of infection, but they can be crossed under appropriate circumstances usually involving efficient routes of administration and high doses of agent. Studies on laboratory animals have shown that intracerebral inoculation is much more efficient than any other route and is followed in decreasing order of efficiency, by intravenous, intraperitoneal and subcutaneous administration. The oral route is less efficient than the parenteral routes. In some cases species barriers can be crossed only after passage of the agent through intermediary species.

Human beings have been naturally exposed to the scrapie agent for at least 200 years, but despite exten-

Requests for reprints should be made to: Permanent Office Biostandards, Case Postale 456, CH-1211 Geneva, Switzerland.

* Final approval of the document by CPMP 11 December 1991. Proposed date for coming into operation, 1 May 1992.

sive epidemiological studies no sign of transmission of scrapie to humans has been detected. In so far as BSE is different from scrapie, it is conceivable that the species barriers may also be different. Therefore, the recommendations below should be followed.

The acceptability of a particular medicinal product containing or derived from bovine materials will be influenced by a number of factors including the selection and processing of source materials, the age and geographical origin of the individual source animal, the intended use of the product, its stipulated dose and route of administration, production process and quality control. The state of science and technology must be taken into consideration. All products will be considered on a case by case basis.

2. Scope of the note for guidance

This note for guidance covers all medicinal products which contain active ingredients and/or excipients derived from bovines, as well as medicinal products for which the production process involves bovine materials.

The note also covers the use of such materials in procedures which are indirectly associated with the manufacturing process, for example, in test media used in the validation of plant and equipment to avoid cross-contamination.

3. Manufacture (including collection of source materials)

The safety of medicinal products can be secured further, and the risk of transmission of infectious agents greatly reduced by combinations of the measures specified in this note for guidance or other appropriate measures. The pharmaceutical manufacturers and the producers of medicinal products of animal origin are responsible for the selection of adequate measures.

3.1. *Animals as source of materials*

Careful selection of source materials is the most important criterion for the safety of medicinal products. The use of source materials from countries where there is a high incidence of BSE is to be avoided.

The following criteria should be taken into account when sourcing materials.

3.1.1. Materials may be sourced from countries which have not reported cases of BSE, if they have an effective veterinary service capable of detecting a low incidence of disease and if BSE is reportable. Official certification should be presented.

In addition, it should be ensured that there is no risk of BSE infection from the following factors:

(a) the feeding to ruminants of ruminant protein derived from the specified offal (brain, spinal cord, spleen, thymus, tonsil and intestine from duodenum to rectum, placenta), either produced in the country or imported from other countries;

(b) the processes used in the rendering industry;

(c) scrapie-associated factors;
- — the incidence and prevalence of scrapie;
- — the ratio of sheep and goats to cattle;
- — the relative geographical distribution of sheep and goats to cattle, where this might have led to the use of sheep material in cattle feed in the past;

(d) importation of cattle above the age of 6 months from countries where a high incidence of BSE has occurred and/or importation of progeny of affected females.

3.1.2. Materials may also be sourced from countries where a low number of cases have occurred, if in addition to the factors in paragraph 3.1.1:

- — BSE has been made legally notifiable;
- — the carcasses of all affected animals are destroyed;
- — the progeny of affected females are not used.

3.1.3. Satisfactory source materials may be obtained from established and monitored herds, where their feeding and breeding history is documented. This is possible even in countries with a high incidence of BSE.

3.2. *Age of animals*

Natural scrapie or BSE has not been detected in animals under the age of 6 months. Therefore, cattle yielding source materials should not be older than 6 months unless otherwise justified.

3.3. *Parts of animal bodies, body fluids and secretions as starting materials*

In the infected animal, different organs and secretions contain different maximum concentrations of infectivity. On the basis of experimental data on transmissible spongiform encephalopathies, organs, tissues and fluids can be classified into four main

groups bearing different potential risks, as shown in the table below. These potential risks, amongst other criteria, should be considered for the selection of source materials.

Although being based on studies of natural scrapie, the classification can be applied to the related diseases in mule deer (CWD) and cattle (BSE), which have similar incubation periods. However, the categories in the table are only indicative and it is important to note the following points:

- the classification of tissues shown in the table is based on titration of infectivity in mice by the intracerebral route.[1–3] In experimental models using agent strains adapted to laboratory animals, higher titres and a slightly different classification of tissues may occur.[4–5] For experimental intraspecies transmission, titres of up to 10^{10} have been reported.[4–5] Therefore, the risks could be higher when medicinal products are manufactured form, and used in, the same species;
- the potential risks will be influenced by the circumstances in which tissues were removed, especially by contact of material of a low-risk group with that of a high-risk group. Thus the contamination of some tissues may be increased if infected animals are slaughtered by penetrative brain stunning, or if the brain and/or spinal cord is sawed;
- dura mater, hypophysis and pineal gland from animals older than 6 months should be regarded as belonging to category II only if contamination with brain tissue can be avoided;
- body fluids should be collected with minimal damage to tissue, and cellular components should be removed; e.g. fetal blood should be collected without contamination from placenta and amniotic fluids.

The information currently available suggests that, given assurances of adequate collection and processing, certain materials and their derivatives are unlikely to present any risk of contamination. These include: milk and its derivatives, e.g. lactose and casein; skin and its derivatives, e.g. gelatine; hair and wool and their derivatives, e.g. wool alcohols and lanolin.

In addition, materials derived from rendered carcasses and subjected to rigorous processes of extraction and purification (e.g. triglycerides, glycerol, sorbitan esters etc. manufactured from tallow) may be considered unlikely to be contaminated.

3.4. *Cellular substrates*

Cell lines known to be capable of concentrating or amplifying agents causing spongiform encephalopathies must not be used in the manufacture of

Relative scrapie infectivity titres in tissues and body fluids from naturally infected sheep and goats with clinical scrapie*

Category I	
High infectivity	Brain, spinal cord (eye)
Category II	
Medium infectivity	Ileum, lymph nodes, proximal colon, spleen, tonsil (dura mater, pineal gland, placenta), cerebrospinal fluid, pituitary, adrenal
Category III	
Low infectivity	Distal colon, nasal mucosa, sciatic nerve, bone marrow, liver, lung, pancreas, thymus
Category IV	
No detectable infectivity†	Blood clot, faeces, heart, kidney, mammary gland, milk, ovary, saliva, salivary gland, seminal vesicle, serum, skeletal muscle, testis, thyroid, uterus, foetal tissue (bile, bone, cartilaginous tissue, connective tissue, hair, skin, urine)

* Tissues in brackets were not titrated in the original studies,[1–3] but their relative infectivity is indicated by other data on spongiform encephalopathies. Materials not listed may be classified by analogy to those mentioned on the basis of their composition.

† No infectivity was transmitted in bioassays involving inoculation of up to 5 mg tissue into rodent brains.

medicinal products, except for reasoned exceptional cases.

4. Procedures which remove or inactivate agents causing spongiform encephalopathies

Removal and inactivation procedures contribute to the reduction of the risk of infection. Their effectiveness in removing infectivity during a given production process must be tested and validated using appropriate model systems (presently, animal infection experiments).

Whereas none of the following procedures may guarantee complete inactivation of the infectious agents, the efficiency of the first three methods on this list is considered greatly superior to that of the remaining ones:

- autoclaving at appropriate conditions (recommended parameters are 134–138°C for 18 min for porous-load autoclaving, and 132°C for 1 h for gravity-displacement autoclaving);
- treatment with sodium hydroxide (preferably: 1 N solution, for 1 h at 20°C);
- treatment with sodium hypochlorite (preferably: solution containing at least 2% available chlorine, for 1 h at 20°C);
- autoclaving at shorter times and/or lower temperatures than those given above;
- extraction by organic solvents (use the organic phase);
- removal of protein by precipitation, ultracentrifugation or absorption;
- preparation of filtrates by passage through 10 filters;
- passage through appropriate chromatograp columns (before re-using treat columns for with at least 0·1 N sodium hydroxide);
- treatment with 6 M urea.[6]

5. Concluding remark

Although these guidelines relate particularly to B and materials of bovine origin, they should be c sidered in relation to material from sheep, goats a other species affected via non-experimental routes agents causing spongiform encephalopathi Finally, while this note for guidance has gene applicability, it may not be necessary to fulfill al the listed measures for all products. The potent risk associated with a given medicinal product v have to be considered individually in the light specific circumstances and current knowledge.

References

1. Hadlow WJ, Kennedy RC, Race RE, Eklund CM. Pathol 1980; 17: 187–199.
2. Hadlow WJ, Kennedy RC, Race RE. J Infect Dis 19 146: 657–664.
3. Kimberlin RH. In: Collier LH, Timbury MC, eds. Top and Wilson's Principles of Bacteriology, Virology a Immunity Vol 4. London: Edward Arnold, 19 671–693.
4. Eklund CM, Kennedy RC, Hadlow WJ. Infect Dis 19 117: 15–22.
5. Diringer H, Hilmert H, Simon D, Werner E, Ehler Eur J Biochem 1983; 134: 555–560.
6. Pocchiari M, Macchi G, Peano S, Conz A. Arch Vriol 19 98: 131–135.

Attorney Docket No. 9013-67 PATENT

IN THE UNITED STATES PATENT AND TRADEMARK OFFICE

In re: Foster et al.
Application No.: 10/518,471
Int'l Filing Date: December 17, 2004
For: ***REMOVAL OF PRION INFECTIVITY***

Confirmation No.: 7924
Group Art Unit: 1746
Examiner: Bibi S. Carrillo

Date: December 8, 2006

Mail Stop RCE
Commissioner for Patents
P.O. Box 1450
Alexandria, VA 22313-1450

Appendix E

Biochemistry and structure of PrP^{C} and PrP^{Sc}

Detlev Riesner

Institut für Physikalische Biologie, Heinrich-Heine-Universität Düsseldorf, Düsseldorf, Germany

In a brief historical description, it is shown that the prion model was developed from the biochemical and biophysical properties of the scrapie infectious agent. The biochemical properties of the prion protein which is the major, if not only, component of the prion are outlined in detail. PrP is a host-encoded protein which exists as PrP^{C} (cellular) in the non-infected host, and as PrP^{Sc} (scrapie) as the major component of the scrapie infectious agent. An overview of the purification techniques is given. Although chemically identical, the biophysical features of PrP^{Sc} are drastically different in respect to solubility, structure, and stability; furthermore, specific lipids and a polyglucose scaffold were found in prions, whereas for nucleic acids their absence could be proven. The structure of recombinant PrP in solution is known from spectroscopic studies and with high resolution from NMR analysis. Structural models of PrP^{Sc} were derived recently from electron microscopic analysis of two-dimensional crystals. Conformational transitions of PrP *in vitro* were studied with different techniques in order to mimic the natural PrP^{C} to PrP^{Sc} conversion. Spontaneous transitions can be induced by solvent changes, but at present infectivity cannot be induced *in vitro*.

The early history of the prion model is the history of the biochemical and biophysical properties of the scrapie infectious agent. In searching for a virus, no viral features were found; however, highly enigmatic properties of the infectious agent were demonstrated, such as absence of particles in the electron microscope, no immune response during the infection, and high resistance of the agent against chemical and physical treatment. As early as 1966 from inactivation studies using ionising and UV-irradiation, Alper *et al*[1] concluded that the target size of the scrapie infectious agent (50–150 kDa) is too small for a virus but more characteristic of a protein. Many experimental results were left unexplained until Prusiner took up the inactivation studies and performed systematic analysis using not only chemical and physical, but also enzymatic procedures. He summarized the results under two groups: (i) procedures which modify or destroy nucleic acids do not inactivate scrapie infectivity; and (ii) procedures which modify or destroy proteins inactivate the infectivity. From that, he came to the conclusion that the scrapie infectious agent could not be a virus but a novel

Correspondence to: Prof. Dr Detlev Riesner, Institut für Physikalische Biologie, Heinrich-Heine-Universität Düsseldorf, Universitäts Strasse 1, 40225 Düsseldorf, Germany

N.B. Colour figures are referred to as 'Plates' and appear in a 'Colour plate section' at the front of this volume

British Medical Bulletin 2003; 66: 21–33
DOI 10.1093/bmb/dg66.021

proteinaceous type of an agent, which he termed 'prion' (proteinaceous infectious particle)[2].

To confirm a protein-like agent, the protein (one or more molecular species) had to be purified and characterized. A hydrophobic and, in mild detergents, insoluble protein of molecular weight 33–35 kDa could be highly enriched. In a collaborative research project involving the laboratories of Prusiner, Hood and Weissmann using the Syrian hamster as the experimental animal, the sequence of a peptide fragment was found; from this, the DNA-sequence was determined, first in a cDNA-library and later in a genomic library. The major component of the prion was shown to be a host-encoded protein, later called prion protein[3,4]. In one sense, the finding raised doubts about the prion model, because no foreign information, even a foreign protein, was found; alternatively, it supported the possibility, which indeed was mentioned earlier as a purely theoretical possibility[5], that rather than a self-replicating protein, an infection-induced synthesis of a host protein might be the basis for prion amplification.

The strong, but not complete, resistance of prions to degradation by proteinase K (and other proteases) had supported the hypothesis of prions. When, however, the prion protein was identified as encoded in the host genome, the protein was found also in the non-infected host[6]. Its resistance against proteinase K digestion was barely measurable, so that a clear biochemical distinction between two isoforms of the prion protein could be drawn: the cellular prion protein PrP^{C} in the non-infected organism, and the scrapie isoform PrP^{Sc} as the major component of the purified infectious agent. It should be emphasized that proteinase K resistance of PrP was used as a biochemical marker for infectivity, and often 'PrP^{Sc}' and 'PrPres' (for resistance) were used synonymously. Later, however, it was shown, that infectivity and proteinase K resistance do not correlate in all cases; therefore, in this chapter, PrP^{Sc} is used for the property of infectivity and PrPres for proteinase K resistance, respectively.

Chemical properties of PrP and recombinant PrP

A few biochemical features of PrP were the basis of the prion hypothesis in the early days. In the mean time, PrP is one of the most intensively studied proteins, its chemical properties are well known whereas the biological function of PrP^{C} is still under discussion as outlined elsewhere in this volume.

Plate I summarizes the amino acid sequence, processing, and post-translational modifications of PrP from the hamster. The final, processed form of PrP contains amino acids 23–231 from the original translation product of 253 amino acids. Peptide 1–22 is cleaved as signal peptide during trafficking,

and peptide 232–253 is replaced by the glycosyl-phosphatidylinositol-anchor (for details see elsewhere in this volume). The cellular form is attached *via* the anchor to the outer membrane. Asparagine residues 181 and 197 carry highly branched glycosyl groups with sialic acid substitutions. PrP is always isolated as a mixture of three forms – unglycosylated, with one glycosyl-, and with two glycosyl-groups. A disulphide bridge is formed between Cys179 and Cys214. As indicated in Plate I, PrP contains 2 hexarepeats and 5 octarepeats in its N-terminus (see Prusiner[7] and Weissmann[8]).

The amino acid sequence is the same whether derived from the genomic DNA sequence or directly by peptide sequencing. PrP^C and PrP^{Sc} are identical with respect to all chemical features described in Plate I. Note, however, that the glycosyl groups are heterogeneous, and only typical glycosyl groups are depicted in Plate I. Since it is nearly impossible to compare quantitatively distributions of different glycosyl groups, the chemical identity of PrP^C and PrP^{Sc} is not completely safe in this respect.

Purification of PrP was attempted first in efforts to purify the infectious agent from the brain of infected animals. This became possible only after the hamster was introduced as experimental animal where there is a relatively short incubation time of 3–5 months instead of one or more years in the case of mouse or sheep. Furthermore, in the hamster the infectious dose (ID_{50}) could be determined not only by end-point titration using about 50 animals for one value, but also by the incubation time assay[9] in 4–6 hamsters. The purification procedure consists of a homogenization of the tissue and a series of precipitations and differential centrifugations. In the standard procedure, the solvent contains detergents, and a protein digestion step with proteinase K is included. Thus, the proteinase K resistance of PrP^{Sc} was essential for the purification, and PrP 27–30 was obtained as the purified product[10]. The criteria for optimization are the total yield of infectivity and the specific infectivity (*i.e.* ID_{50}/g of material).

Besides the need for PrP^{Sc} purification, for many studies purified PrP^C is also required. Although the amount of PrP^C in brain is very high in contrast to other tissues, it represents less than 0.1% of the total central nervous system proteins. For example, from 100 hamster brains only a few micrograms of purified PrP^C were obtained in an optimal procedure.

Obviously, expression of recombinant PrP in *Escherichia coli* was required. First attempts to isolate PrP from *E. coli* yielded either low expression levels or low purification efficiency because of the instability and insolubility of the protein. Furthermore, the disulphide bond in PrP, which is essential for correct folding of PrP, is not formed under the reducing conditions in the cytoplasm of *E. coli*. Attempts to fuse PrP with proteins that target the product in the periplasm and thereby spontaneously form the disulphide bond *in vivo* were not effective in

producing larger quantities of PrP. Therefore, recombinant PrP was purified and afterwards reconstituted by denaturing under harsh conditions (8 M urea or 5 M guanidinium hydrochloride), the disulphide bond was formed under oxidizing conditions, and than PrP was renatured by dialysing out the denaturant[11]. This strategy is now used for the purification of recombinant PrP in high amounts.

Eukaryotic expression systems are of particular interest because they yield post-translationally modified PrP, *i.e.* a PrP which is very similar or identical with PrP^C. Many eukaryotic cell systems including those of yeast and mammals were tested for expression of PrP. However, in most of these cases, difficulties occurred (unstable transfection, low levels of expression, insolubility of the protein, or difficulties in purifying PrP) and prevented those procedures becoming standard.

Finally, a transgenic mammalian cell system of Chinese hamster ovary (CHO) cells was established that generated PrP^C at high levels of expression (~14-fold higher than in hamster brain). By this method, purified PrP^C in amounts of 10–100 μg can be prepared[12]. Although this yield is still rather low in comparison to the yield of recombinant PrP purified from *E. coli* cells, purified PrP^C is now available in amounts sufficient for some biophysical studies.

Chemical properties of PrP^{Sc}

Purified prions, either in the form of 'full-length' PrP^{Sc} or as PrP 27–30, are insoluble, even in mild detergents. In electron micrographs, fibrillar structures also called prion rods are visible (Fig. 1). After staining with

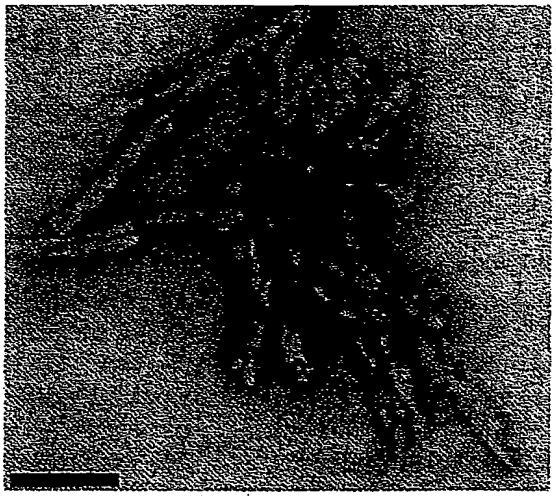

Fig. 1 Prion rods. As obtained from a purification procedure including detergents and proteinase K-treatment.

Congo Red, they show the typical fluorescence birefringence of amyloids[13]. Similar structures were detected in thin sections of the brain of infected animals, which were called originally scrapie associated fibrils (SAF)[14]. It should be noted that, in the brains of CJD or Kuru victims, PrP deposits can be detected as diffuse deposits, amyloidic fibres, condensed plaques, or florid plaques.

The high tendency to aggregate correlates with a PrP^{Sc}-specific resistance against digestion with proteinase K. In Plate II, the Western blot of an SDS-gel electrophoresis of PrP^{C} and PrP^{Sc}, without and with proteinase K digestion, respectively, is depicted. The characteristic three bands of PrP (*i.e.* without, with one and with two glycosyl groups) are visible; they disappear completely after proteinase K digestion of PrP^{C} which results in small peptides. In the case of PrP^{Sc}, however, the bands remain nearly undiminished in intensity although shifted to lower molecular weight. These are the N-terminally truncated forms of PrP^{Sc}, called PrP 27–30. From the right panel of Plate II, it can be seen that the 'full-length'-PrP is cleaved around amino acid 90. The cleavage product (PrP 27–30) is fully infectious and, indeed, it is also the product of the purification procedure described above[10]. Furthermore, it should be noted that all presently available routine tests for BSE and scrapie are based on the proteinase K resistance of PrP 27–30.

The prion model might well be explained on the basis of conformational changes of the prion protein which are induced directly or indirectly by the invading PrP^{Sc}. The phenomenon of prion strains, however, is hard to explain in a similar manner. Although different physicochemical properties were found with different prion strains[15], these could not be attributed to different conformations of single PrP molecules but only to the highly aggregated and insoluble PrP. Even if the principal replication features of prions did not depend on nucleic acids, it was argued that at least the strain specificity might be determined by nucleic acid molecules[16]. Many attempts had been undertaken to find nucleic acids, all without success, which did not prove, however, the absence of nucleic acids. One series of studies was arranged in a way that nucleic acids either would have been found or would be excluded as essential components to prion infectivity[17,18]. Using highly purified infectious material, the number of nucleic acid molecules irrespective of their chemical nature and structure but depending on their size were determined quantitatively and related to the number of infectious units. For all nucleic acids larger than about 80 (in later work 50) nucleotides, less than one molecule of nucleic acid was determined per infectious unit. Consequently, infectious units exist without a nucleic acid – and the virus hypothesis was disproven finally with quantitative biophysical methods.

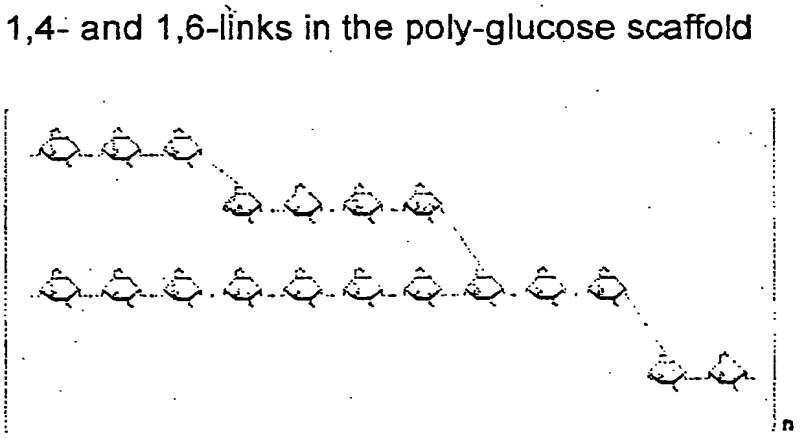

Fig. 2 Schematic presentation of the polyglucose scaffold as found in prion rods. The estimated molecular weight is above 200,000.

The lipophilic nature of highly purified prions suggested that not only a glycolipid anchor is linked to PrP but, in addition, lipids might be associated non-covalently with PrP. A chemical analysis revealed specific lipids which amounted to around 1% of purified prions[19]. These are sphingomyelin, α-hydroxy-cerebroside and cholesterol depending on the method of purification. Both lipids are known to be components of the outside of the cell membrane in caveolae-like sites, where PrP^C also accumulates. It could not be shown that the lipids are essential for infectivity, but their presence in prions might indicate the origin of prions, namely the site of PrP^C accumulation on the outside of the cell membrane.

Early experiments, in which prion rods were digested extensively with proteinase K, had shown that the rod-like structure was maintained in electron micrographs even if PrP was digested by more than 99%[20]. This result had pointed to an additional structural component. It was identified much later as polymeric sugar consisting of α-1,4-linked and 1,4,6-branched polyglucose[21]. Thus, this sugar component is clearly different from the glycosyl groups which are attached covalently to PrP. A schematic presentation is given in Figure 2. Since the polysaccharide amounted to up to 10% (w/w) of highly purified prions, it might be regarded as a structural scaffold contributing to the high chemical and physical stability of prions.

Structure of PrP^C and PrP^{Sc}

It has been indicated above that PrP^C and PrP^{Sc} are different in respect to solubility, fibril formation, proteinase K resistance and other features. These differences could be either a consequence of ligands bound to one

Table 1 Secondary structure of PrP in different isoforms

	α-helix (%)	β-sheet (%)
PrP^C	43	–
PrP^{Sc}	20	34
PrP 27–30	29	31

isoform but not to the other or a consequence of a different secondary and tertiary structure of PrP^C and PrP^{Sc}, respectively. First indications for clear differences in the secondary structure came from spectroscopic measurements applying circular dichroism and infrared spectroscopy[22,23]. From those measurements, α-helix and β-sheet contents could be determined. The numbers given in Table 1 are not very accurate, since the analysis on PrP^{Sc} had to be carried out on insoluble samples; however, they show clearly that PrP^C is dominated by α-helices and has only little β-sheet content, whereas PrP^{Sc}, *i.e.* 'full-length', or PrP 27–30 are characterized by similar amounts of α-helices and β-sheets.

Natural PrP^C could not be used to apply NMR spectroscopy or X-ray analysis for determination of the exact three-dimensional structure. The amount of material available was too small, the samples were not sufficiently pure, and the concentration was too low. These three hurdles were only overcome with recombinant PrP. In addition, recombinant PrP was synthesized in a form labelled with ^{15}N or ^{13}C. Even then, it took several years before the groups of Wüthrich[24] and a little later of James[25] analysed the structure of the C-terminal part of PrP, *i.e.* amino acids 121–231. As shown in Plate III for PrP of mouse and of man[26], the structure consists of three α-helices (amino acids 144–154, 175–193 and 200–219) and a small antiparallel β-sheet (amino acids 128–131 and 161–164). When the structure of 'full-length' PrP (*i.e.* amino acids 23–231) was analysed it was evident that the C-terminal part (*i.e.* amino acids 126–231) contained the complete globular part of the structure, whereas the N-terminus (*i.e.* amino acids 23–125) was more or less flexible[27]. Close to the small β-sheet, the disulphide bridge connects helix 2 and helix 3. The region between the β-sheet and helix 2 (amino acids 166–171) could be determined only with less accuracy possibly because of some structural flexibility. This region, however, is of particular functional interest. Different lines of evidence such as antibody binding, transgenic animals with mutations in that region, binding of the hypothetical factor X, *etc.* argue that the species barrier might be localized in that region. Furthermore, the minor differences in the structure of mouse and hamster PrP on the one hand and of bovine[28] and human PrP on the other are restricted to that part of the molecule.

It should be noted that the structure described above is the best description of the PrP^C structure presently available, but that it was

obtained from recombinant PrP. The glycosyl-groups of PrP^C probably do not alter the structure significantly, but the fact that PrP^C is attached to the membrane by the glycolipid anchor might have more influence, particularly if one considers the structure of the N-terminus which was found unstructured when free in solution (see above). Furthermore, it is known that the N-terminus and, in particular, the octarepeat of the N-terminus bind 4–6 copper ions in a co-operative manner which definitely would induce more structure than presently known from the NMR analysis.

The NMR-structure of PrP is a monomeric structure. Several reports in the literature indicate that PrP in its α-helical structure can form dimers under physiological or close to physiological conditions[29,30]. Dimers in solution show the intact intramolecular disulphide bridge. Consequently, dimerization is not induced by oxidizing the disulphide bridge and reforming it in an intermolecular structure. The latter situation was, however, found in a recent crystal structure of a dimer of PrP (120–231)[31]; dimers were formed by domain swapping and intermolecular disulphide bridging. Whether this structure is a consequence of the long-time crystallization, or might indicate a physiological state, cannot be stated at present.

As mentioned above, PrP^{Sc} or PrP 27–30 are not accessible to structural analysis by NMR or X-ray analysis because of their insolubility. Attempts were made[32] to use the structure described above as a starting model, change α-helices into β-sheets and, in this way, develop a model for PrP^{Sc}. These models assume that helix 2 and helix 3 are unchanged in accordance with antibody binding data, but they are incomplete in the sense that they are models for isolated molecules whereas PrP^{Sc} as well as PrP 27–30 were found only in aggregated forms. Thus, one has to assume that the PrP^{Sc} structure is stabilized by intermolecular interactions.

A new approach was followed by Wille from Prusiner's laboratory who was able to prepare two-dimensional crystalline-like arrays of PrP^{Sc}- or PrP^{Sc}-like molecules[33]. Those samples were studied by electron microscopy and, because of the crystalline-like arrangement, images could be reconstructed from the repetitive unit with fairly high resolution. A hexagonal symmetry was visible, but it could not be decided whether one unit is built from 3 or 6 molecules. The electron density map could be fitted best if, instead of β-sheets, a β-helix was assumed. The structure of the β-helix type is known from other fibrillar proteins; spectroscopically, β-sheets and β-helices cannot be differentiated, so that the new model would not contradict earlier spectroscopic studies. The model is depicted in Plate 1V. In summary, the β-helical N-terminus is located in the inner part of the hexagonal unit, with the helices 2 and 3 at the outer side and the glycosyl-groups pointing into the space between the hexagonal units. Most probably, the

model shown in Plate IV is not the final description of the structure of PrP^{Sc}, but it is the best model currently available and takes into account both electron microscopic and spectroscopic data as well as the intermolecular stabilization of the PrP^{Sc} structure.

Conformational transitions of PrP *in vitro*

Structural and other chemical and physical properties of PrP^{C} and PrP^{Sc} in the purified state have been described above. PrP^{C} was characterized by α-helical structure, solubility as a monomeric or dimeric molecule, and proteinase K sensitivity. Since no functional test for PrP^{C} is available, it is more accurate to speak about a PrP^{C}-like conformation when the such properties are found. Similarly, for PrP^{Sc}, a β-sheet-rich structure, insoluble aggregates, and proteinase K resistance are typical, but these features are not sufficient for PrP^{Sc}, because PrP^{Sc} stands for infectivity and, presently, the re-establishment of infectivity has not been achieved. Thus, the properties of PrP^{Sc} as mentioned above are those of a PrP^{Sc}-like molecule and do not infer infectivity.

Conformational transitions might be either denaturation processes of PrP^{C} or PrP^{Sc}, transitions between PrP^{C} and PrP^{Sc} induced by varying solvent conditions, or induction of the PrP^{C} to PrP^{Sc} transition by an existing seed of PrP^{Sc} (as described in detail elsewhere in this volume).

The denaturation of the globular domain of recombinant PrP (121–231) by addition of up to 8 M urea was analyzed quantitatively by recording the ellipticity at 222 nm[34]. One co-operative transition was obtained at pH 7.0 with a free energy of –28.6 kJ/mol for structure formation. At pH 4.0, an intermediate state could be identified with lowered α-helicity and increased β-sheet content; at present, it cannot be decided whether the intermediate would also be an intermediate on the pathway to PrP^{Sc}-like conformations. From the reversibility of the denaturation process, it was concluded that the PrP^{C}-like conformation is the state of lowest free energy in buffer without detergent. This conclusion might be restricted, however, to the fragment PrP (121–231).

Similar experiments, but also taking into account the mechanism of refolding by kinetic analysis, were carried out on recombinant PrP (89–231) from mouse which is the recombinant equivalent of PrP 27–30[35]. In this fragment, β-sheet-rich oligomers and even fibrils were formed at pH 3.6. However, after switching from the fully denaturing conditions of 10 M urea to native conditions without urea, first the monomeric α-helical conformation and from that (in a very slow process of hours or even days) β-sheet oligomers and finally fibrils were formed. The presence of urea during the incubation speeded up the formation of the β-sheet-rich conformation, and the presence of 5 M urea directly

induced formation of β-sheet-rich oligomers without running through the α-helical state. Consequently, at acidic pH, folding of PrP to the α-helical state is under kinetic control and the thermodynamically stable state is the β-sheet rich state.

More close to the natural conditions of the PrP^{C} to PrP^{Sc} transition were experiments in which the PrP^{C}-like, α-helical state was established first as it is in the non-infected organism[36]. Then the transition to the PrP^{Sc}-like conformation was induced by slightly denaturing conditions, (*e.g.* 1 M guanidinium hydrochloride). Also, these experiments were carried out at acidic pH (4.0), and the conversion process could be induced by a wide variety of conditions combining mild denaturants and different salts. In accordance with renaturation experiments (see above), it was found that β-sheet formation is always connected with aggregation and that the most stable state, at least at acidic pH, is the β-sheet-rich aggregated state. An exception was shown under conditions reducing the disulphide bridge; it was reported that acidic and reducing conditions could induce a β-sheet-rich and monomeric state[37]. It is not known whether this finding is relevant to PrP^{C} to PrP^{Sc} conversion in nature because the intramolecular disulphide bridge is present in both states and in all other conversion experiments the disulphide bridge was not opened transiently[38].

The earliest studies on the *in vitro* conversion were carried out with natural PrP and at neutral pH[39]. Infectious PrP 27–30 was converted to an α-helical, oligomeric and non-infectious form by addition of 0.3% sodium-dodecylsulphate (SDS). Further addition of 30% acetonitrile or mere dilution of SDS to 0.01%[40], re-established a β-sheet-rich, aggregated and partially proteinase K-resistant conformation. Although natural PrP was used which was infectious before the conversion, infectivity could not be re-established. These experiments were closest to natural conditions if the low concentrations of SDS were regarded as a membrane-like environment. It was also shown that the conversion occurs in steps, first fast formation of β-sheet structure concomitant with forming small oligomers, then larger oligomers in minutes to an hour, and finally large insoluble aggregates in hours to days. Applying the same conversion system to recombinant PrP (90–231), systematic studies of the influence of varying SDS concentrations were carried out and several intermediate states described (Fig. 3)[30]. In 0.06–0.1% SDS, an α-helical dimer is present as a thermodynamically stable state which is converted in a co-operative manner in 0.04–0.06% SDS to a β-sheet-rich oligomeric state. As recently determined (Nagel-Steger *et al*, unpublished), the oligomeric state with 12–16 molecules is of particular interest for further biophysical studies since it is stable in solution. In low SDS concentrations (< 0.02% SDS), large insoluble aggregates (see above) are formed which also remain stable after the SDS has been

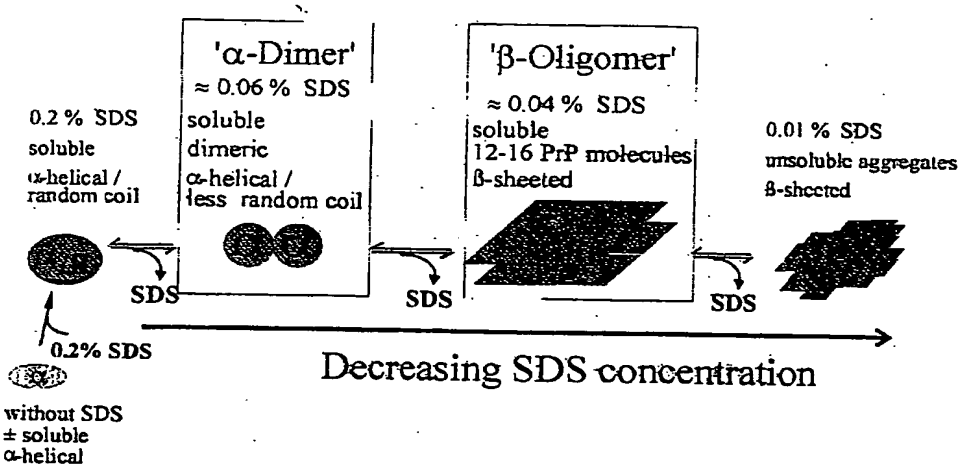

Fig. 3 Intermediates in the *in vitro* conversion of recombinant PrP (90–231).

washed out completely. In buffer without detergent at pH 7, the PrP^C-like as well as the PrP^{Sc}-like conformations can be established, but the stable state is the PrP^{Sc}-like conformation, and the conversion can be induced by different detergents, even in very low concentrations (see also Xiong *et al*[41]).

Conclusions

What is the conclusion from all the *in vitro* conversion studies? Evidently, the thermodynamically stable state is the PrP^{Sc}-like state, and this would be true for lysosomal acidic pH or the cell-surface neutral pH. A high activation barrier renders the transition very slow (*i.e.* hours, days or even weeks). Formation of the β-sheet-rich structure is always correlated with oligomerization at least if the naturally occurring disulphide bridge is intact. Whether β-sheet oligomers are intermediates on the pathway to PrP^{Sc} or a dead-end product is at present an artificial discussion because the PrP^{Sc}-like state as available is not infectious and a final decision on the right pathway cannot be made. If the PrP^C-conformation is not the thermodynamically stable state, but only metastable, the question remains why a transition to PrP^{Sc} does not occur much more frequently in nature as a spontaneous transition. It is, however, not a discrepancy if one takes into account that PrP^C is anchored in the lipid membrane, and all studies described were carried out in aqueous buffer. Consequently, as an additional transition of PrP^C, one has to include the distribution between the aqueous and the lipid

phase which would definitely stabilize PrP^C in nature to prevent a spontaneous transition.

Acknowledgement

The author thanks his co-workers E Birkmann, C Dumpitak, K Elfrink, H Gruber, and Drs K Jansen and J Schell for their help in preparing the manuscript.

References

1 Alper T, Haig DA, Clarke MC. The exceptionally small size of the scrapie agent. *Biochem Biophys Res Commun* 1966; 22: 278–84
2 Prusiner SB. Novel proteinaceous infectious particles cause scrapie. *Science* 1982; 216: 136–44
3 Oesch B, Westaway D, Walchli M *et al.* A cellular gene encodes scrapie PrP 27–30 protein. *Cell* 1985; 40: 735–46
4 Basler K, Oesch B, Scott M *et al.* Scrapie and cellular PrP isoforms are encoded by the same chromosomal gene. *Cell* 1986; 46: 417–28
5 Griffith JS. Self-replication and scrapie. *Nature* 1967; 215: 1043–4
6 Barry RA, Kent SB, McKinley MP *et al.* Scrapie and cellular prion proteins share polypeptide epitopes. *J Infect Dis* 1986; 153: 848–54
7 Prusiner SB. Scrapie prions. *Annu Rev Microbiol* 1989; 43: 345–74
8 Weissmann C. Molecular biology of prion diseases. *Trends Cell Biol* 1994; 4: 10–4
9 Prusiner SB, Cochran SP, Groth DF, Downey DE, Bowman KA, Martinez HM. Measurement of the scrapie agent using an incubation time interval assay. *Ann Neurol* 1982; 11: 353–8
10 McKinley MP, Meyer RK, Kenaga L *et al.* Scrapie prion rod formation *in vitro* requires both detergent extraction and limited proteolysis. *J Virol* 1991; 65: 1340–51
11 Mehlhorn I, Groth D, Stockel J *et al.* High-level expression and characterization of a purified 142-residue polypeptide of the prion protein. *Biochemistry* 1996; 35: 5528–37
12 Blochberger TC, Cooper C, Peretz D *et al.* Prion protein expression in Chinese hamster ovary cells using a glutamine synthetase selection and amplification system. *Protein Eng* 1997; 10: 1465–73
13 Prusiner SB, McKinley MP, Bowman KA *et al.* Scrapie prions aggregate to form amyloid-like birefringent rods. *Cell* 1983; 35: 349–58
14 Merz PA, Somerville RA, Wisniewski HM, Iqbal K. Abnormal fibrils from scrapie-infected brain. *Acta Neuropathol* 1981; 54: 63–74
15 Safar J, Wille H, Itri V *et al.* Eight prion strains have PrP(Sc) molecules with different conformations. *Nat Med* 1998; 4: 1157–65
16 Weissmann C. A 'unified theory' of prion propagation. *Nature* 1991; 352: 679–83
17 Meyer N, Rosenbaum V, Schmidt B *et al.* Search for a putative scrapie genome in purified prion fractions reveals a paucity of nucleic acids. *J Gen Virol* 1991; 72: 37–49
18 Kellings K, Meyer N, Mirenda C, Prusiner SB, Riesner D. Further analysis of nucleic acids in purified scrapie prion preparations by improved return refocusing gel electrophoresis (RRGE). *J Gen Virol* 1992; 73: 1025–9
19 Klein TR, Kirsch D, Kaufmann R, Riesner D. Prion rods contain small amounts of two host sphingolipids as revealed by thin-layer chromatography and mass spectrometry. *Biol Chem* 1998; 379: 655–66
20 McKinley MP, Braunfeld MB, Bellinger CG, Prusiner SB. Molecular characteristic of prion rods purified from scrapie-infected hamster brain. *J Infect Dis* 1986; 154: 110–20
21 Appel TR, Dumpitak Ch, Mathiesen U, Riesner D. Prion rods contain an inert polysaccharide scaffold. *Biol Chem* 1999; 380: 1295–306

22 Caughey BW, Dong A, Bhat KS, Ernst D, Hayes SF, Caughey WS. Secondary structure analysis of the scrapie-associated protein PrP (27–30) in water by infrared spectroscopy. *Biochemistry* 1991; 30: 7672–80

23 Safar J, Roller PP, Gajdusek DC, Gibbs Jr CJ. Conformational transitions, dissociation, and unfolding of scrapie amyloid (prion) protein. *J Biol Chem* 1993; 268: 20276–84

24 Riek R, Hornemann S, Wider G, Billeter M, Glockshuber R, Wuthrich K. NMR structure of the mouse prion protein domain PrP(121–321). *Nature* 1996; 382: 180–2

25 James TL, Liu H, Ulyanov NB *et al.* Solution structure of a 142-residue recombinant prion protein corresponding to the infectious fragment of the scrapie isoform. *Proc Natl Acad Sci USA* 1997; 94: 10086–91

26 Zahn R, Liu A, Lührs T *et al.* NMR solution structure of the human prion protein. *Proc Natl Acad Sci USA* 2000; 97: 145–50

27 Riek R, Hornemann S, Wider G, Glockshuber R, Wüthrich K. NMR characterization of the full-length recombinant murine prion protein, mPrP(23–231). *FEBS Lett* 1997; 413: 282–8

28 Garcia FL, Zahn R, Riek R, Wüthrich K. NMR structure of the bovine prion protein. *Proc Natl Acad Sci USA* 2000; 97: 8334–9

29 Meyer RK, Lustig A, Oesch B, Fatzer R, Zurbriggen A, Vandeveld M. A monomer–dimer equilibrium of a cellular prion protein (PrP^{C}) not observed with recombinant PrP. *J Biol Chem* 2000; 275: 38081–7

30 Jansen K, Schäfer O, Birkmann E *et al.* Structural intermediates in the putative pathway from the cellular prion protein to the pathogenic form. *Biol Chem* 2001; 382: 683–91

31 Knaus KJ, Morillas M, Swietnicki W, Malone M, Surewicz WK, Yee VC. Crystal structure of the human prion protein reveals a mechanism for oligomerization. *Nat Struct Biol* 2001; 8: 770–4

32 Pan KM, Baldwin M, Nguyen J *et al.* Conversion of alpha-helices into beta-sheets features in the formation of the scrapie prion protein. *Proc Natl Acad Sci USA* 1993; 90: 10962–6

33 Wille H, Michelitsch MD, Guénebaut V *et al.* Structural studies of the scrapie prion protein by electron crystallography. *Proc Natl Acad Sci USA* 2002; 99: 3563–8

34 Hornemann S, Glockshuber R. A scrapie-like unfolding intermediate of the prion protein domain PrP(121–231) induced by acidic pH. *Proc Natl Acad Sci USA* 1998; 95: 6010–4

35 Baskakov IV, Legname G, Prusiner SB, Cohen FE. Folding of prion protein to its native α-helical conformation is under kinetic control. *J Biol Chem* 2001; 276: 19687–90

36 Morillas M, Swietnicki W, Gambetti P, Surewicz WK. Membrane environment alters the conformational structure of the recombinant human prion protein. *J Biol Chem* 1999; 274: 36859–65

37 Jackson GS, Hosszu LLP, Power A *et al.* Reversible conversion of monomeric human prion protein between native and fibrilogenic conformations. *Science* 1999; 283: 1935–7

38 Welker E, Raymond LD, Scheraga HA, Caughey B. Intramolecular versus intermolecular disulfide bonds in prion proteins. *J Biol Chem* 2002; 277: 33477–81

39 Riesner D, Kellings K, Post K *et al.* Disruption of prion rods generates spherical particles composed of four to six PrP 27–30 molecules that have a high α-helical content and are non-infectious. *J Virol* 1996; 70: 1714–22

40 Post K, Pitschke M, Schäfer O *et al.* Rapid acquisition of β-sheet structure in the prion protein prior to multimer formation. *Biol Chem* 1998; 379: 1307–17

41 Xiong L-W, Raymond LD, Hayes SF, Raymond GJ, Caughey B. Conformational change, aggregation and fibril formation induced by detergent treatments of cellular prion protein. *J Neurochem* 2001; 79: 669–78

Clinical Chemistry 48:12
2105–2114 (2002)

Review

Protein Conformation and Diagnostic Tests: The Prion Protein

BRIAN J. BENNION and VALERIE DAGGETT*

Background: **Many clinical diagnostic tests depend on the accurate detection and quantification of proteins and peptides and their functions. Alterations of protein structure, and the resulting consequences on dynamics, can affect the outcome of laboratory tests. These changes can be a result of mutations, other in vivo factors, or even the experimental conditions of the diagnostic test.**
Approach: **The relationship between protein structure and dynamics and experimentally observable properties used in diagnostic assays are discussed in light of transmissible spongiform encephalopathies, or prion diseases.**
Content: **This review describes current efforts and possible future directions of prion diagnostic development. Recent advances in therapeutic development are also addressed.**
Summary: **The intent of the review is to highlight the role of protein dynamics and conformational change in protein-based diagnostics and treatments for prion disease.**

Protein Conformation and Dynamics in Protein-based Diagnostic Assays

Most proteins assume a distinct three-dimensional structure in vivo and in vitro, and this native structure is necessary for function. A protein's structure is determined by its amino acid sequence and the surrounding environment. There are various levels of structure: primary structure refers to the amino acid sequence; secondary structure refers to the fold of the peptide, i.e., α-helices, β-strands, and turns; and tertiary structure describes the three-dimensional structure and is determined by the packing of the secondary structural elements and the amino acid side chains. As a protein or peptide unfolds, interactions are disrupted and both secondary and tertiary structure can be lost. In addition, the folded and unfolded states of proteins are in equilibrium. Even under conditions that favor the folded state, a protein is not locked into a single conformation. The amino acids are free to interact and move according to the forces placed on them by neighboring atoms and the solvent, producing many conformations that may differ only very slightly (conformers).

Protein motion occurs on a wide spectrum with respect to time. Bond vibration and rotations occur on a femtosecond timescale (10^{-15} s), whereas amino acid side chains move on a picosecond to nanosecond timescale (10^{-12}–10^{-9} s). Small segments of the peptide backbone can reposition themselves in a matter of nanoseconds to microseconds (10^{-9}–10^{-6} s). The arrangement of surface amino acids can be affected by such dynamic behavior. Such changes in the surface of a protein can alter potential binding sites for other molecules. Complete folding of a protein can occur in microseconds to milliseconds or hours, depending on the sequence and solvent environment. Furthermore, proteins and peptides can adopt different, folded structures under different conditions *(1–3)*. Even slight changes in binding epitopes attributable to either localized or more dramatic conformational changes of a protein can have profound effects on antibody-based diagnostic tests. This issue is particularly pertinent and potentially problematic in the case of the development of diagnostic tests for transmissible spongiform encephalopathies, or prion diseases.

Conformational Change and Disease: Transmissible Spongiform Encephalopathies

There is currently much interest in transmissible spongiform encephalopathies (TSEs)[1] because of outbreaks of

Department of Medicinal Chemistry, Box 357610, University of Washington, Seattle, WA 98195-7610.
*Author for correspondence. E-mail daggett@u.washington.edu.
Received May 9, 2002; accepted September 19, 2002.

[1] Nonstandard abbreviations: TSE, transmissible spongiform encephalopathy; BSE, bovine spongiform encephalopathy; CJD, Creutzfeldt–Jakob disease; CWD, chronic wasting disease; PrP^{C}, cellular prion protein; PrP^{Sc}, scrapie prion protein; GPI, glycosylphosphatidylinositol; FTIR, Fourier transform infrared; NMR, nuclear magnetic resonance; FDA, Food and Drug Administration; EDRF, erythroid differentiation-related factor; and LTBR, lymphotoxin β-receptor.

bovine spongiform encephalopathy (BSE, or mad cow disease) in the United Kingdom and elsewhere *(4, 5)*. BSE began to receive a great deal of media attention in the mid to late 1990s when massive herd culls occurred in Great Britain and the incidence of Creutzfeldt–Jakob disease (CJD) increased dramatically among young people *(4, 6, 7)*. Recent reports of chronic wasting disease (CWD) in elk and deer from the Western United States and Canada, as well as scrapie in sheep in the Northeast, continue to keep TSEs in the news headlines and a priority among government agencies *(8, 9)*.

Prion diseases affect the central nervous system and are a result of a conformational change in the prion protein, often leading to prion protein-based plaques. In humans, these diseases can be sporadic, inherited, or infectious disorders. This protein is responsible for the following diseases in humans: Kuru, Gerstmann–Sträussler–Scheinker disease (GSS), fatal familial insomnia (FFI), CJD, and the BSE-linked, variant CJD (vCJD). These diseases are always fatal. Inherited disease maps exclusively to mutations in the prion protein. The infectious nature of this disease differs from that of other infectious diseases in that the pathogen is a proteinaceous particle lacking nucleic acids; thus, the "protein-only" hypothesis was proposed *(6)*.

The essential component of prions is the scrapie prion protein (PrP^{Sc}; or PrP^{res}, for the protease-resistant form). PrP^{Sc} is chemically indistinguishable from the normal, cellular prion protein (PrP^{C}; or PrP^{sen}, as it is sensitive to proteases) *(10)*; however, their secondary and tertiary structures differ *(11–17)*. PrP^{C} is a monomeric, glycosylated, glycosylphosphatidylinositol (GPI)-linked extracellular protein that appears to play a role in signal transduction *(18)* and/or in the maintenance of the proper copper ion concentration *(19–21)*. In contrast, PrP^{Sc} adopts an oligomeric arrangement and has no known function. Fourier transform infrared (FTIR) and circular dichroism spectroscopy studies indicate that PrP^{C} is highly helical (42%) with little β-sheet structure (3%) *(15)*. In contrast, PrP^{Sc} contains less helical structure (30%) and a large amount of β-structure (43%). PrP^{C} can be converted to the lethal PrP^{Sc} conformation on contact with PrP^{Sc} *(22–24)*. These results, and others, suggest that a conversion of α-helices to β-sheets is a critical feature in the formation of PrP^{Sc} from PrP^{C} and that the protein can aid in its own conversion *(24)*. Several mechanisms have been proposed for the spontaneous and/or assisted conversion of endogenous PrP^{C} to PrP^{Sc} *(24)*. Residues in close proximity to the C-terminal end of PrP^{C} have been associated with PrP^{Sc} binding, which is subsequently followed by conversion of PrP^{C} *(25)*. A confounding factor in conversion is that PrP^{Sc} is conformationally heterogeneous, which appears to be important in determining strain differences and perhaps species barriers *(23, 26–28)*. Unfortunately, high-resolution structures exist only for portions of PrP^{C} (Fig. 1). There are many other fascinating aspects of this system, but unfortunately they cannot be described here; the reader is directed to an excellent series of reviews edited by B. Caughey for more details *(29)*.

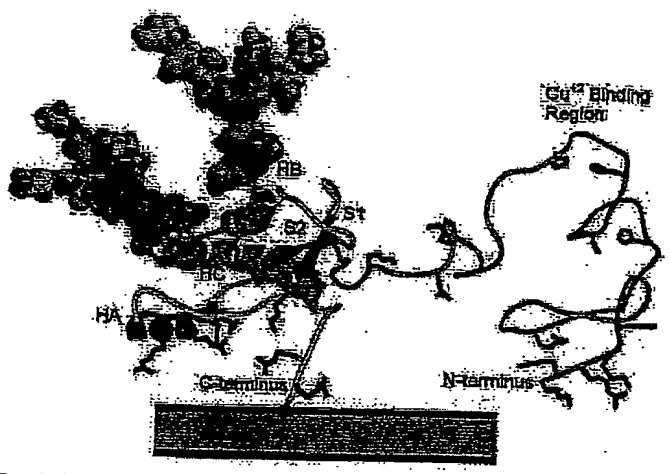

Fig. 1. Model of the soluble prion protein.

Residues 125–231 are from the NMR structure *(79)* modeled with carbohydrates (in *space-filling* representation), the N-terminal region (residues 23–124) as random coil (*light orange*), and the GPI-membrane anchor (*gray*). Secondary structure is displayed as *ribbons*: helix A (*HA*; residues 144–156; *red*), helix B (*HB*; residues 177–193; *green*), helix C (*HC*; residues 200–223; *cyan*), β-strands *S1* (residues 128–131; *red*), and *S2* (residues 160–164; *dark red*). Histidine sidechains involved in copper binding are shown in *green (20)*. Lysine and arginine residues are shown in stick representation (*blue*). For a further description of the model, see DeArmond et al. *(80)*.

Given the lack of detailed structural information regarding the conversion process of the prion protein as well as PrP^{Sc} and its many possible conformers, we have been performing molecular dynamics simulations, beginning with PrP^{C}, in which we destabilize the protein by lowering the pH *(21, 30, 31)* as is believed to occur in vivo. Such an approach can provide atomic-resolution information about the putative conversion process as well as possible PrP^{Sc} models. However, these models must be carefully compared with experimental data to ensure that they are realistic. In any case, to illustrate some of the complexities involved in the conversion of PrP and in developing diagnostics for PrP^{Sc}, we provide some of these preliminary models for PrP^{Sc}, along with nuclear magnetic resonance (NMR)-derived models for PrP^{C}, in Fig. 2. Structures for the hamster, bovine, and human forms of the prion protein are shown in the cellular and putative disease-causing conformations, illustrating how the same amino acid sequence can adopt different conformations. Several antigenic sites for PrP^{C} are highlighted (Fig. 2 and Table 1), as these are the sites exploited in the antibody-based diagnostics described below. In extreme examples such as these, the surface of the protein can change dramatically so that epitopes found in PrP^{C} are unavailable for binding in PrP^{Sc}. For example, the 3F4 epitope (red patch on the structures in Fig. 2) is less accessible in the simulated PrP^{Sc} form, which is consistent with experimental findings *(32)*.

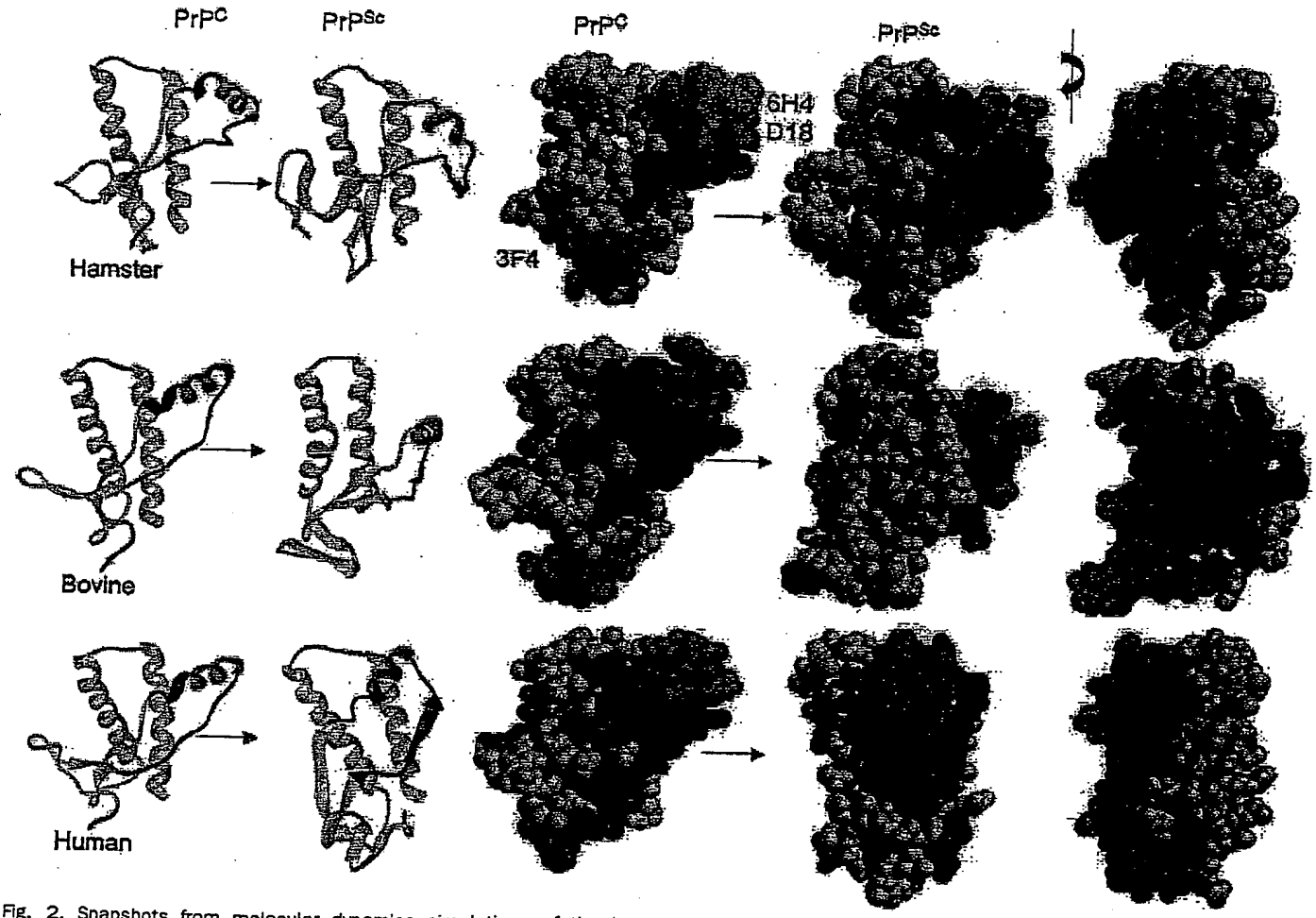

Fig. 2. Snapshots from molecular dynamics simulations of the hamster, bovine, and human prion proteins in ribbon and space-filling representations, before molecular dynamics simulations were started (PrP^C) and after 10 ns at low pH (yielding putative PrP^{Sc} conformations) *(31)*. The starting PrP^C structures were the NMR structures determined experimentally with the addition of the important N-terminal residues to the bovine and human fragments [hamster *(79)*; bovine *(81)*; human *(82)*]. Each structure is aligned so that helices B and C are in the background with secondary structure displayed as ribbons. Effects of protein dynamics on the epitopes for D18, 6H4, and 3F4 are shown in space-filling models next to their main chain representations. In addition, the space-filling models of PrP^{Sc} were rotated 90 degrees in the structures at the *far right*. Epitopes are colored as follows: D18 (residues 132–156), *blue* and *light blue*; 6H4 (residues 144–152), *light blue*; and 3F4 (residues 109–112), *red*.

Table 1. Antibody detection of PrP: Epitopes, conformation recognized, and current or proposed applications.[a]

Antibody	Epitope, residues	Conformation recognized	Diagnostic agent	Therapeutic agent
3F4[b]	109–112	PrP^C		
D13[b]	95–103	PrP^C		X[c]
6H4[d]	144–152	PrP^C + PrP^{Sc}	X[e]	
D18[f]	132–156	PrP^C		X[c]

[a] Current information about diagnostics and therapeutics development can be found at http://www.priondata.org/.
[b] Data from Peretz et al. *(32)*. Also note that both 3F4 and D13 can recognize denatured PrP^{Sc}.
[c] Data from Peretz et al. *(75)*.
[d] Data from Korth et al. *(78)*.
[e] "Prionics Check" by Prionics AG (http://www.prionics.ch/).
[f] Data from Williamson et al. *(76)*.

Rationale for Development of Diagnostics for the Prion Protein

The protein-only hypothesis is important from a scientific point of view because it challenges the dogma regarding the transfer of biological information. From a public health point of view, a new route of disease transmission exists, and the ramifications are potentially enormous. Important sectors of the economy are susceptible to problems posed by transmissible prion diseases, with agriculture being one of the most vulnerable for several reasons. The first reason is the possibility of contamination of the food supply; the second reason is that the resulting loss incurred by agricultural producers when infection is discovered and eradicated can be enormous. Contamination of the food supply can occur in various

ways, with transmission by meat products being only one possible route. Animal-based food supplements are found throughout the processed food and health supplements industries (*33*). Cosmetics may also contain oils, fats, or other rendered animal products (*34*). Furthermore, traditional medicines made from animal parts pose a risk (*35*). Individuals infected by ingesting contaminated food pose a risk to blood supplies and tissue banks. The American Red Cross and US Food and Drug Administration (FDA) have acknowledged this particular risk recently, and they have established guidelines to restrict possible contamination (*36*). Other sources of potential infection include pharmaceuticals that rely on animal remains, either in the manufacturing process or in the final product. The pharmaceutical industry was warned recently by the US FDA to restrict the use of animal-derived materials in the production of vaccines and other therapeutics (*37*). Several recent studies have shown the great difficulties in estimating the future risk of infection in humans and animals, further necessitating the development and widespread use of sensitive, reliable, and inexpensive TSE detection methods (*38–41*).

Rapid, specific, ultrasensitive, robust, and noninvasive diagnostic tools are desired for the prevention of transmission of prion diseases. These diagnostics are needed, especially in areas at high risk of transmission to large numbers, such as cattle herds and human patients reliant on chronic therapy regimens that include animal or even human-derived pharmaceuticals. Until recently, the only definitive diagnosis of BSE was by autopsy. Prion detection with the new antibody-based assays is now relatively rapid (8–24 h) (*42*) compared with past tests, which were long-term projects (>260 days for mouse infectivity assays). However, brain tissue samples are still required for these faster assays. Tonsil biopsies have been proposed as a less invasive alternative to brain biopsies (*43*), and a patent application has been filed. In addition, the detection of surrogate proteins (tau, 14-3-3, S100, and neuron-specific enolase) in cerebrospinal fluid has been proposed (*44*). These studies are promising, but an invasive lumbar puncture is required. Other methods for determining PrP^{Sc} in central nervous system tissues include fluorescence correlation spectroscopy (*45*) and FTIR spectroscopy (*46*). The fluorescence correlation spectroscopy method has been shown to have 100% specificity and a sensitivity 20 times that of current Western blot techniques. Kneipp et al. (*45*) have shown that disease-specific changes in several parts of the brain can be detected by FTIR microspectroscopy. This method does not rely completely on the presence of PrP^{Sc} for detection but rather monitors the change in infrared absorbances in carbohydrates and lipids. Data for other tissues and double-blind studies have not been published.

No absolute lethal prion dose or incubation time has been determined for cattle or humans (*38, 39*), which places rigorous requirements on diagnostic sensitivity. Lack of specificity could allow real infections to proceed undetected (false-negative results), whereas false-positive outcomes could lead to unnecessary expense and disrupted lives. An example of the havoc created by a false-positive result was experienced by a patient at our institution who was diagnosed with an extremely aggressive form of cancer (gestational trophoblastic tumors) (*47*). The diagnosis was apparently based on the AxSYM β-Human Chorionic Gonadotropin test manufactured by Abbott Laboratories. Unnecessary chemotherapy sessions and surgeries were performed as a result of a diagnostic test that purportedly gave a false-positive result 44 times, highlighting the general need for multiple diagnostic tests for a particular condition. Ethical questions aside, several biochemical problems exist in the development of prion diagnostic assays.

Standard immunometric diagnostics rely on binding events predicated on the target protein adopting a single conformation. However, in the case of infectious prions, PrP^{Sc} appears to adopt a variety of conformations (*23, 26, 27*), possibly requiring separate antibodies for detection. The sensitivity must be such that it is possible to detect prion protein in body tissues more accessible than the central nervous system (e.g., blood and urine). However, it is not known whether all conformations of PrP^{Sc} cause disease (*16*). Here we review several diagnostic assays in use or in development for prion diseases; we also examine emerging technologies that address some of the concerns outlined above. Although diagnostic tests that detect the infectious form of the protein before the onset of clinical symptoms are of paramount importance for the detection and disposal of contaminated material, correct diagnosis of prion diseases is important, even after clinical signs appear, to provide appropriate treatment when such agents become available, especially because prion diseases may be misdiagnosed as Alzheimer disease (*48*). Therefore, in addition to discussing potential diagnostic tests, we also briefly summarize recent studies focusing on the development of therapeutic agents against prion diseases.

Diagnostic Tests in Use and under Development for the Prion Protein

PROCEDURES USING BRAIN TISSUE

In July 1999, the European Commission requested an evaluation of four promising prion diagnostic assays. These four candidates were selected from a total of 30 applications. Each assay was tested under double-blind conditions in four categories: specificity, sensitivity, limit of detection, and reproducibility. A brief description of each assay (*42*) is given below:

Test A: Diagnostic by E.G. & G Wallace Ltd. This test is under development and uses a two-site noncompetitive immunometric procedure with two different monoclonal antibodies. A small sample of brainstem (100 mg) is taken from the animal, cell membranes are disrupted, and proteins are extracted by use of a chaotropic agent.

Extracts are then digested with two different concentrations of proteinase K, and the analyte is concentrated by centrifugation. After resuspension in 6 mol/L guanidinium hydrochloride, the extract is diluted 1:50 and subjected to a time-resolved fluorescence immunoassay, DELFIA, for detection of PrP^{Sc} (specifics regarding the antibodies used and their respective PrP epitopes were not provided). In its current state of development, the test requires <24 h, although this could be reduced with automation.

Test B: Diagnostic by Prionics AG. "Prionics Check" is an immunoblotting test based on a Western blotting procedure for the detection of PrP^{Sc} that uses the 6H4 mouse-derived monoclonal antibody (epitope, human residues 144–152; recognition sequence, DYEDRYYRE; Table 1 and Fig. 2). The test procedure can be summarized briefly as follows: A piece of brain stem or cervical spinal cord (typically 0.5 g of tissue) is homogenized in a plastic, single-use container. The homogenate is then digested with proteinase K, boiled in sodium dodecyl sulfate sample buffer, and loaded on a sodium dodecyl sulfate–polyacrylamide gel. After electrophoretic separation, proteins are transferred to a membrane, and PrP^{Sc} is detected with the antibody coupled to a chemiluminescent marker. The minimum time to complete the test is 7–8 h.

Test C: Diagnostic by Enfer Scientific Ltd. (Protherics). The Enfer test is a novel, high-throughput chemiluminescent ELISA that can be completed in <4 h; it uses a polyclonal anti-PrP antibody (no specific information regarding the antibody was provided) for detection. The test itself includes a rapid sample extraction procedure, coupled to a simple ELISA technique. For detection, a polyclonal primary antibody and a horseradish peroxidase-conjugated secondary antibody are used with an enhanced chemiluminescent reagent.

Test D: Diagnostic by CEA-Bio-Rad. The CEA-Bio-Rad test, originally developed by the Commissariat a l'Energie Atomique, is a sandwich immunoassay for PrP^{Sc} carried out after denaturation and concentration steps. Two monoclonal antibodies are used (details regarding the antibodies are not available). In its current state of development, the test takes <24 h to complete; this could be reduced with automation.

Summary of test results. Each of the previous assays was tested under double-blind conditions in four categories: specificity, sensitivity, limits of detection, and reproducibility. Results reported to the European Commission are summarized in Table 2. The Bio-Rad product (Test D) performed well. Subsequent studies using a commercial form of the Bio-Rad assay have been conducted with similar results *(49)*. As stated previously, these tests are used for deceased cattle. The European Commission has started evaluating another set of "rapid" postmortem diagnostics, with field trials imminent *(50)*. No commercially available human test exists at this time.

Table 2. Test results of PrP diagnostic tests from the European Commission.[a]

	Test A	Test B[b]	Test C[c]	Test D[d]
Sensitivity, %	70	100	100	100
Specificity, %	90	100	100	100
Titer				
10^{-1}	6/6	6/6	6/6	6/6
$10^{-1.5}$	0/20	15/20	20/20	20/20
$10^{-2.0}$		0/20	20/20	20/20
$10^{-2.5}$			0/20	20/20
$10^{-3.0}$				18/20
$10^{-3.5}$				1/20
				0/20

[a] Tests B, C, and D correctly identified all duplicate samples. No analysis of the relationship between test quantification and tissue location was reported. Data from Valleron et al. *(42)*.
[b] http://www.prionics.ch/.
[c] http://www.protherics.com/.
[d] http://www.bio-rad.com/.

DETECTION OF PRION PROTEIN IN PERIPHERAL TISSUES

Progress has been made recently in detecting prion protein from peripheral tissues as well as increasing the sensitivity of the current assays. In addition, several studies have reported progress in methods to increase the concentration of prion protein to enhance sensitivity. We report on four of these areas below.

Detection of prion protein in blood. RNA aptamer technology has been proposed as a diagnostic tool *(51)* and as a method to disinfect donated blood *(52, 53)*. Patent applications have been filed for this technology *(52, 54)* with at least one company, V.I. Technologies (Watertown, MA), solidly promoting their blood disinfectant abilities *(53)*. In the study by Weiss et al. *(51)*, two RNA aptamers highly specific for PrP^{C} were generated. RNA oligomers that recognized PrP^{C} contained four sets of three-guanine base repeats that formed a "G quartet scaffold". The RNA binding site mapped to the NH_2 terminus of PrP^{C} (residues 23–52). In studies with scrapie-infected brain homogenates, only PrP^{C} was detected by the RNA aptamers. Although the Weiss group has filed a patent application for a blood-based diagnostic *(53)*, no further studies have been published addressing this use. V.I. Technologies use proprietary nucleotide aptamers licensed from William James at Oxford University in their blood disinfectant protocol. Like the Weiss study, the aptamers in the V.I. protocol have an affinity for PrP^{C}; however, the V.I. protocol does suggest that aptamer-dependent clearance of PrP^{Sc} is possible, although few data have been published to support this assertion *(53)*.

Schmerr et al. *(55)* are also working on a prion diagnostic protocol that uses readily accessible blood samples. The method, which uses capillary electrophoresis and

fluorescently labeled markers, has detected very small amounts of PrP^{Sc} in blood from sheep and elk. A peptide consisting of residues 218–232 was labeled with fluorescein at its NH_2 terminus during synthesis. Antibodies to this peptide were raised in rabbits and isolated by affinity chromatography. These antibodies also reacted against scrapie-infected brain samples. In control studies, capillary electrophoresis led to two fluorescence peaks, one for the free peptide and another for the peptide-antibody-prion complex. A positive result for scrapie is indicated by a dramatic reduction in the free peptide peak and a corresponding increase in the immunocomplex peak. Infected and healthy sheep and elk were tested at several time intervals. In one case, an elk in the wild tested negative in the first screen and then was found to be positive for CWD several months later, before the onset of clinical symptoms.

The sensitivity of this diagnostic technique was tremendous; only 50 amol/L (10^{-18} mol/L) fluorescent marker was used. However, the extraction of prion protein from the blood samples was not detailed for "proprietary" reasons. PrP^{Sc} concentration enhancement is directly linked to the extraction procedure; therefore, it is not clear what effect the extraction step had on the detection of the peptide-antibody-prion complex peak. Specificity was not addressed explicitly in this study, nor were immunocomplex affinity data reported. Because the detection of scrapie consists of peak differences, nonspecific binding may contribute to the results. Double-blind studies using this method have not been reported. Another confounding element is the use of fetal bovine serum in the assay, which could be contaminated. This method is promising because it uses only very small quantities of material and each assay can be completed in several minutes. However, a recent report by Brown et al. *(56)* describes their difficulties in reproducing the results of Schmerr et al. *(55)*

Detection of prion protein in urine. The first potential prion diagnostic to test urine samples was described recently by Shaked et al. *(57)*. The protocol relies on the prion protein being small enough to be filtered by the kidneys, such that it is concentrated several hundred times over its concentration in blood. Dialysis was also performed during purification, which appeared to increase sensitivity, although rigorous testing by serial dilutions was not reported. Although not double-blind, the protocol did show some specificity and all controls were correctly identified. A larger, double-blind study that includes serial dilutions is needed to address specificity, sensitivity, and reproducibility. The purification portion of the protocol was not dependent on prion strain per se, but the quantification depended on the conformation of the prion protein through use of the 3F4 murine-derived hamster antibody (epitope, hamster sequence residues 109–112; recognition sequence, MKHM; Fig. 2 and Table 1) and 6H4 (epitope, human sequence residues 144–152; recognition sequence, DYEDRYYRE; Fig. 2 and Table 1). This diagnostic exploits the fact that the binding epitope is the same in the hamster and human proteins. Infection of Syrian hamsters with enriched urine prion protein (denoted by the authors as $UPrP^{Sc}$) appeared to alter the time course of infection. Prion protein was observed in urine from animals near day 60. Additionally, one apparently healthy $UPrP^{Sc}$-infected hamster was sacrificed at 120 days after infection, and PrP^{Sc} was found in the brain of this animal. However, no fatalities had occurred at the time of publication (>270 days after infection). The apparent lack of clinical symptoms in PrP^{Sc}-positive hamsters was thought to be the result of a subclinical prion infection. No double-blind studies were reported.

Enrichment of prion protein in biological samples. Because it is theoretically possible that a small number of PrP^{Sc} molecules can cause infection, highly sensitive assays a necessary. In this regard, Saborio et al. *(58)* recent developed a PCR-like prion-protein amplification metho that might serve as a front end to the various tes described above. In this study, potentially infectious brai homogenate was mixed with fresh, prion-free brain ma ter, and the conversion process was allowed to proceed, originally pioneered by Caughey's group *(16)*. Becaus the conversion tends to be inefficient and the newl converted protein is often hidden in the background the assay, Saborio et al. *(58)* introduced a cyclical protoc involving incubation and sonication. After the initi incubation, the sample is sonicated to break up the newl formed prion aggregate and more normal brain matter i added. Five cycles of incubation/sonication produce 97% conversion. The authors addressed sensitivity b serial dilution studies. Although the evidence is impres sive, with PrP^{Sc} detection at >10 000-fold dilution, it i somewhat hampered by low-resolution immunoblotting Other than controls, double-blind studies were not reported. The throughput is limited by the time of each cycle, currently reported to be 1 h. However, the trade-off in cycle time may be balanced by increased sensitivity The protocol, as published, appears to be independent o prion strain, but the authors suggest that this protocol may not work when the samples to be amplified are not from brain tissue. Additionally, they note that a catalyst in brain homogenate may be required for proper PrP^{Sc} amplification.

Detection of prion disease by altered gene expression. It is natural to assume that most diagnostics for prion diseases would use methods to detect PrP^{Sc}. However, other organs and tissues may be affected during TSE infection before the onset of clinical symptoms. For example, the lymphoreticular system, and the spleen in particular, has been implicated in the pathology of TSEs *(59)*. Consequently, Miele et al. *(59)* investigated altered gene expression in spleens from prion-infected mice by differential-display reverse transcription-PCR. In so doing, they

identified a 0.5-kb gene corresponding to the erythroid differentiation-related factor (EDRF) from 10 000 transcripts. EDRF expression was reduced in prion-infected mice compared with control animals. EDRF is expressed in spleen, bone marrow, and blood in several lines of mice *(59)*. However, EDRF is expressed only in blood and bone marrow in healthy sheep, cattle, and humans. EDRF expression decreases 20% by 40 days postinfection in mice, and it is <10% at the final stage of the disease (162 days postinfection). Studies with TSE-infected sheep and cattle also show a decrease in EDRF expression in both blood and bone marrow. The authors demonstrated that erythroid cells are solely responsible for the expression of EDRF, but it is not clear why infection causes a decrease in the expression of this protein.

In light of this method being a potential diagnostic tool, several issues should be addressed. One issue is that sensitivity was shown qualitatively by comparing EDRF in TSE-infected animals and controls. Although a substantial decrease in EDRF expression was seen 40 days postinfection, clinical symptoms seemed to be present at this time point as well. More precise data are needed earlier in the course of the disease. Time course data were not presented for other animals or for humans, which have longer incubation periods. Application of this method as a diagnostic tool depends on observing down-regulation of EDRF expression before the onset of clinical symptoms. Nonetheless, a nice feature of this protocol is that it could potentially circumvent the problems associated with multiple conformations of PrP^{Sc} and the possible need for PrP^{Sc} conformation-specific probes.

DEVELOPMENT OF PRION THERAPEUTICS

As research progresses on the cause, transmission, and detection of TSEs, studies focusing on treatment and prevention are appearing in greater numbers. Promising small-molecule-based treatments have been described in the last several years, primarily from the research groups of Caughey and Prusiner. As early as 1992, Congo red and various sulfonated glycans were shown to inhibit formation of PrP^{Sc} *(60, 61)*. Protection was obtained if these and other, more toxic drug classes [polyene antibiotics and anthracycline *(62)*] were administered very near to the actual time of infection. Caughey's group *(62, 63)* also examined other, less toxic, actively transported compounds containing derivatized porphyrins and phthalocyanines, with IC_{50} values in the range of 0.5–1 μmol/L.

In addition, Prusiner's group *(64)* have explored the use of branched polyamines for the treatment of TSEs with some success, as well as the synthesis of molecules to mimic PrP^{C} regions containing mutations that prevent the proposed binding of protein X *(65)*. Caughey's group described lysosomotropic and cysteine protease inhibitor compounds that inhibit PrP^{Sc} accumulation in cell cultures *(66)*. CJD therapy using flupirtine, which blocks apoptosis induced by PrP^{Sc}, has been reported *(67, 68)*. More recently, Korth et al. *(69)* have shown that two FDA-approved drugs, quinacrine and chlorpromazine, inhibit PrP^{Sc} formation in cellular assays. At least one study has linked the protective effects of quinacrine to inhibition of 5-lipooxygenase and reduction of neurotoxicity in cells inoculated with PrP106–126 *(70)*. The main difference between these two compounds and other isosteric molecules is, for example, the rotational freedom of the aliphatic chain in chlorpromazine vs the fixed configuration of chlorprothixen. Consequently, further research into the role of the aliphatic chain in prohibiting prion conversion appears to be warranted. Given that these drugs are already approved and side-effect profiles are well documented, Korth et al. *(69)* advocate the use of these compounds in individuals currently suffering from prion diseases. In a preliminary trial with quinacrine at the University of California-San Francisco, the progression of CJD was slowed, at least in one of two CJD-afflicted volunteers *(71)*. Unfortunately, both patients subsequently died, but the disease had already progressed very far when treatment began. The death of one patient may have been linked to the high doses of quinacrine that were administered *(72)*. Larger trials involving quinacrine are currently being pursued in the United Kingdom *(71)* and at the University of California-San Francisco. Korth et al. *(69)* also suggest that quinacrine should be used in animals to treat and possibly halt transmission in contaminated herds, thereby hopefully removing the need for massive herd culls to contain outbreaks of the disease.

Other possible therapeutic interventions targeting different pathways in prion infection have been reviewed *(73)*. One promising postexposure treatment involves blockade of lymphotoxin β-receptor (LTBR) in the lymphoreticular system. A recent study by Oldstone et al. *(74)* has reported on the lack of prion infection in LTBR knockout mice that were fed PrP^{Sc}. Progression of prion infection occurred more rapidly in lymphotoxin α-receptor-null mice, and suppression of follicular dendritic cells and CD11c(+) did nothing to alter the kinetics of neuroinvasion of prions. The authors propose that LTBR blockade is a viable intervention and should be pursued *(74)*.

Both the Caughey and Prusiner research groups are also pursuing peptide- and protein-based inhibition of PrP^{C}-PrP^{Sc} binding. Following up on their previous studies, Caughey's group has shown that peptide fragments from the C-terminal portion of the Syrian hamster PrP^{C} protein inhibit PrP^{Sc} binding and consequently conversion of endogenous PrP^{C} to the protease-resistant form *(25)*. Two peptides (residues 166–179 and 200–223) in particular show promise. Data from cell-free conversion assays indicate that complete inhibition of conversion is obtained at a peptide concentration of 50 μmol/L, with IC_{50} values of 10–15 μmol/L. Random mutations to these peptides severely reduce their ability to inhibit conversion. Inhibition occurs when the peptides adopt β-sheet structure. The sensitivity of this method was addressed in several experiments involving many peptides. Encourag-

ingly, their data show complete inhibition of $PrP^C \rightarrow PrP^{Sc}$ conversion for several of the peptides.

One of the latest advances in the possible treatment of prion diseases with protein-based molecules involves antibody-based inhibition of prion propagation with clearance of infectivity *(75)*. Several antibodies that bind to a variety of epitopes on PrP^C were investigated, and two in particular, D13 and D18, displayed dose-dependent clearance of PrP^{Sc} with IC_{50} values of 12 and 9 nmol/L, respectively *(32, 75–77)*. Experiments were also conducted to determine whether infectious prion protein reappeared when the antibodies were removed. The D18 antibody (Fig. 2 and Table 1) effectively prevented re-emergence of PrP^{Sc} when cells were first grown in antibody culture for at least 2 weeks before the antibody was removed from the medium. The antibody concentration used in these studies was 10 mg/L, and the IC_{50} for D18 was 0.45 mg/L. The authors propose that the antibody binds to the nascent prion protein before the binding of template PrP^{Sc} or other unknown factors. Animal studies were also conducted in which mice were inoculated with mouse ScN2a cells treated with various antibodies. Those animals that received D18 (binds residues 132–156), D13 (binds residues 95–104), or R2 (binds residues 225–231 and 29–37) antibodies were free from disease after 265 days *(75)*. Because the antibodies bind to PrP^C, the strain issue should not be a concern; however, antibody-related loss of native PrP^C function may be an issue if long-term therapy is necessary.

Conclusions

Protein motion can have profound effects on protein-protein interactions, specifically antibody-epitope recognition. For the prion protein, the same amino acid sequence can produce different folded structures, which can hide or create new epitopes. This phenomenon contributes to the already difficult and critically important task of detecting prions in TSEs such as BSE and CJD.

Fortunately, progress has been made in the last 2 years in the field of TSE detection in animals. Current assays provide fairly sensitive and specific results in <24 h *(42)*, which represents a substantial improvement over the previous biological assays (>260 days). However, major limiting factors to these commercial diagnostics include dependence on brain samples from deceased animals as well as issues of sensitivity and specificity. Furthermore, we still lack a commercial test for TSEs in humans.

Several promising technologies have recently been reported that deal with improved TSE detection in animals and proposed diagnostics for humans. Tissue sample accessibility is very important for a mainstream diagnostic tool, and in this regard, the blood and urine assays hold great promise. Sensitivity is crucial for catching presymptomatic cases of TSE disease; methods for amplification and enrichment of infectious prion protein may be very useful to achieve this goal. Advances in analytical methods will also contribute greatly to development of sensitive diagnostics. In addition, there are several promising therapeutic avenues being explored that involve small molecules, peptides, and proteins.

We thank Darwin Alonso for critical reading of the text and contributions to the figures. This work was supported by the National Institutes of Health (Grant GM 50789 to V.D.) and a National Institute of General Medical Sciences National Research Service Award (Grant GM-07750 to B.J.B.).

References

1. Carr CM, Chaudhry C, Kim PS. Influenza hemagglutinin is spring-loaded by a metastable native conformation. Proc Natl Acad Sci U S A 1997;94:14306–13.
2. Ye S, Goldsmith EJ. Serpins and other covalent protease inhibitors. Curr Opin Struct Biol 2001;11:740–5.
3. Carrell RW, Gooptu B. Conformational changes and disease—serpins, prions and Alzheimer's. Curr Opin Struct Biol 1998;8: 799–809.
4. Schiermeier Q. Testing times for BSE [News]. Nature 2001;409: 658–9.
5. Giles J. Mad cow disease comes to Japan [News]. Nature 2001; 413:240.
6. Prusiner SB. Prions. Proc Natl Acad Sci U S A 1998;95:13363–83.
7. Prusiner SB. Prion diseases and the BSE crisis [Review]. Science 1997;278:245–51.
8. Sink M. Coloradoans fear the spread of a kind of mad elk disease. New York Times 2001;October 23. http://www.nytimes.com/2001/10/23/national/23ELK.html (Accessed October 2001).
9. Veneman AM. Declaration of emergency. Fed Regist 2001;66: 49342–3.
10. Stahl N, Baldwin MA, Teplow DB, Hood L, Gibson BW, Burlingame AL, et al. Structural studies of the scrapie prion protein using mass spectrometry and amino acid sequencing. Biochemistry 1993;32:1991–2002.
11. Basler K, Oesch B, Scott M, Westaway D, Waelchli M, Groth DF, et al. Scrapie and cellular PrP isoforms are encoded by the same chromosomal gene. Cell 1986;46:417–28.
12. Caughey B, Raymond GJ, Ernst D, Race RE. N-Terminal truncation of the scrapie-associated form of Prp by lysosomal protease(s)—implications regarding the site of conversion of Prp to the protease-resistant state. J Virol 1991;65:6597–603.
13. Stahl N, Prusiner SB. Prions and prion proteins. FASEB J 1991; 5:2799–807.
14. Caughey B, Raymond GJ. The scrapie-associated form of PrP is made from a cell surface precursor that is both protease- and phospholipase-sensitive. J Biol Chem 1991;266:18217–23.
15. Pan KM, Baldwin M, Nguyen J, Gasset M, Serban A, Groth D, et al. Conversion of α-helices into β-sheets features in the formation of the scrapie prion proteins. Proc Natl Acad Sci U S A 1993;90: 10962–6.
16. Kocisko DA, Come JH, Priola SA, Chesebro B, Raymond GJ, Lansbury PT, et al. Cell-free formation of protease-resistant prion protein. Nature 1994;370:471–4.
17. Kocisko DA, Priola SA, Raymond GJ, Chesebro B, Lansbury PT Jr, Caughey B. Species specificity in the cell-free conversion of prion protein to protease-resistant forms: a model for the scrapie species barrier. Proc Natl Acad Sci U S A 1995;92:3923–7.
18. Mouillet-Richard S, Ermonval M, Chebassier C, Laplanche JL,

Lehmann S, Launay JM, et al. Signal transduction through prion protein. Science 2000;289:1925–8.
19. Brown DR, Schmidt B, Kretzschmar HA. Effects of copper on survival of prion protein knockout neurons and glia. J Neurochem 1998;70:1686–93.
20. Burns CS, Aronoff-Spencer E, Dunham CM, Lario P, Avdievich NI, Antholine WE, et al. Molecular features of the copper binding sites in the octarepeat domain of the prion protein. Biochemistry 2002;41:3991–4001.
21. Alonso DOV, Daggett V. Simulations and computational analyses of prion protein conformations [Review]. Adv Protein Chem 2001; 57:107–37.
22. Horiuchi M, Caughey B. Prion protein interconversions and the transmissible spongiform encephalopathies [Review]. Structure Fold Des 1999;7:R231–40.
23. Safar J, Wille H, Itri V, Groth D, Serban H, Torchia M, et al. Eight prion strains have $PrP^{(Sc)}$ molecules with different conformations. Nat Med 1998;4:1157–65.
24. Caughey B. Interactions between prion protein isoforms: the kiss of death? [Review]. Trends Biochem Sci 2001;26:235–42.
25. Horiuchi M, Baron GS, Xiong LW, Caughey B. Inhibition of interactions and interconversions of prion protein isoforms by peptide fragments from the C-terminal folded domain. J Biol Chem 2001; 276:15489–97.
26. Cohen FE, Prusiner SB. Pathologic conformations of prion proteins [Review]. Annu Rev Biochem 1998;67:793–819.
27. Wadsworth JDF, Hill AF, Joiner S, Jackson GS, Clarke AR, Collinge J. Strain-specific prion-protein conformation determined by metal ions. Nat Cell Biol 1999;1:55–9.
28. Peretz D, Williamson RA, Legname G, Matsunaga Y, Vergara J, Burton DR, et al. A change in the conformation of prions accompanies the emergence of a new prion strain. Neuron 2002;34: 854–6.
29. Caughey B, ed. Prion proteins. Advances in protein chemistry, Vol. 57. San Diego: Academic Press, 2001:405pp.
30. Alonso DOV, DeArmond SJ, Cohen FE, Daggett V. Mapping the early steps in the pH-induced conformational conversion of the prion protein. Proc Natl Acad Sci U S A 2001;98:2985–9.
31. Alonso DOV, An C, Daggett V. Simulations of biomolecules: characterization of the early steps in the pH-induced conformational conversion of the hamster, bovine, and human forms of the prion protein. Philos Trans R Soc Lond A 2002;360:1–13.
32. Peretz D, Williamson RA, Matsunaga Y, Serban H, Pinilla C, Bastidas RB, et al. A conformational transition at the N terminus of the prion protein features in formation of the scrapie isoform. J Mol Biol 1997;273:614–22.
33. Food and Drug Administration. Office of Regulatory Affairs. BSE Import Bulletin 99B-14, 2001. http://www.cfsan.fda.gov/~comm/bseimport.html (Accessed May 2000).
34. Food and Drug Administration. Center for Food Safety. Applied nutrition: domestic and international cosmetic rules, 2001. http://www.cfsan.fda.gov/~comm/cp29001.html and http://www.cfsan.fda.gov/~comm/cp29002.html (Accessed May 2002).
35. Norton SA. Raw animal tissues and dietary supplements [Letter]. N Engl J Med 2000;343:304–5.
36. Food and Drug Administration. Revised preventative measures for blood products, 2001. http://www.fda.gov/ohrms/dockets/ac/01/briefing/3817b1.htm (Accessed May 2002).
37. Centers for Disease Control. Public health service recommendations for the use of vaccines manufactured with bovine-derived materials, 2001. http://www.cdc.gov/mmwr/preview/mmwrhtml/mm4950a4.htm (Accessed May 2002).
38. Ferguson NM, Ghani AC, Donnelly CA, Hagenaars TJ, Anderson RM. Estimating the human health risk from possible BSE infection of the British sheep flock [Letter]. Nature 2002;415:420–4.
39. d'Aignaux JN, Cousens SN, Smith PG. Predictability of the UK variant Creutzfeldt-Jakob disease epidemic. Science 2001;294: 1729–31.
40. Valleron AJ, Boelle PY, Will R, Cesbron JY. Estimation of epidemic size and incubation time based on age characteristics of vCJD in the United Kingdom. Science 2001;294:1726–8.
41. Kao RR, Gravenor MB, Baylis M, Bostock CJ, Chihota CM, Evans JC, et al. The potential size and duration of an epidemic of bovine spongiform encephalopathy in British sheep. Science 2002;295: 332–5.
42. Moynagh J. The evaluations of tests for the diagnosis of transmissible spongiform encephalopathy in bovines. European Commission, 1999. http://europa.eu.int/comm/food/fs/bse/bse12_en.html (Accessed May 2002).
43. Hill AF, Butterworth RJ, Joiner S, Jackson G, Rossor MN, Thomas DJ, et al. Investigation of variant Creutzfeldt-Jakob disease and other human prion diseases with tonsil biopsy samples. Lancet 1999;353:183–9.
44. Bieschke J, Giese A, Schulz-Schaeffer W, Zerr I, Poser S, Eigen M, et al. Ultrasensitive detection of pathological prion protein aggregates by dual-color scanning for intensely fluorescent targets. Proc Nat Acad Sci U S A 2000;97:5468–73.
45. Kneipp J, Beekes M, Lasch P, Naumann D. Molecular changes of preclinical scrapie can be detected by infrared spectroscopy. J Neurosci 2002;22:2989–97.
46. Otto M, Wiltfang J, Cepek L, Neumann M, Mollenhauer B, Steinacker P, et al. Tau protein and 14-3-3 protein in the differential diagnosis of Creutzfeldt-Jakob disease. Neurology 2002;58: 192–7.
47. Jennifer Rufer v. Abbott Laboratories and the University of Washington Medical Center. Benyon, M. Case 99-2-270908-Seattle (King County Superior Court, 2001).
48. Alperovitch A. Epidemiology of Creutzfeldt-Jakob disease—past and present uncertainties. Eur J Neurol 1996;3:500–6.
49. Desiys JP, Comoy E, Hawkins S, Simon S, Schimmel H, Wells G, et al. Public health—screening slaughtered cattle for BSE [Communication]. Nature 2001;409:476–8.
50. European Commission. Opinion of the SSC on design of a field trial for the evaluation of new rapid BSE post mortem tests. Scientific Steering Committee, 2002. http://europa.eu.int/comm/food/fs/sc/ssc/out246_en.pdf (Accessed May 2002).
51. Weiss S, Proske D, Neumann M, Groschup MH, Kretzschmar HA, Famulok M, et al. RNA aptamers specifically interact with the prion protein PrP. J Virol 1997;71:8790–7.
52. Weiss S. PrP^{Sc}-specific nucleic acids, method for their production, and diagnostic and therapeutic use. PCT Int Appl Wo (Lasmezas, Corinne Ida, Fr), 2000:48pp.
53. Hope J, Roth N, Hatigi L, Watson S, Richmond-Chew T, Wiltshire V, et al. High efficiency removal of prion proteins from red cell concentrates by the INACTINE™ process. Watertown, MA: VI Technologies Inc, 2001.
54. James WS. Nucleic acid aptamer ligands specific for an isoform of the prion protein. PCT Int Appl Wo (Isis Innovation Limited, UK), 2001:46 pp.
55. Schmerr MJ, Jenny AL, Bulgin MS, Miller JM, Hamir AN, Cutlip RC, et al. Use of capillary electrophoresis and fluorescent labeled peptides to detect the abnormal prion protein in the blood of animals that are infected with a transmissible spongiform encephalopathy. J Chromatogr A 1999;853:207–14.
56. Brown P, Cervenakova L, Diringer H. Blood infectivity and the prospects for a diagnostic screening test in Creutzfeldt-Jakob disease. J Lab Clin Med 2001;137:5–13.
57. Shaked GM, Shaked Y, Kariv-Inbal Z, Halimi M, Avraham I,

Gabizon R. A protease-resistant prion protein isoform is present in urine of animals and humans affected with prion diseases. J Biol Chem 2001;276:31479–82.

58. Saborio GP, Permanne B, Soto C. Sensitive detection of pathological prion protein by cyclic amplification of protein misfolding [Letter]. Nature 2001;411:810–3.
59. Miele G, Manson J, Clinton M. A novel erythroid-specific marker of transmissible spongiform encephalopathies. Nat Med 2001;7: 361–4.
60. Caughey B, Race RE. Potent inhibition of scrapie-associated Prp accumulation by Congo red. J Neurochem 1992;59:768–71.
61. Caughey B, Raymond GJ. Sulfated polyanion inhibition of scrapie-associated Prp accumulation in cultured cells. J Virol 1993;67: 643–50.
62. Caughey WS, Raymond LD, Horiuchi M, Caughey B. Inhibition of protease-resistant prion protein formation by porphyrins and phthalocyanines. Proc Natl Acad Sci U S A 1998;95:12117–22.
63. Priola SA, Raines A, Caughey WS. Porphyrin and phthalocyanine antiscrapie compounds. Science 2000;287:1503–6.
64. Supattapone S, Nguyen HOB, Cohen FE, Prusiner SB, Scott MR. Elimination of prions by branched polyamines and implications for therapeutics. Proc Natl Acad Sci U S A 1999;96:14529–34.
65. Perrier V, Wallace AC, Kaneko K, Safar J, Prusiner SB, Cohen FE. Mimicking dominant negative inhibition of prion replication through structure-based drug design. Proc Natl Acad Sci U S A 2000;97:6073–8.
66. Doh-Ura K, Iwaki T, Caughey B. Lysosomotropic agents and cysteine protease inhibitors inhibit scrapie-associated prion protein accumulation. J Virol 2000;74:4894–7.
67. Perovic S, Pialoglou P, Schroder HC, Pergande G, Muller WE. Flupirtine increases the levels of glutathione and Bc1–2 in hNT (human Ntera/D1) neurons: mode of action of the drug-mediated anti-apoptotic effect. Eur J Pharmacol 1996;317:157–64.
68. Otto M, Boekhoff I, Ratzka P, Wiltfang J, Riedemann C, Kropp S, et al. First therapeutic experience with flupirtine in patients with Creutzfeldt-Jakob disease. J Neurol 1998;245:846.
69. Korth C, May BCH, Cohen FE, Prusiner SB. Acridine and phenothiazine derivatives as pharmacotherapeutics for prion disease. Proc Natl Acad Sci U S A 2001;98:9836–41.
70. Stewart LR, White AR, Jobling MF, Needham BE, Maher F, Thyer J, et al. Involvement of the 5-lipoxygenase pathway in the neurotoxicity of the prion peptide PrP106–126. J Neurosci Res 2001;65: 565–72.
71. Will RG, Knight RSG. Potential treatments for Creutzfeldt-Jakob Disease, 2002. http://www.cjd.ed.ac.uk/TREAT.htm (Accessed May 2002).
72. First CJD drug trial patient dies, 2001. http://news.bbc.co.uk/1/hi/health/1687339.stm (Accessed July 2002).
73. Aguzzi A, Glatzel M, Montrasio F, Prinz M, Heppner FL. Interventional strategies against prion diseases. Nat Rev Neurosci 2001; 2:745–9.
74. Oldstone MB, Race R, Thomas D, Lewicki H, Homann D, Smelt S, et al. Lymphotoxin-α- and lymphotoxin-β-deficient mice differ in susceptibility to scrapie: evidence against dendritic cell involvement in neuroinvasion. J Virol 2002;76:4357–63.
75. Peretz D, Williamson RA, Kaneko K, Vergara J, Leclerc E, Schmitt-Ulms G, et al. Antibodies inhibit prion propagation and clear cell cultures of prion infectivity [Letter]. Nature 2001;412:739–43.
76. Williamson RA, Peretz D, Pinilla C, Ball H, Bastidas RB, Rozenshteyn R, et al. Mapping the prion protein using recombinant antibodies. J Virol 1998;72:9413–8.
77. Leclerc E, Peretz D, Ball H, Sakurai H, Legname G, Serban A, et al. Immobilized prion protein undergoes spontaneous rearrangement to a conformation having features in common with the infectious form. EMBO J 2001;20:1547–54.
78. Korth C, Stierli B, Streit P, Moser M, Schaller O, Fischer R, et al. Prion (PrP^{Sc})-specific epitope defined by a monoclonal antibody [Letter]. Nature 1997;390:74–7.
79. James TL, Liu H, Ulyanov NB, Farr-Jones S, Zhang H, Donne DG, et al. Solution structure of a 142-residue recombinant prion protein corresponding to the infectious fragment of the scrapie isoform. Proc Natl Acad Sci U S A 1997;94:10086–91.
80. DeArmond SJ, Qiu Y, Sanchez H, Spilman PR, Ninchak-Casey A, Alonso D, et al. PrP^{C} glycoform heterogeneity as a function of brain region: implications for selective targeting of neurons by prion strains. J Neuropathol Exp Neurol 1999;58:1000–9.
81. Garcia FL, Zahn R, Riek R, Wuthrich K. NMR structure of the bovine prion protein. Proc Natl Acad Sci U S A 2000;97:8334–9.
82. Zahn R, Liu AZ, Luhrs T, Riek R, von Schroetter C, Garcia FL, et al. NMR solution structure of the human prion protein. Proc Natl Acad Sci U S A 2000;97:145–50.